

Supporting Information for:

Red-shifted tetra-*ortho*-halo-azobenzenes for photo-regulated transmembrane anion transport

Aidan Kerckhoffs, Zonghua Bo, Samuel Penty, Fernanda Duarte*, and Matthew J. Langton*

Contents

1. Materials and methods	2
2. Synthesis and characterization	3
3. Photo-switching experiments	66
4. NMR titration experiments	72
5. Anion transport studies	83
6. Computational	92
7. References	99

1. Materials and methods

All reagents and solvents were purchased from commercial sources and used without further purification. Lipids were purchased from Avanti Polar Lipids and used without further purification. Where necessary, solvents were dried by passing through an MBraun MPSP-800 column and degassed with nitrogen. Triethylamine was distilled from and stored over potassium hydroxide. Column chromatography was carried out on Merck® silica gel 60 under a positive pressure of nitrogen. Where mixtures of solvents were used, ratios are reported by volume. NMR spectra were recorded on a Bruker AVIII 400, Bruker AVII 500 (with cryoprobe) and Bruker AVIII 500 spectrometers. Chemical shifts are reported as δ values in ppm. Mass spectra were carried out on a Waters Micromass LCT and Bruker microTOF spectrometers. Fluorescence spectroscopic data were recorded using a Horiba Duetta fluorescence spectrophotometer, equipped with Peltier temperature controller and stirrer. UV-Vis spectra were recorded on a V-770 UV-Visible/NIR Spectrophotometer equipped with Peltier temperature controller and stirrer using quartz cuvettes of 1 cm path length. Experiments were conducted at 25°C unless otherwise stated. Vesicles were prepared as described below using Avestin “LiposoFast” extruder apparatus, equipped with polycarbonate membranes with 200 nm pores. GPC purification of vesicles was carried out using GE Healthcare PD-10 desalting columns prepacked with Sephadex G 25 medium.

Abbreviations

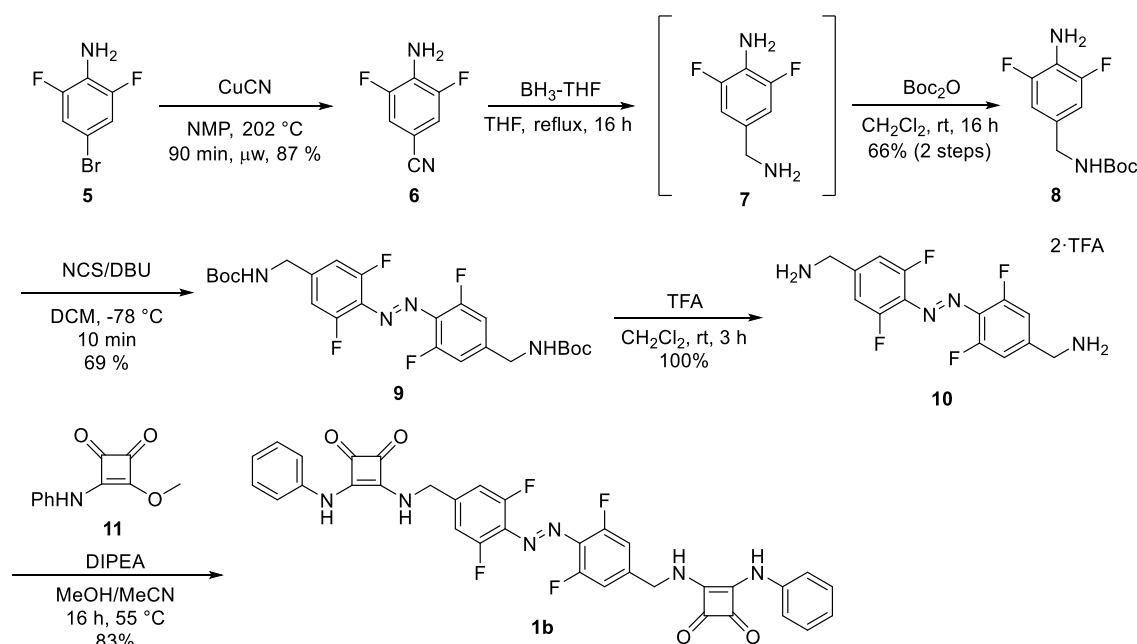
Boc: tert-butyloxycarbonyl; CF: 5(6)-Carboxyfluorescein; DBU: 1,8-Diazabicyclo[5.4.0]undec-7-ene; DCM: Dichloromethane; DIPEA: *N,N*-Diisopropylethylamine; DMF: *N,N*-Dimethylformamide; DMSO: Dimethylsulfoxide; DPPC: 1,2-dipalmitoyl-*sn*-glycero-3-phosphocholine; EYPG: egg-yolk phosphatidylglycerol; HEPES: *N*-(2-hydroxyethyl)piperazine-*N'*-(2-ethanesulfonic acid); HPTS: 8-hydroxy-1,3,6-pyrenetrisulfonate; HRMS: High resolution mass spectrometry; KF: Potassium Fluoride; KOH: Potassium hydroxide; LUVs: large unilamellar vesicles; MeCN: Acetonitrile; MeOH: Methanol; NCS: *N*-Chlorosuccinimide; Phth: Phthaloyl; POPC: 1-palmitoyl-2-oleoyl-*sn*-glycero-3-phosphocholine; rt: Room temperature; TFA: Trifluoroacetic acid; THF: Tetrahydrofuran.

2. Synthesis and characterization

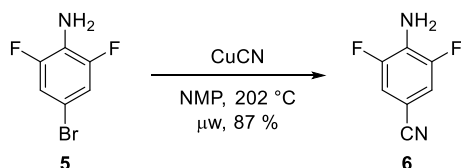
General comments.

Compounds **11** and **37** were prepared according to literature procedures.^[1]

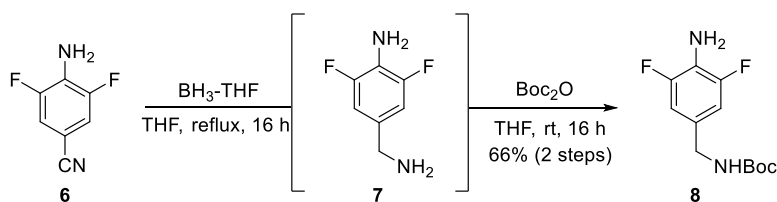
All novel compounds were characterised by ¹H and ¹³C NMR, UV-Vis and high-resolution mass spectrometry. Azobenzene derivatives were formed as a mixture of *E* and *Z* isomers. Peaks for the *E* isomer are reported (major product). Thermal relaxation to achieve 100% *E* isomer was achieved by heating the sample in DMSO at 80 °C prior to NMR titration experiments or anion transport assays. For carriers **1-4**, ¹H NMR spectra are provided for both 100% *E*-azobenzene isomer (heated dark state) and where available, 77% *cis* isomer (green light photo-stationary state for carrier **1b** and red light photo-stationary state for carriers **2-4**).



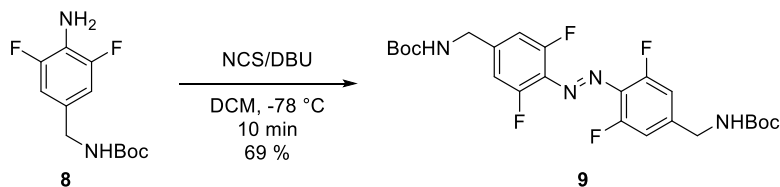
Scheme S1. Synthesis of tetra-*ortho*-fluoro azobenzene anionophore **1b**



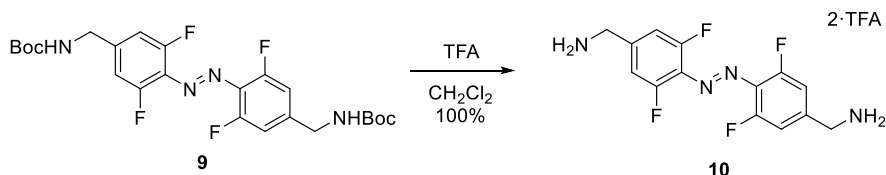
4-amino-3,5-difluorobenzonitrile 6. A suspension of 4-bromo-2,6-difluoroaniline **5** (6.5 g, 31.1 mmol) and copper(I) cyanide (4.2 g, 146.6 mmol, 1.5 eq) in dry NMP (15 mL) was heated to 202 °C under microwave irradiation for 90 minutes under N₂. The reaction was poured onto 15% ammonia solution (300 mL), then extracted with 50:50 Hexane:EtOAc (3x 150 mL). The combined organic layers were washed with water (5x 150 mL), 5% LiCl solution, then were concentrated in vacuo. The resulting residue was purified by silica gel column chromatography (50% CH₂Cl₂ in hexane) to obtain the title compound as a white crystalline solid (4.16 g, 27 mmol, 87%). ¹H NMR (400 MHz, Chloroform-d) δ 7.17 (dd, J = 6.0, 2.3 Hz, 2H), 4.29 (s, 2H). Data consistent with that given in the literature.^[2]



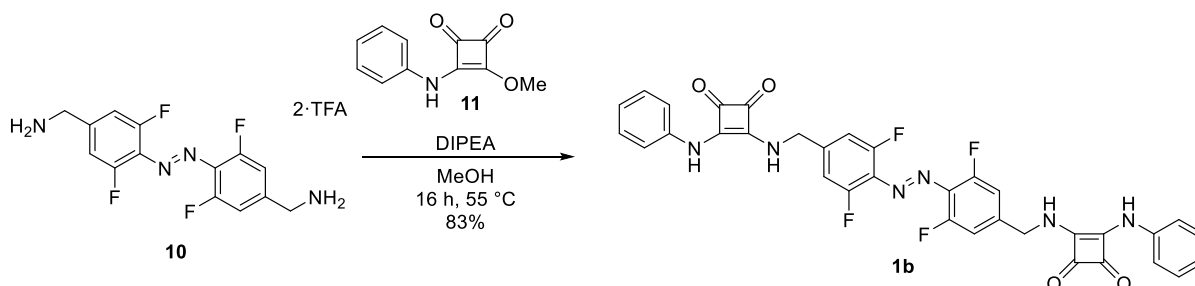
tert-butyl (4-amino-3,5-difluorobenzyl)carbamate 8. To a solution at 0°C of 4-amino-3,5-difluorobenzonitrile **6** (3.85 g, 25 mmol) in THF (20 mL) was added dropwise 1M BH₃-THF solution (100 mL, 100 mmol, 4 equiv). The mixture was stirred under reflux for 16 h. 100 mL of MeOH were then added, and the resulting mixture was refluxed for 1 h. The solvent was removed *in vacuo*. The resulting residue was re-dissolved in EtOAc (300 mL) and washed with water (3 x 50 mL) and brine (1 x 50 mL). The organic layers were concentrated *in vacuo* to afford crude amine **7**. ¹H NMR (400 MHz, Acetone) δ 6.97 – 6.77 (m, 1H), 4.29 (s, 1H). This was immediately dissolved in CH₂Cl₂ (60 mL). Boc₂O (5.45g, 25 mmol, 1 equiv) in CH₂Cl₂ (30 mL) was added dropwise to the solution of **7**. The reaction was stirred for 16 h at rt. The solvent was concentrated and the residue was purified by silica gel flash column chromatography (6:1 hexane-acetone) to afford the title compound as a white solid (4.26 g, 66%). ¹H NMR (400 MHz, CDCl₃) δ 6.82 – 6.69 (m, 2H), 4.80 (s, 1H), 4.17 (d, *J* = 6.1 Hz, 2H), 3.82 – 3.54 (br s, 2H), 1.46 (s, 9H). ¹³C NMR (101 MHz, CDCl₃) δ 155.85, 151.92 (dd, *J* = 240.8, 8.2 Hz), 128.40 (t, *J* = 7.83 Hz), 122.83 (t, *J* = 16.5 Hz), 109.92 (dd, *J* = 15.1, 7.5 Hz), 79.66, 43.67, 28.35. HRMS-ESI (*m/z*) Calculated for C₁₂H₁₆O₂N₂F₂ [M+Na]⁺, 281.1072; found 281.1072.



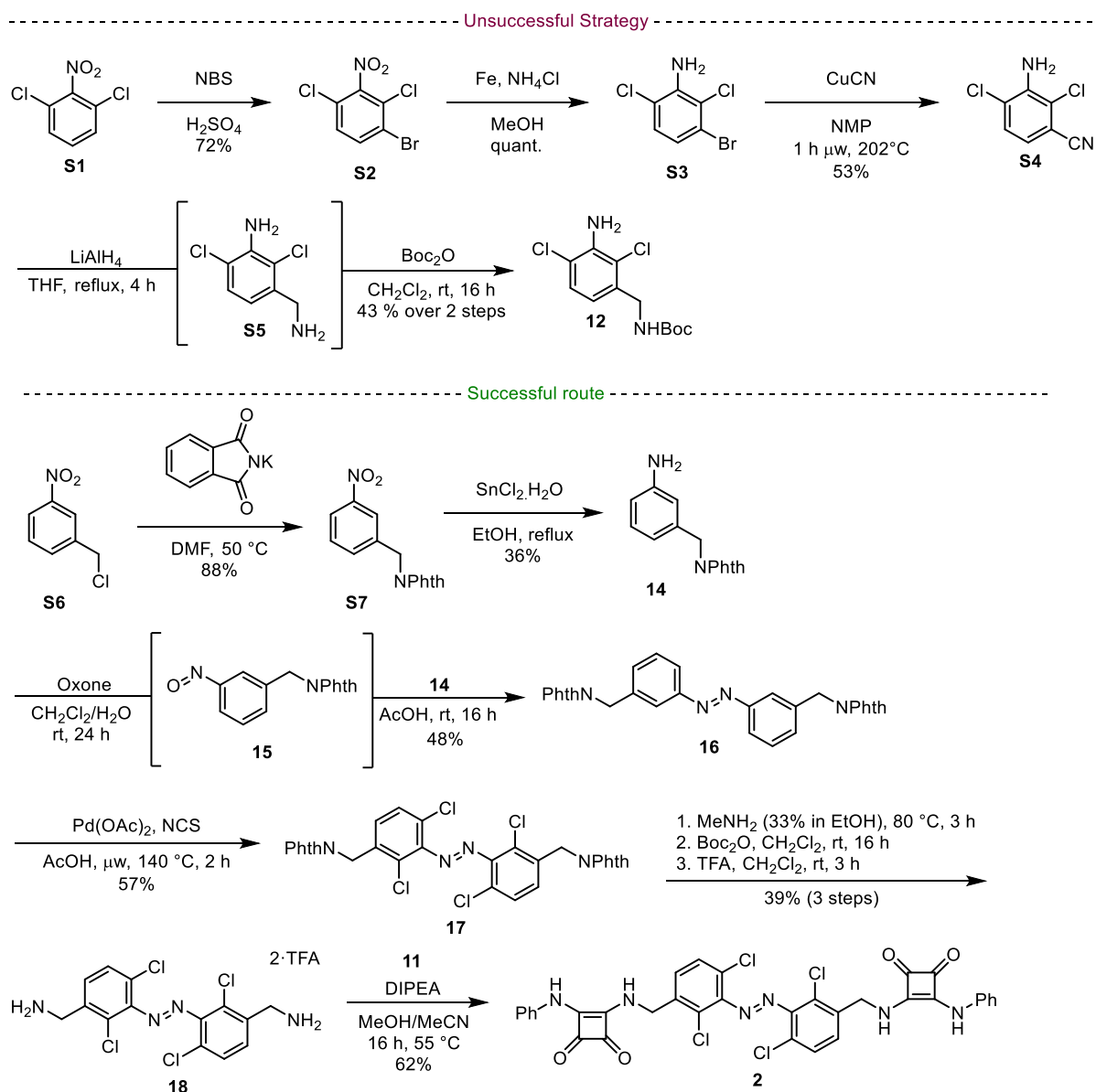
Azobenzene 9. To a solution of **8** (303 mg, 1.17 mmol) in CH₂Cl₂ (17 mL) was added DBU (350 mg, 2.34 mmol, 2 eq). The solution was stirred at room temperature for 5 min before being cooled down to –78 °C. NCS (313 mg, 2.34 mmol, 2 eq) was added. The orange solution was stirred for 10 min at –78 °C before quenching with saturated bicarbonate solution (15 mL). The organic layer was separated, washed sequentially with 15 mL of water (5 x 15 mL) and 1N HCl (15 mL), dried over anhydrous sodium sulfate, and concentrated to dryness *in vacuo*. The residue was purified by silica gel flash chromatography (5% EtOAc in CH₂Cl₂) to afford the title compound as an orange solid as a mixture of isomers (205 mg, 402 μmol, 69%, 11:9 ratio of *E*-**9** and *E*-**9** as indicated by ¹H NMR analysis). *E*-**9**: ¹H NMR (400 MHz, Chloroform-*d*) δ 6.99 (d, *J* = 10.1 Hz, 4H), 4.99 (s, 2H), 4.35 (d, *J* = 6.4 Hz, 4H), 1.47 (s, 18H). ¹³C NMR (101 MHz, Chloroform-*d*) δ 155.95, 155.04 (dd, *J* = 261.7, 4.53 Hz), 144.60 (m), 130.69 (t, *J* = 9.8 Hz), 111.14 (d, *J* = 21 Hz), 80.40, 44.02, 28.50. HRMS-ESI (*m/z*) Calculated for C₂₄H₂₈F₄N₄O₄ [M+H]⁺, 513.2119; found 513.2119.



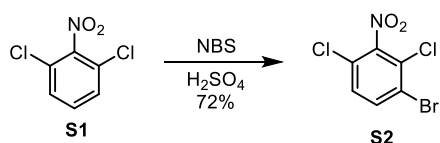
TFA Salt 10. To a solution of **9** (200 mg, 0.39 mmol) in CH_2Cl_2 (4.5 mL) was added TFA (0.57 mL). The reaction was stirred for 3 hours. The TFA was removed under a nitrogen stream, after which the residue was dried to afford the title compound as an orange solid (210 mg, 0.39 mmol, 100%, 73:27 of **E-10** and **Z-10**). **E-10**: ^1H NMR (400 MHz, Methanol- d_4) δ 7.34 (s, 4H), 4.23 (s, 4H). ^{13}C NMR (101 MHz, Methanol- d_4) δ 156.73 (dd, $J = 266.2$ Hz, 3.53 Hz), 139.76 (t, $J = 10.23$ Hz), 132.66 (t, $J = 10.21$ Hz), 114.48 (d, $J = 22.3$ Hz), 43.22. HRMS-ESI (m/z) Calculated for $\text{C}_{14}\text{H}_{12}\text{F}_4\text{N}_4$ $[\text{M}+\text{H}]^+$, 313.1071; found 313.1070.



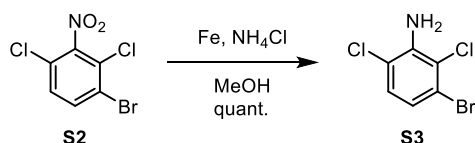
Transporter 1b. Diamine **10** (50 mg, 92.5 μmol) was dissolved in MeOH (1 mL). DIPEA (86.2 μL , 0.5 mmol, 6 equiv) was added dropwise. Monosquaramide **11** (38 mg, 185 μmol , 2 equiv) in MeCN (1 mL) was added dropwise, and the solution was stirred at 55°C for 16 h. The reaction was then cooled to rt and the solid precipitate was isolated by vacuum filtration and washed with MeOH and MeCN, then dried under high vacuum to afford the title compound as an orange solid (50.3 mg, 76.8 μmol , 83%). **E-1b**: ^1H NMR (500 MHz, DMSO) δ 9.79 (br s, 2H), 8.08 (br s, 2H), 7.44 (d, $J = 8.2$ Hz, 4H), 7.41 (d, $J = 10.6$ Hz, 4H), 7.37 – 7.33 (m, 4H), 7.04 (t, $J = 7.3$ Hz, 2H), 4.92 (d, $J = 6.5$ Hz, 4H). ^{13}C NMR (126 MHz, DMSO) δ 183.97, 180.84, 168.88, 164.30, 154.78 (dd, $J = 260.2$, 4.6 Hz), 145.29 (t, $J = 9.4$ Hz), 138.87, 129.57 (t, $J = 9.9$ Hz), 129.36, 122.82, 117.91, 111.86 (dd, $J = 20.7$, 3.3 Hz), 46.22. HRMS-ESI (m/z) calculated for $\text{C}_{34}\text{H}_{21}\text{F}_4\text{N}_6\text{O}_4^-$ $[\text{M}-\text{H}]^-$, 653.1566, found 653.1581.



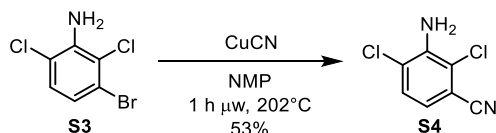
Scheme S2. Synthesis of meta-substituted azobenzene anionophore **2**



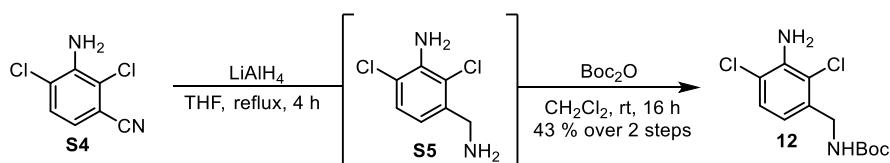
Aryl bromide S2. Prepared according to a modified literature procedure.^[3] To a stirring solution of **S1** (3.93 g, 20.5 mmol) in concentrated sulphuric acid (110 mL) under inert atmosphere was added N-bromosuccinimide (3.64 g, 20.5 mmol) at rt and the resulting suspension was heated to 60 °C and stirred for 16 h. The reaction was poured into ice-cold water (100 mL) and extracted with EtOAc (2 x 100 mL). The organic layers were concentrated then recrystallized from hexane to afford the title compound as white crystals (4.0 g, 14.8 mmol, 72%). ¹H NMR (400 MHz, DMSO) δ 8.11 (d, *J* = 8.9 Hz, 1H), 7.79 (d, *J* = 8.8 Hz, 1H). Data consistent with that given in the literature.^[3]



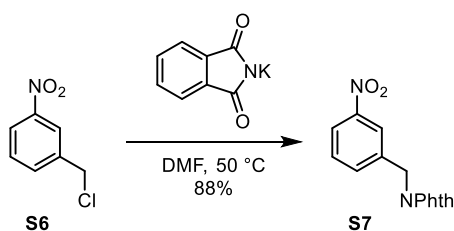
Aniline S3. To a solution of **S2** (4.0 g, 14.77 mmol) in MeOH (100 mL) equipped with a large stirring bar was added Fe powder (4.12 g, 73.83 mmol, 5 eq) and ammonium chloride (3.95 g, 73.83 mmol, 5 eq). The suspension was stirred vigorously at 80 °C (bath temperature) for 4 hours. The solution was filtered over celite and the filtrate was concentrated in vacuo to afford the title compound as a white solid (3.55 g, 14.74 mmol, 100%). ¹H NMR (400 MHz, CDCl₃) δ 7.05 (d, *J* = 8.6 Hz, 1H), 6.95 (d, *J* = 8.6 Hz, 1H), 4.61 (br s, 2H). ¹³C NMR (101 MHz, CDCl₃) δ 141.64, 128.16, 121.84, 121.41, 119.85, 118.33. HRMS-ESI (m/z) Calculated for C₆H₄Cl₂NBr [M+H]⁺, not found under any conditions.



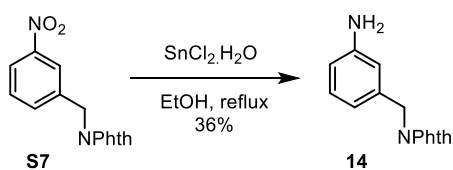
Nitrile S4. In a microwave vial was added **S3** (3.5 g, 14.53 mmol) and CuCN (1.69 g, 18.89 mmol, 1.3 eq). The vial was purged with N₂ for 10 minutes. Then, 20 mL degassed NMP was added, the tube was sealed and reaction was heated to 202 °C under microwave irradiation for 1h. The reaction was cooled, poured over ice water ammonia solution and extracted with 50:50 hexane:EtOAc 3x. The combined organic layers were sequentially washed with water and 5% LiCl solution, then concentrated. The resulting residue was purified by silica gel flash chromatography (50% CH₂Cl₂ in hexane) to afford the title compound as a white solid (1.44 g, 7.70 mmol, 53%, 90% purity). ¹H NMR (400 MHz, CDCl₃) δ 7.28 (d, *J* = 8.3 Hz, 1H), 7.00 (d, *J* = 8.3 Hz, 1H), 4.72 (br s, 2H). ¹³C NMR (101 MHz, CDCl₃) δ 141.48, 128.27, 124.07, 122.11, 121.06, 116.06, 112.33. HRMS-EI (m/z) Calculated for C₇H₄Cl₂N₂ 185.9752; found 185.9748



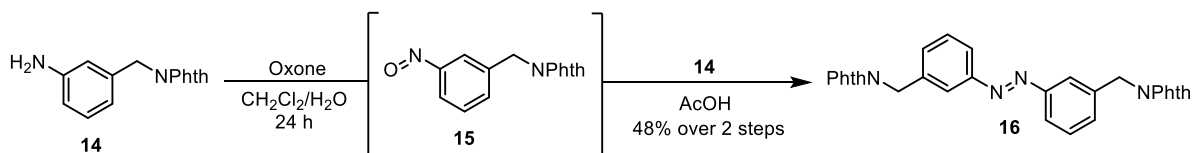
Carbamate 12. To a suspension of LiAlH₄ (733 mg, 19.25 mmol, 2.5 eq) in dry THF (40 mL) was added **S4** (1.44 g, 7.70 mmol, 1.0 eq) in THF (60 mL). The suspension was refluxed for 4 hours. The reaction mixture was cooled, diluted in Et₂O (150 mL), then water (730 μL), 2.5M NaOH (730 μL), and water (2 mL) was added dropwise. The suspension was stirred for 15 minutes, and then anhydrous MgSO₄ was added (Fieser work-up). The solution was filtered, then concentrated to afford crude **S5** without further purification (1.35 g). ¹H NMR (400 MHz, CDCl₃) δ 7.13 (d, *J* = 8.2 Hz, 1H), 6.68 (d, *J* = 8.2 Hz, 1H), 4.50 (br s, 2H), 3.84 (s, 2H), 1.85 – 1.72 (br s, 2H). **S5** was dissolved in CH₂Cl₂ (25 mL), then Boc₂O (1.51 g, 6.93 mmol, 0.9 eq) in CH₂Cl₂ (15 mL) was added dropwise. The reaction was stirred at room temperature for 16 h. The reaction was concentrated, then purified by silica gel flash chromatography (80% CH₂Cl₂ in hexane) to afford the title compound as a white solid (734 mg, 3.32 mmol, 43%). ¹H NMR (400 MHz, CDCl₃) δ 7.15 (d, *J* = 8.3 Hz, 1H), 6.71 (d, *J* = 8.3 Hz, 1H), 4.92 (s, 1H), 4.33 (d, *J* = 6.0 Hz, 2H), 1.45 (s, 9H). ¹³C NMR (126 MHz, CDCl₃) δ 155.85, 140.38, 135.78, 127.49, 118.81, 118.76, 118.10, 79.85, 42.86, 28.53. HRMS-ESI (m/z) Calculated for C₁₂H₁₆Cl₂N₂O₂ [M+Na]⁺, 313.0481; found 313.0481.



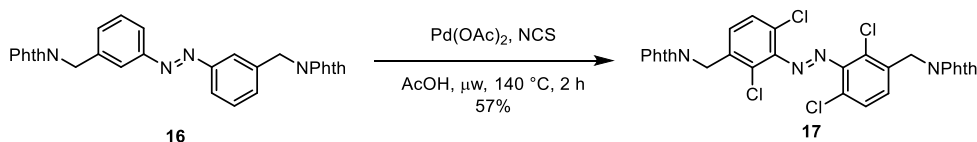
Phthalimide S7. Prepared according to a modified literature procedure.^[4] 3-nitrobenzyl chloride **S6** (2 g, 11.7 mmol) was dissolved in DMF (10 mL). Potassium phthalimide (2.27 g, 12.2 mmol, 1.05 eq) was added and the reaction was stirred at 50 °C for 16 hours. The DMF was removed in vacuo at 70 °C. To the residue was added water (15 mL) and EtOAc (4 mL) and the biphasic mixture was stirred vigorously for 30 minutes. The precipitated solid was filtered, washed with EtOAc and dried to afford the title compound as a white solid (2.9 g, 10.27 mmol, 88%). ¹H NMR (400 MHz, CDCl₃) δ 8.28 (t, *J* = 2.0 Hz, 1H), 8.14 (ddd, *J* = 8.2, 2.3, 1.1 Hz, 1H), 7.91 – 7.85 (m, 2H), 7.79 – 7.73 (m, 3H), 7.51 (t, *J* = 7.9 Hz, 1H), 4.94 (s, 2H). Data consistent with that given in the literature.^[4]



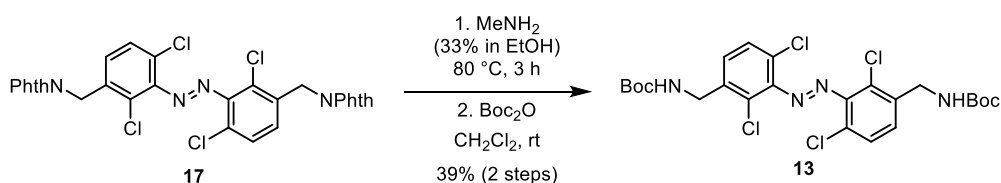
Phthalimide 14. Prepared according to a modified literature procedure.^[4] **S7** (2.9 g, 10.25 mmol) was dissolved in EtOH (50 mL). SnCl₂·H₂O (9.2 g, 41 mmol, 4 eq) was added and the reaction was refluxed for 16 hours. The mixture was concentrated and suspended in 60 mL 4N NaOH and 40 mL EtOAc and the biphasic mixture was stirred vigorously for 30 minutes at 0 °C. The precipitated solid was filtered, washed with EtOAc and dried to afford a solid, which was recrystallised from MeCN to afford the title compound light green crystals (930 mg, 10.3 mmol, 36%). ¹H NMR (400 MHz, CDCl₃) δ 7.84 (dd, *J* = 5.5, 3.1 Hz, 2H), 7.73 – 7.67 (m, 2H), 7.09 (t, *J* = 7.8 Hz, 1H), 6.82 (dt, *J* = 7.6, 1.3 Hz, 1H), 6.75 (t, *J* = 2.0 Hz, 1H), 6.58 (ddd, *J* = 8.0, 2.4, 1.0 Hz, 1H), 4.75 (s, 2H), 3.65 (s, 2H). Data consistent with that given in the literature.^[4]



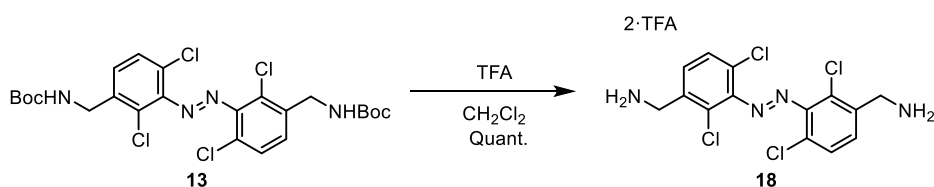
Azobenzene 16. A solution of **14** (650 mg, 2.58 mmol) in CH₂Cl₂ (50 mL), was treated with a solution of Oxone® (7.6 g, 23 mmol, 9.0 equiv.) in H₂O (50 mL) at 23 °C. The resulting biphasic reaction mixture was stirred vigorously at room temperature overnight. Subsequently, the phases were separated and the aqueous phase was extracted with CH₂Cl₂. The combined organic extracts were washed sequentially with a 1M aqueous hydrochloric acid solution (50 mL), saturated aqueous sodium bicarbonate solution (50 mL), and H₂O (50 mL). The washed organic layer was treated with **14** (780 mg, 8.37 mmol, 1.2 equiv.) and AcOH (40 mL). The CH₂Cl₂ was then removed under reduced pressure at 35 °C and the solution was stirred overnight. The AcOH was then removed under reduced pressure. The residue was purified by flash silica gel chromatography (CH₂Cl₂) to yield the title compound as an orange solid as a mixture of isomers (620 mg, 1.24 mmol, 48%). **E-16:** ¹H NMR (400 MHz, CDCl₃) δ 7.96 (t, *J* = 1.9 Hz, 2H), 7.89 – 7.83 (m, 4H), 7.80 (dt, *J* = 7.9, 1.5 Hz, 2H), 7.74 – 7.69 (m, 4H), 7.54 (dt, *J* = 7.7, 1.5 Hz, 2H), 7.45 (t, *J* = 7.7 Hz, 2H), 4.95 (s, 4H). ¹³C NMR (126 MHz, CDCl₃) δ 168.15, 152.96, 137.59, 134.17, 132.24, 131.24, 129.58, 123.61, 123.50, 122.11, 41.49. HRMS-ESI (*m/z*) Calculated for C₃₀H₂₀N₄O₄ [M+H]⁺, 501.1557; found 501.1556



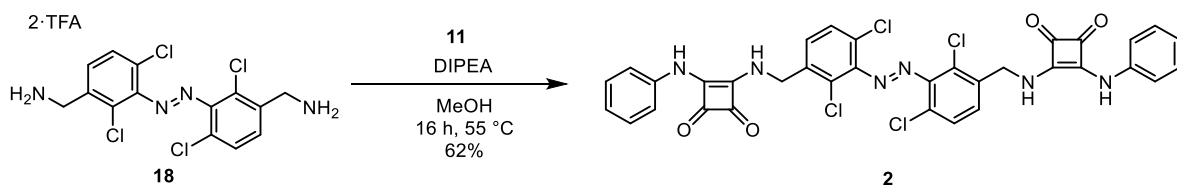
Azobenzene 17. Azobenzene **16** (300 mg, 0.6 mmol, 1.0 eq), NCS (400 mg, 3 mmol, 5.0 eq) and Pd(OAc)_2 (16.15 mg, 72 μmol , 0.10 eq) were suspended in AcOH (6 mL) under a N_2 -atmosphere in a microwave vial. The tube was sealed and the reaction was heated to 140 °C under microwave irradiation for 2h. The dark red solution was cooled, concentrated and redissolved in CH_2Cl_2 . The organic layer was washed with water, then concentrated in *vacuo*. The brown oil was purified by silica gel flash chromatography (8% acetone in 1:1 hexane: CH_2Cl_2) to afford the title compound as an orange solid as a mixture of isomers (220 mg, 0.34 mmol, 57%). **E-17**: $^1\text{H NMR}$ (400 MHz, CDCl_3) δ 7.90 (dd, $J = 5.5, 3.1$ Hz, 4H), 7.79 – 7.75 (m, 4H), 7.39 (d, $J = 8.5$ Hz, 2H), 7.23 (d, $J = 8.4$ Hz, 2H), 5.05 (s, 4H). $^{13}\text{C NMR}$ (126 MHz, CDCl_3) δ 167.80, 148.00, 134.35, 133.98, 131.93, 129.04, 128.85, 126.81, 125.55, 123.66, 39.32. HRMS-ESI (m/z) Calculated for $\text{C}_{30}\text{H}_{16}\text{Cl}_4\text{N}_4\text{O}_4$ [$\text{M}+\text{Na}$] $^+$, 658.9823; found 658.9816



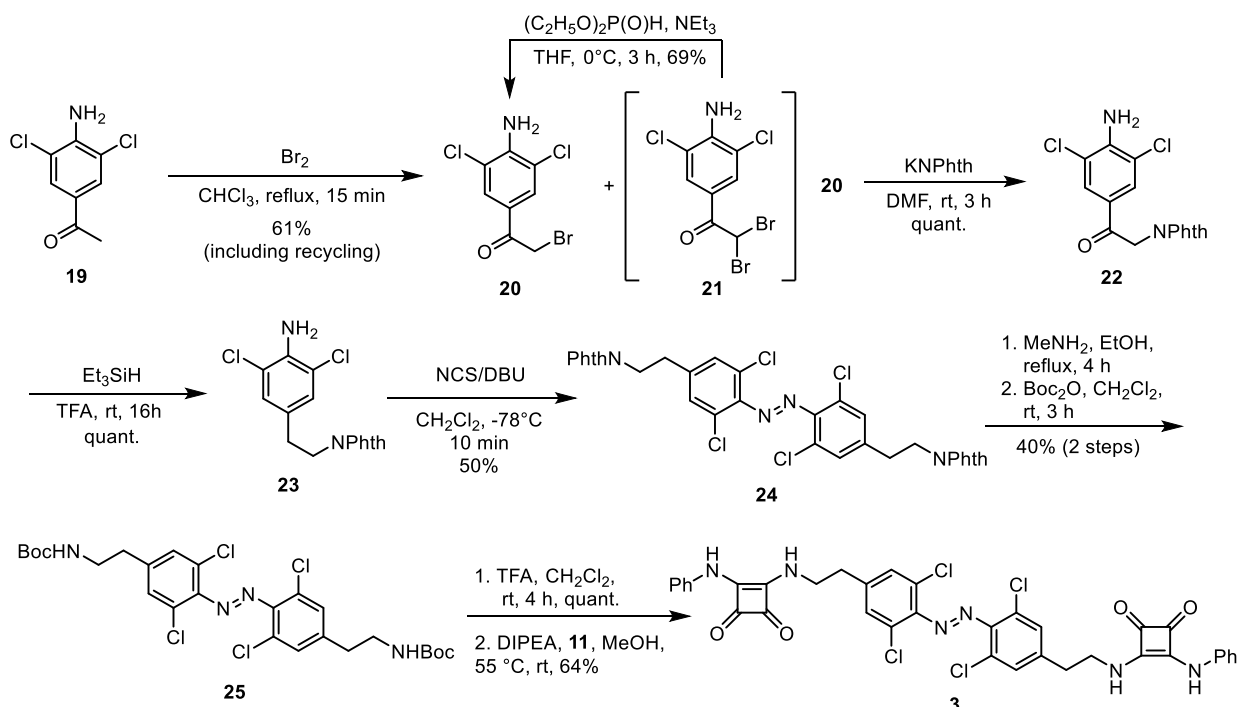
Azobenzene 13. Phthalimide **17** (210 mg, 329 μmol) was dissolved in 33% MeNH_2 solution in ethanol (5 mL). The reaction was stirred refluxed for 3 h. The solvent was removed *in vacuo*. The resulting residue was dissolved in CH_2Cl_2 (5 mL). To this was added Boc_2O (163 mg, 744 μmol , 2.2 eq) in CH_2Cl_2 (5 mL). The reaction was stirred at rt for 16 h and the solvent was then removed *in vacuo*. The residue was purified by silica gel flash column chromatography (1.5% EtOAc in CH_2Cl_2) to afford the title compound as an orange solid as a mixture of isomers (76 mg, 131 μmol , 39 %, 3:2 ratio of **E-13** and **Z-13** as indicated by $^1\text{H NMR}$ analysis). **E-13**: $^1\text{H NMR}$ (400 MHz, CDCl_3) δ 7.38 (d, $J = 8.3$ Hz, 2H), 7.33 (d, $J = 8.5$ Hz, 2H), 5.00 (s, 2H), 4.39 (d, $J = 6.4$ Hz, 4H), 1.39 (s, 18H). $^{13}\text{C NMR}$ (126 MHz, CDCl_3) δ 155.75, 147.89, 137.07, 129.62, 129.16, 126.86, 125.23, 80.03, 42.39, 28.40. HRMS-ESI (m/z) Calculated for $\text{C}_{24}\text{H}_{28}\text{Cl}_4\text{N}_4\text{O}_4$ [$\text{M}+\text{H}$] $^+$, 577.0937; found 577.0933.



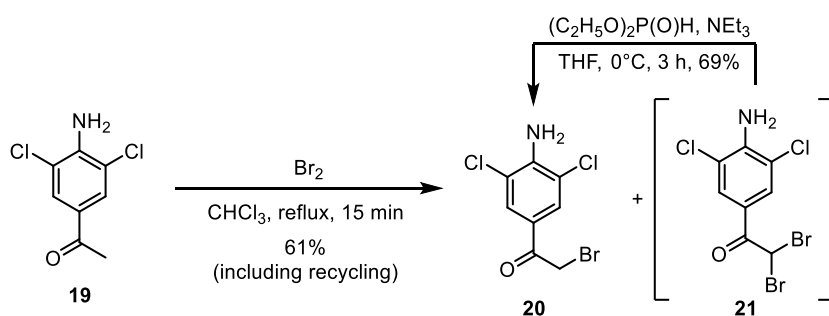
TFA salt 18. To a solution of **13** (60 mg, 104 μmol) in CH_2Cl_2 (1 mL) was added TFA (133 μL). The reaction was stirred at room temperature for 2 hours. The TFA was removed under a stream of nitrogen, then dried *in vacuo* to afford the title compound as an orange solid (63 mg, 104 μmol , 100%, 5:2 ratio of **E-18** and **Z-18** as indicated by $^1\text{H NMR}$ analysis). **E-18**: $^1\text{H NMR}$ (400 MHz, MeOD) δ 7.72 (d, $J = 8.4$ Hz, 2H), 7.63 (d, $J = 8.4$ Hz, 2H), 4.39 (s, 4H). $^{13}\text{C NMR}$ (126 MHz, MeOD) δ 147.83, 131.92, 131.12, 129.80, 127.55, 126.85, 39.93. HRMS-ESI (m/z) Calculated for $\text{C}_{14}\text{H}_{12}\text{Cl}_4\text{N}_4$ [$\text{M}+\text{H}$] $^+$, 376.9889; found 376.9890.



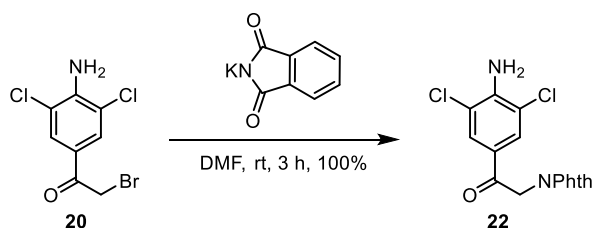
Carrier 2. Amine **18** (23 mg, 37 μmol) was dissolved in MeOH (0.5 mL). DIPEA (40 μL , 0.23 mmol, 6 eq) was added dropwise. Monosquaramide **11** (15.2 mg, 75 μmol , 2 eq) in MeCN (0.5 mL) was added, and the solution was heated at 55 °C for 16 hours. The reaction was cooled to rt and the solid precipitate was filtered and washed sequentially with MeOH and MeCN, then collected and dried under high vacuum to afford the title compound as an orange solid (16.8 mg, 23.4 μmol , 62%). *E-2*: ^1H NMR (400 MHz, DMSO) δ 9.81 (s, 2H), 8.14 (s, 2H), 7.78 (d, $J = 8.4$ Hz, 2H), 7.65 (d, $J = 8.5$ Hz, 2H), 7.44 (d, $J = 8.1$ Hz, 4H), 7.35 (t, $J = 7.7$ Hz, 4H), 7.04 (t, $J = 7.2$ Hz, 2H), 5.01 (s, 4H). ^{13}C NMR (126 MHz, DMSO) δ 183.84, 180.74, 168.91, 164.22, 146.87, 138.86, 137.32, 130.42, 129.86, 129.39, 125.72, 124.31, 122.87, 118.18, 44.96. HRMS-ESI (m/z) Calculated for $\text{C}_{34}\text{H}_{22}\text{Cl}_4\text{N}_6\text{O}_4$ [$\text{M}-\text{H}$] $^-$, 717.0373; found 717.0376.



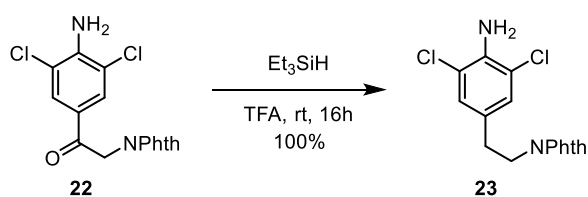
Scheme S3. Synthesis of ethyl-substituted azobenzene anionophore **3**



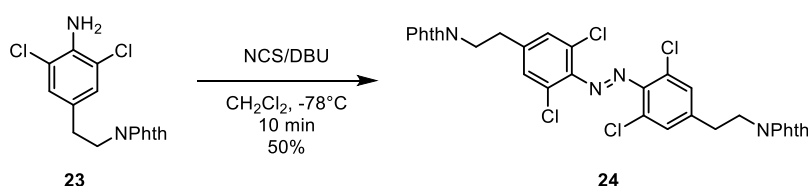
Bromide 20 and 21. To a solution of compound **19** (5 g, 24.5 mmol) in CHCl_3 (100 mL) was added Br_2 (1.64 mL, 31.85 mmol, 1.3 equiv) dropwise with vigorous stirring. The reaction was stirred under reflux for 15 min and then cooled to rt. 10 % sodium thiosulphate solution was added dropwise until the reaction mixture had lost its brown colour. The reaction mixture was then neutralised with 10% NaHCO_3 solution. The organic layer was concentrated, then purified by silica gel column chromatography (50% Hexane in CH_2Cl_2) to afford **20** and **21** as white solids. Compound **20** (2.92 g, 10.3 mmol, 42%): $^1\text{H NMR}$ (400 MHz, d_6 -DMSO) δ 7.87 (s, 2H), 6.58 (s, 2H), 4.76 (d, $J = 1.3$ Hz, 2H). Data consistent with that given in the literature.^[5] Compound **21** (2.47 g, 6.8 mmol, 28%): $^1\text{H NMR}$ (400 MHz, CDCl_3) δ 7.98 (s, 2H), 6.53 (s, 1H), 5.13 (s, 2H). Data consistent with that given in the literature.^[6] To improve the yield of desired compound **20**, isolated compound **21** was dissolved in THF (15ml) and cooled to 0°C . A solution of diethyl phosphite (879 μL , 6.8 mmol, 1 equiv) and NEt_3 (1.05 mL, 7.48 mmol, 1.1 equiv.) in THF (6 ml) was added dropwise with vigorous stirring. The reaction was brought to rt and stirred for 3 h. 200 mL ice water was poured into the reaction mixture. The precipitate was collected and dried by vacuum filtration to afford 1.33 g of **20** (Total yield: 4.25 g, 15.9 mmol, 61.3%).



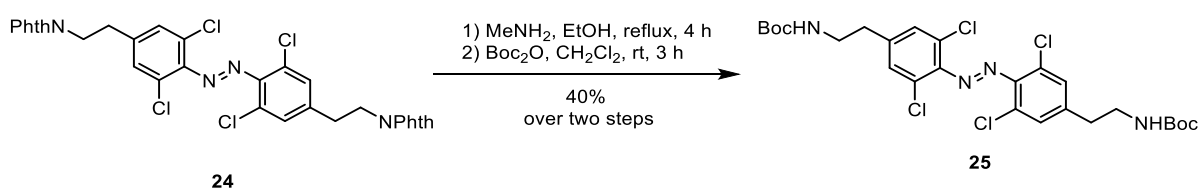
Phthalimide 22. To a solution of **20** (4.25 g, 15.0 mmol) in DMF (20 mL) was added potassium phthalimide (3.34 g, 16.5 mmol, 1.1 equiv). The reaction was stirred at rt for 3 h and monitored by TLC. 300 mL of cold water was added to form a precipitate, which was isolated by vacuum filtration then dried to afford the title compound as a white solid (5.2 g, 15.0 mmol, quant). $^1\text{H NMR}$ (400 MHz, d_6 -DMSO) δ 7.96 (s, 2H), 7.95 – 7.88 (m, 4H), 6.65 (s, 2H), 5.13 (s, 2H). $^{13}\text{C NMR}$ (126 MHz, d_6 -DMSO) δ 188.49, 167.56, 146.39, 134.80, 131.57, 128.70, 123.37, 122.27, 117.46, 43.87. HRMS-ESI (m/z) calculated for $\text{C}_{16}\text{H}_{10}\text{Cl}_2\text{N}_2\text{O}_3^+$ [$\text{M}+\text{H}$] $^+$, 349.0141; found 349.0141.



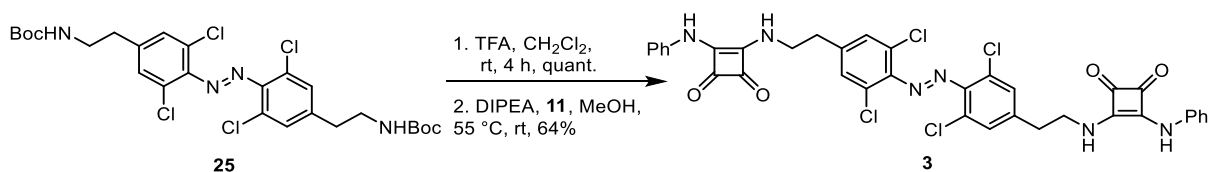
Aniline 23. To a solution of compound **22** (6.00 g, 17.2 mmol) in TFA (50 mL) at 0°C was added dropwise triethylsilane (6.86 mL, 43.0 mmol, 2.5 equiv) under a nitrogen atmosphere with vigorous stirring. The reaction was brought to rt and stirred for 16 h. The mixture was diluted with 200 mL of water and brought to pH 9 by the addition of 10% NaOH solution (~ 100 mL) to form a precipitate, which was isolated by vacuum filtration then dried to afford the title compound as a white solid (5.76 g, 17.2 mmol, quant.). ¹H NMR (400 MHz, DMSO) δ 7.87 – 7.79 (m, 4H), 7.05 (s, 2H), 5.30 (s, 2H), 3.75 (t, *J* = 7.0 Hz, 2H), 2.77 (t, *J* = 7.0 Hz, 2H). ¹³C NMR (101 MHz, DMSO) δ 167.71, 139.46, 134.47, 131.44, 128.16, 127.28, 123.06, 118.00, 38.68, 32.13. HRMS-ESI (*m/z*) calculated for C₁₆H₁₃Cl₂N₂O₂⁺ [M+H]⁺, 335.0349, found 335.0350.



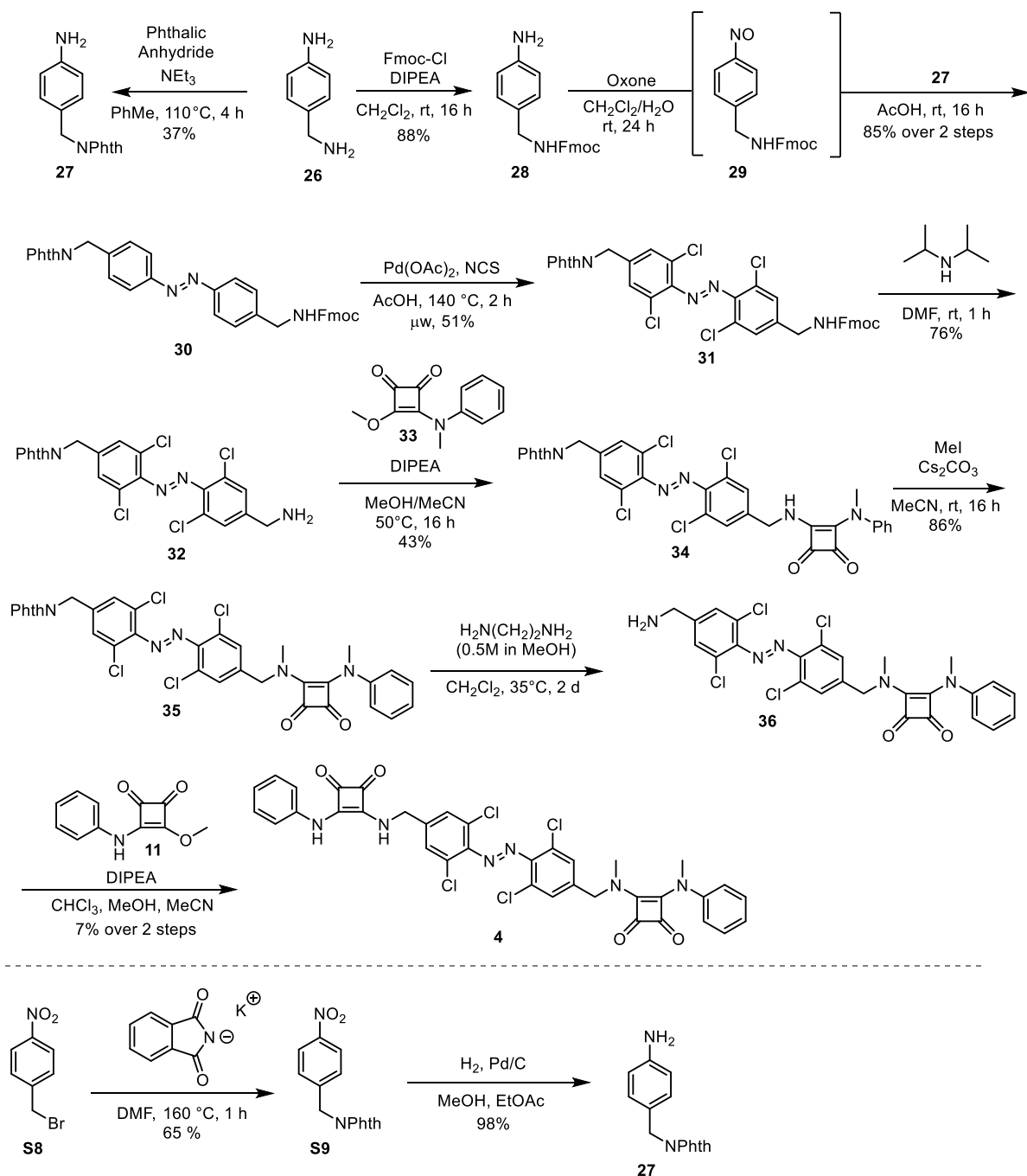
Protected azobenzene 24. To a solution of **23** (3.82 g, 11.4 mmol) in CH₂Cl₂ (150 mL) was added DBU (3.40 mL, 22.8 mmol, 2 equiv). The solution was stirred at rt for 5 min before being cooled to –78°C. *N*-chlorosuccinimide (3.04 g, 22.8 mmol, 2 equiv) was added. The solution was stirred at –78°C for 10 min before quenching by addition of saturated sodium bicarbonate solution (150 mL). The organic layer was washed with water (5 x 150 mL) and 1 M HCl (150 mL), dried over anhydrous MgSO₄ and concentrated *in vacuo*. The residue was purified by silica gel flash column chromatography (CH₂Cl₂) to afford the title compound as an orange brown solid as a mixture of isomers (1.89 g, 2.84 mmol, 50%): **E-24** ¹H NMR (500 MHz, CDCl₃) δ 7.87 (dd, *J* = 5.5, 3.1 Hz, 4H), 7.75 – 7.73 (m, 4H), 7.37 (s, 4H), 3.98 – 3.94 (m, 4H), 3.05 – 2.99 (m, 4H). ¹³C NMR (126 MHz, CDCl₃) δ 168.20, 146.30, 140.63, 134.29, 132.07, 129.93, 127.72, 123.57, 38.50, 33.92. HRMS-ESI (*m/z*) calculated for C₃₂H₂₁Cl₄N₄O₄⁺ [M+H]⁺, 665.0317; found 665.0306.



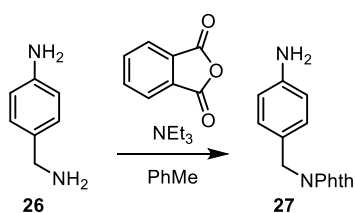
Protected azobenzene diamine 25. Compound **24** (400 mg, 600 μmol) was dissolved in 33% MeNH₂ solution in ethanol (9.6 mL). The reaction was stirred under reflux for 4 h. The solvent was removed *in vacuo*. The resulting residue (243 mg) was dissolved in CH₂Cl₂ (10 mL). To this was added Boc₂O (122 mg, 557 μmol) in CH₂Cl₂ (10 mL). The reaction was stirred at rt for 3 h and the solvent was then removed *in vacuo*. The crude was purified by silica gel flash column chromatography (10% EtOAc in CH₂Cl₂) to afford the title compound as an orange solid as a mixture of isomers (146 mg, 240.78 μmol, 40 %): **E-25**: ¹H NMR (400 MHz, CDCl₃) δ 7.29 (s, 4H), 4.58 (s, 2H), 3.40 (q, *J* = 6.7 Hz, 4H), 2.83 (t, *J* = 6.7 Hz, 4H), 1.45 (s, 18H). ¹³C NMR (126 MHz, CDCl₃) δ 155.90, 146.11, 141.94, 129.92, 127.65, 79.79, 41.41, 35.54, 28.51. HRMS-ESI (*m/z*) calculated for C₂₆H₃₂Cl₄N₄O₄Na⁺ [M+Na]⁺, 629.1042; found 629.1037.



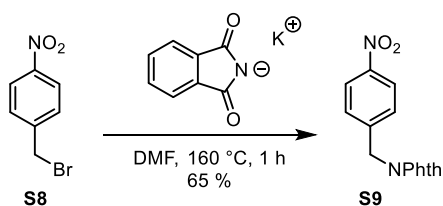
Carrier 11. To a solution of **25** (70 mg, 115 μmol) in CH_2Cl_2 (1.6 mL) was added TFA (0.2 mL). The reaction was stirred at rt for 4 h. The TFA and solvent were removed by evaporation under a stream of nitrogen and then under high vacuum to afford the deprotected amine as an orange salt (73 mg, 115 μmol , quant.). $^1\text{H NMR}$ (400 MHz, CD_3OD) δ 7.51 (s, 4H), 3.22 (d, $J = 7.4$ Hz, 4H), 3.00 (t, $J = 7.4$ Hz, 4H). HRMS-ESI (m/z) calculated for $\text{C}_{16}\text{H}_{17}\text{Cl}_4\text{N}_4\text{Na}^+$ $[\text{M}+\text{H}]^+$, 407.0173; found 407.0173. The diamine (23 mg, 39 μmol) was dissolved in MeOH (0.5 mL). DIPEA (40 μL , 0.23 mmol, 6 eq) was added dropwise. Monosquaramide **11** (15.6 mg, 77 μmol , 2 eq) in MeCN (0.5 mL) was added, and the solution was heated at 55 $^\circ\text{C}$ for 16 hours. The reaction was cooled to rt and the solid precipitate was filtered and washed sequentially with MeOH and MeCN, then collected and dried under high vacuum to afford the title compound as an orange solid (20 mg, 39 μmol , 69%). **E-3:** $^1\text{H NMR}$ (400 MHz, DMSO-d_6) δ 9.67 (br s, 2H), 7.66 (s, 4H), 7.57 (s, 2H), 7.39 (d, $J = 6.7$ Hz, 4H), 7.32 (t, $J = 7.8$ Hz, 4H), 7.02 (t, $J = 7.3$ Hz, 2H), 3.94 (s, 4H), 3.01 (t, $J = 6.9$ Hz, 4H). $^{13}\text{C NMR}$ (126 MHz, DMSO) δ 184.55, 180.97, 169.57, 164.24, 145.34, 143.28, 139.40, 130.81, 129.81, 126.63, 123.14, 118.54, 44.62, 36.33. HRMS-ESI (m/z) Calculated for $\text{C}_{36}\text{H}_{26}\text{Cl}_4\text{N}_6\text{O}_4$ $[\text{M}-\text{H}]^-$, 745.0697; found 745.0690



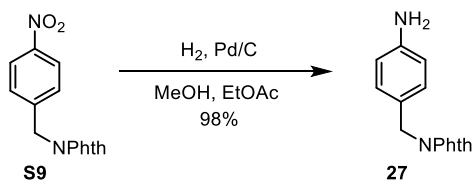
Scheme S4. Synthesis of non-symmetric azobenzene derivatives



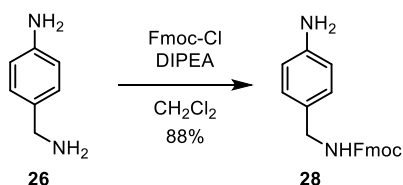
Phthalimide 27. Prepared according to a modified literature procedure.^[7] Amine **26** (1 g, 8.2 mmol, 1 eq) and triethylamine (3.4 mL, 24.6 mmol, 3 eq) were suspended in toluene (10 mL). phthalic anhydride (0.78 mL, 4.5 mmol, 1 eq) suspended in toluene (300 mL) was added dropwise over 4 hours at reflux temperature. The solution was hot filtered and the filtrate concentrated and purified by silica gel flash chromatography (dry load, 4% EtOAc in CH₂Cl₂) to afford the title compound as a light yellow solid (766 mg, 3.0 mmol, 37%). ¹H NMR (400 MHz, DMSO) δ 7.92 – 7.79 (m, 4H), 6.98 (d, *J* = 8.4 Hz, 2H), 6.48 (d, *J* = 8.4 Hz, 2H), 5.04 (s, 2H), 4.56 (s, 2H). Data consistent with that given in the literature.^[7]



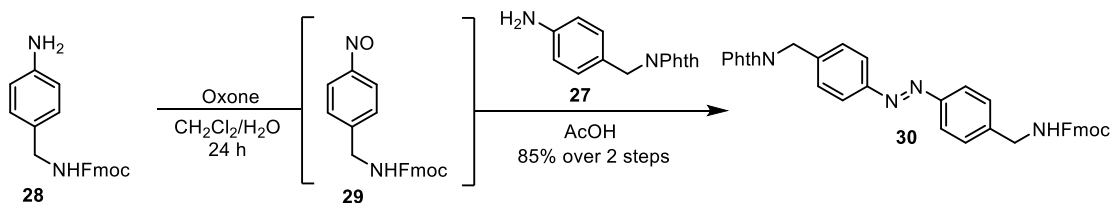
Phthalimide S9. Prepared according to a modified literature procedure.^[8] P-nitrobenzyl bromide **S8** (7 g, 32.40 mmol) was dissolved in DMF (45 mL). Potassium phthalimide (6.3 g, 34 mmol, 1.05 eq) was added and the reaction was stirred at reflux temperature for 1 h. The reaction was cooled, and ice water was added. The filtrate was dissolved in hot EtOAc (300 mL), and allowed to recrystallize for two days at room temperature in a 500 mL flask. The solid was collected and washed with cold EtOAc to afford the title compound as white crystals (5.9 g, 20.9 mmol, 65%). ¹H NMR (400 MHz, CDCl₃) δ 8.22 – 8.15 (m, 2H), 7.88 (dd, *J* = 5.4, 3.1 Hz, 2H), 7.75 (dd, *J* = 5.5, 3.1 Hz, 2H), 7.62 – 7.56 (m, 2H), 4.93 (s, 2H).^[8]



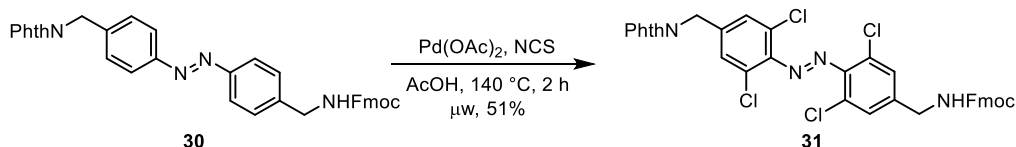
Phthalimide 27. Nitro compound **S9** (3 g, 22.0 mmol) was dissolved in 40% MeOH in EtOAc (160 mL). The reaction was placed under nitrogen, then 10% Pd/C (300 mg) was added. The reaction was stirred under H₂ atmosphere for 16 hours, filtered over celite, then concentrated to afford the title compound as a white solid (2.3 g, 21.7 mmol, 98%). ¹H NMR (400 MHz, DMSO) δ 7.92 – 7.79 (m, 4H), 6.98 (d, *J* = 8.4 Hz, 2H), 6.48 (d, *J* = 8.4 Hz, 2H), 5.04 (s, 2H), 4.56 (s, 2H). Data consistent with that given in the literature.^[7]



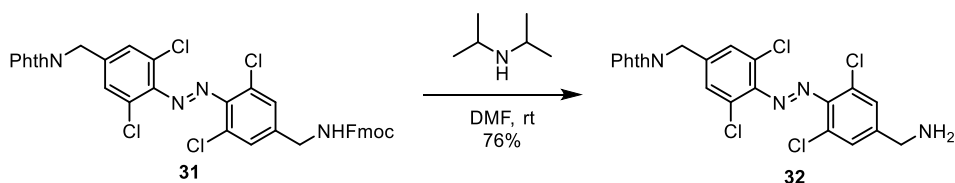
Fmoc building block 28. Prepared according to a modified literature procedure.^[9] 4-aminobenzylamine **26** (550 mg, 4.5 mmol, 1 eq) and DIPEA (0.78 mL, 4.5 mmol, 1 eq) were dissolved in CH₂Cl₂ (50 mL). Fmoc-Cl (1.16 g, 4.5 mmol, 1 eq) in CH₂Cl₂ (10 mL) was added dropwise at 0 °C. The reaction was stirred at room temperature for 16 hours, after which a white precipitate had formed. The organic layer was washed with water, then concentrated in vacuo. The crude was purified by silica gel flash chromatography (dry load, 10% EtOAc in CH₂Cl₂) to afford the title compound as a white solid (1.37 g, 4.0 mmol, 88%). ¹H NMR (400 MHz, Chloroform-d) δ 7.75 (d, *J* = 7.56 Hz, 2H), 7.58 (d, *J* = 7.40 Hz, 2H), 7.39 (t, *J* = 7.34 Hz, 2H), 7.29 (t, *J* = 7.30 Hz, 2H), 7.21 (t, *J* = 6.96 Hz, 1H), 7.05 (d, *J* = 8.10 Hz, 2H), 6.62 (d, *J* = 8.34 Hz, 2H), 5.01 (s br, 1H), 4.42 (d, *J* = 7.18 Hz, 2H), 4.24 (s, 2H), 3.72 (br s, 2H). Data consistent with that given in the literature.^[9]



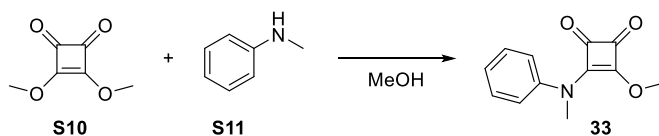
Azobenzene 30. A solution of **28** (855 mg, 2.77 mmol, 1.4 equiv.) in CH₂Cl₂ (50 mL), was treated with a solution of Oxone® (5.43 g, 17.84 mmol, 9.0 equiv.) in H₂O (50 mL) at 23 °C. The resulting biphasic reaction mixture was stirred vigorously at room temperature overnight, after which the organic layer turned green. Subsequently, the phases were separated and the aqueous phase was extracted with CH₂Cl₂ (2x50 mL). The combined organic extracts were washed sequentially with a 1M aqueous hydrochloric acid solution (50 mL), saturated aqueous sodium bicarbonate solution (50 mL), and H₂O (50 mL). The washed organic layer was treated with **27** (500 mg, 1.98 mmol, 1.0 equiv.) and AcOH (40 mL). The CH₂Cl₂ was removed under reduced pressure at 35 °C and the solution was stirred for 16 hours. The AcOH was removed under reduced pressure. The residue was purified by flash silica gel chromatography (CH₂Cl₂ to 1% Acetone in CH₂Cl₂) to yield the title compound as an orange solid (1.0 g, 1.69 mmol, 85%). **E-30:** ¹H NMR (400 MHz, CDCl₃) δ 7.91 – 7.80 (m, 6H), 7.79 – 7.74 (m, 2H), 7.72 (dd, *J* = 5.5, 3.1 Hz, 2H), 7.64 – 7.54 (m, 4H), 7.43 – 7.34 (m, 4H), 7.31 (t, *J* = 7.5 Hz, 2H), 5.15 (br t, *J* = 6.2 Hz, 1H), 4.92 (s, 2H), 4.50 (d, *J* = 6.7 Hz, 2H), 4.45 (d, *J* = 6.2 Hz, 2H), 4.23 (t, *J* = 6.7 Hz, 1H); ¹³C NMR (126 MHz, CDCl₃) δ 168.13, 156.60, 152.27, 152.12, 143.99, 141.66, 141.49, 139.34, 134.25, 132.21, 129.48, 128.22, 127.84, 127.20, 125.13, 123.60, 123.37, 123.34, 120.14, 66.84, 47.46, 44.89, 41.44. HRMS-ESI (*m/z*) Calculated for C₃₇H₂₈N₄O₄ [M+H]⁺, 593.2183; found 593.2180



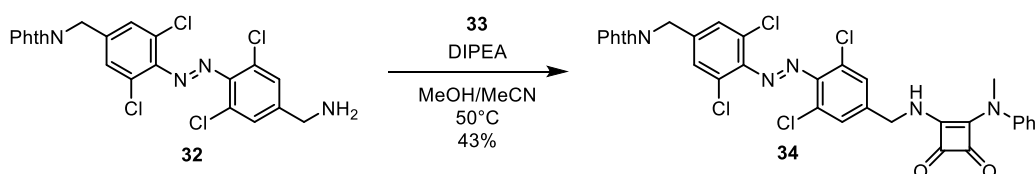
Azobenzene 31. This reaction was split into three 1 g batches due to microwave vial size restrictions. **30**, (1 g, 1.69 mmol, 1.0 eq), NCS (1.13 mg, 8.44 mmol, 5.0 eq) and Pd(OAc)₂ (46 mg, 0.2 mmol, 0.12 eq) were dissolved in AcOH (17 mL) under a N₂-atmosphere in a 20 mL pressure tube. The tube was sealed and reaction was heated to 140 °C under microwave irradiation for 2h. The dark red solution was cooled, concentrated and redissolved in CH₂Cl₂. The organic layer was washed sequentially with sat. aq. NaCl and phosphate buffer (pH 7), and then concentrated in vacuo. The three batches were combined and purified by silica gel flash chromatography (CH₂Cl₂) to afford the title compound as a dark red solid as a mixture of isomers (1.96 g, 2.68 mmol, 51% [\sim 90% purity]). **E-31**: ¹H NMR (400 MHz, CDCl₃) δ 7.88 (td, J = 5.3, 2.2 Hz, 2H), 7.76 (dd, J = 5.4, 3.1 Hz, 2H), 7.74 – 7.62 (m, 2H), 7.58 (d, J = 6.2 Hz, 2H), 7.53 (s, 2H), 7.45 – 7.31 (m, 4H), 7.26 – 7.15 (m, 2H), 5.21 (br t, J = 6.6 Hz, 1H), 4.84 (s, 2H), 4.62 – 4.41 (m, 1H), 4.38 (d, J = 6.6 Hz, 2H), 4.22 (t, J = 6.7 Hz, 1H). ¹³C NMR (126 MHz, CDCl₃) δ 167.73, 156.24, 147.60, 147.13, 145.69, 143.31, 141.06, 138.44, 134.36, 131.91, 129.49, 129.17, 128.33, 128.24, 128.07, 128.03, 125.44, 123.67, 120.09, 66.59, 47.24, 43.89, 40.35. HRMS-ESI (m/z) Calculated for C₃₇H₂₄Cl₄N₄O₄ [M-H]⁻, 729.0624; found 729.024



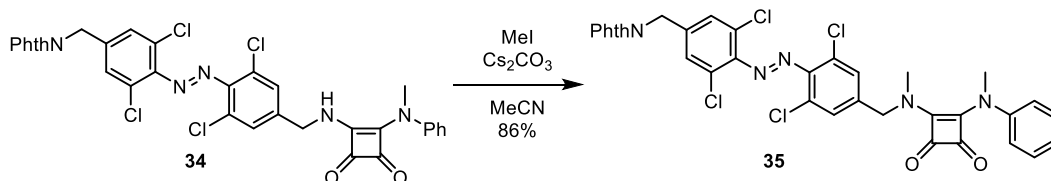
Amine 32. **31** (1.1 g, 1.51 mmol) was dissolved in DMF (8 mL). Diisopropylamine (341 μ L, 1.96 mmol, 1.3 eq) was added, and the reaction was stirred at room temperature for 1 hour, after which a precipitate had formed. The DMF was azeotropically removed under reduced pressure with toluene. The residue was purified by silica gel flash chromatography (100:3:1 CH₂Cl₂:MeOH:NEt₃) to afford the title compound as a dark red solid as a mixture of isomers (580 mg, 1.14 mmol, 76%), which is used immediately in the next step. **E-32**: ¹H NMR (400 MHz, CDCl₃) δ 7.92 – 7.85 (m, 2H), 7.79 – 7.72 (m, 2H), 7.52 (s, 2H), 7.44 (s, 2H), 4.84 (s, 2H), 3.91 (s, 2H). HRMS-ESI (m/z) Calculated for C₂₂H₁₄Cl₄N₄O₂ [M+H]⁺, 506.9944; found 506.9943



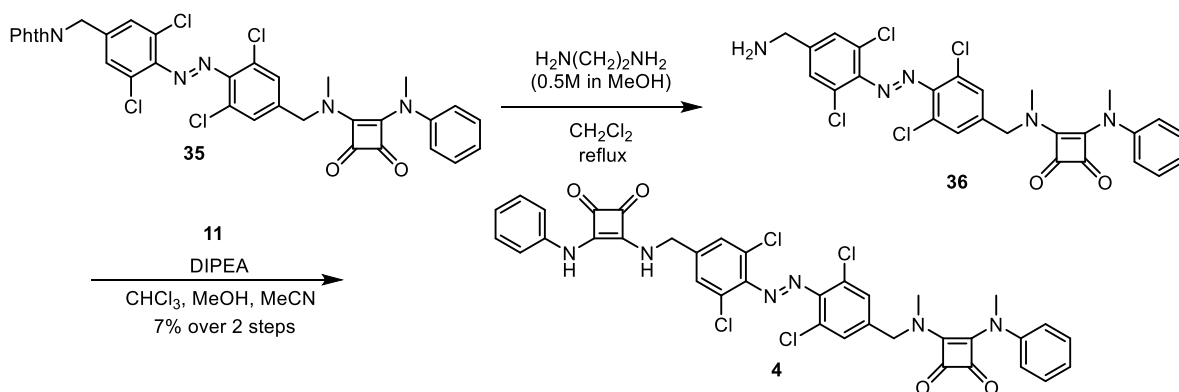
Monosquaramide 33. To a stirred solution of **S10** (100 mg, 0.70 mmol, 1 eq) in methanol (1 mL) was added N-methylaniline **S11** (68 μ L, 0.7 mmol, 1 eq) and the mixture was allowed to stir at room temperature for 90 hours. The reaction was concentrated and purified by silica gel flash chromatography (6 % MeCN in CH₂Cl₂) to afford the title compound as a white solid (75 mg, 0.345 mmol, 49%). ¹H NMR (400 MHz, CDCl₃) δ 7.46 – 7.38 (m, 2H), 7.33 – 7.27 (m, 1H), 7.20 – 7.13 (m, 2H), 4.52 – 4.19 (br s, 3H), 3.73 (s, 3H). ¹³C NMR (126 MHz, CDCl₃) δ 189.00, 184.58, 177.99, 170.78, 141.56, 129.16, 127.17, 123.14, 60.75, 39.39. HRMS-ESI (m/z) Calculated for C₁₂H₁₁NO₃ [M+H]⁻, 218.0812; found 218.0810



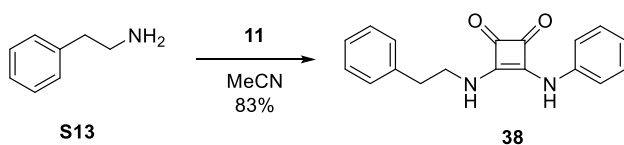
Squaramide 34. **32** (580 mg, 1.14 mmol) and **33** (272 mg, 1.26 mmol, 1.1 eq) were dissolved in MeOH (10 mL) and MeCN (5 mL). DIPEA (437 μ L, 2.51 mmol, 2.2 eq) was added. The reaction was stirred at 50 °C for 6 hours. The reaction was concentrated, then purified by silica gel flash chromatography (5% to 8% MeCN in CH_2Cl_2) to afford the title compound as an orange solid as a mixture of isomers (270 mg, 0.49 mmol, 43%). **E-34:** ^1H NMR (400 MHz, CDCl_3) δ 7.92 – 7.86 (m, 2H), 7.78 – 7.73 (m, 2H), 7.52 (s, 2H), 7.50 – 7.45 (m, 2H), 7.37 – 7.30 (m, 1H), 7.28 (s, 2H), 7.15 – 7.10 (m, 2H), 4.84 (s, 2H), 4.80 (d, J = 6.6 Hz, 2H), 4.29 (t, J = 6.5 Hz, 1H), 3.80 (s, 3H). ^{13}C NMR (126 MHz, CDCl_3) δ 184.52, 184.29, 167.88, 166.79, 165.86, 147.19, 147.05, 141.48, 140.27, 138.78, 134.52, 132.02, 130.08, 129.66, 128.44, 128.03, 127.84, 127.56, 123.82, 123.13, 47.14, 40.48, 39.17. HRMS-ESI (m/z) Calculated for $\text{C}_{33}\text{H}_{21}\text{Cl}_4\text{N}_5\text{O}_4$ $[\text{M}+\text{H}]^+$, 692.0420; found 692.0416



Squaramide 35. **34** (270 mg, 390 μ mol) was dissolved in MeCN (5 mL). Cs_2CO_3 (950 mg, 2.29 mmol, 7.5 eq) and MeI (364 μ L, 5.84 mmol, 15 eq) were stirred vigorously for 16 h at rt. The reaction was concentrated, then diluted in CH_2Cl_2 and washed with water to remove salts. The organic layer was concentrated and purified by silica gel flash chromatography (7% Acetone in 50:50 CH_2Cl_2 :PhMe) to afford the title compound as an orange solid as a mixture of isomers (236 mg, 333 μ mol, 86%). **E-35:** ^1H NMR (400 MHz, CDCl_3) δ 7.92 – 7.86 (m, 2H), 7.79 – 7.73 (m, 2H), 7.54 (s, 2H), 7.39 (t, J = 7.7 Hz, 2H), 7.27 (s, 2H), 7.21 (t, J = 7.6 Hz, 1H), 7.12 – 7.07 (m, 2H), 4.85 (s, 2H), 4.71 (s, 2H), 3.80 (s, 3H), 2.30 (s, 3H). ^{13}C NMR (126 MHz, CDCl_3) δ 186.00, 185.29, 170.45, 167.87, 166.88, 147.27, 147.07, 144.70, 138.81, 138.32, 134.52, 132.02, 130.13, 129.67, 128.76, 128.00, 127.86, 126.51, 123.83, 122.03, 54.72, 40.48, 39.49, 38.79. HRMS-ESI (m/z) Calculated for $\text{C}_{34}\text{H}_{23}\text{Cl}_4\text{N}_5\text{O}_4$ $[\text{M}+\text{H}]^+$, 706.0577; found 706.0577



Control compound 4. Phthalimide **35** (80 mg, 113 μmol) was dissolved in CH_2Cl_2 (4 mL). Ethylenediamine (0.5M in MeOH) (1.36 mL, 680 μmol , 6 eq) was added, and the reaction was stirred at 43 degrees bath temperature for 48 hours. The reaction was concentrated in vacuo (do not exceed 40 $^\circ\text{C}$). The orange residue was purified by flash-column chromatography (5% MeOH in CH_2Cl_2) to afford 12 mg (20.8 μmol) of intermediate amine **36**. ^1H NMR (400 MHz, CDCl_3) δ 7.48 – 7.43 (s, 2H), 7.42 – 7.37 (m, 2H), 7.29 (s, 2H), 7.24 – 7.19 (m, 1H), 7.12 – 7.08 (m, 2H), 4.72 (s, 2H), 3.93 (s, 2H), 3.82 (s, 3H), 2.31 (s, 3H). The residue was immediately dissolved in 1:1 MeOH/ CHCl_3 (0.5 mL) and DIPEA (7 μL , 41.6 μmol , 2 eq) was added. Monosquaramide **11** (4.22 mg, 20.8 μmol , 1 eq) in MeCN (0.5 mL) was added, and the reaction was stirred at 55 $^\circ\text{C}$ for 16 hours. The reaction was cooled to rt and the solid precipitate was filtered and washed sequentially with MeOH and MeCN, then collected and dried under high vacuum to afford the title compound as an orange solid (6.2 mg, 7 μmol , 7% over 2 steps). **E-4:** ^1H NMR (400 MHz, DMSO) δ 9.81 (s, 1H), 8.12 (s, 1H), 7.75 (s, 2H), 7.68 (s, 2H), 7.47 – 7.41 (m, 2H), 7.39 – 7.28 (m, 6H), 7.21 – 7.16 (m, 1H), 7.04 (tt, $J = 7.3, 1.2$ Hz, 1H), 4.90 (d, $J = 5.5$ Hz, 2H), 4.78 (s, 2H), 3.68 (s, 3H), 2.24 (s, 3H). ^{13}C NMR (126 MHz, DMSO) δ 186.02, 184.51, 184.01, 180.81, 170.82, 168.80, 166.24, 164.33, 145.68, 145.49, 144.31, 142.74, 140.18, 138.87, 129.40, 129.35, 129.17, 128.85, 126.40, 126.31, 125.37, 122.83, 121.61, 118.23, 53.25, 45.80, 38.33, 38.12. HRMS-ESI (m/z) Calculated for $\text{C}_{36}\text{H}_{26}\text{Cl}_4\text{N}_6\text{O}_4$ [M-H] $^-$, 745.0697; found 745.0687.



Control 38. Phenethylamine (24 μL , 189 μmol , 1.1 eq) was added to **11** (35 mg, 172 μmol , in MeCN), and the reaction was stirred at room temperature for 16 hours. The solid precipitate was filtered and washed sequentially with MeOH and MeCN, then collected and dried under high vacuum to afford the title compound as a white solid (42 mg, 143 μmol , 83 %). ^1H NMR (500 MHz, DMSO) δ 9.63 (s, 1H), 7.64 (s, 1H), 7.40 (d, $J = 8.0$ Hz, 2H), 7.32 (t, $J = 7.6$ Hz, 4H), 7.27 (d, $J = 7.4$ Hz, 2H), 7.23 (t, $J = 7.2$ Hz, 1H), 7.02 (t, $J = 7.3$ Hz, 1H), 3.87 (m, 2H), 2.90 (t, $J = 7.1$ Hz, 2H). ^{13}C NMR (126 MHz, DMSO) δ 184.00, 180.31, 169.14, 163.54, 138.97, 138.38, 129.33, 128.82, 128.45, 126.38, 122.58, 117.97, 44.91, 36.88. HRMS-ESI (m/z) Calculated for $\text{C}_{18}\text{H}_{15}\text{N}_2\text{O}_2$ [M+H] $^+$, 291.1139; found 291.1140.

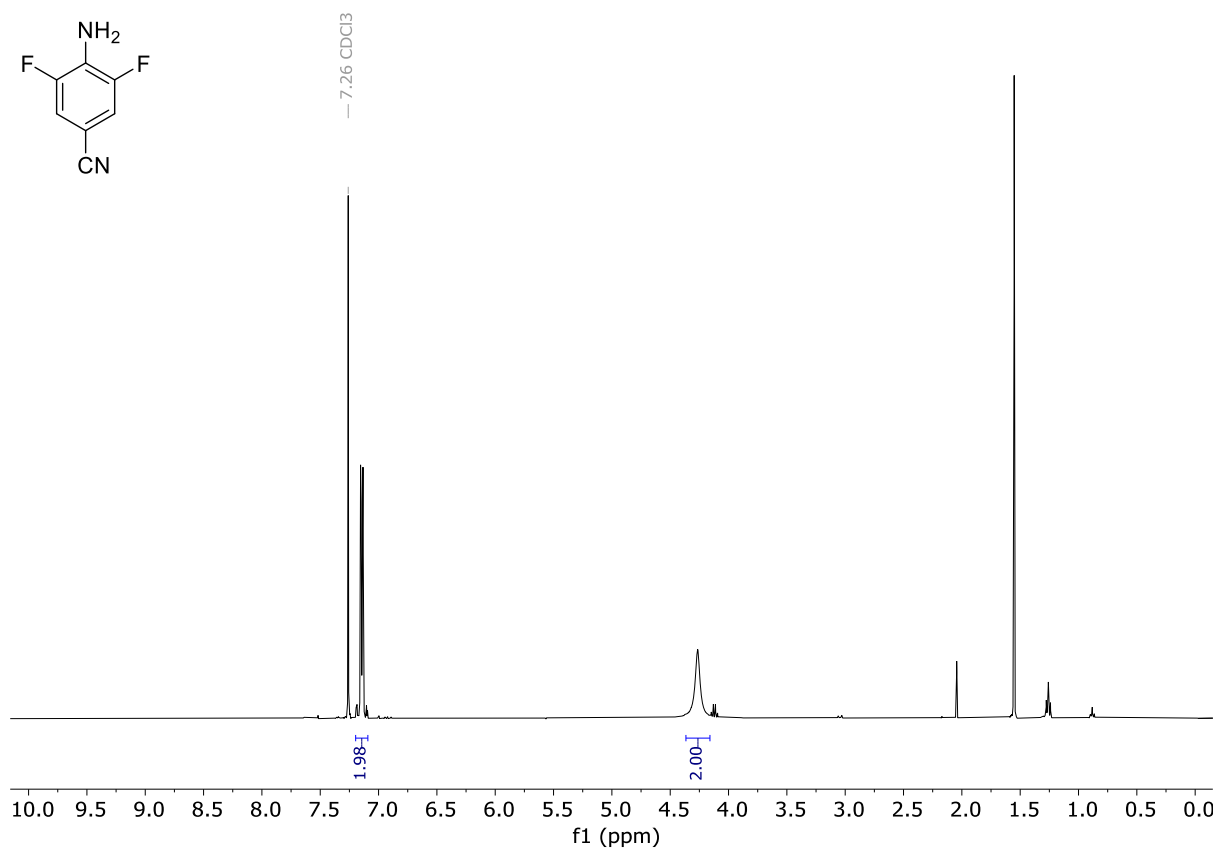


Figure S1. ^1H NMR spectrum of **6** (Chloroform-*d*, 298 K).

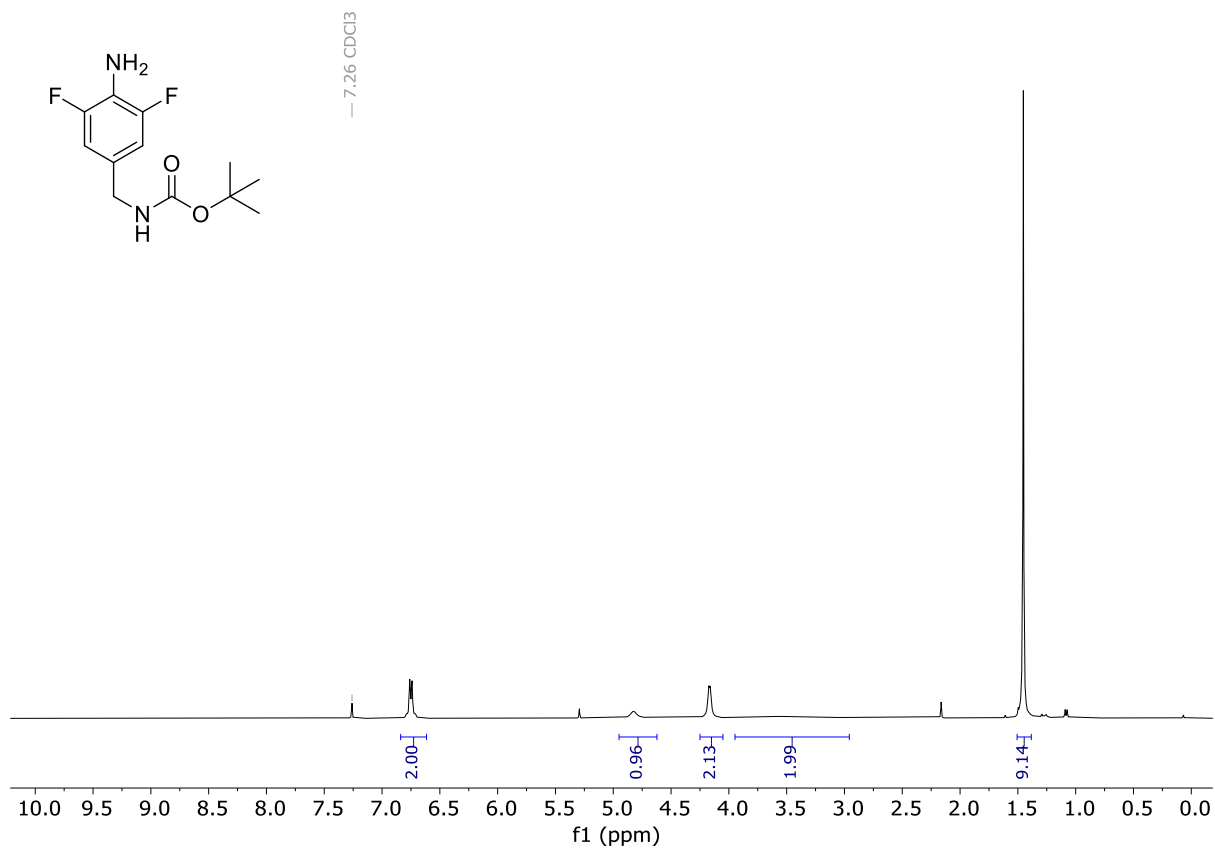


Figure S2. ¹H NMR spectrum of **8** (Chloroform-*d*, 298 K).

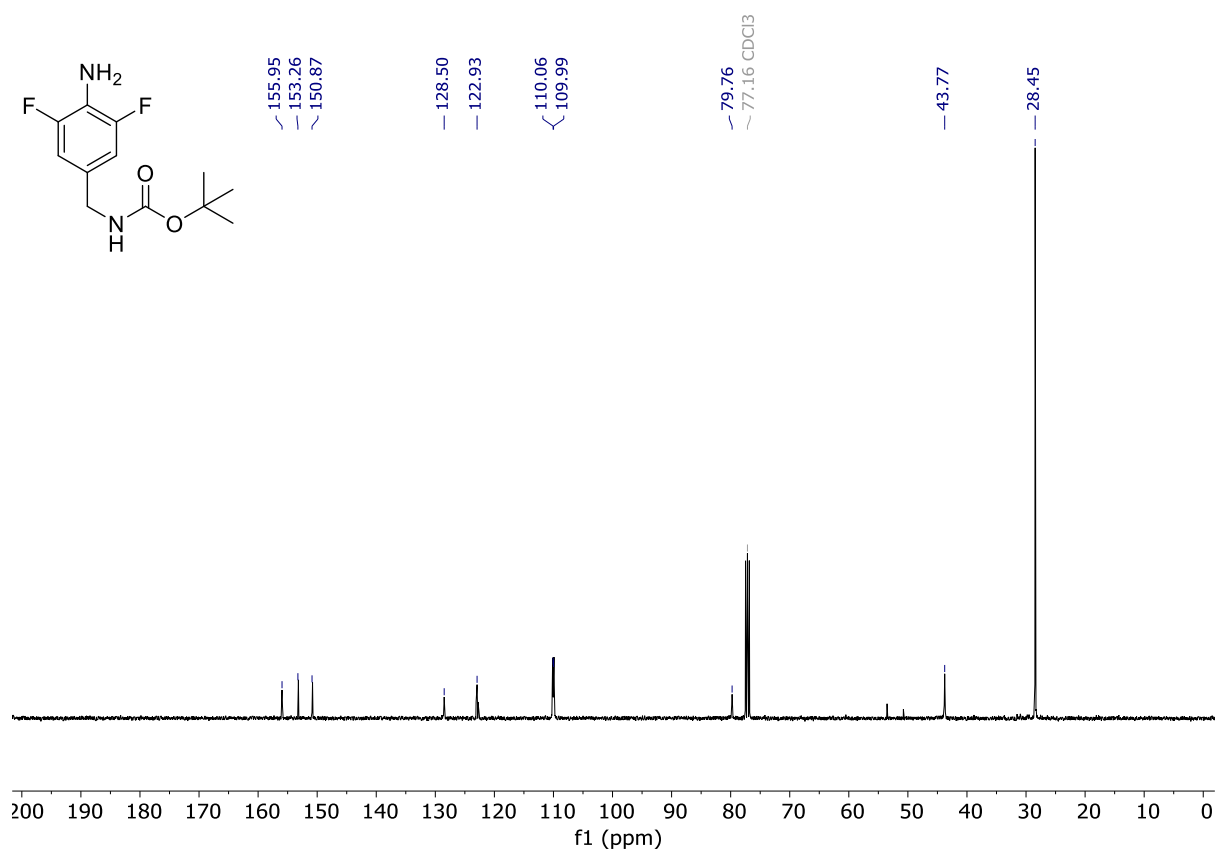


Figure S3. ¹³C NMR spectrum of **8**. (Chloroform-*d*, 298 K).

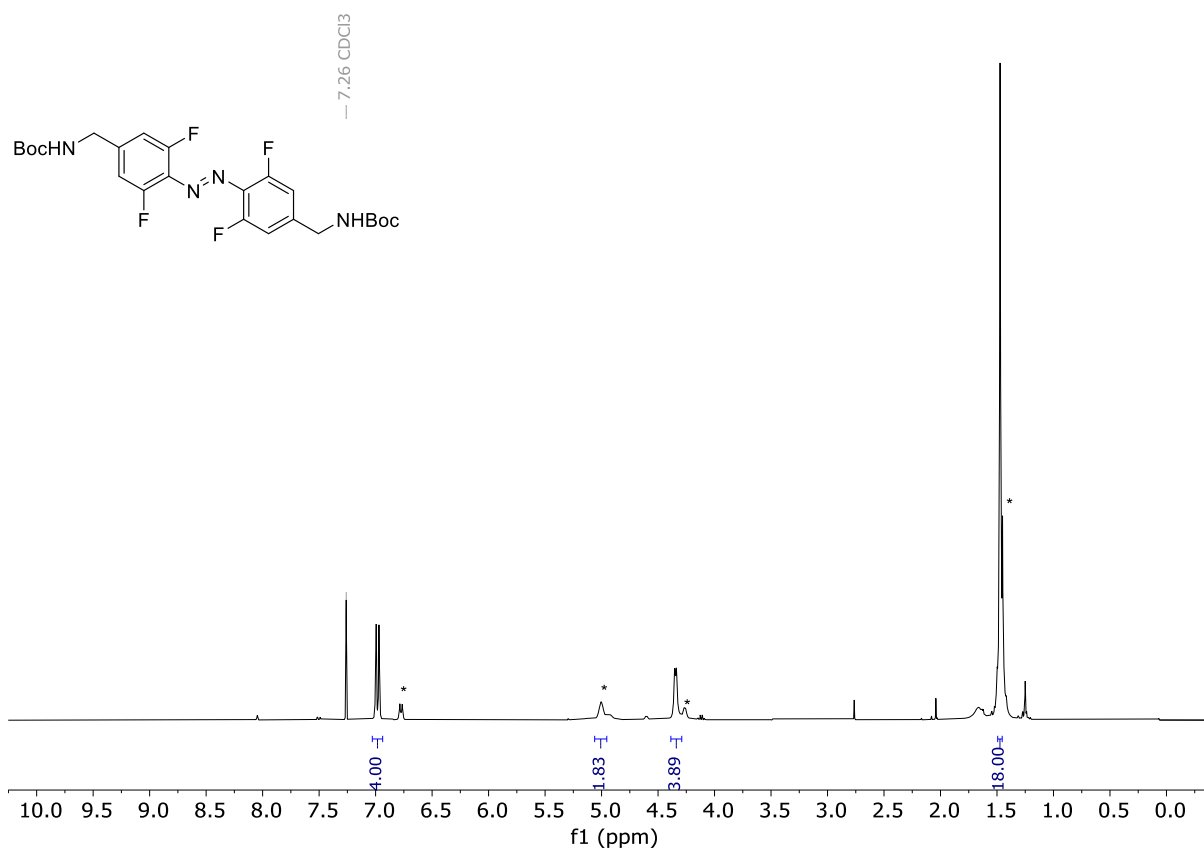


Figure S4. ¹H NMR spectrum of *E*-9 (Chloroform-*d*, 298 K). *Z*-9 signals labelled as *.

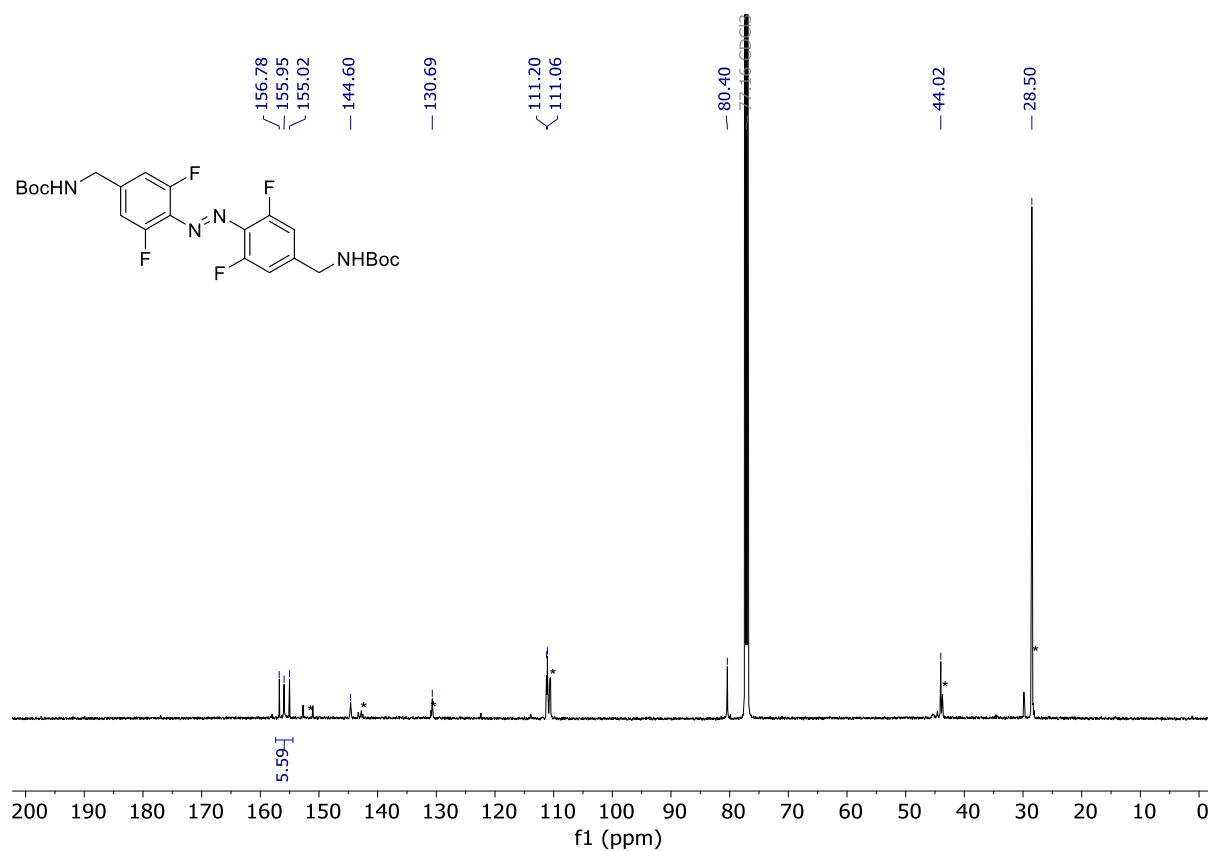


Figure S5. ¹³C NMR spectrum of *E*-9. (Chloroform-*d*, 298 K). *Z*-9 signals labelled as *.

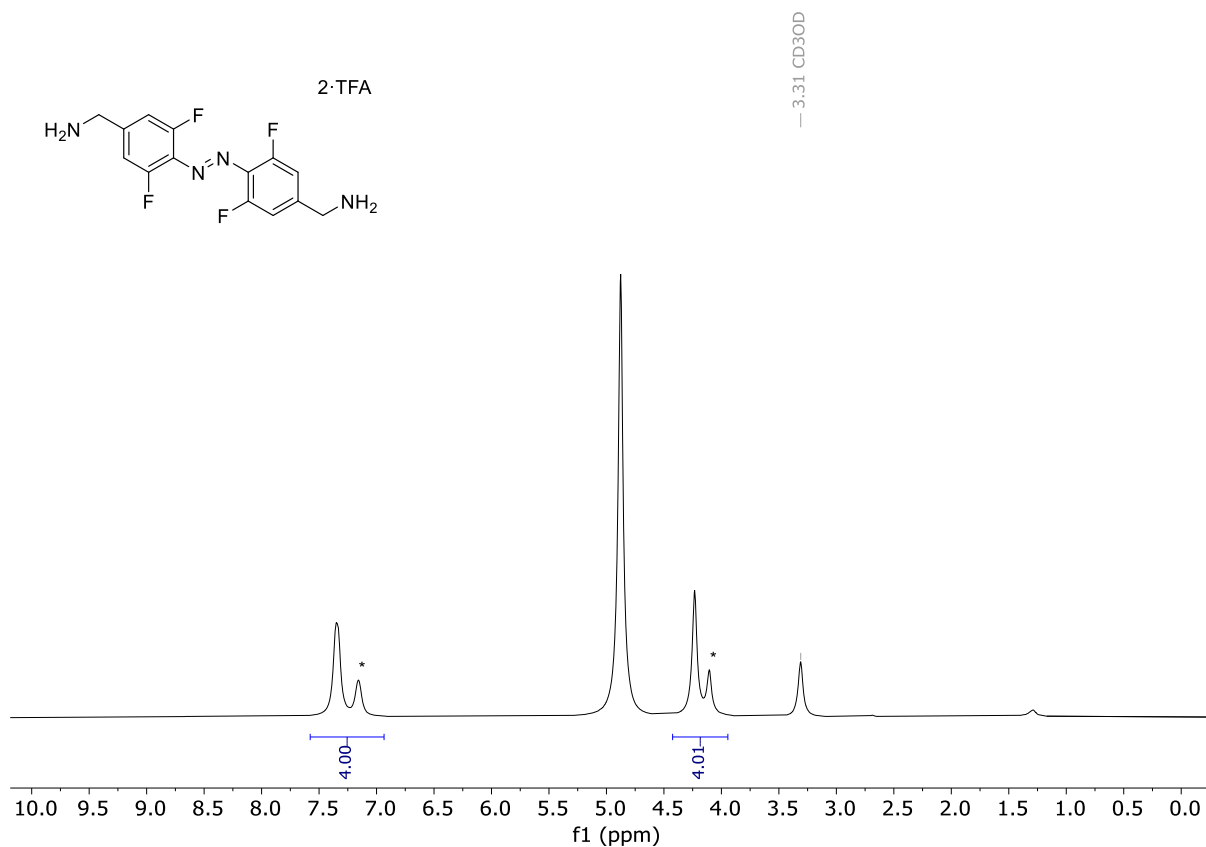


Figure S6. ^1H NMR Spectrum of **10** (Methanol- d_4 , 298 K). **Z-10** signals labelled as *.

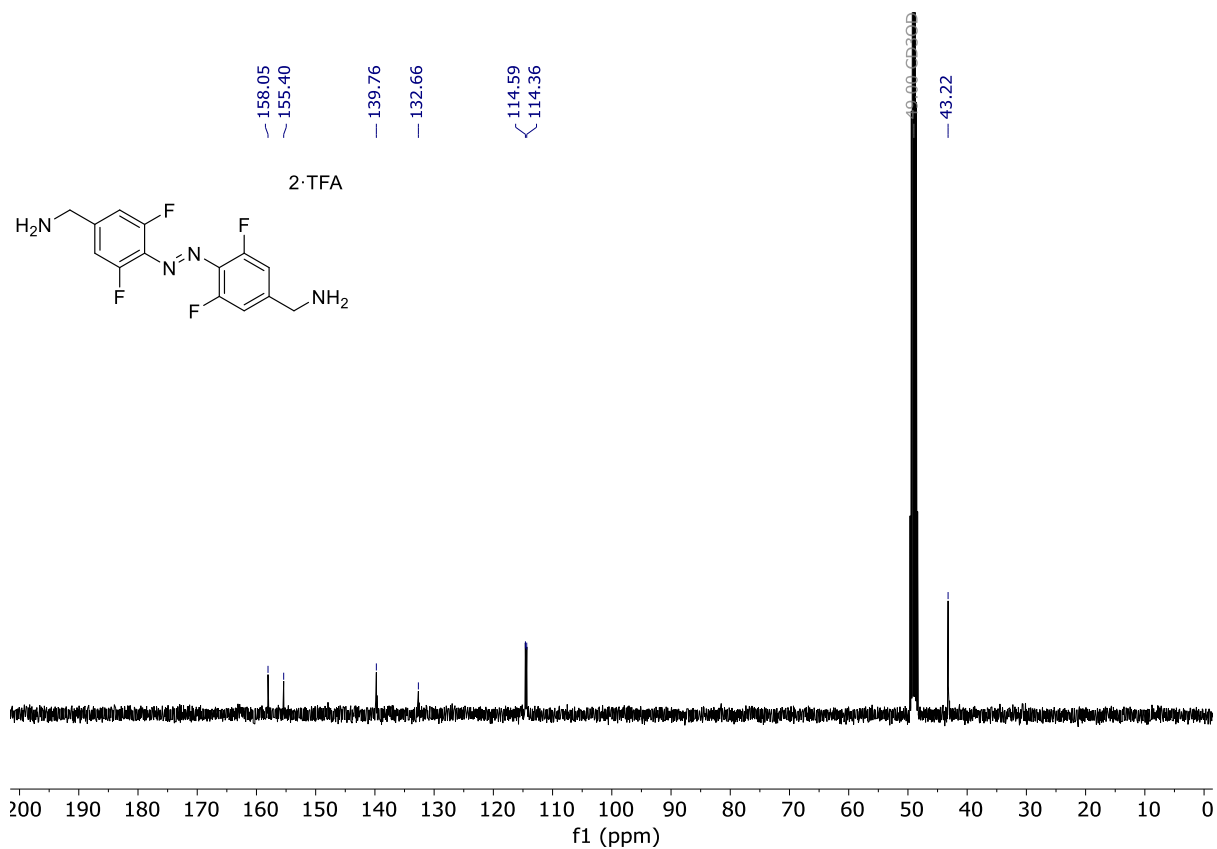


Figure S7. ^{13}C NMR Spectrum of **10**, (Methanol- d_4 , 298 K). **Z-10** signals labelled as *.

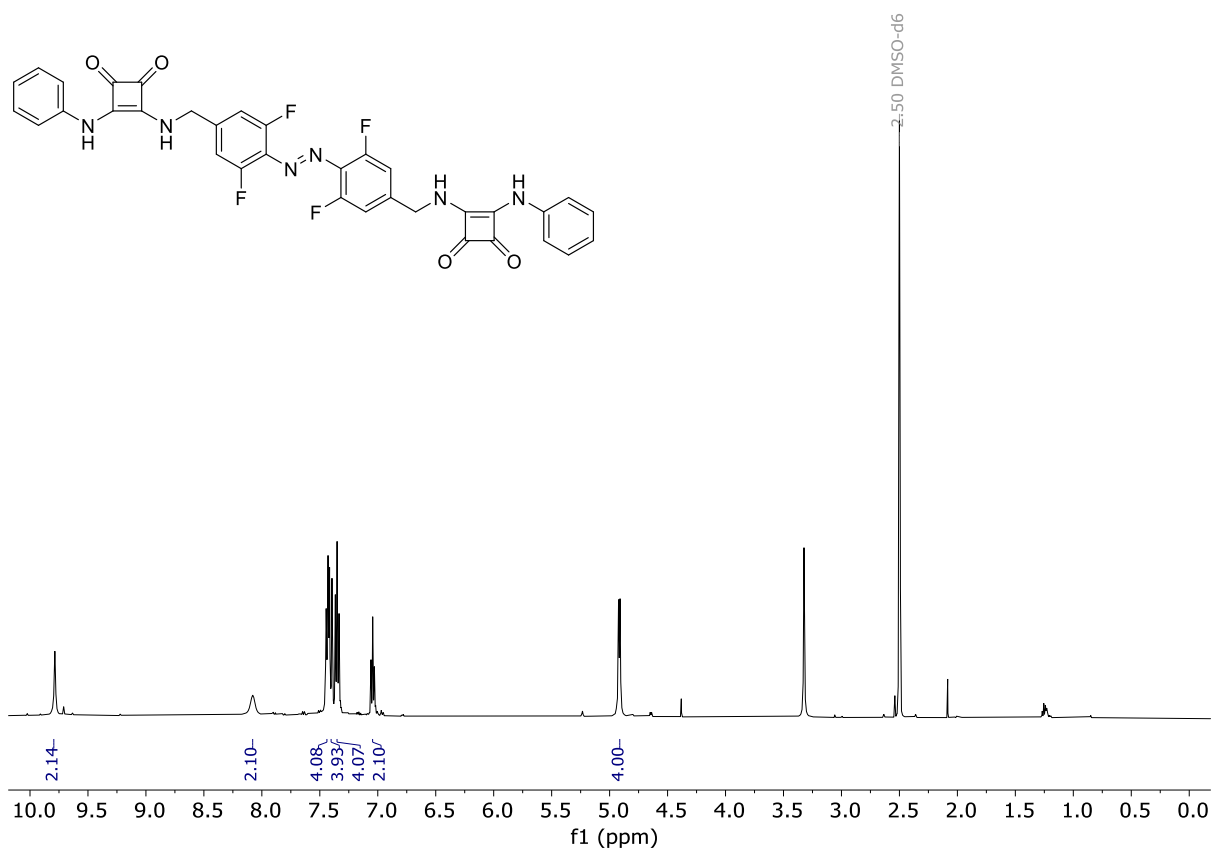


Figure S8. ¹H NMR Spectrum of **1b** (DMSO-d₆, 298 K).

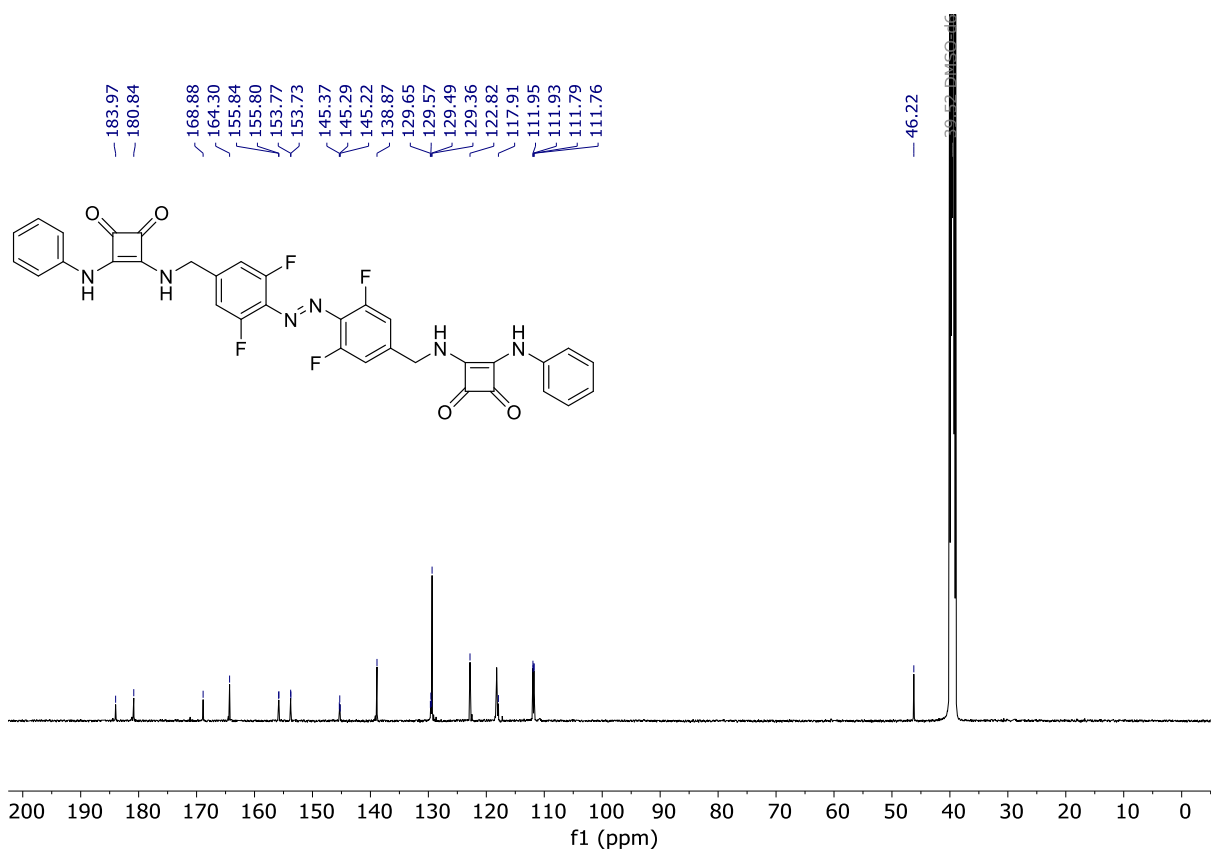


Figure S9. ¹³C NMR Spectrum of **1b** (DMSO-d₆, 298 K).

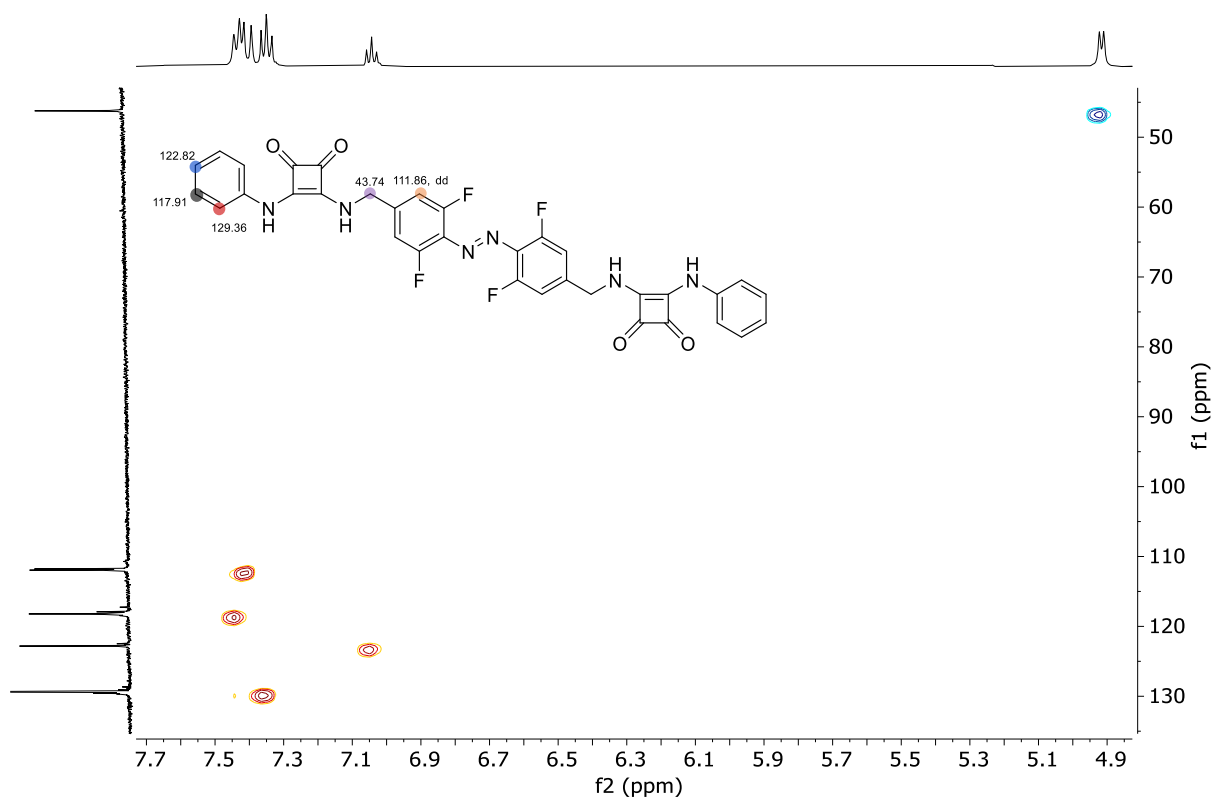


Figure S10. HSQC of **1b**. Key ^1H - ^{13}C correlations highlighted. (DMSO- d_6 , 298 K).

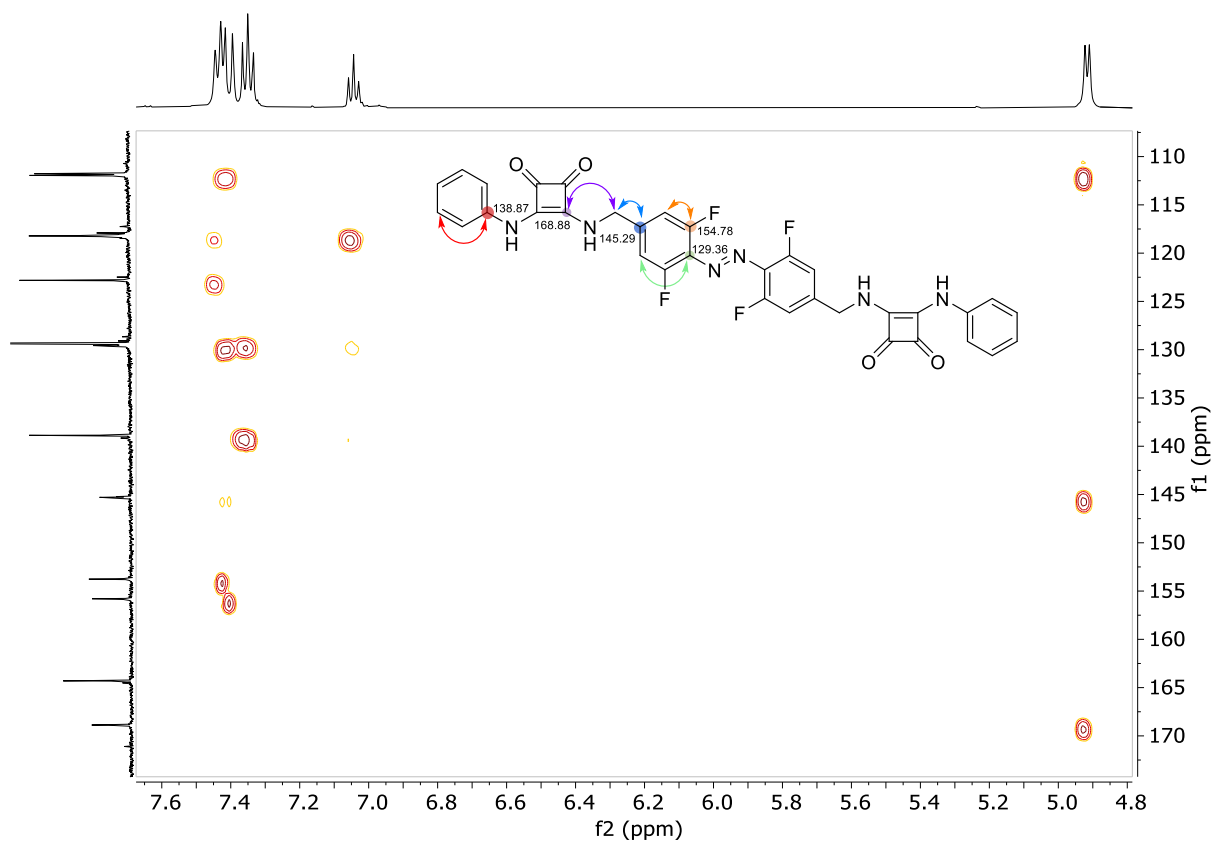


Figure S11. HMBC of **1b**. Key ^1H - ^{13}C correlations highlighted. (DMSO- d_6 , 298 K).

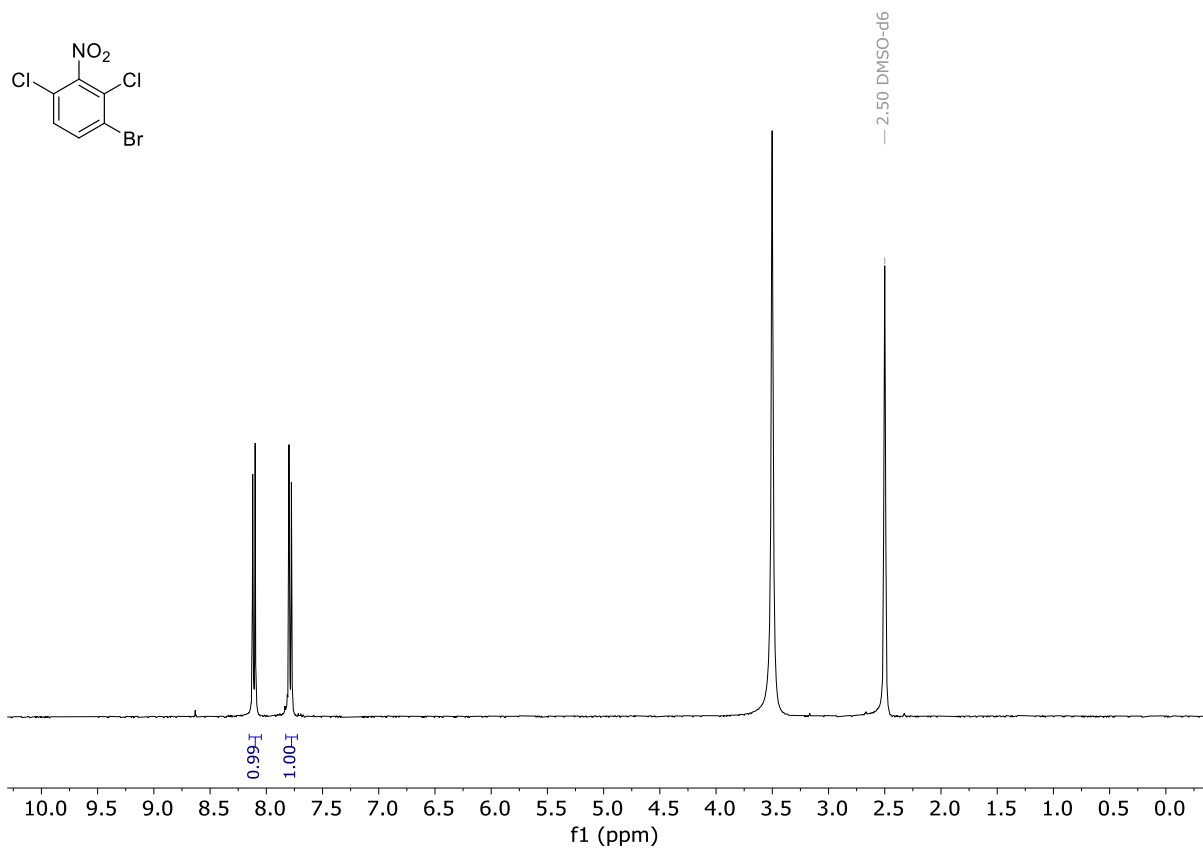


Figure S12. ^1H NMR spectrum of **S2** (DMSO- d_6 , 298 K).

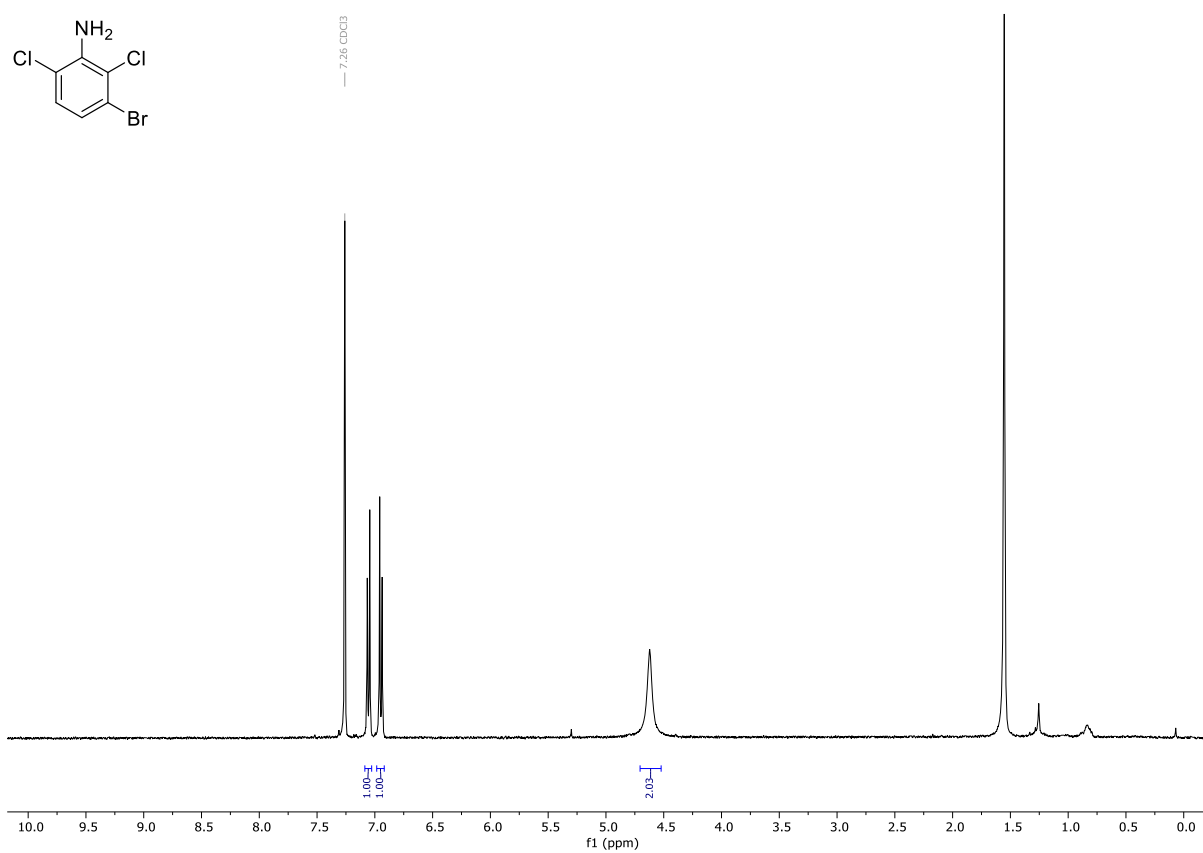


Figure S13. ^1H NMR spectrum of **S3** (Chloroform- d , 298 K).

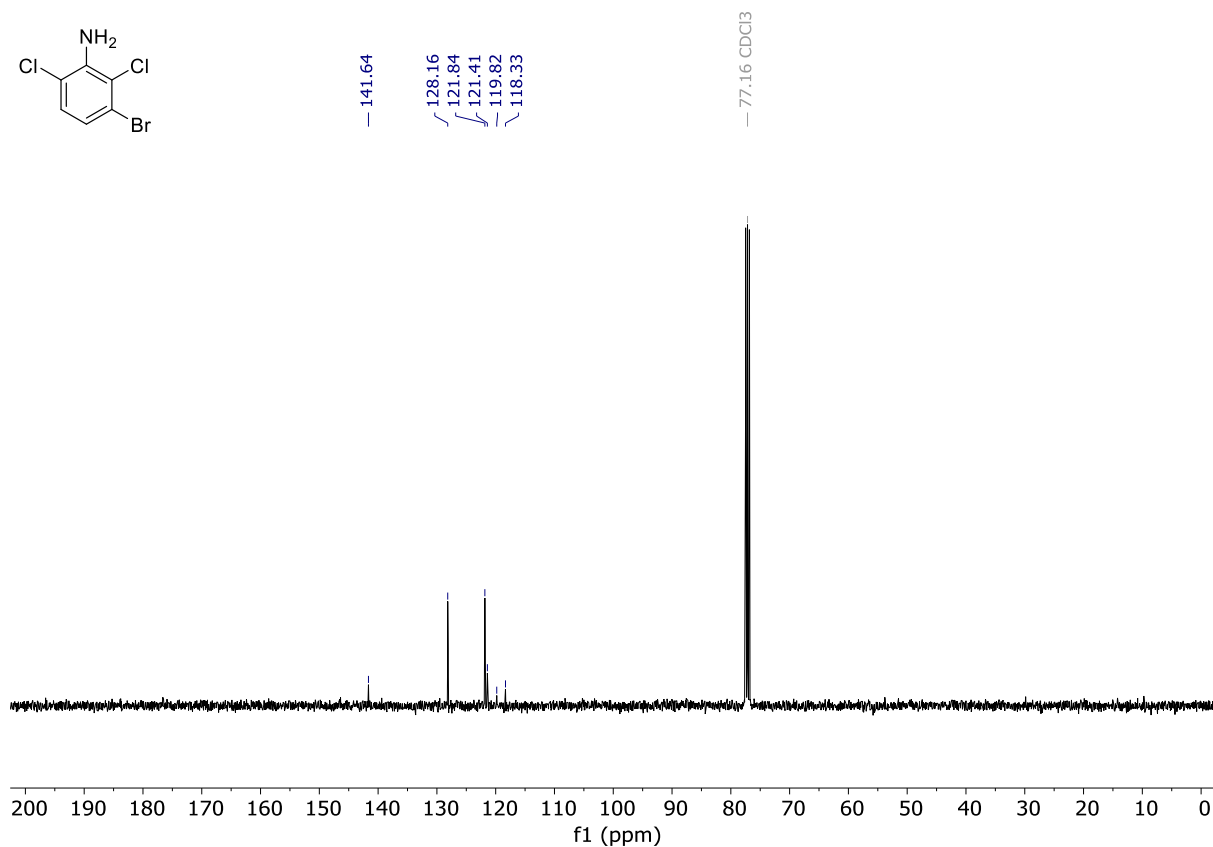


Figure S14. ¹³C NMR spectrum of S3. (Chloroform-*d*, 298 K).

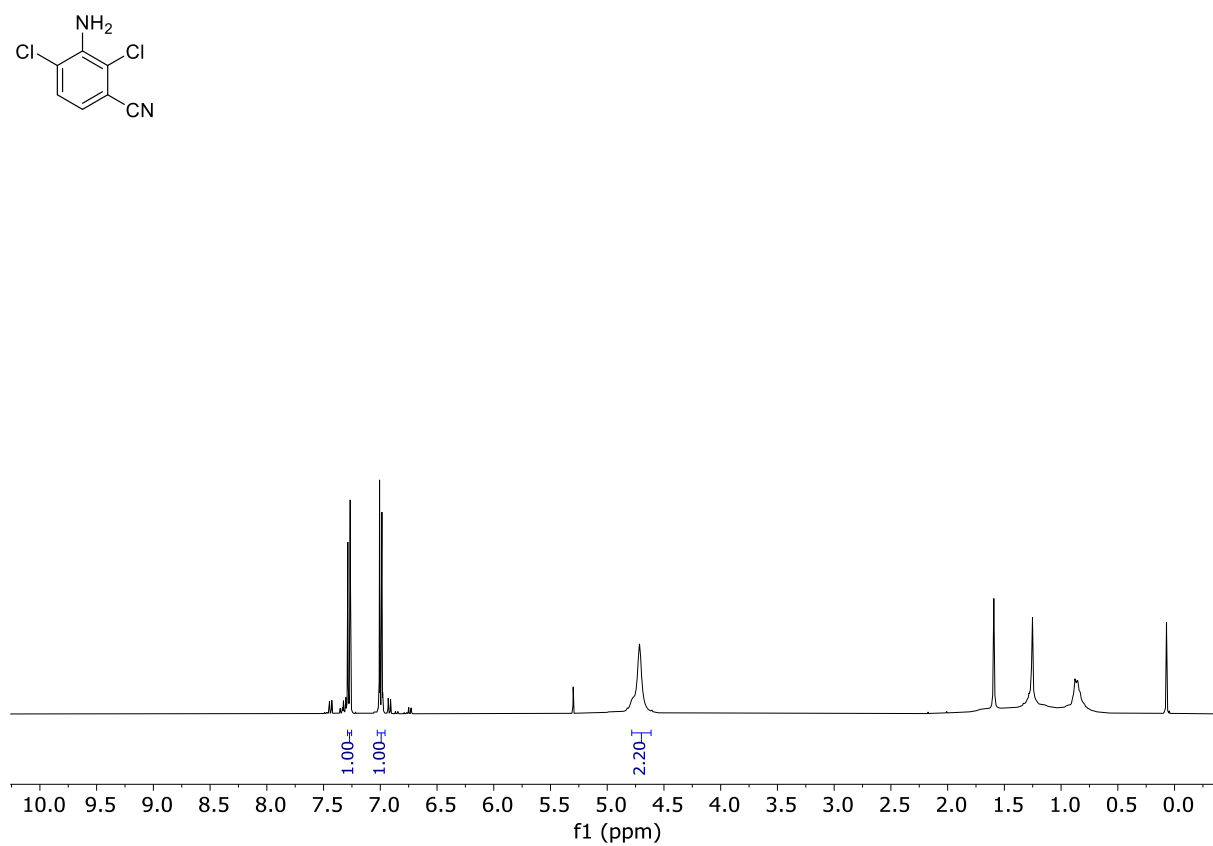


Figure S15. ¹H NMR spectrum of S4 (Chloroform-*d*, 298 K).

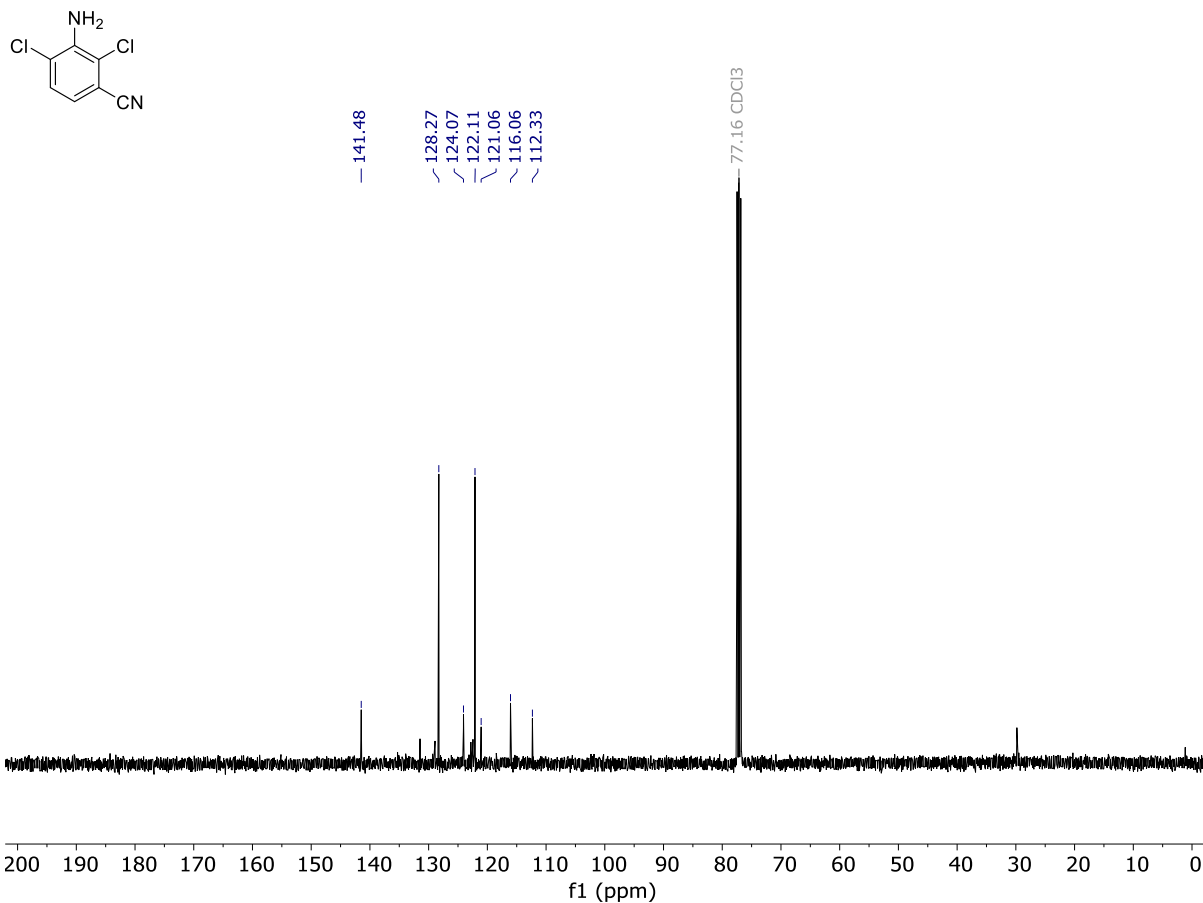


Figure S16. ^{13}C NMR spectrum of **S4**. (Chloroform-*d*, 298 K).

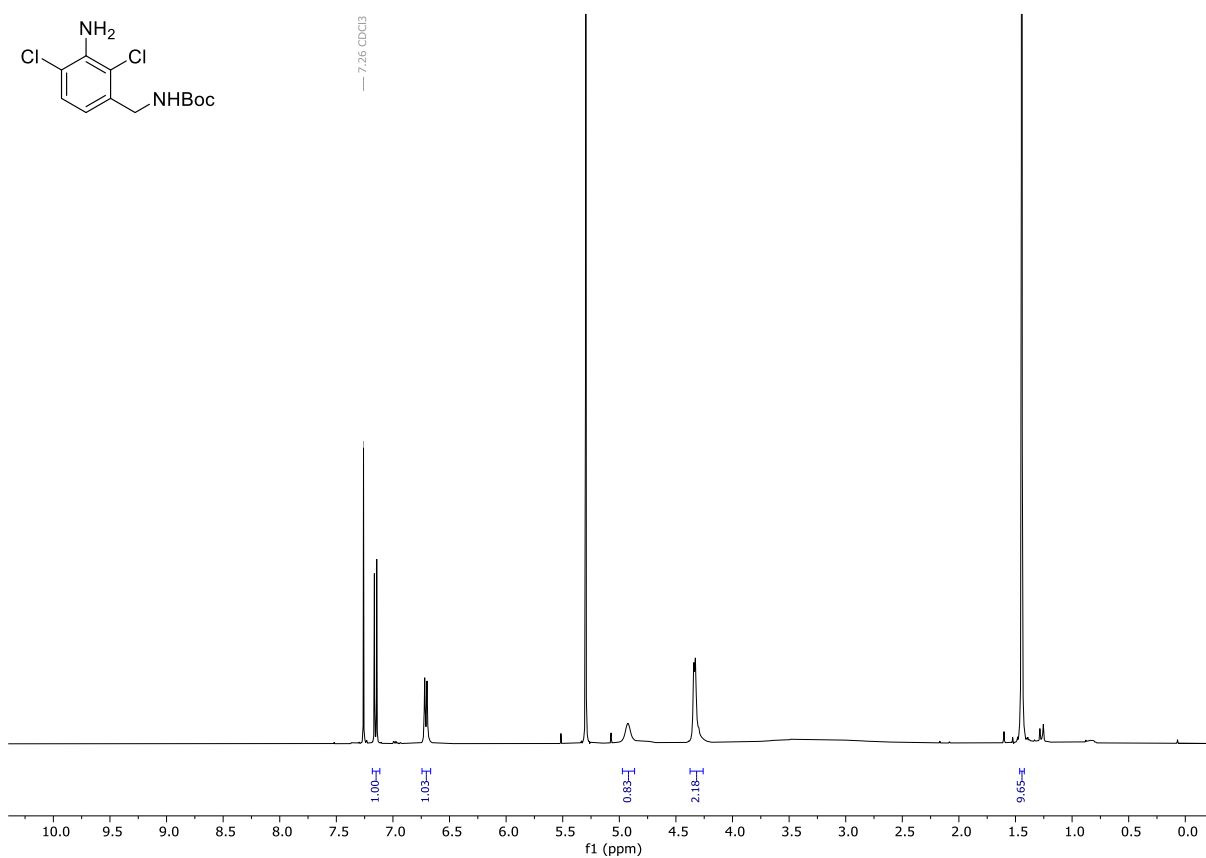


Figure S17. ^1H NMR spectrum of **12**. (Chloroform-*d*, 298 K).

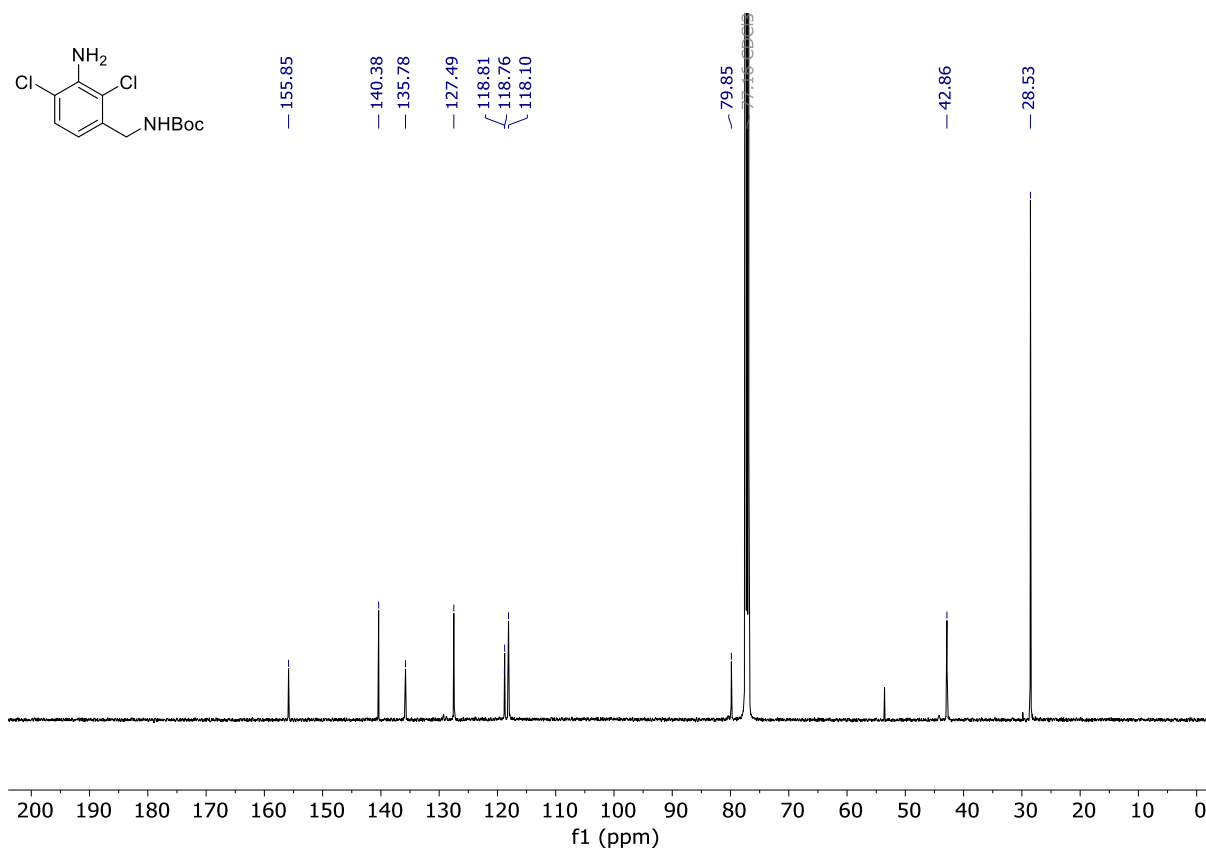


Figure S18. ¹³C NMR spectrum of **12** (Chloroform-*d*, 298 K).

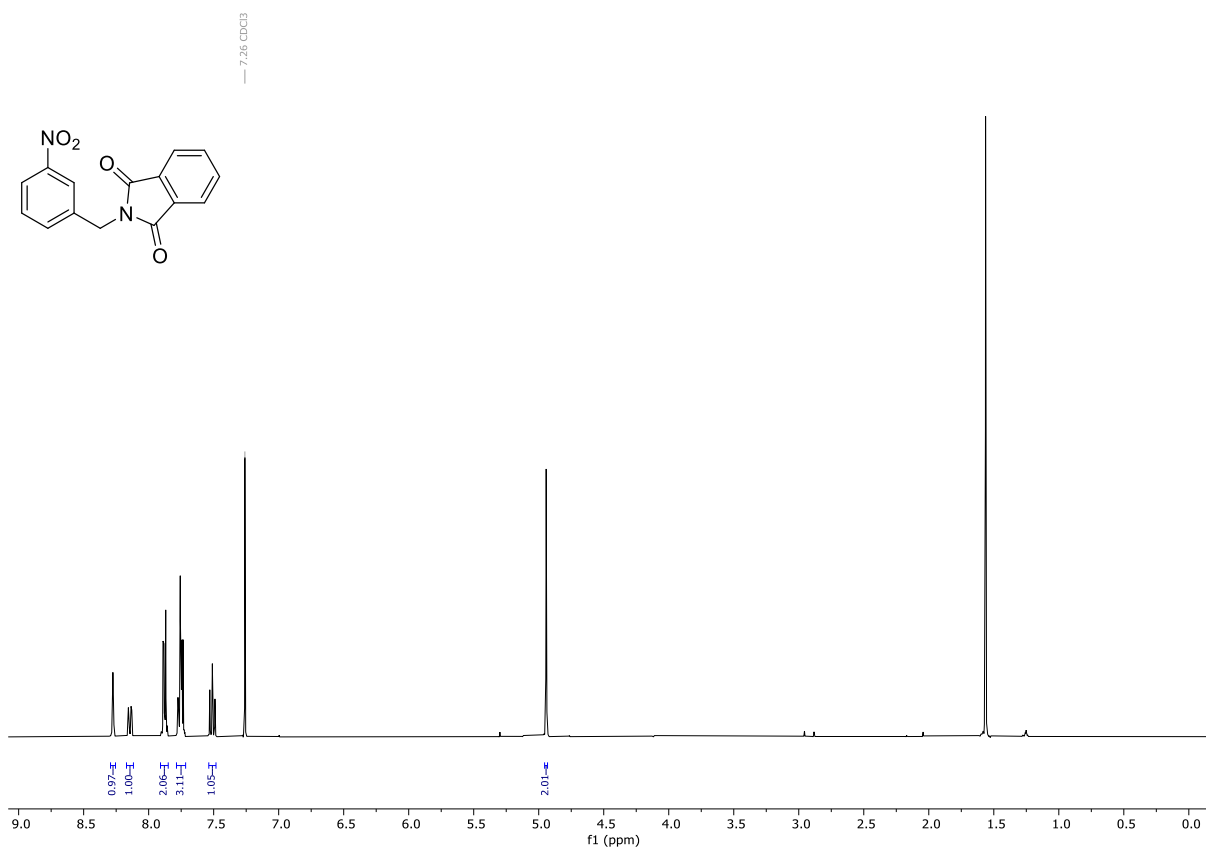


Figure S19. ¹H NMR spectrum of **S7** (Chloroform-*d*, 298 K).

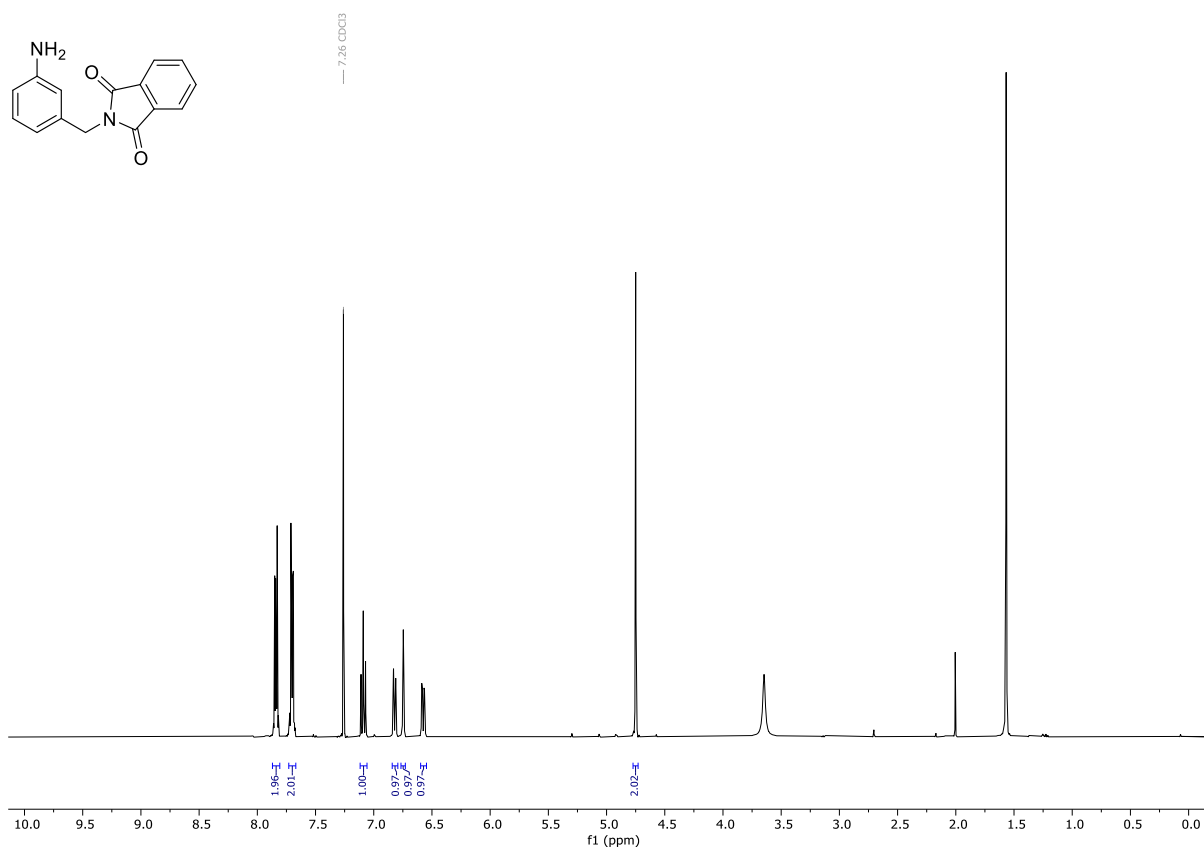


Figure S20. ¹H NMR spectrum of **14** (Chloroform-*d*, 298 K).

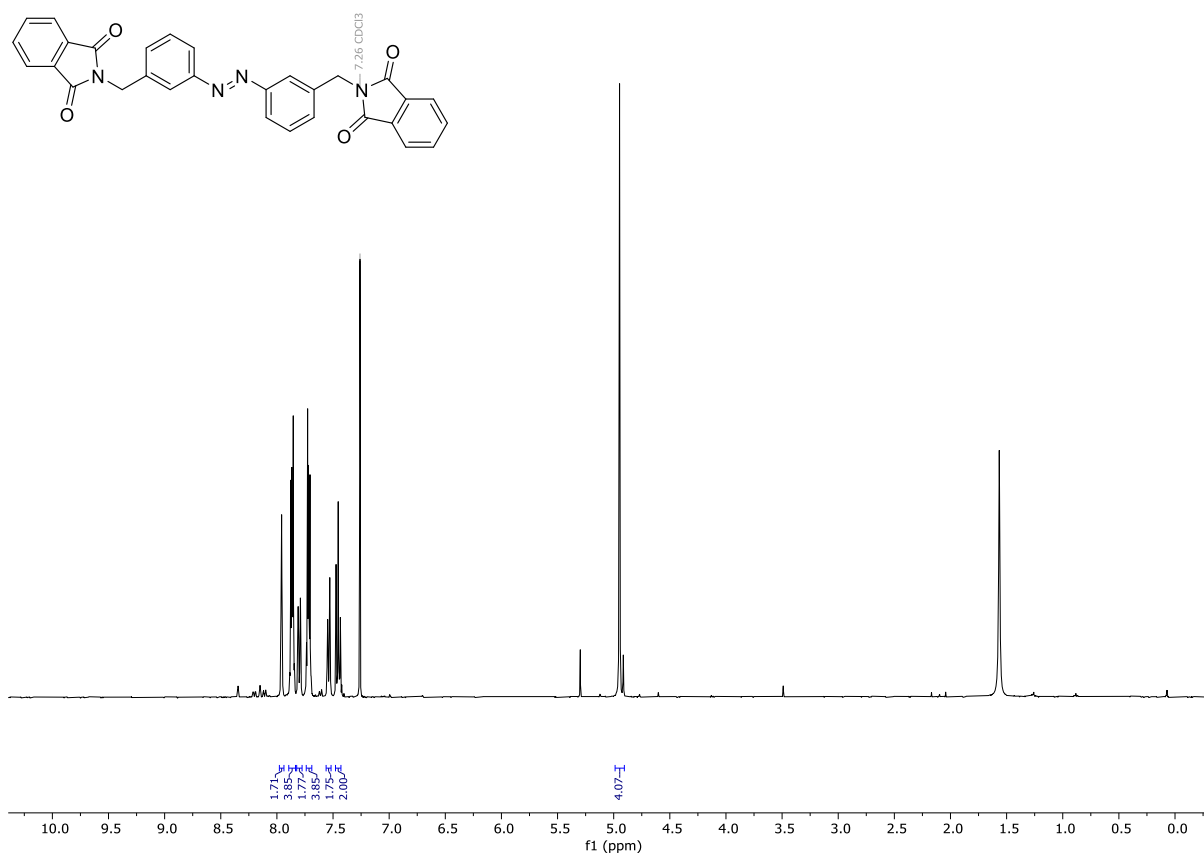


Figure S21. ¹H NMR spectrum of **E-16** (Chloroform-*d*, 298 K).

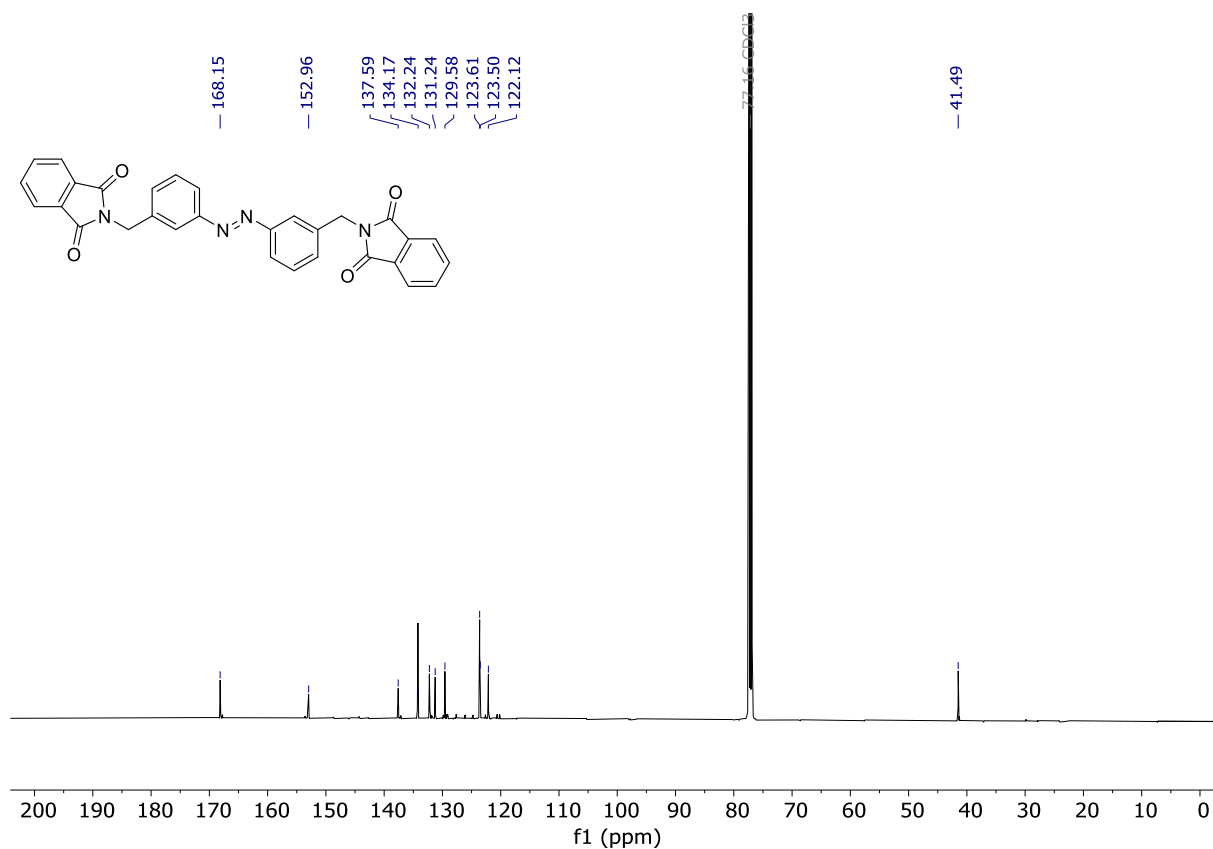


Figure S22. ^{13}C NMR spectrum of *E*-16. (Chloroform-*d*, 298 K).

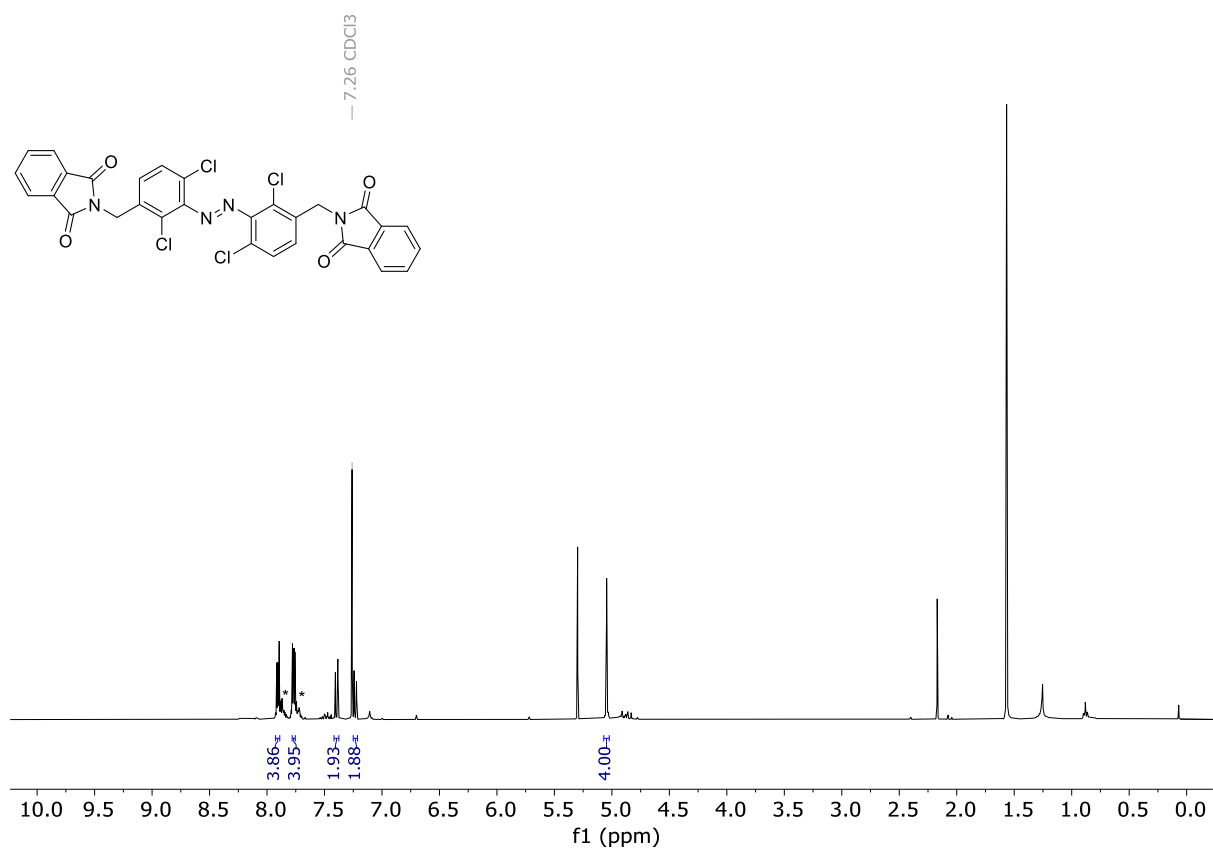


Figure S23. ^1H NMR spectrum of *E*-17 (Chloroform-*d*, 298 K). *Z*-17 signals labelled as *.

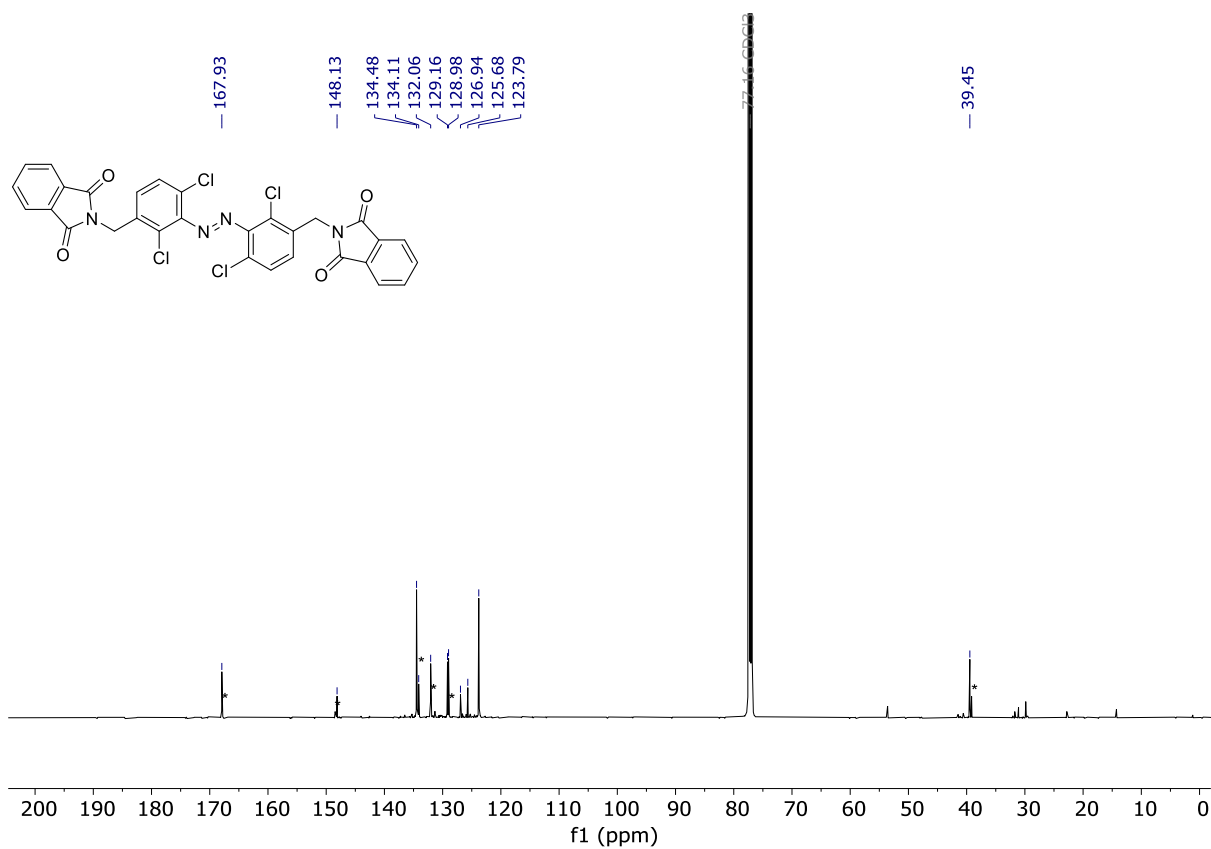


Figure S24. ¹³C NMR spectrum of *E-17*. (Chloroform-*d*, 298 K). *Z-16* signals labelled as *.

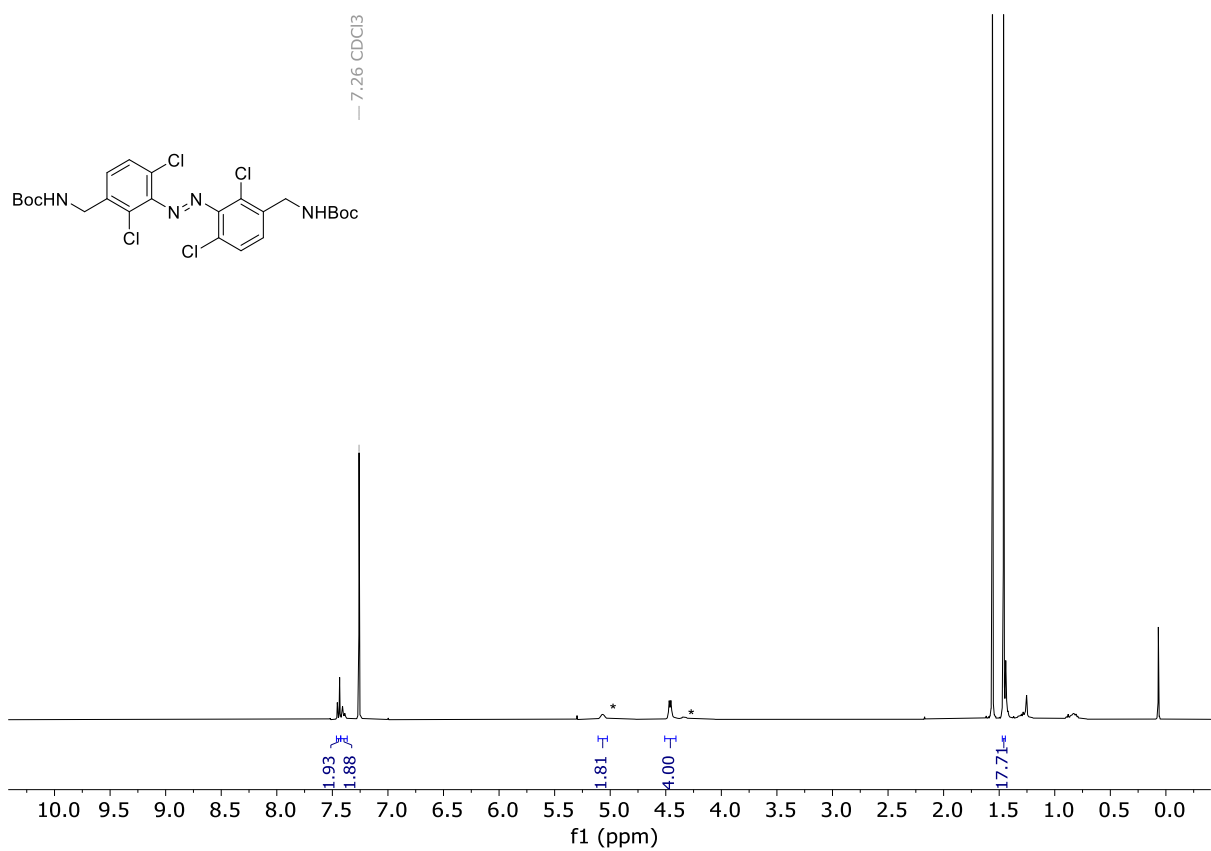


Figure S25. ¹H NMR spectrum of *E-13* (Chloroform-*d*, 298 K). *Z-13* signals labelled as *.

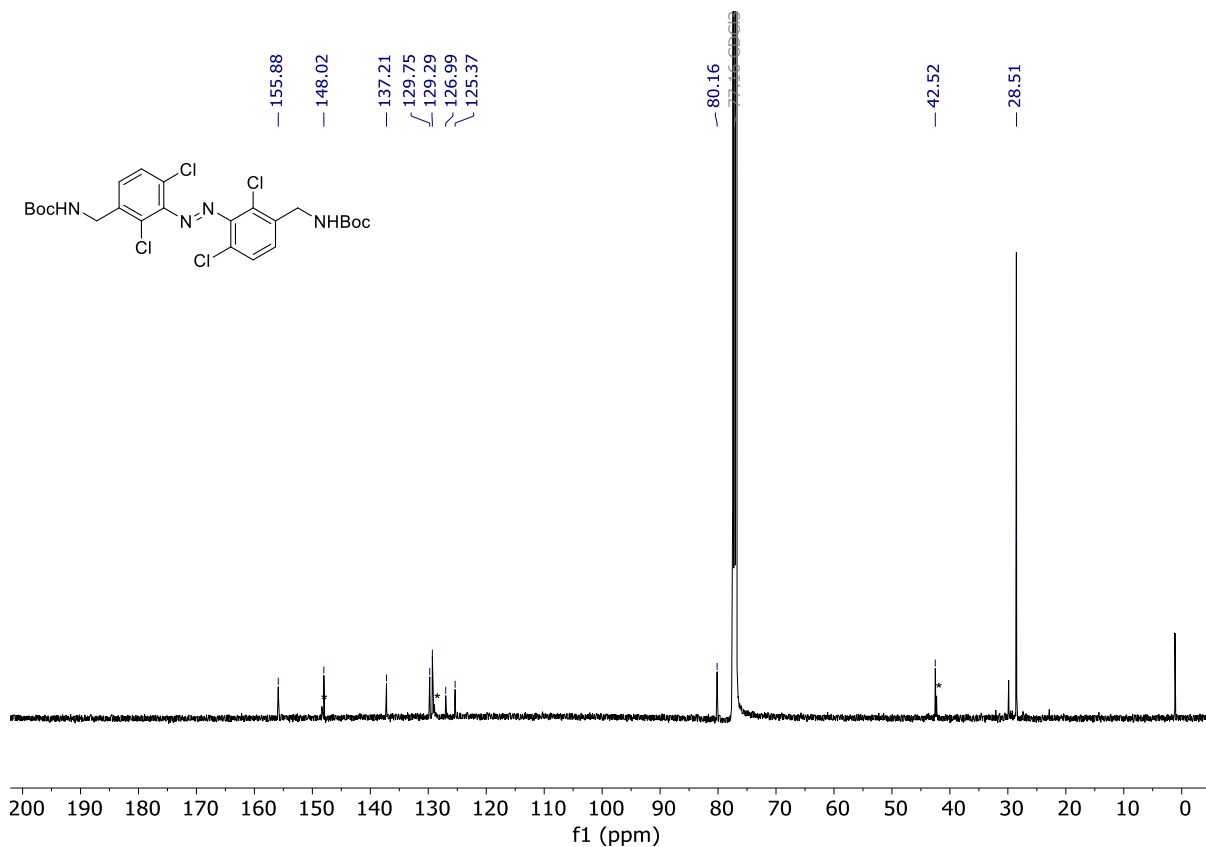


Figure S26. ¹³C NMR spectrum of *E*-13. (Chloroform-*d*, 298 K). *Z*-13 signals labelled as *.

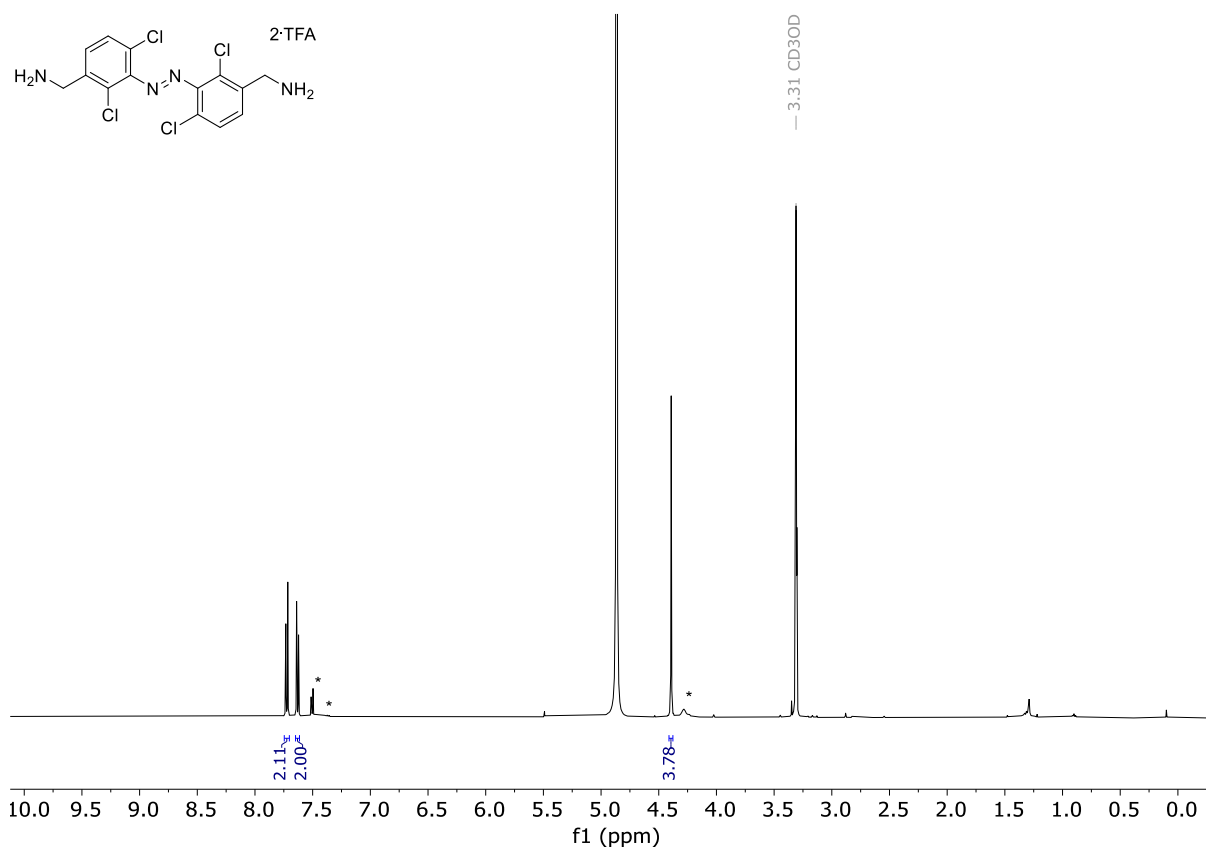


Figure S27. ¹H NMR Spectrum of *E*-18, (Methanol-*d*₄, 298 K). *Z*-18 signals labelled as *.

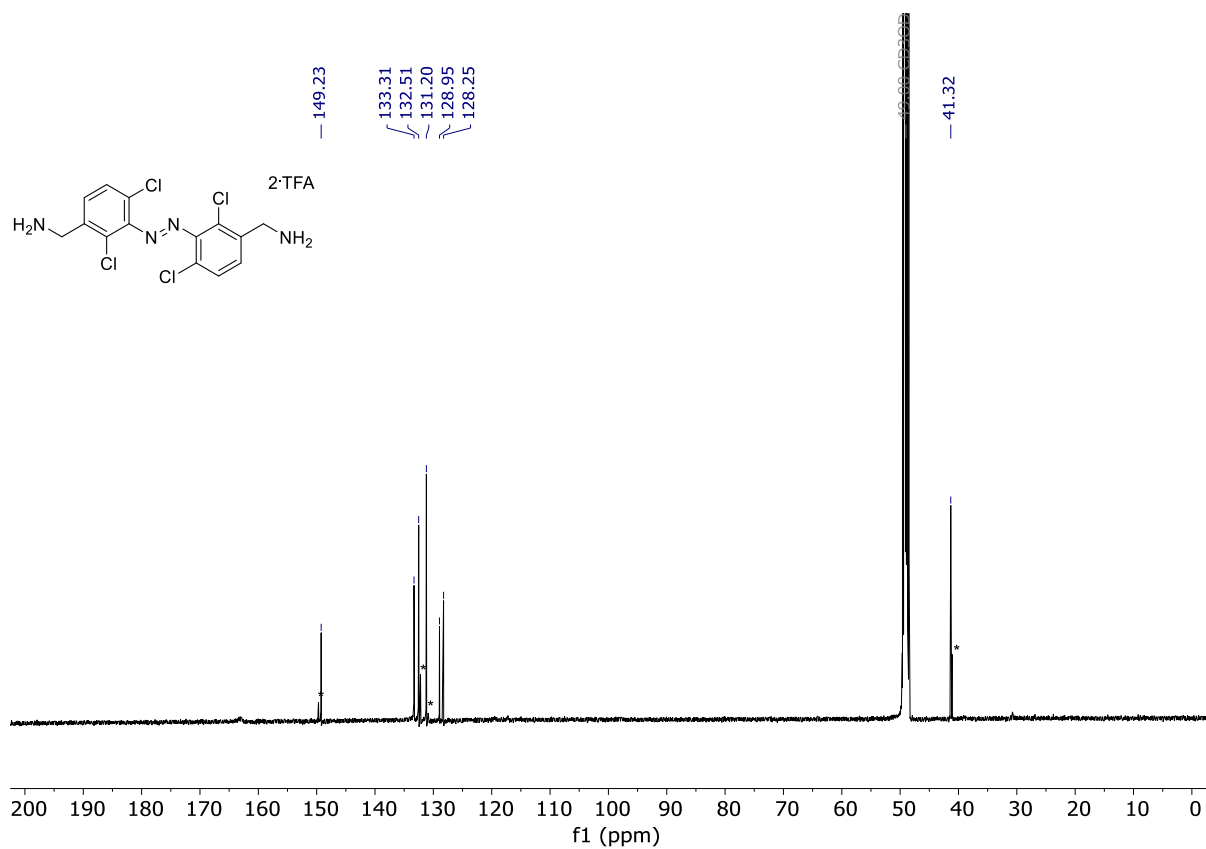


Figure S28. ^{13}C NMR Spectrum of **E-18**, (Methanol- d_4 , 298 K). **Z-18** signals labelled as *.

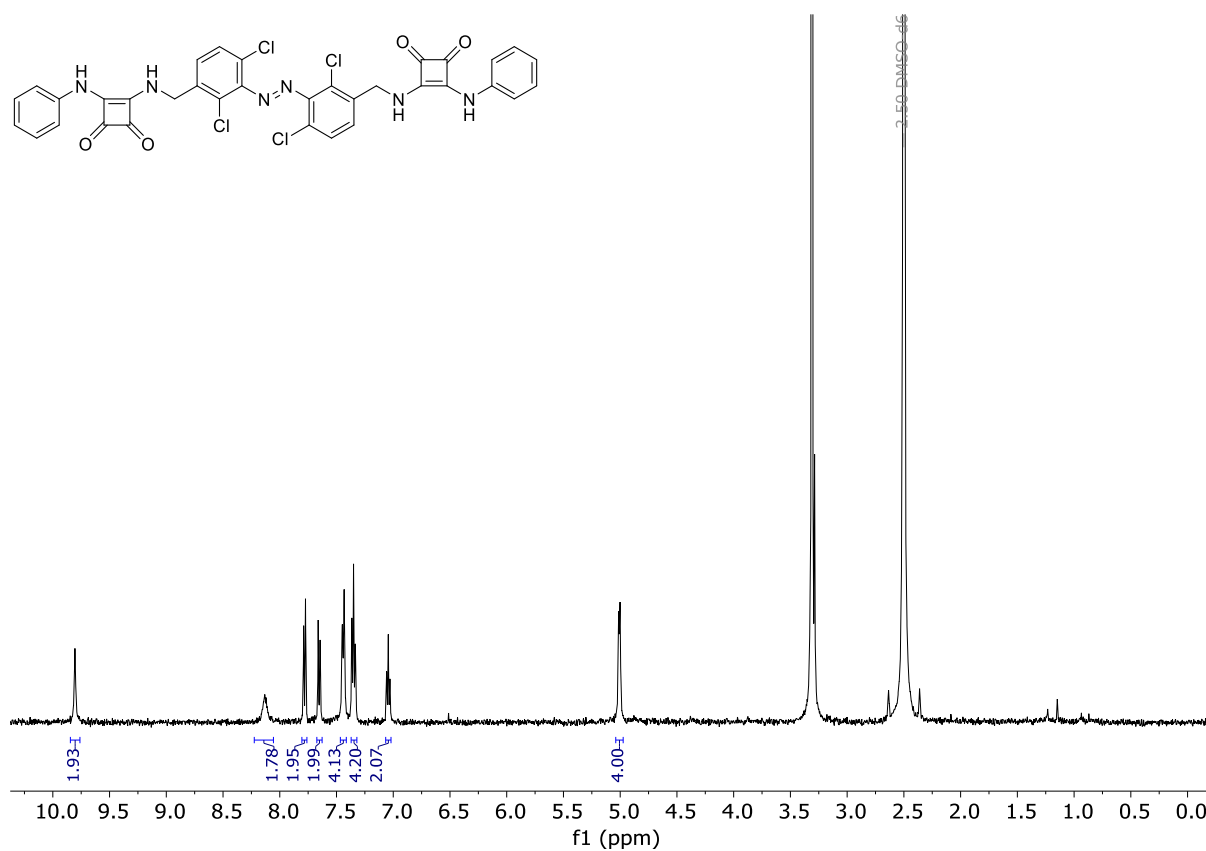


Figure S29. ^1H NMR Spectrum of **E-2**. (DMSO- d_6 , 298 K).

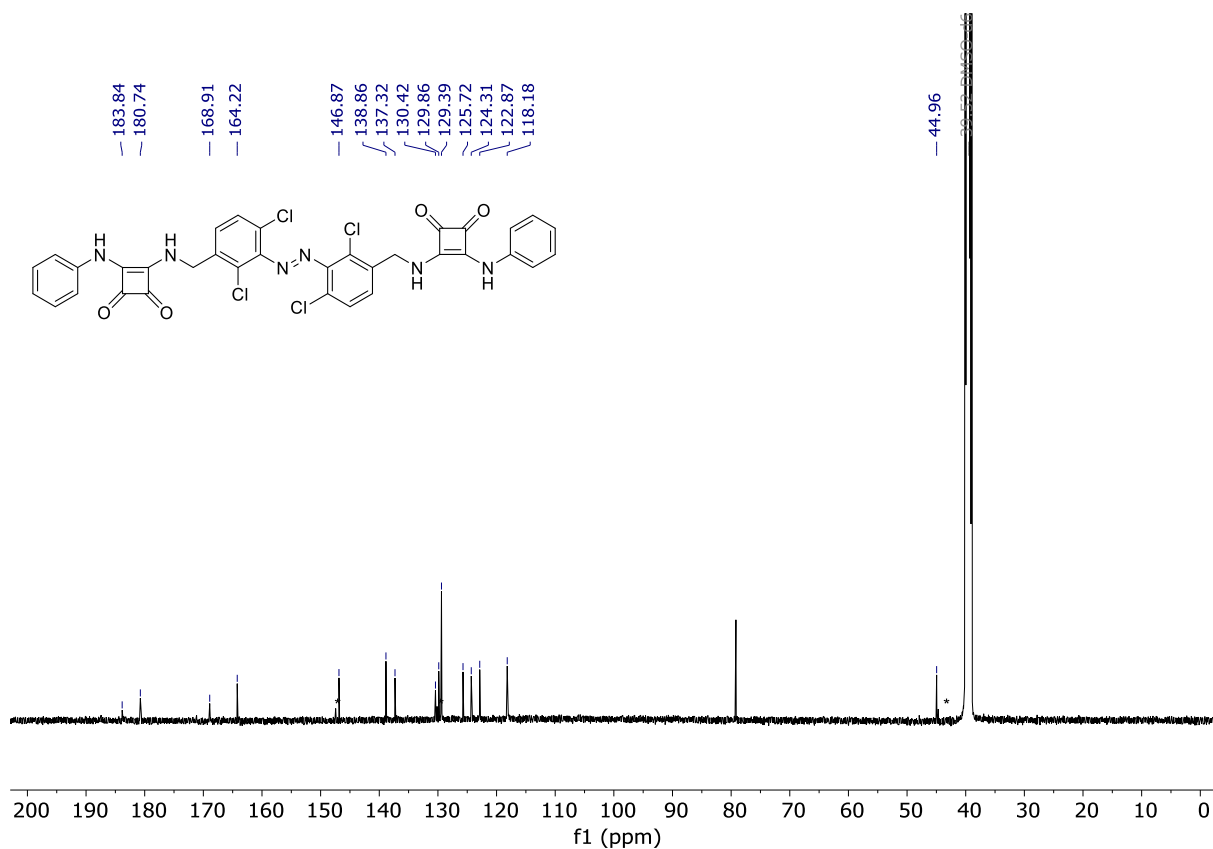


Figure S30. ^{13}C NMR Spectrum of *E-2*. (DMSO- d_6 , 298 K). *Z-2* signals labelled as *.

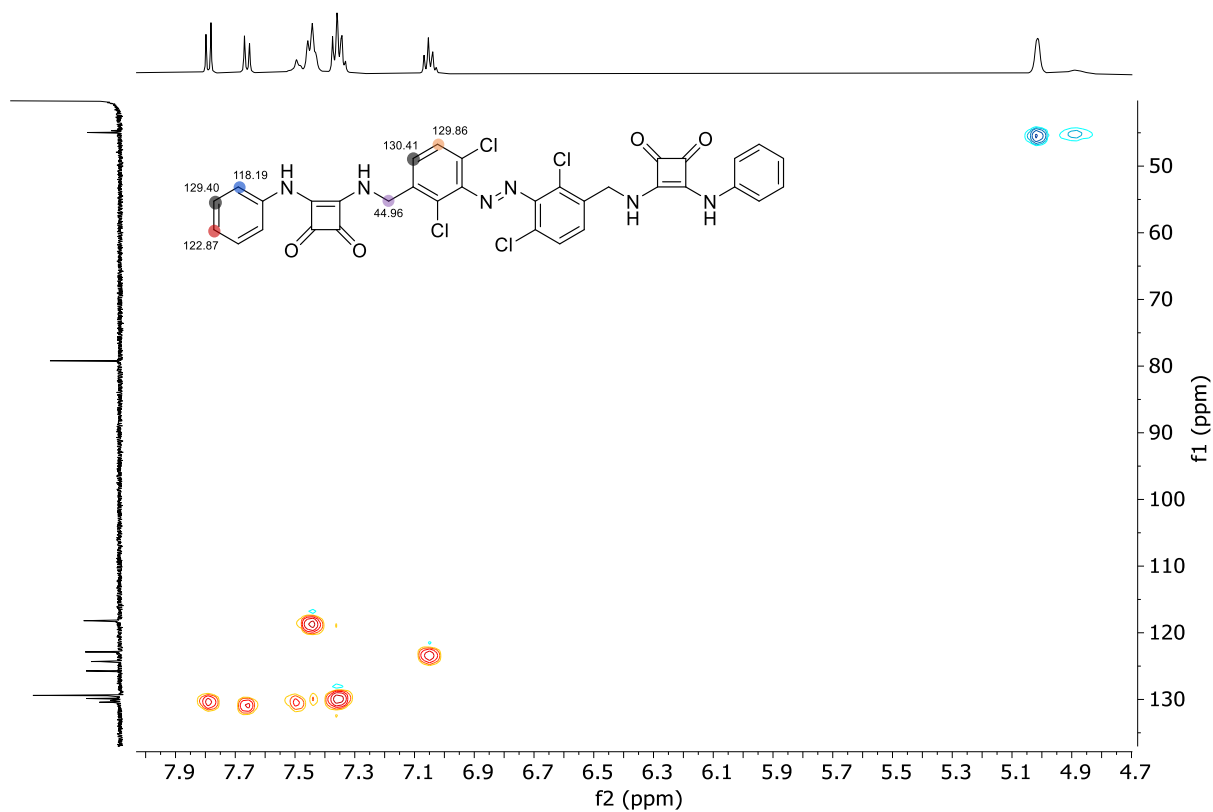


Figure S31. HSQC of *E-2*. Key ^1H - ^{13}C correlations highlighted. (DMSO- d_6 , 298 K).

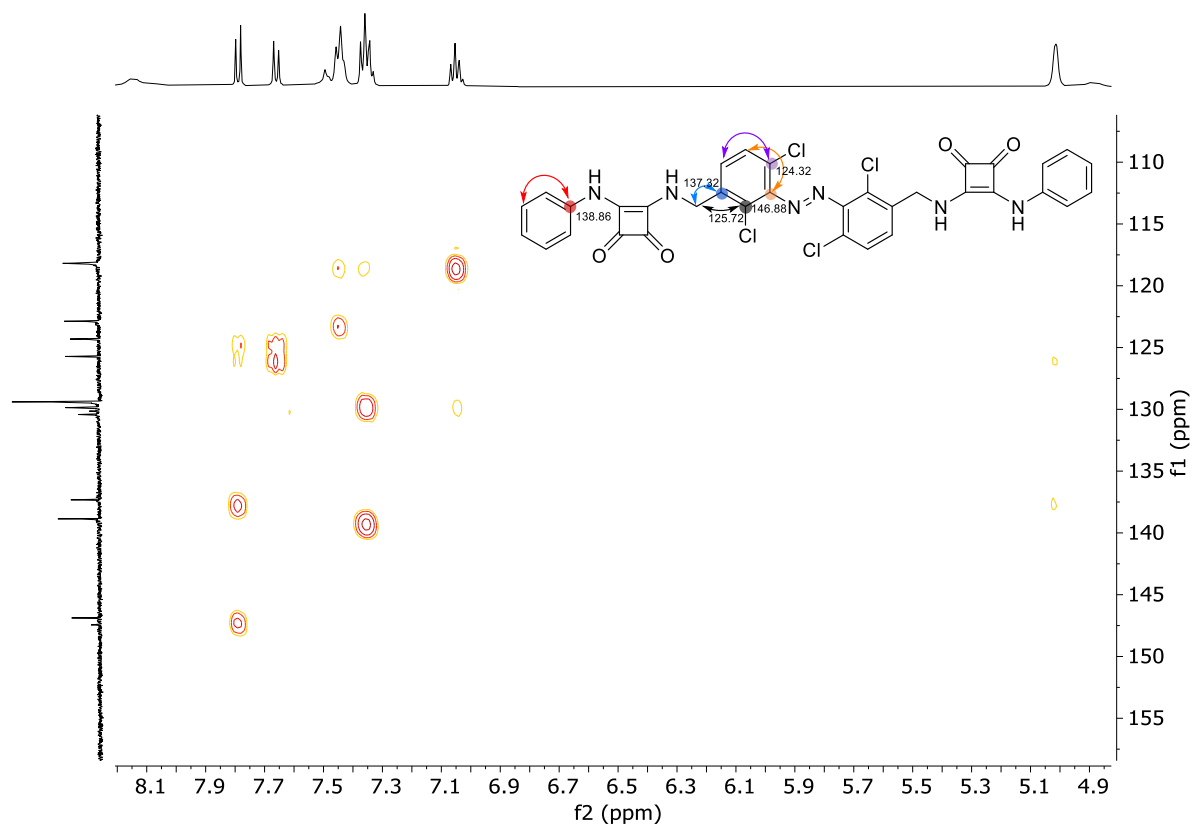


Figure S32. HSQC of **E-2**. Key ^1H - ^{13}C correlations highlighted. (DMSO- d_6 , 298 K).

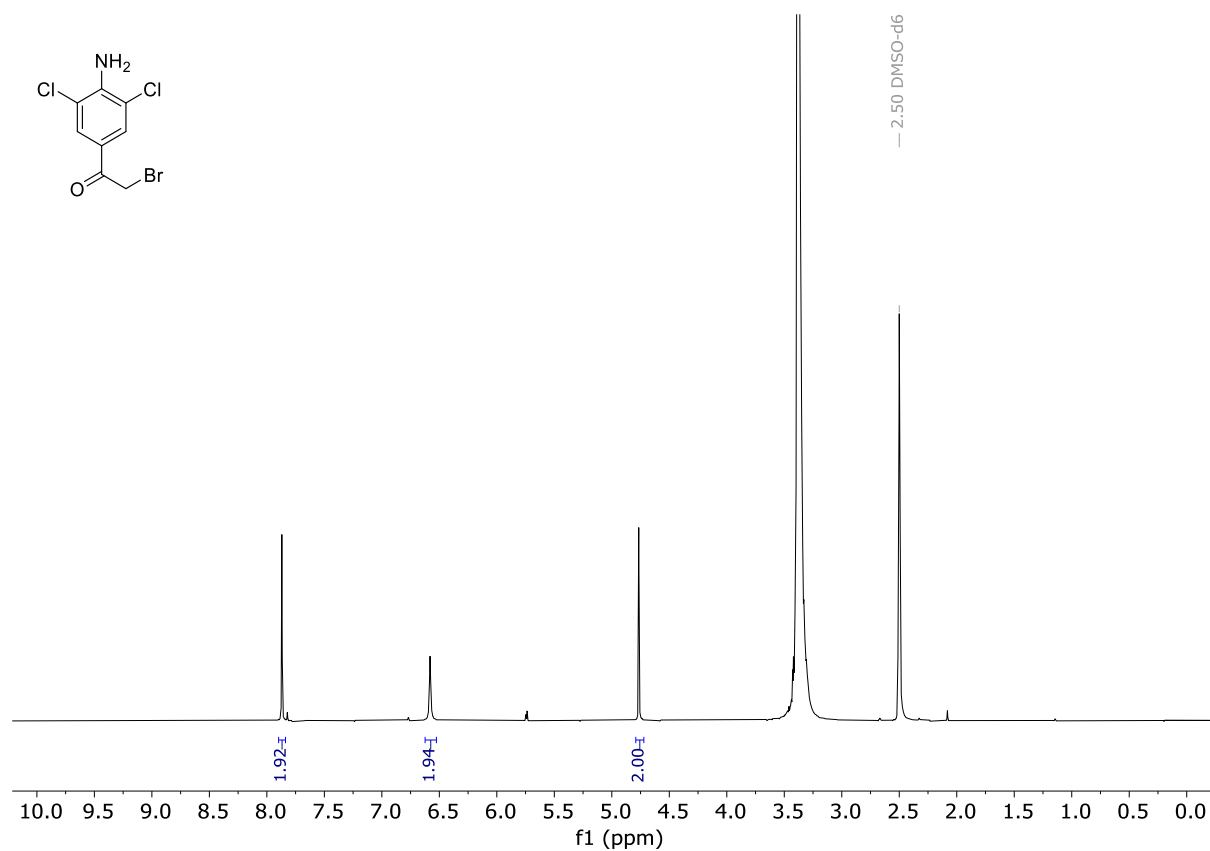


Figure S33. ^1H NMR Spectrum of **20**. (DMSO- d_6 , 298 K).

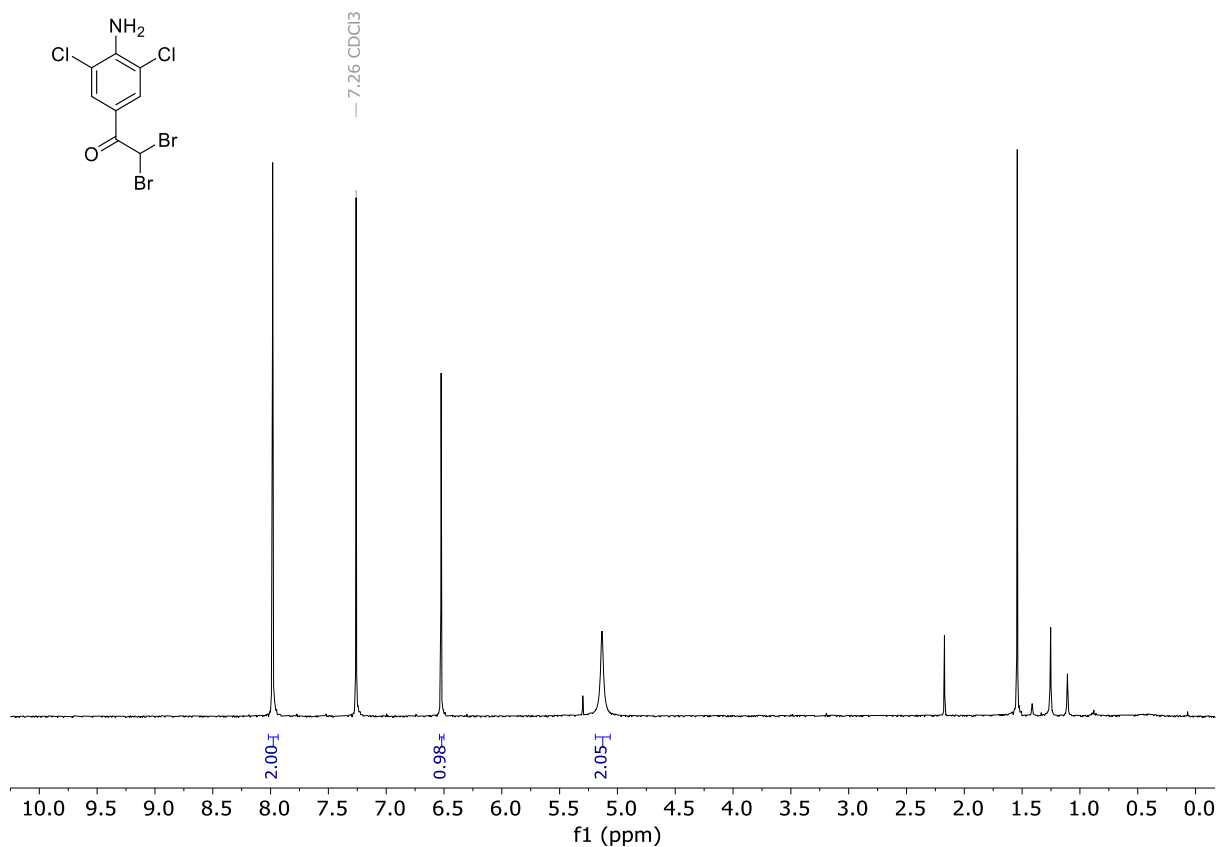


Figure S34. ¹H NMR Spectrum of **21**. (Chloroform-*d*, 298 K).

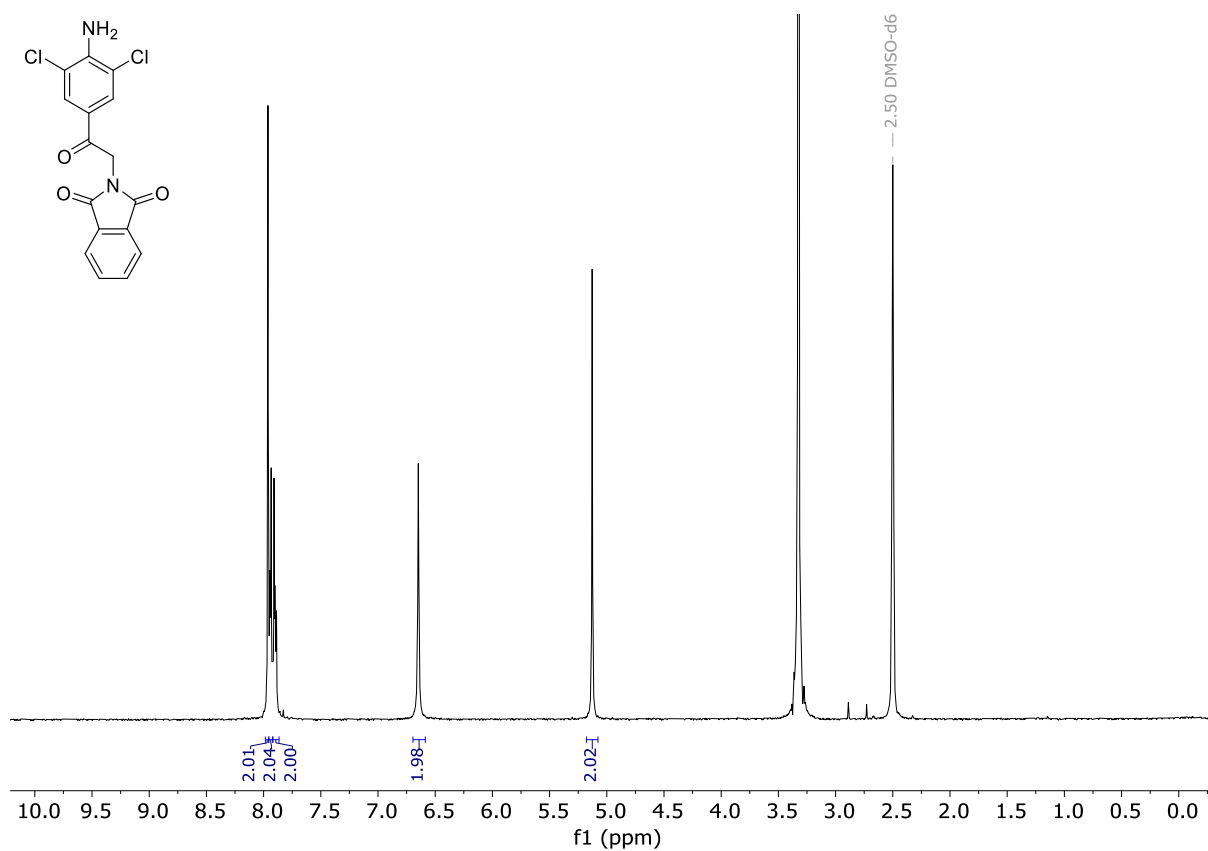


Figure S35. ¹H NMR Spectrum of **22**. (DMSO-*d*₆, 298 K).

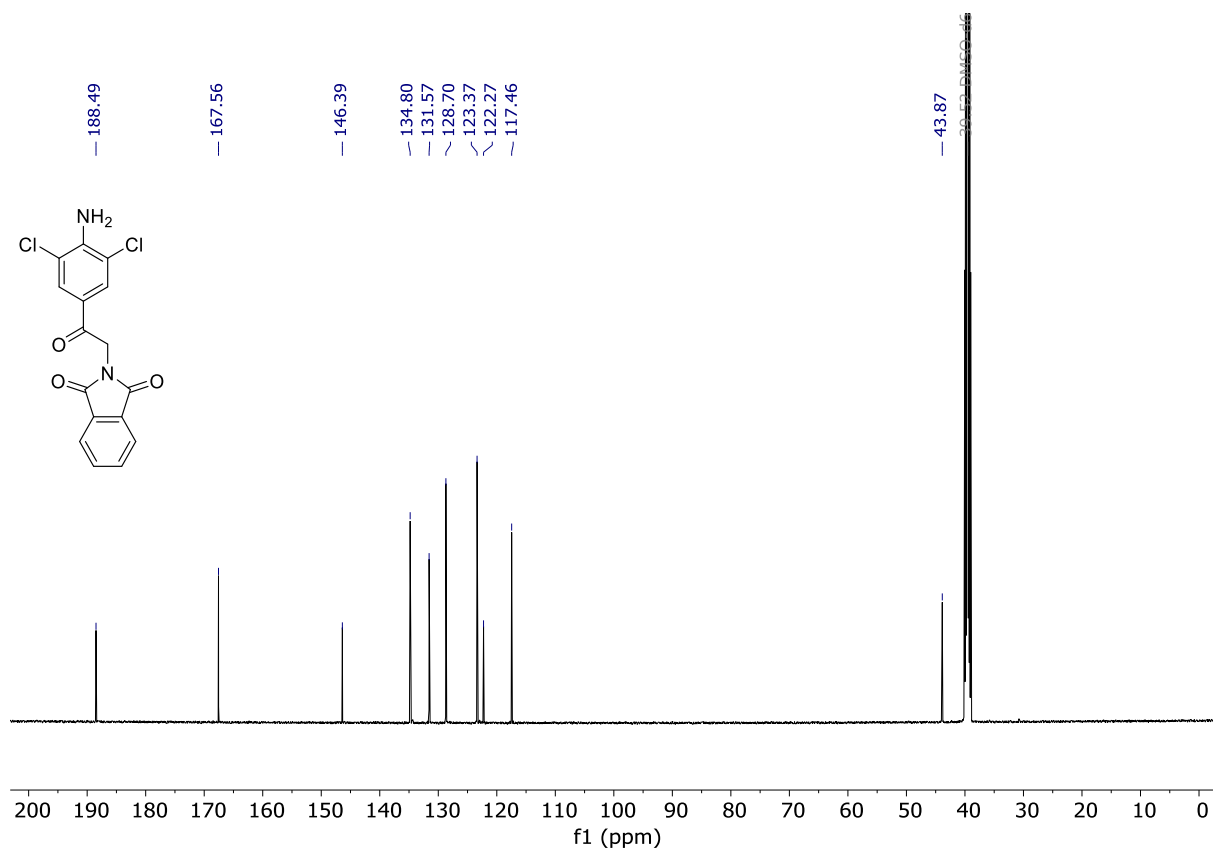


Figure S36. ¹³C NMR Spectrum of **22**. (DMSO-d₆, 298 K).

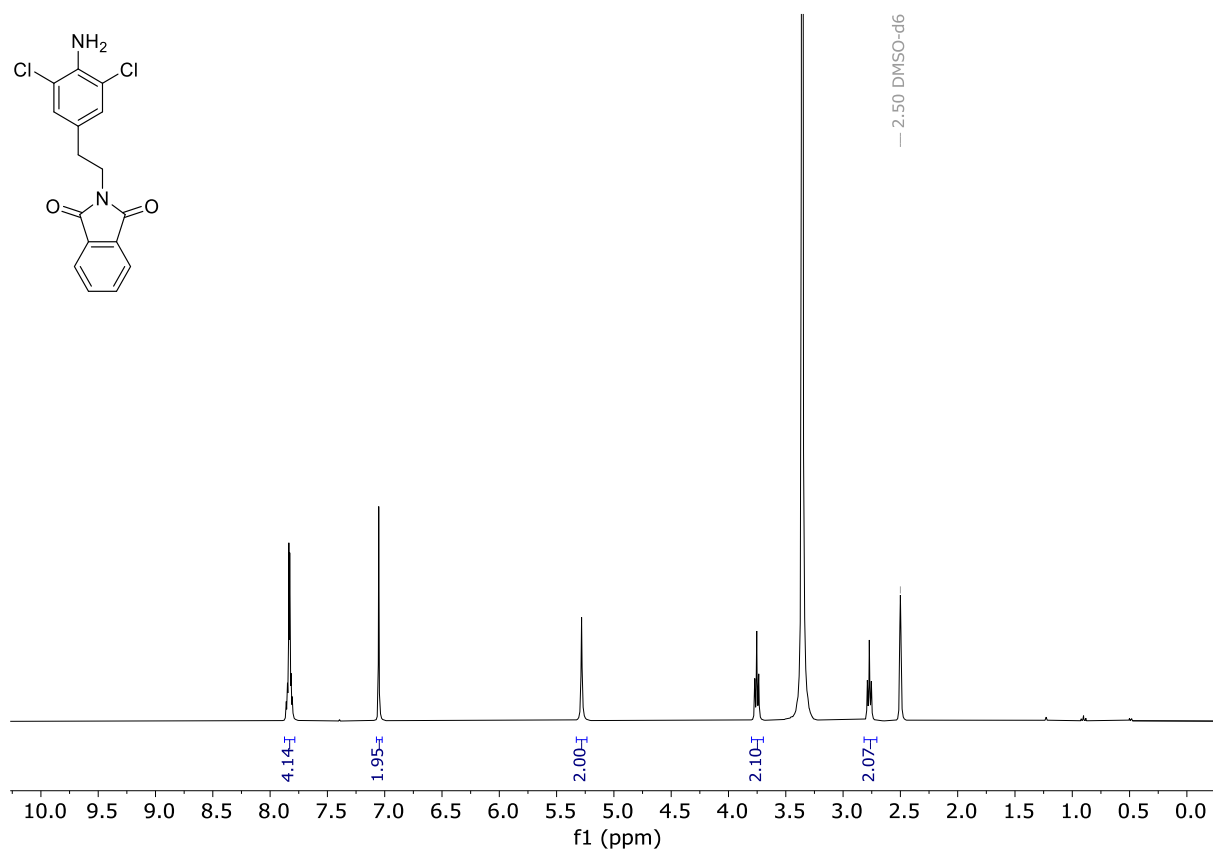


Figure S37. ¹H NMR Spectrum of **23**. (DMSO-d₆, 298 K).

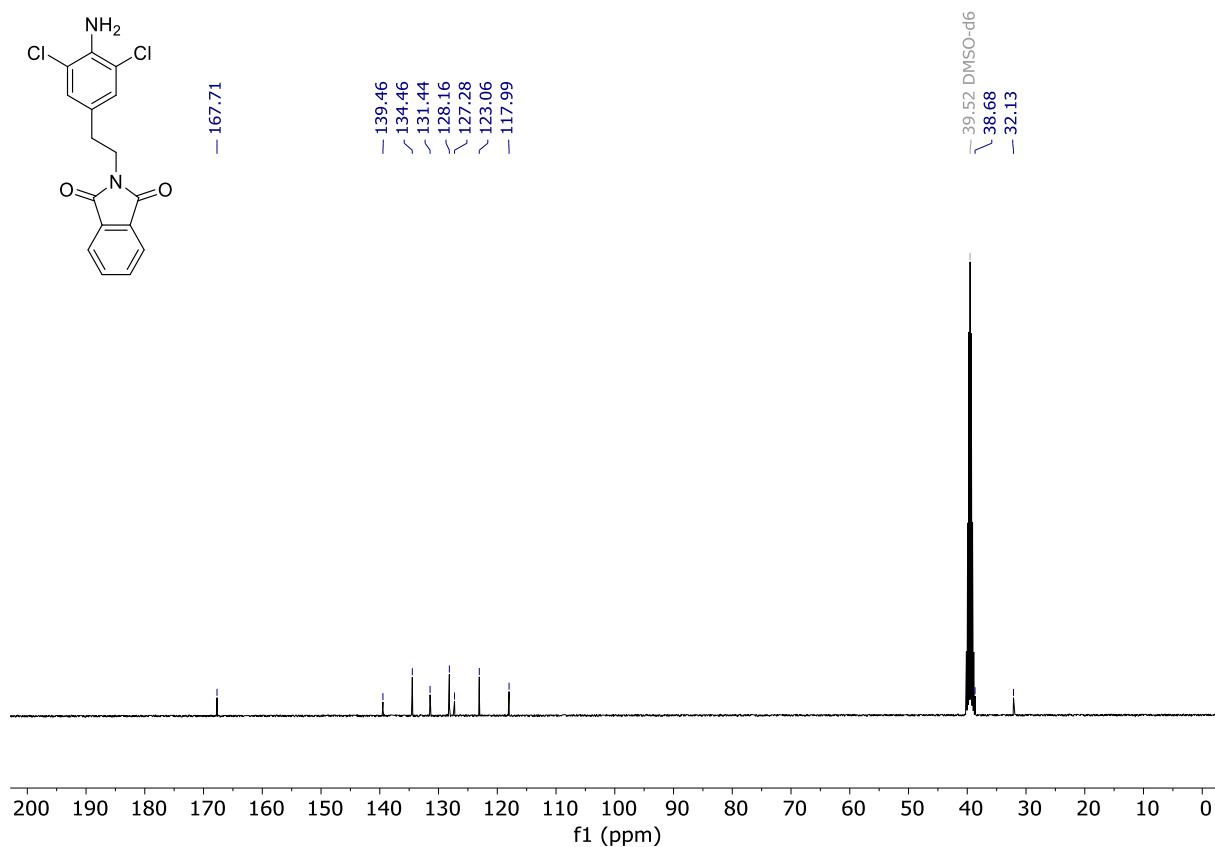


Figure S38. ^{13}C NMR Spectrum of **23**. (DMSO-d₆, 298 K).

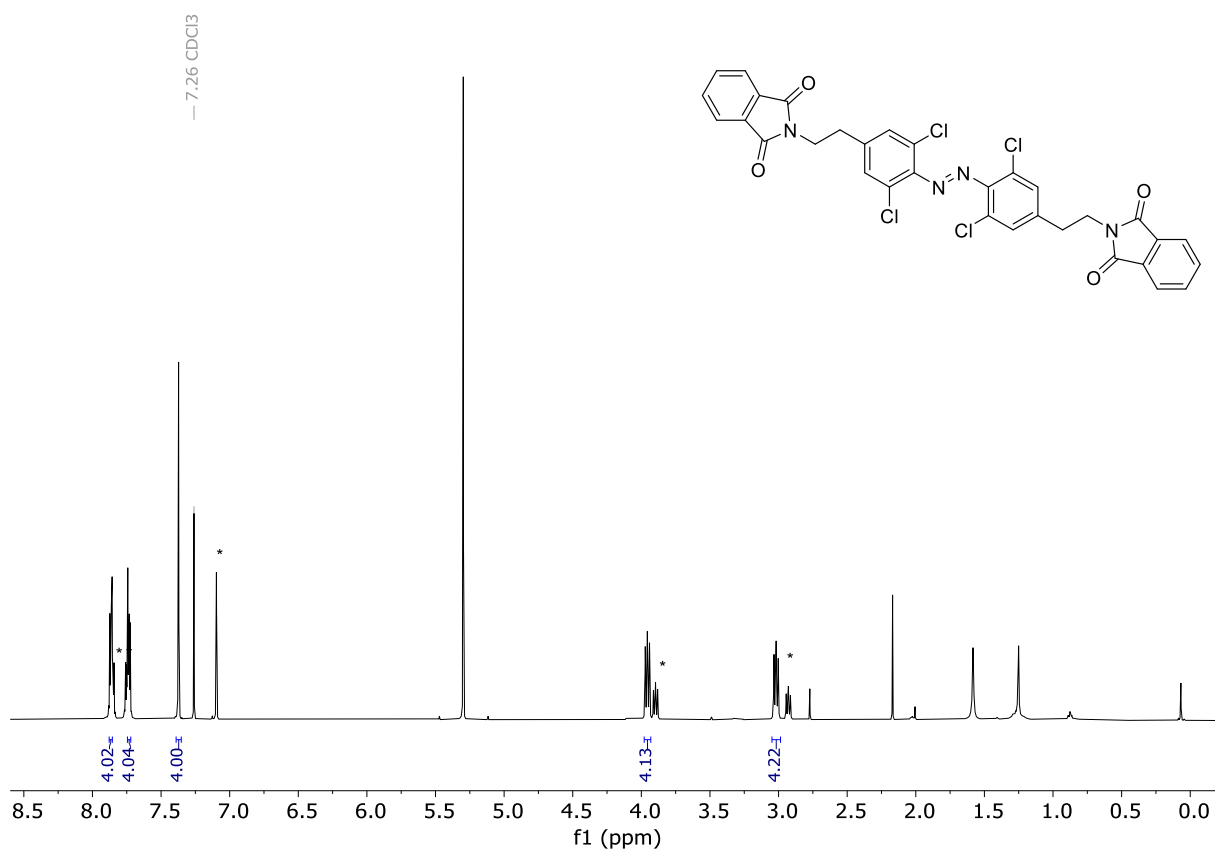


Figure S39. ^1H NMR spectrum of **E-24** (Chloroform-d, 298 K). **Z-24** signals labelled as *

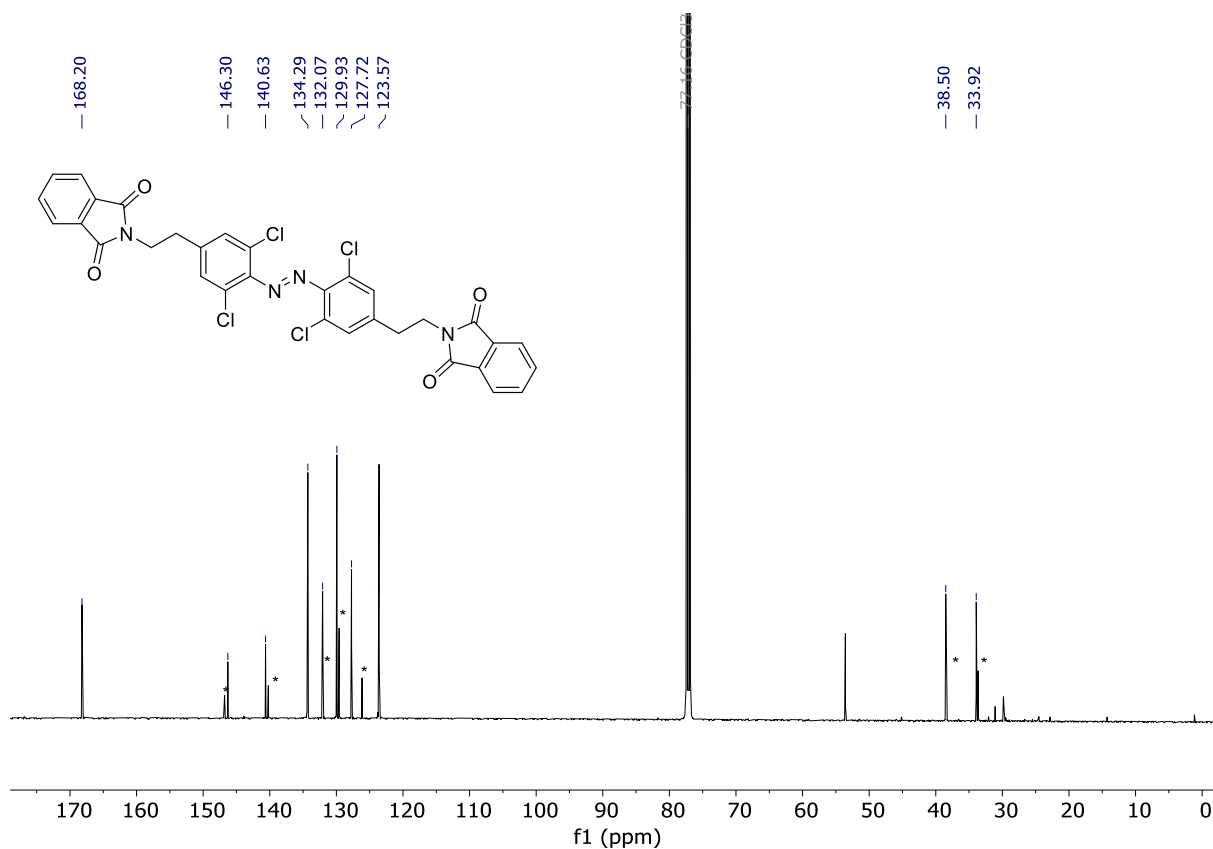


Figure S40. ^{13}C NMR spectrum of *E*-24 (Chloroform-*d*, 298 K). *Z*-24 signals labelled as *

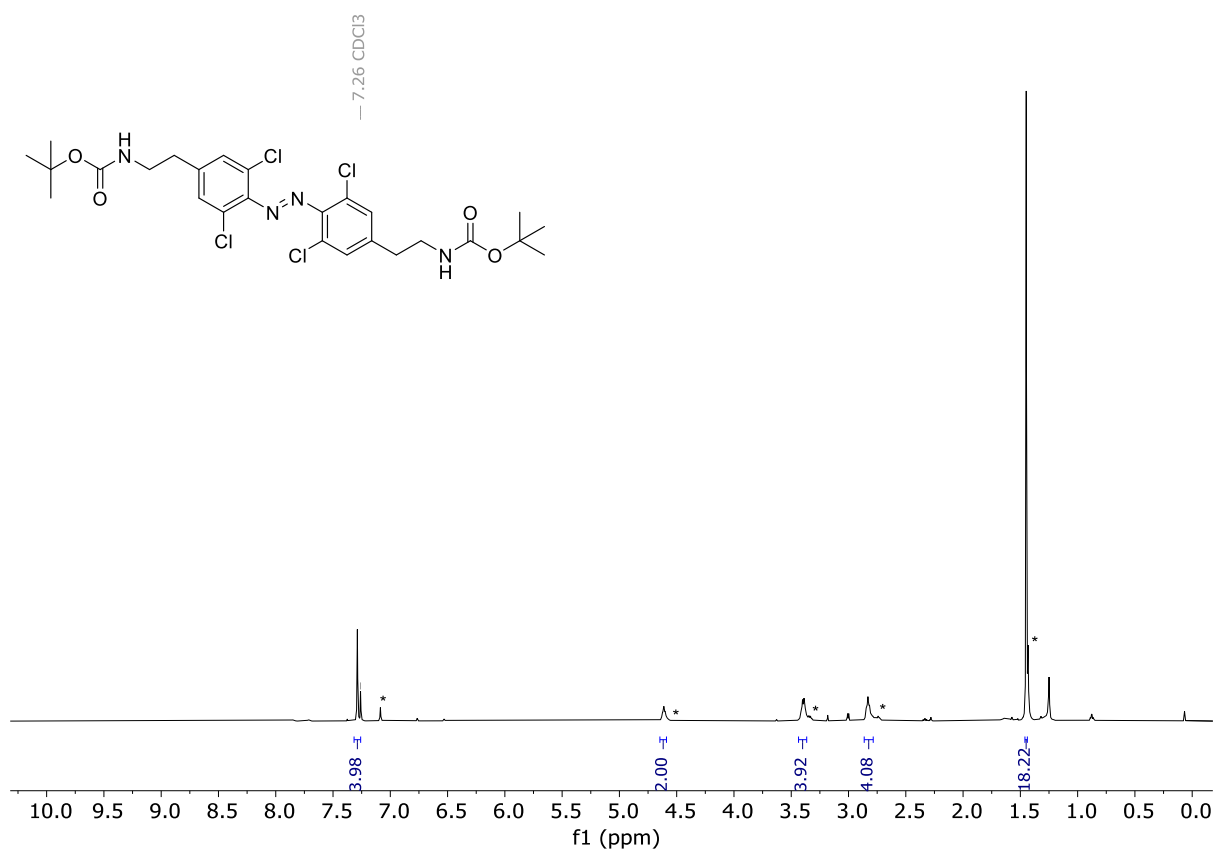


Figure S41. ^1H NMR spectrum of *E*-25 (Chloroform-*d*, 298 K). *Z*-25 signals labelled as *

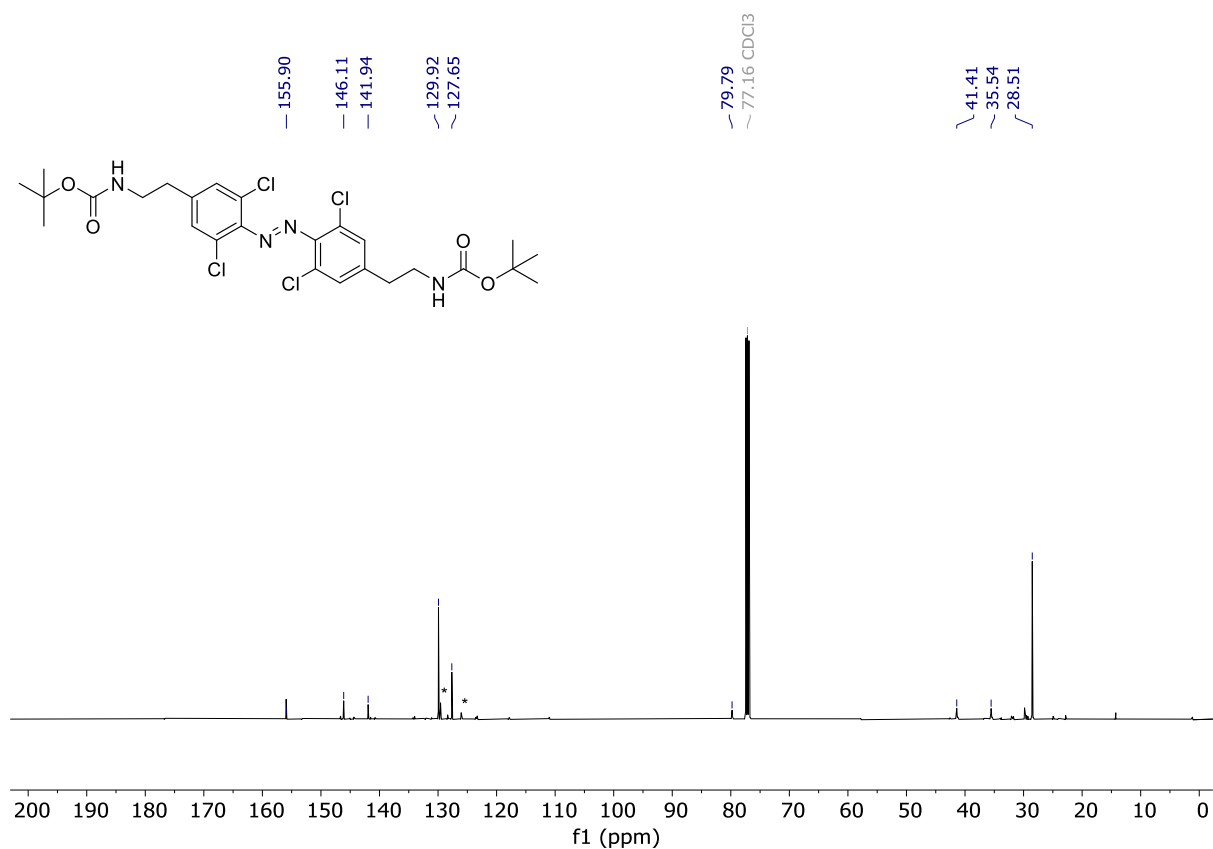


Figure S42. ^{13}C NMR spectrum of *E*-25 (Chloroform-*d*, 298 K). *Z*-25 signals labelled as *.

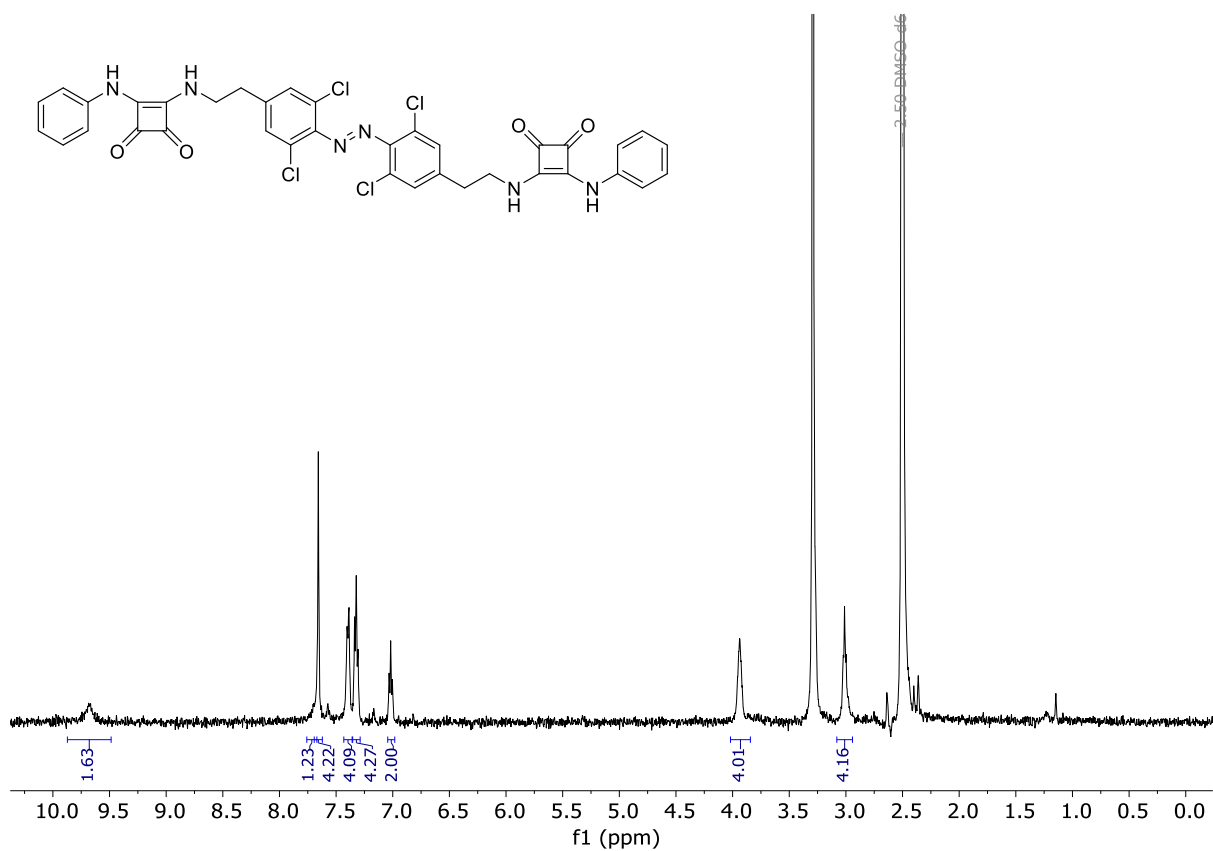


Figure S43. ^1H NMR spectrum of *E*-3 (DMSO-*d*₆, 298 K). *Z*-3 signals labelled as *.

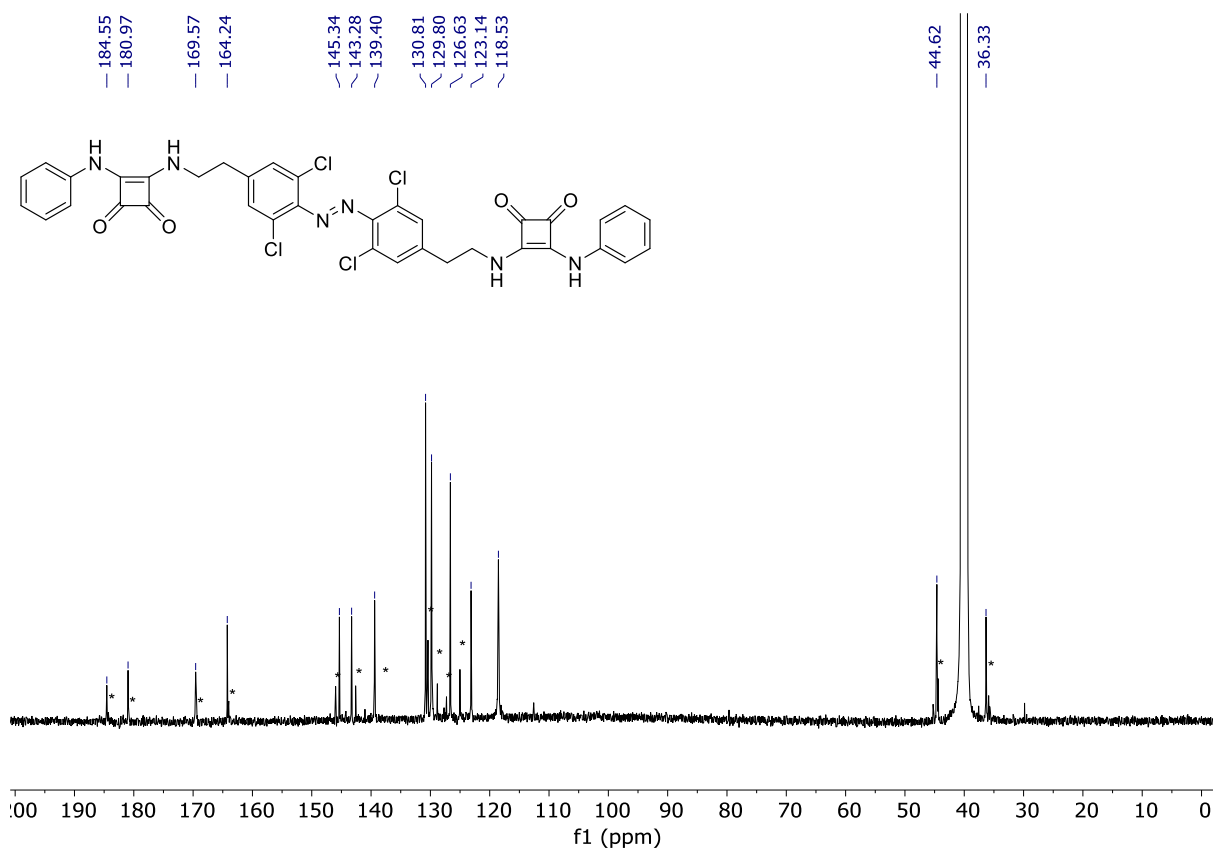


Figure S44. ^{13}C NMR Spectrum of *E-3*. (DMSO- d_6 , 298 K). *Z-3* signals labelled as *.

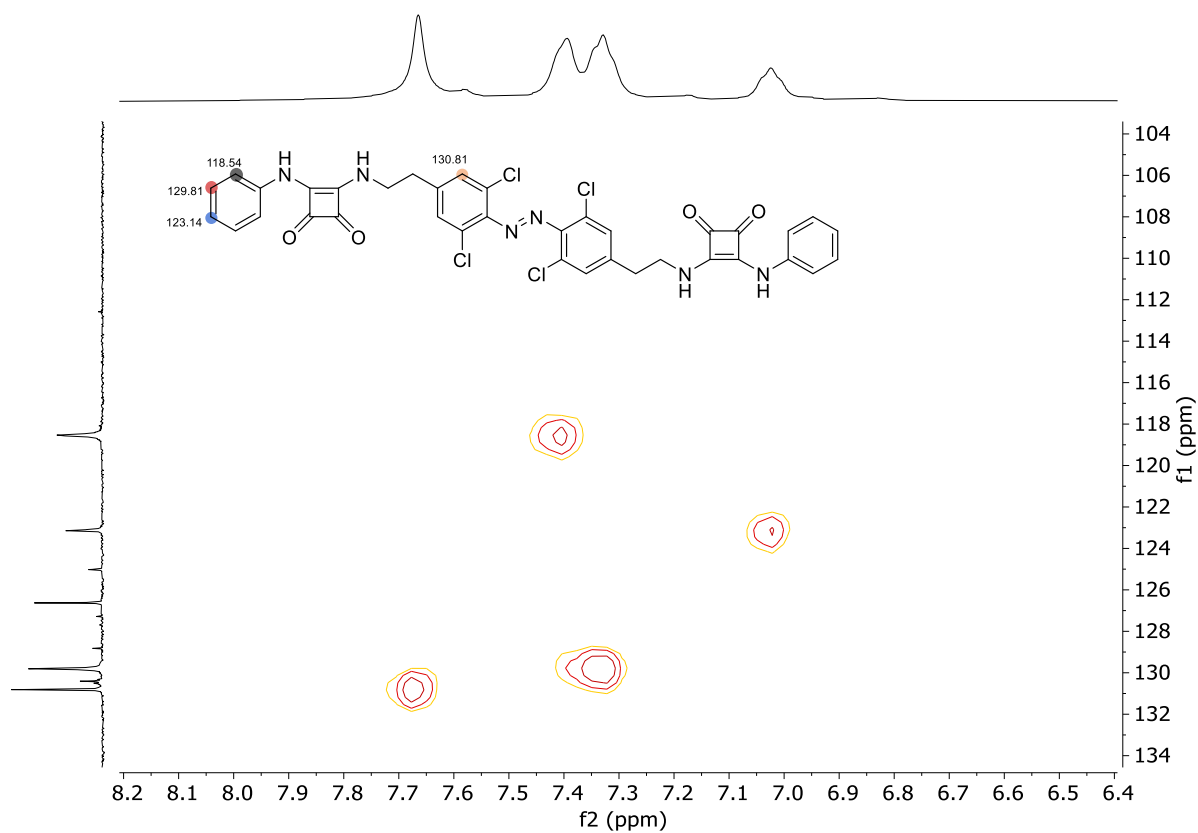


Figure S45. HSQC of **3**. Key aromatic ^1H - ^{13}C correlations highlighted. (DMSO- d_6 , 298 K).

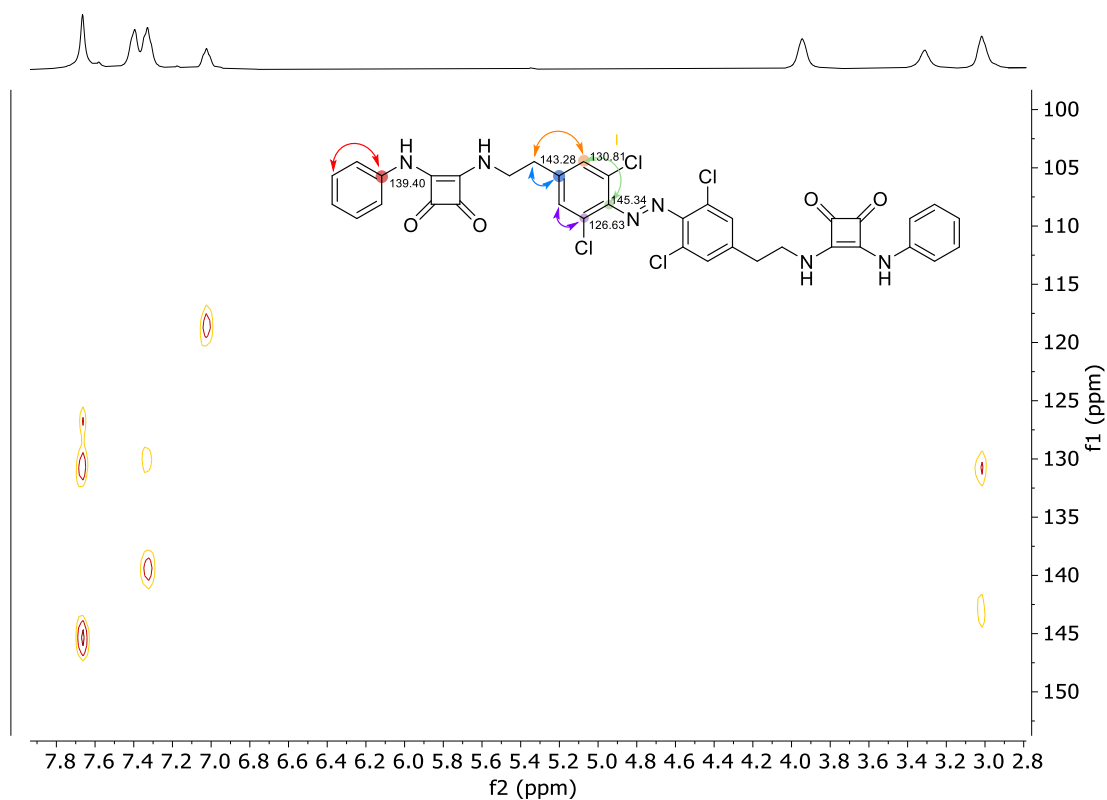


Figure S46. HMBC of **3**. Key ^1H - ^{13}C correlations highlighted. (DMSO- d_6 , 298 K).

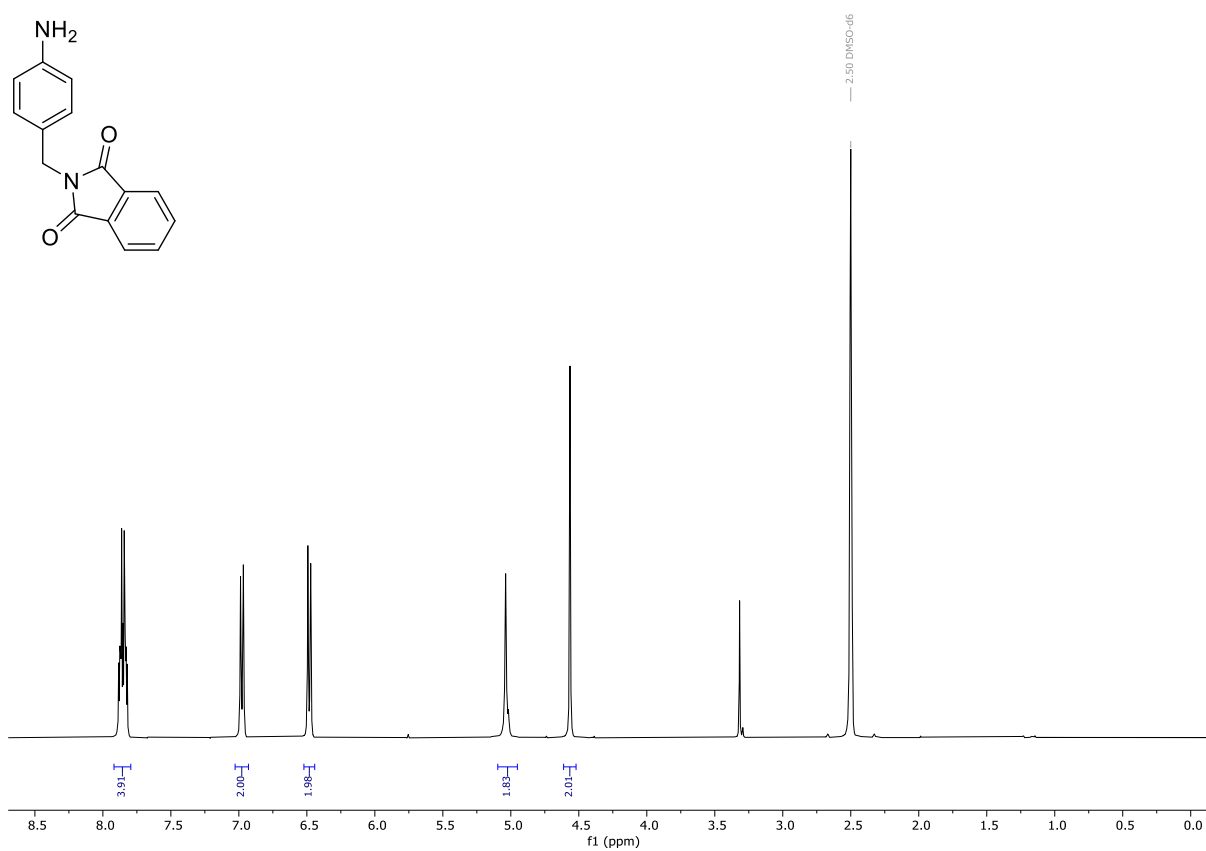


Figure S47. ^1H NMR Spectrum of **27** (DMSO- d_6 , 298 K).

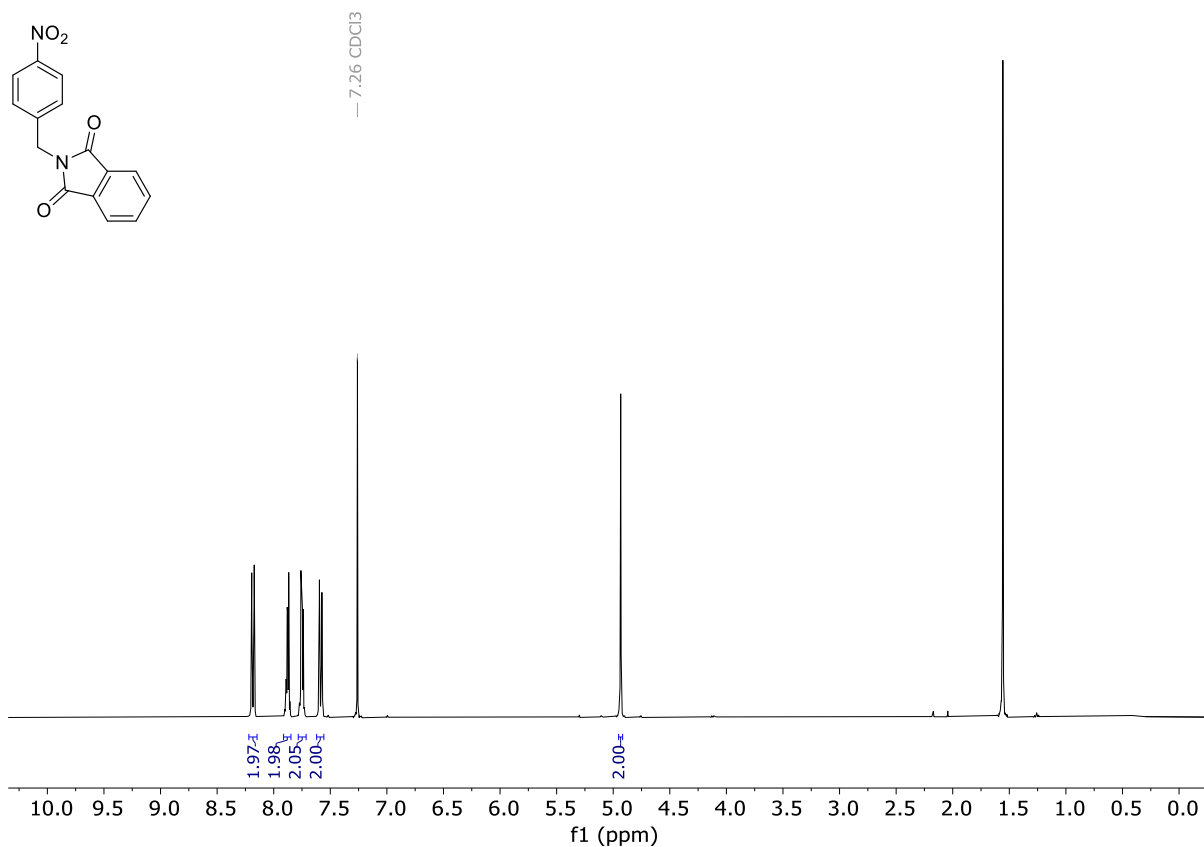


Figure S48. ¹H NMR spectrum of **S9** (Chloroform-*d*, 298 K).

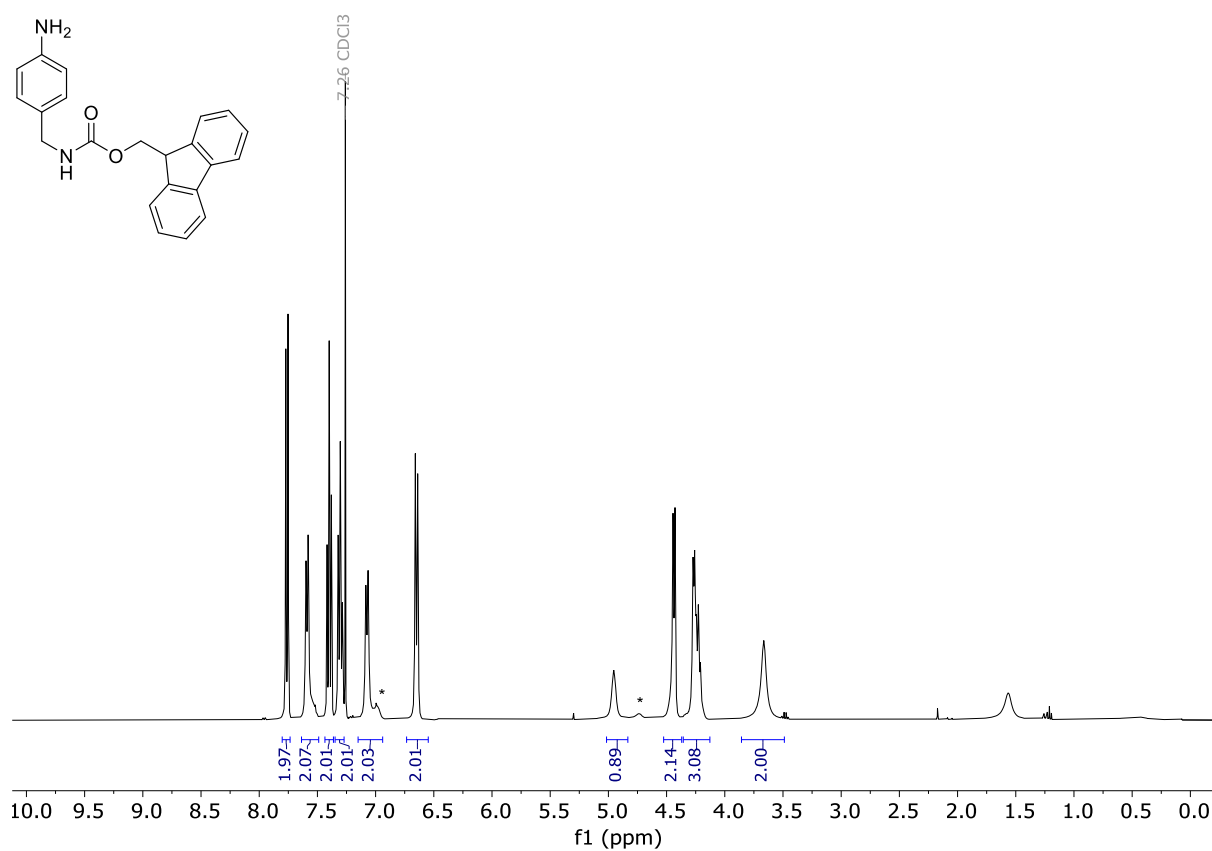


Figure S49. ¹H NMR spectrum of **28** (Chloroform-*d*, 298 K). Minor rotameric signals labelled as *

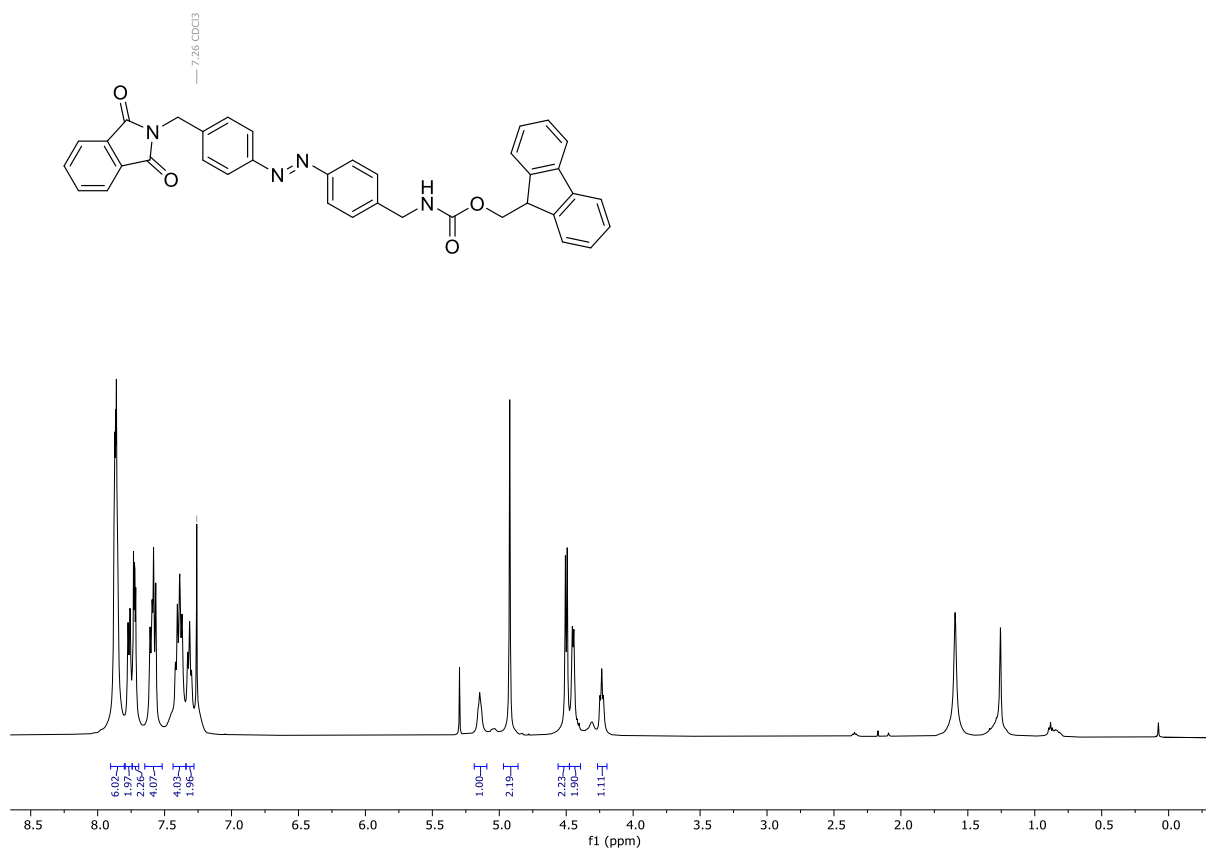


Figure S50. ^1H NMR spectrum of *E-30* (Chloroform-*d*, 298 K).

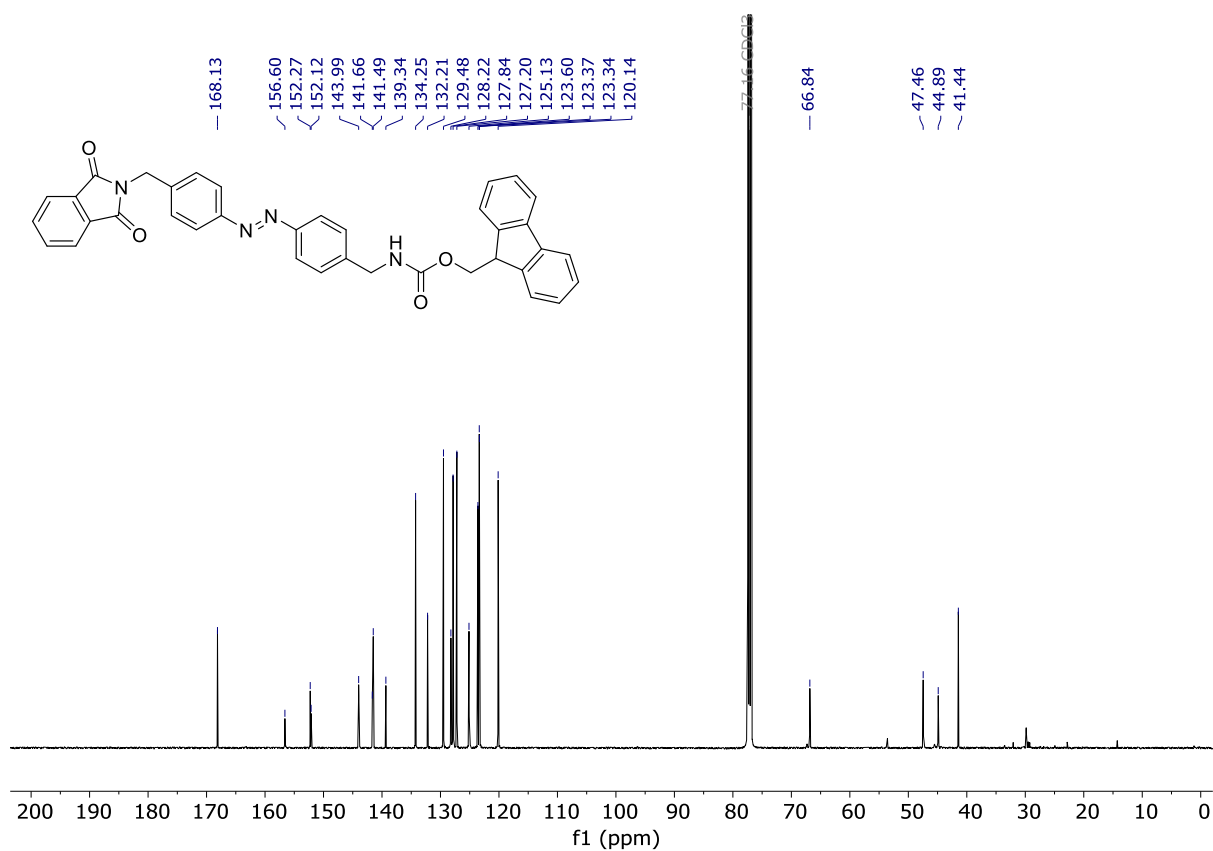


Figure S51. ^{13}C NMR spectrum of *E-30* (Chloroform-*d*, 298 K).

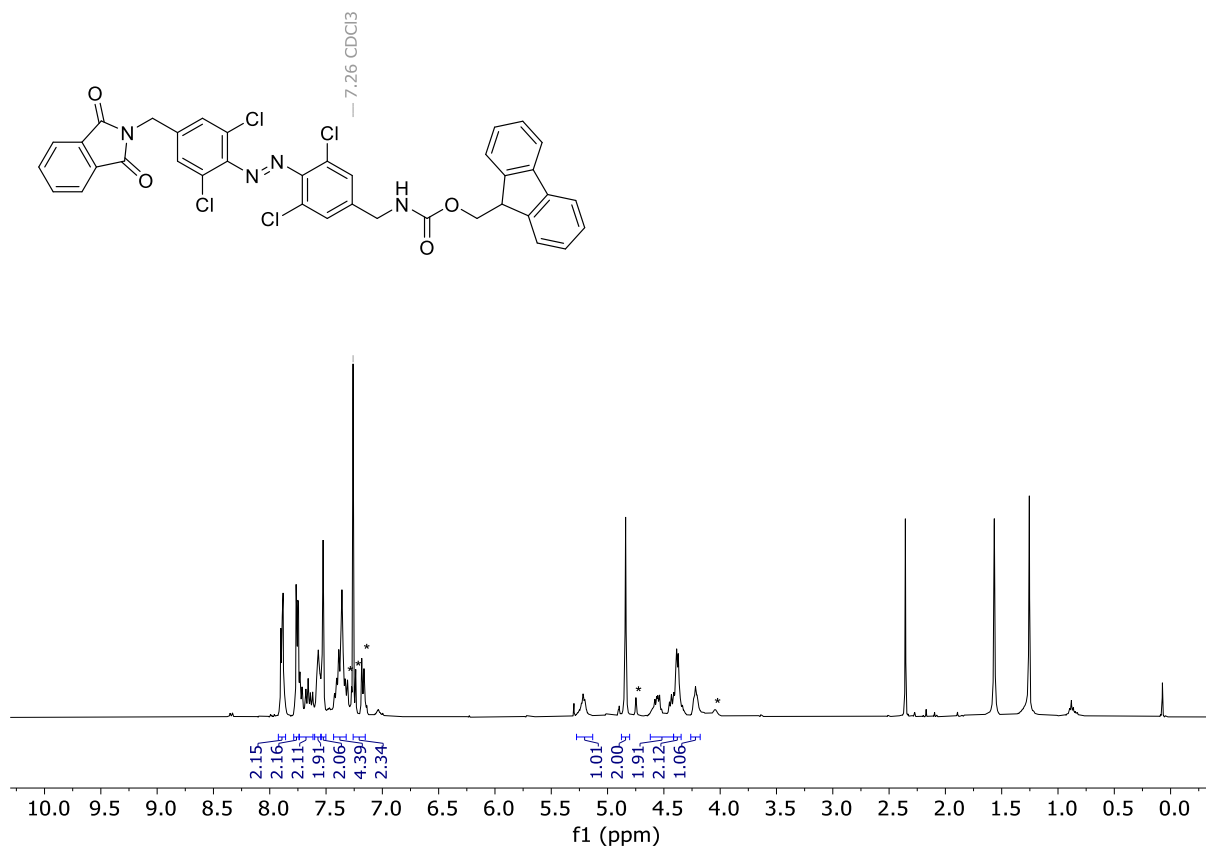


Figure S52. ^1H NMR spectrum of *E*-31 (Chloroform-*d*, 298 K).

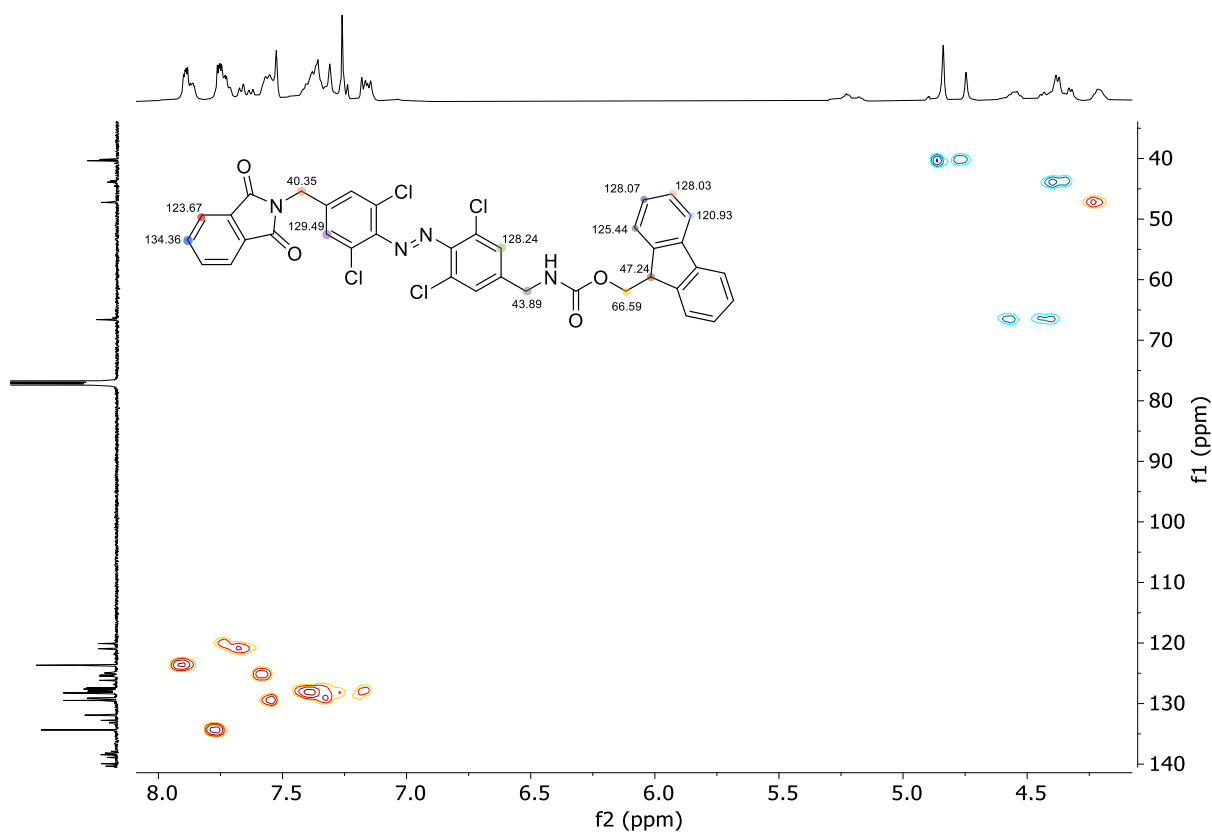


Figure S53. HSQC of *E*-31. Key ^1H - ^{13}C correlations highlighted. (Chloroform-*d*, 298 K).

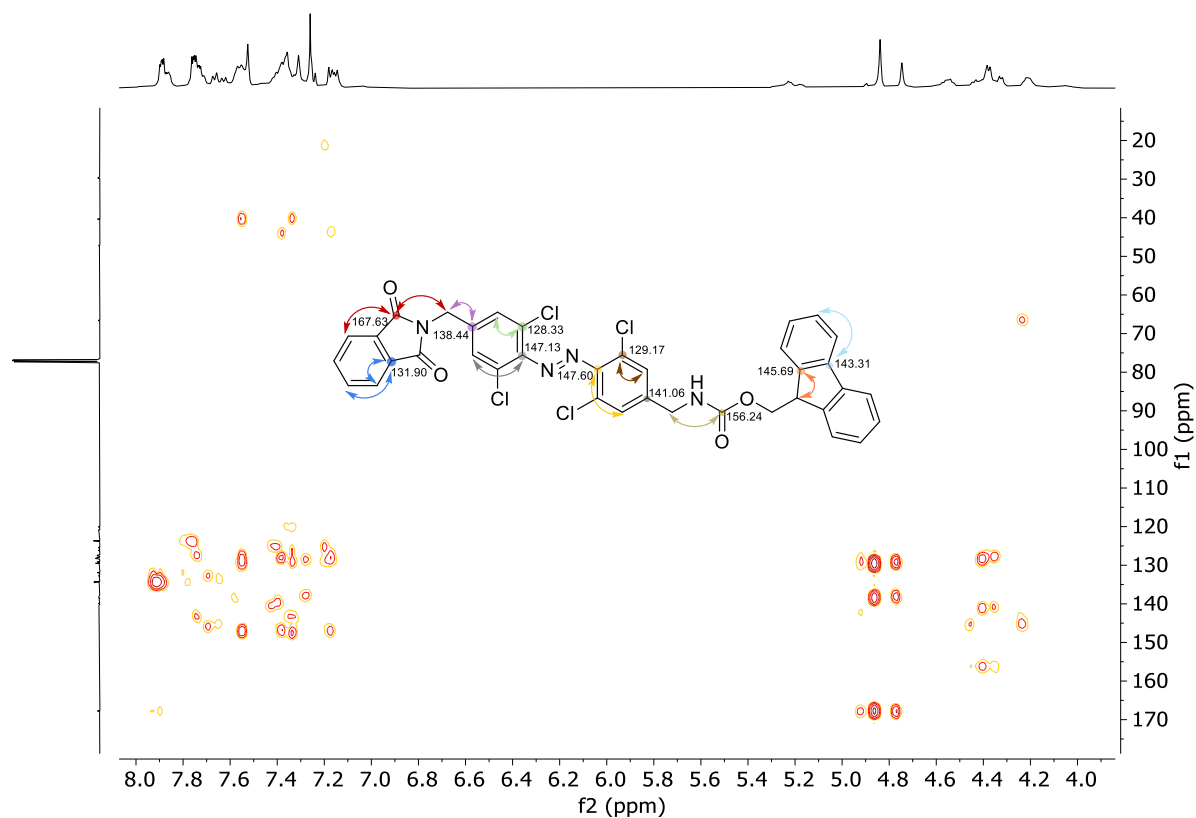


Figure S54. HMBC of *E-31*. Key ^1H - ^{13}C correlations highlighted. (Chloroform-*d*, 298 K).

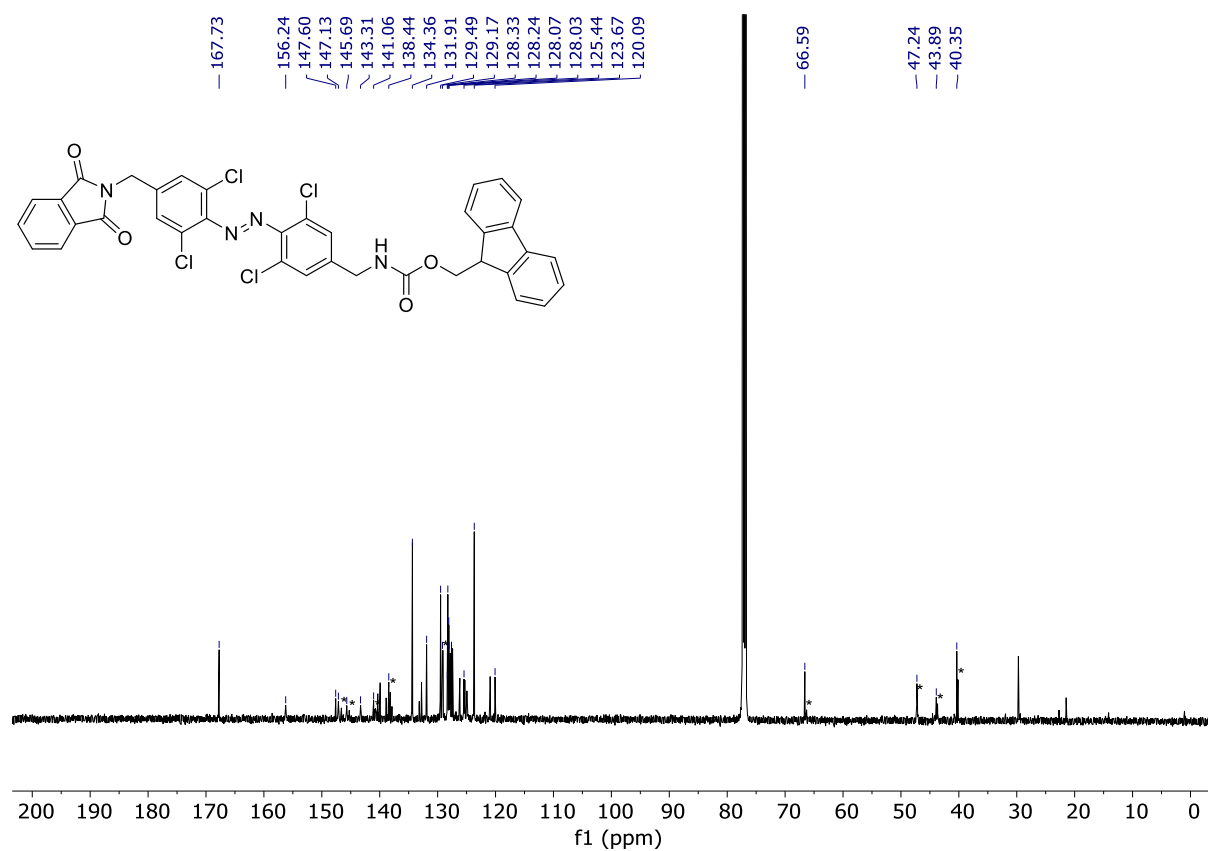


Figure S55. ^{13}C NMR spectrum of *E-31* (Chloroform-*d*, 298 K). *Z-31* peaks labelled as *

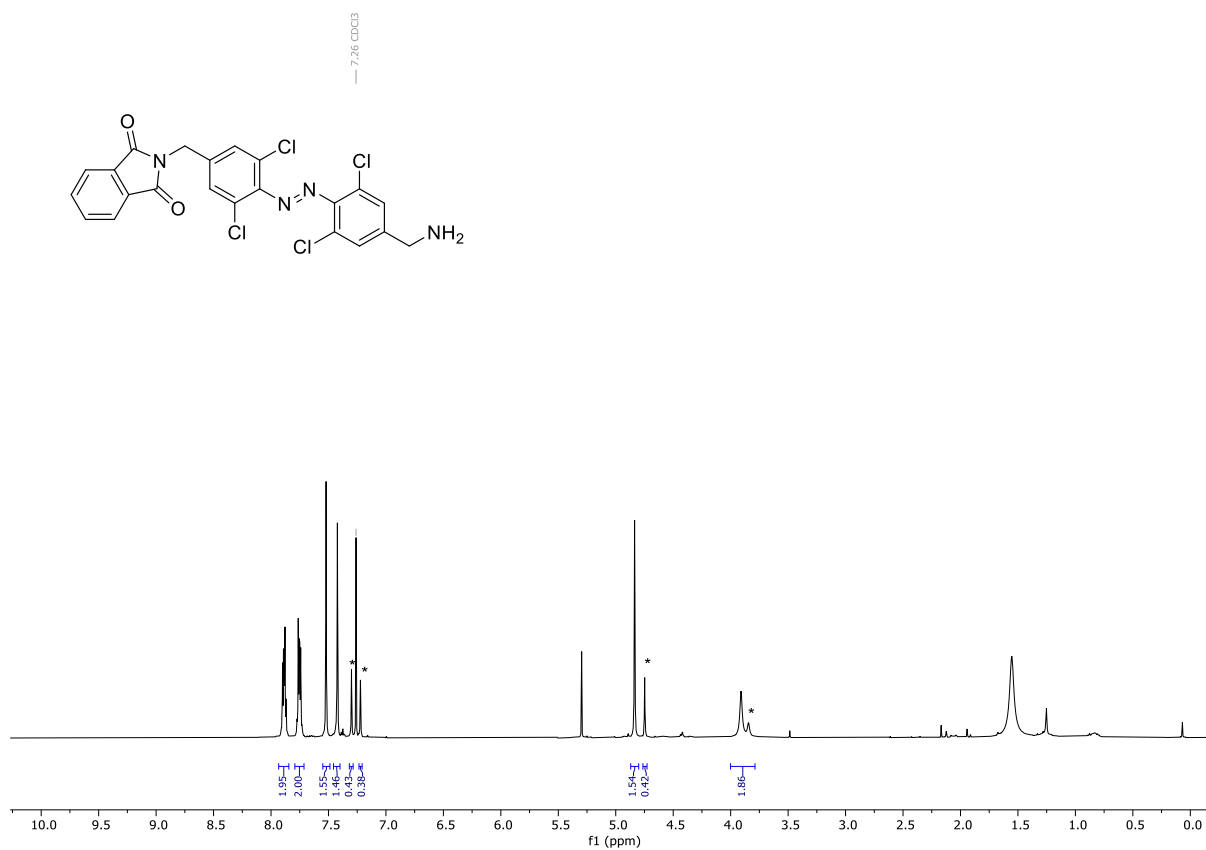


Figure S56. ¹H NMR spectrum of *E*-32 (Chloroform-*d*, 298 K). *Z*-32 signals labelled as *.

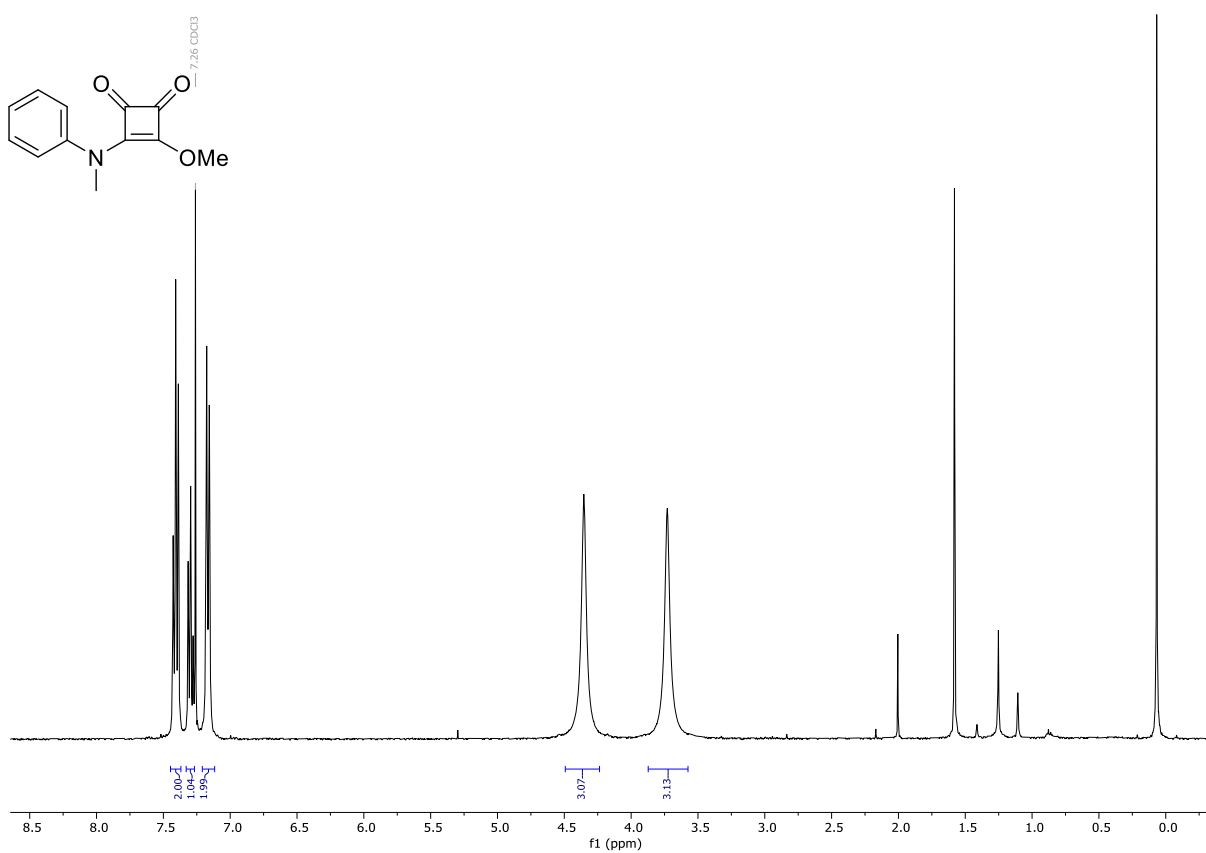


Figure S57. ¹H NMR spectrum of 33 (Chloroform-*d*, 298 K).

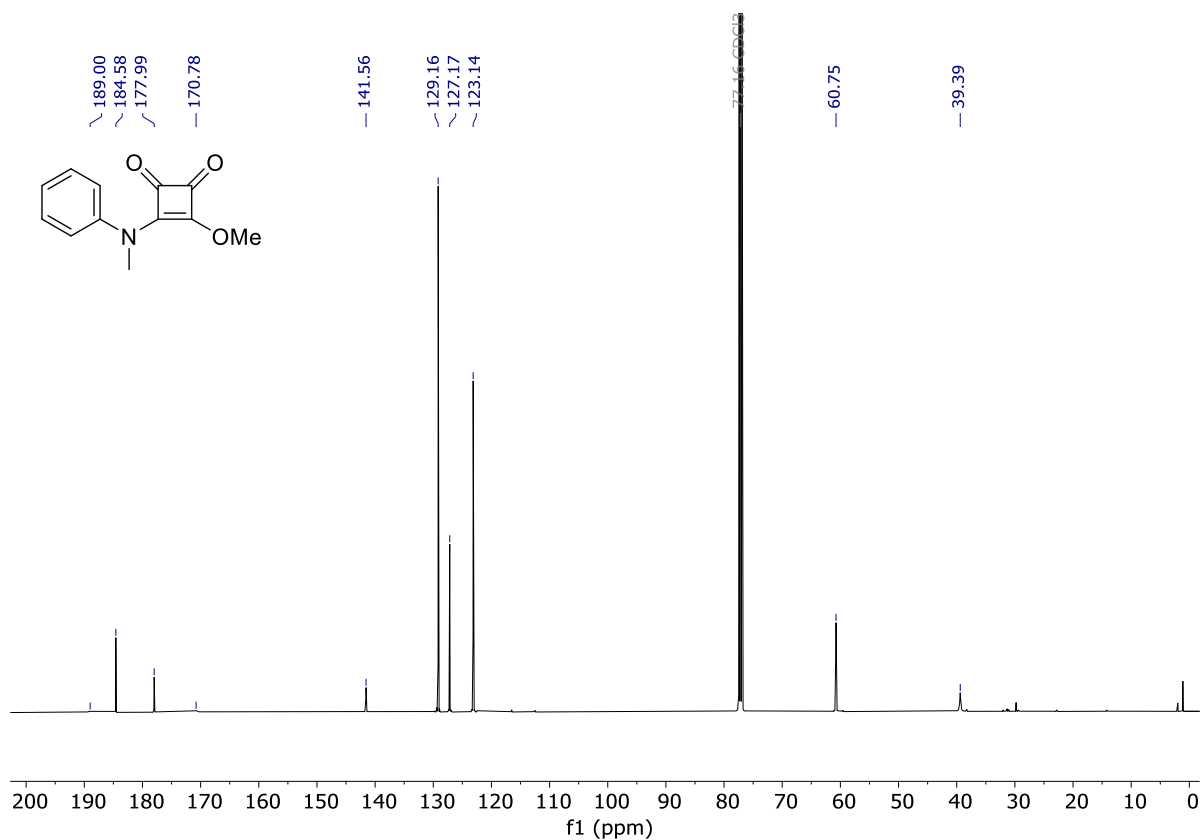


Figure S58. ^{13}C NMR spectrum of **33** (Chloroform-*d*, 298 K).

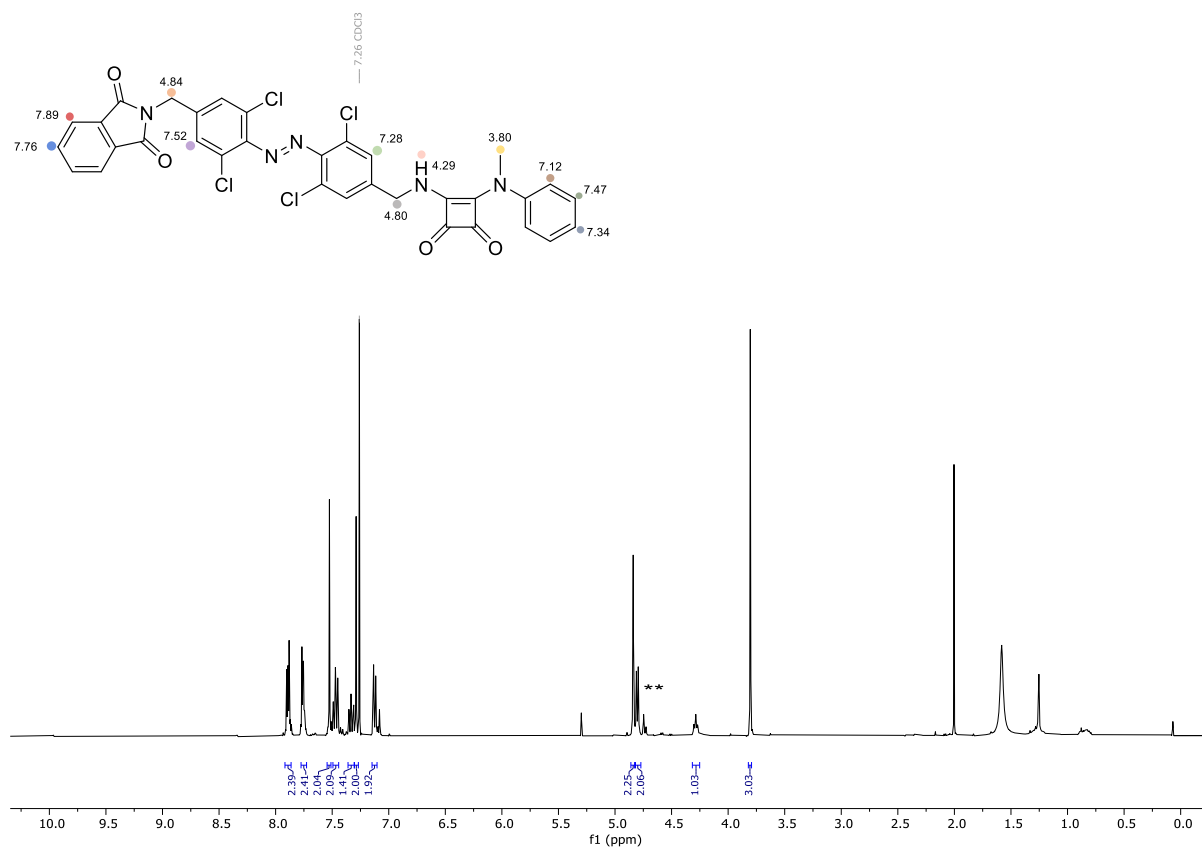


Figure S59. ^1H NMR spectrum of **E-34** (Chloroform-*d*, 298 K). **Z-34** signals labelled as *.

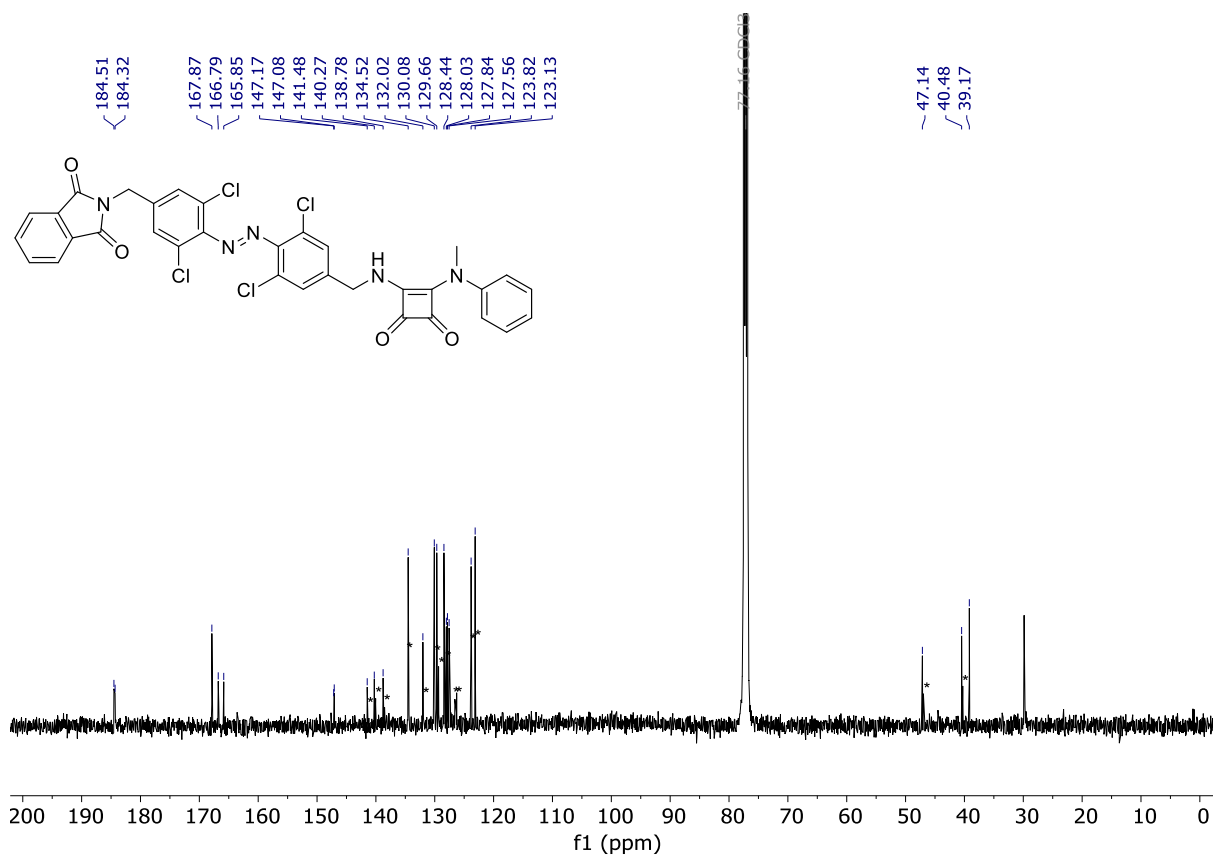


Figure S60. ^{13}C NMR spectrum of *E-34* (Chloroform-*d*, 298 K).

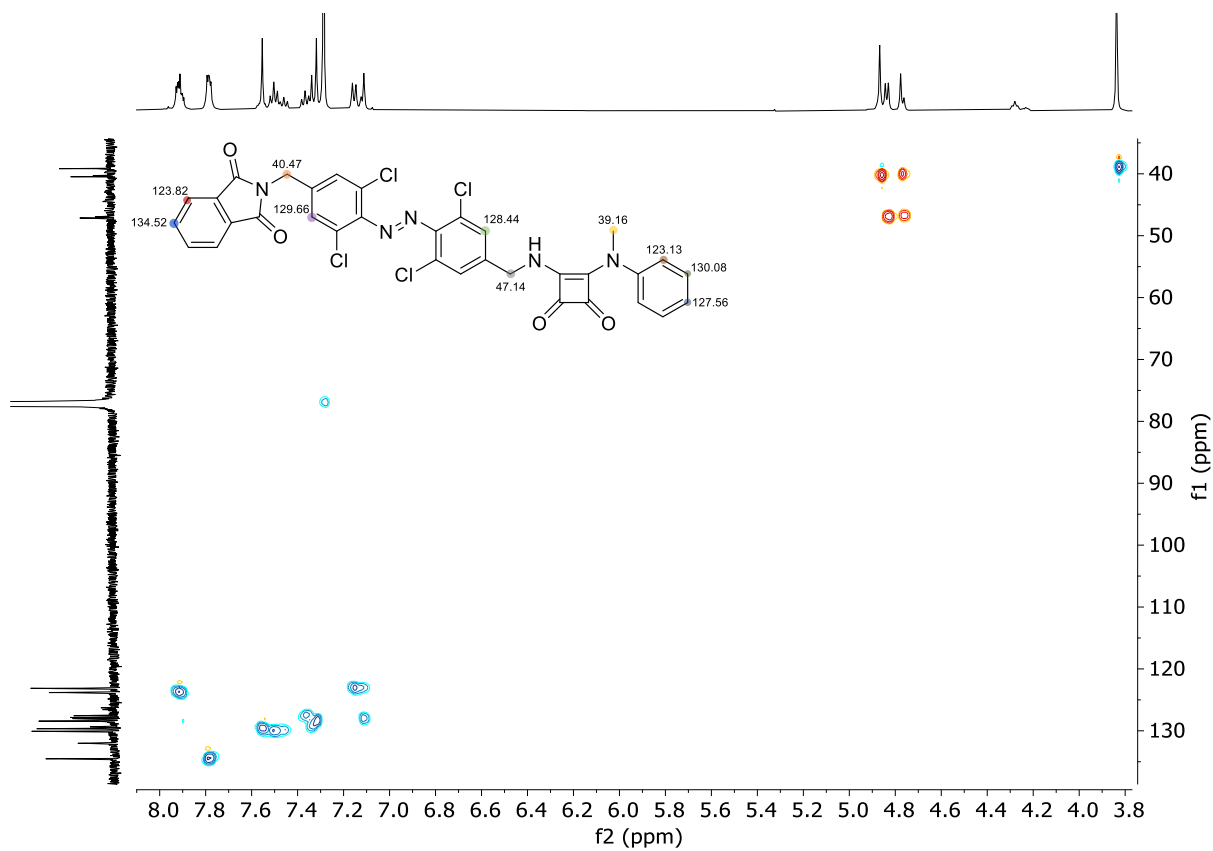


Figure S61. HSQC of *E-34*. Key ^1H - ^{13}C correlations highlighted. (Chloroform-*d*, 298 K).

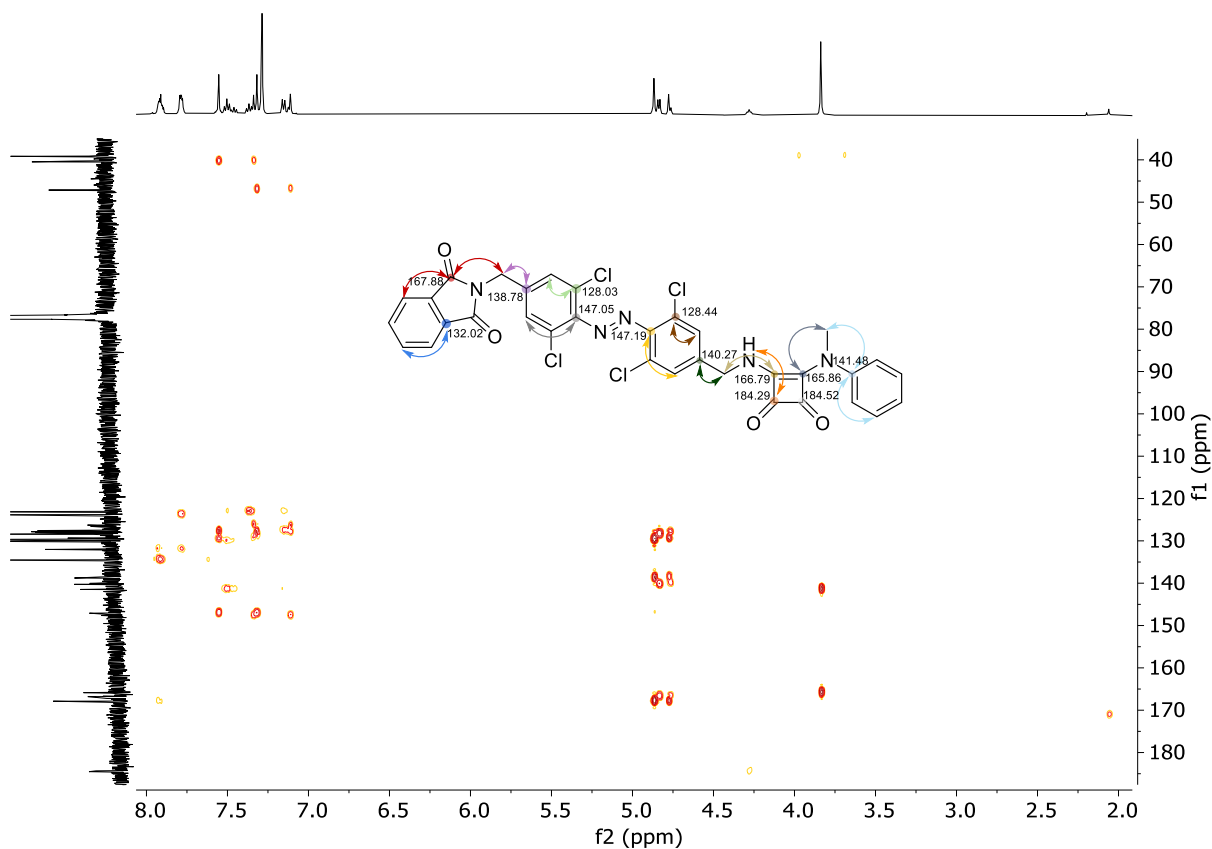


Figure S62. HMBC of *E-34*. Key ^1H - ^{13}C correlations highlighted. (Chloroform-*d*, 298 K).

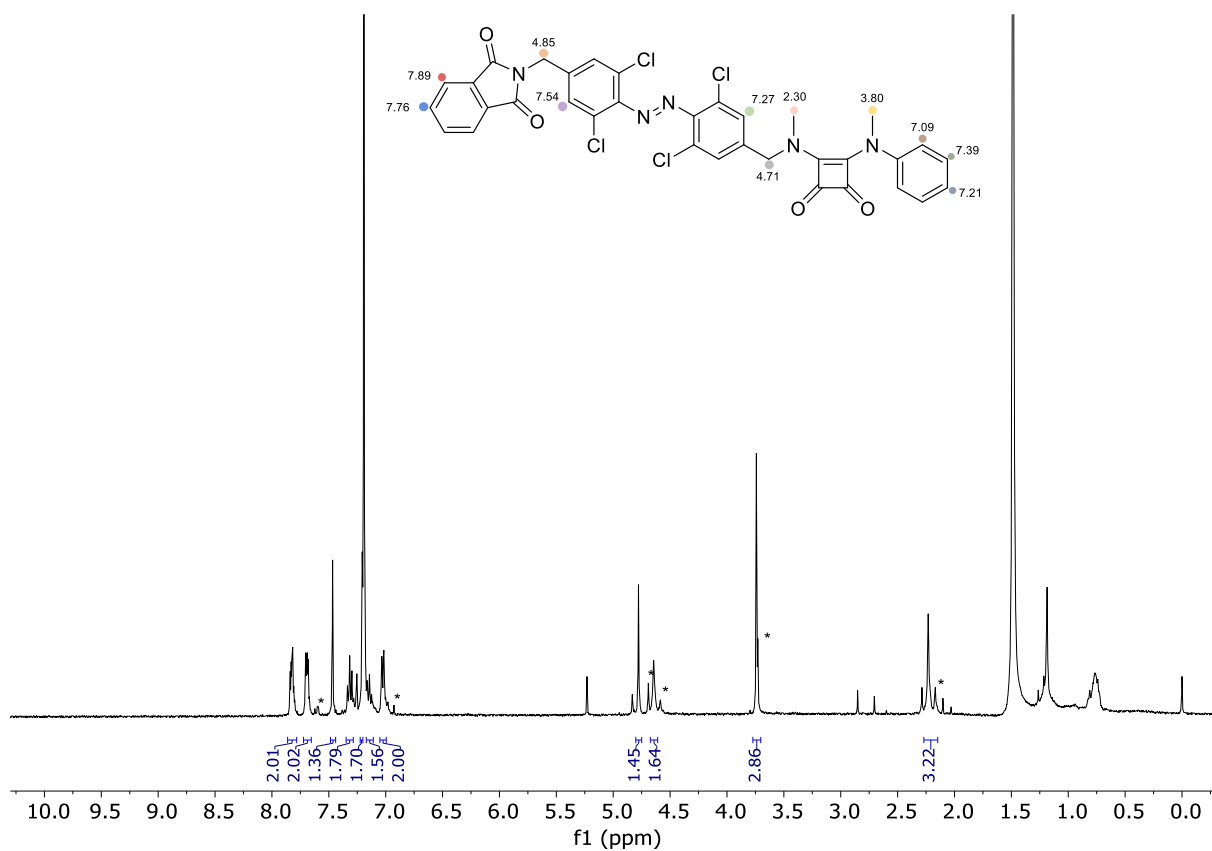


Figure S63. ^1H NMR spectrum of *E-35* (Chloroform-*d*, 298 K). *Z-35* signals labelled as *.

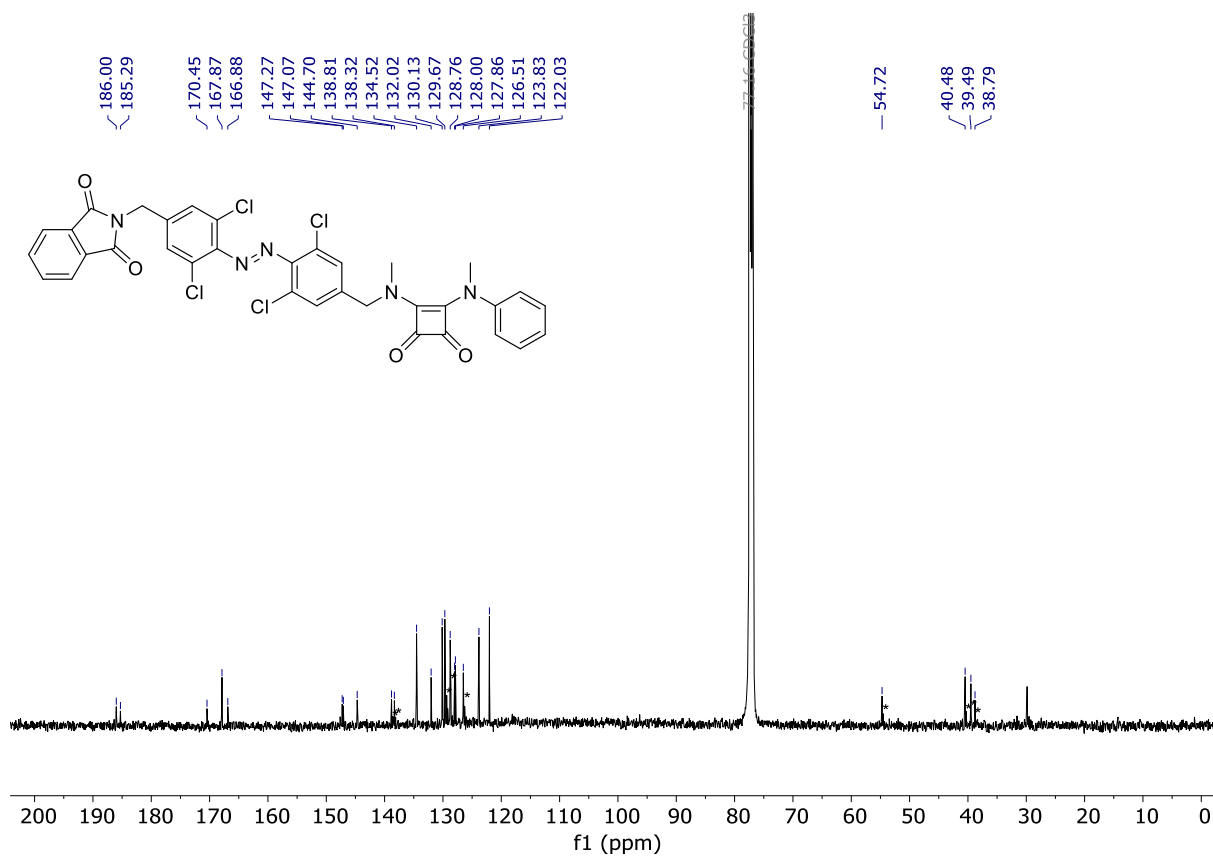


Figure S64. ^{13}C NMR spectrum of *E-35* (Chloroform-*d*, 298 K).

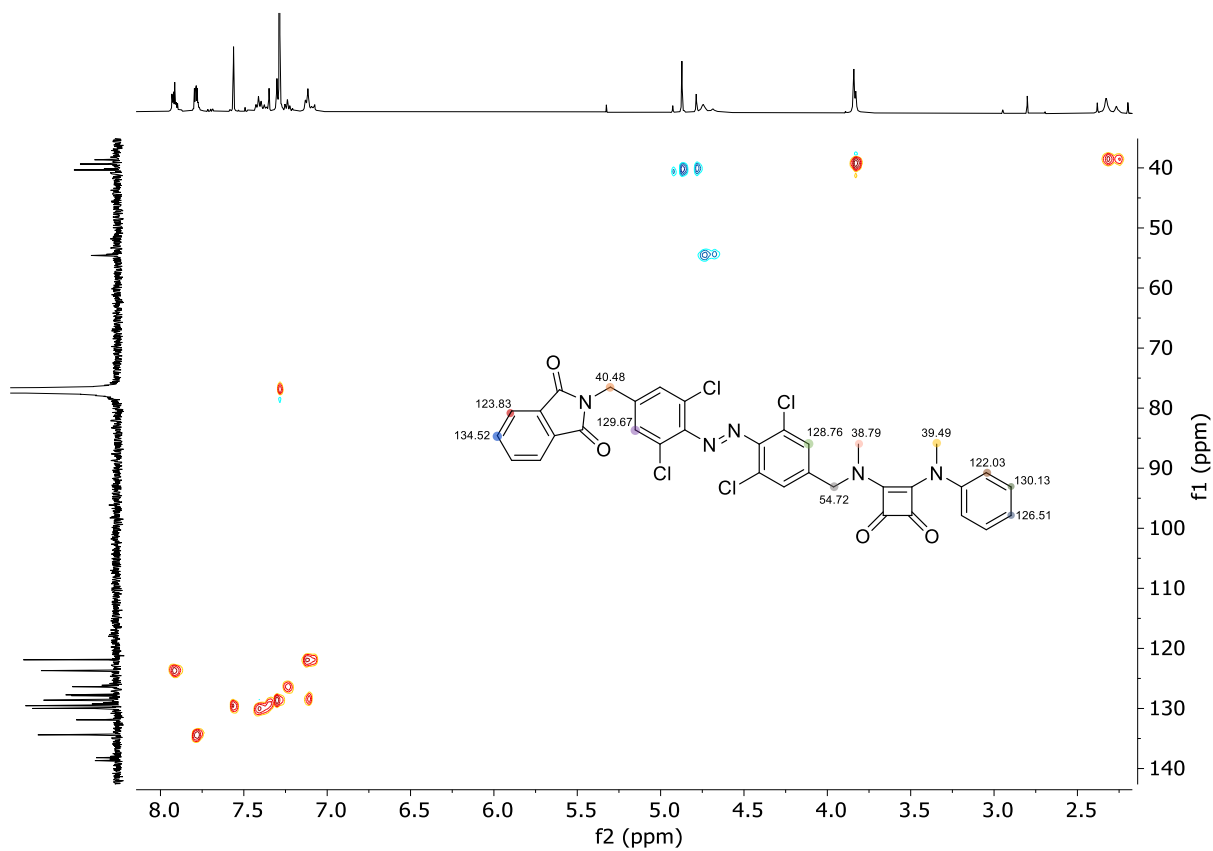


Figure S65. HSQC of *E-35*. Key ^1H - ^{13}C correlations highlighted. (Chloroform-*d*, 298 K).

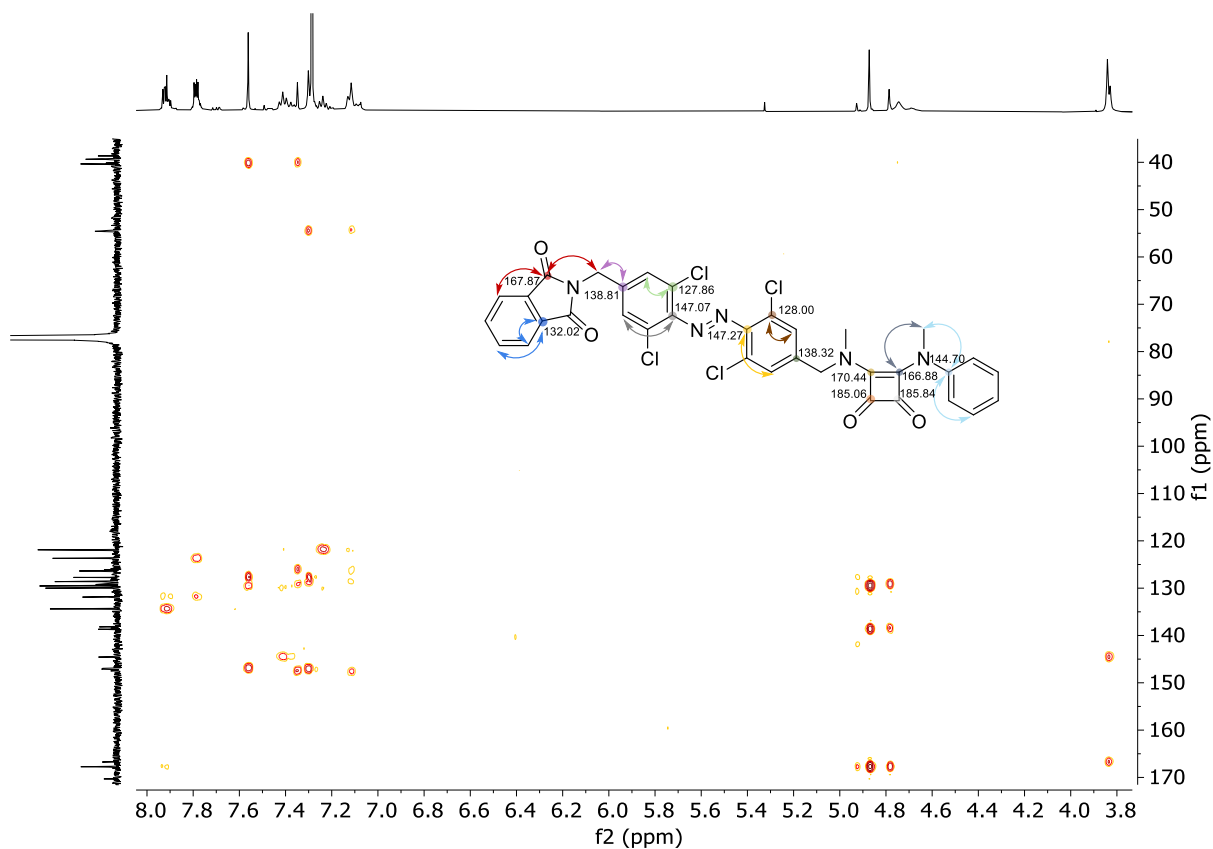


Figure S66. HMBC of *E*-**35**. Key ^1H - ^{13}C correlations highlighted. (Chloroform-*d*, 298 K).

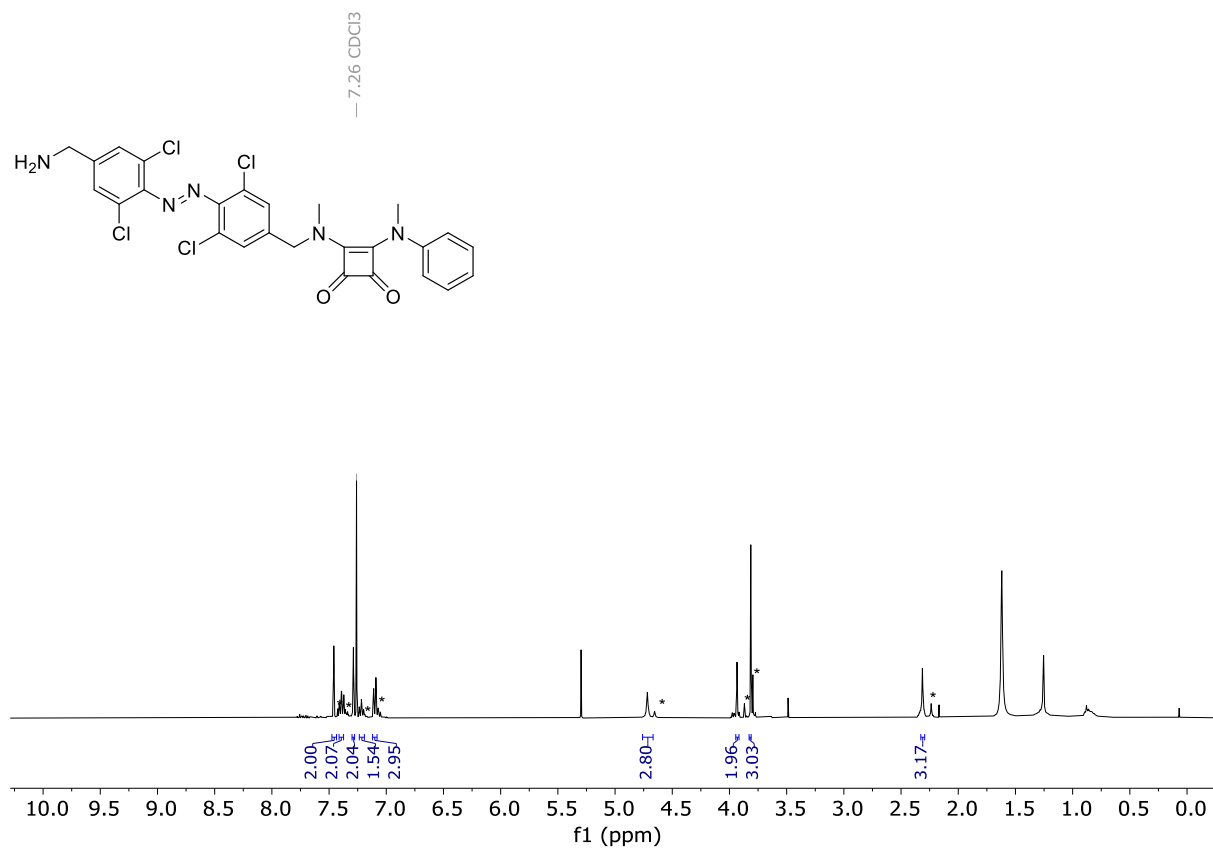


Figure S67. ^1H NMR spectrum of **36** (Chloroform-*d*, 298 K). *Z*-**36** signals labelled as *.

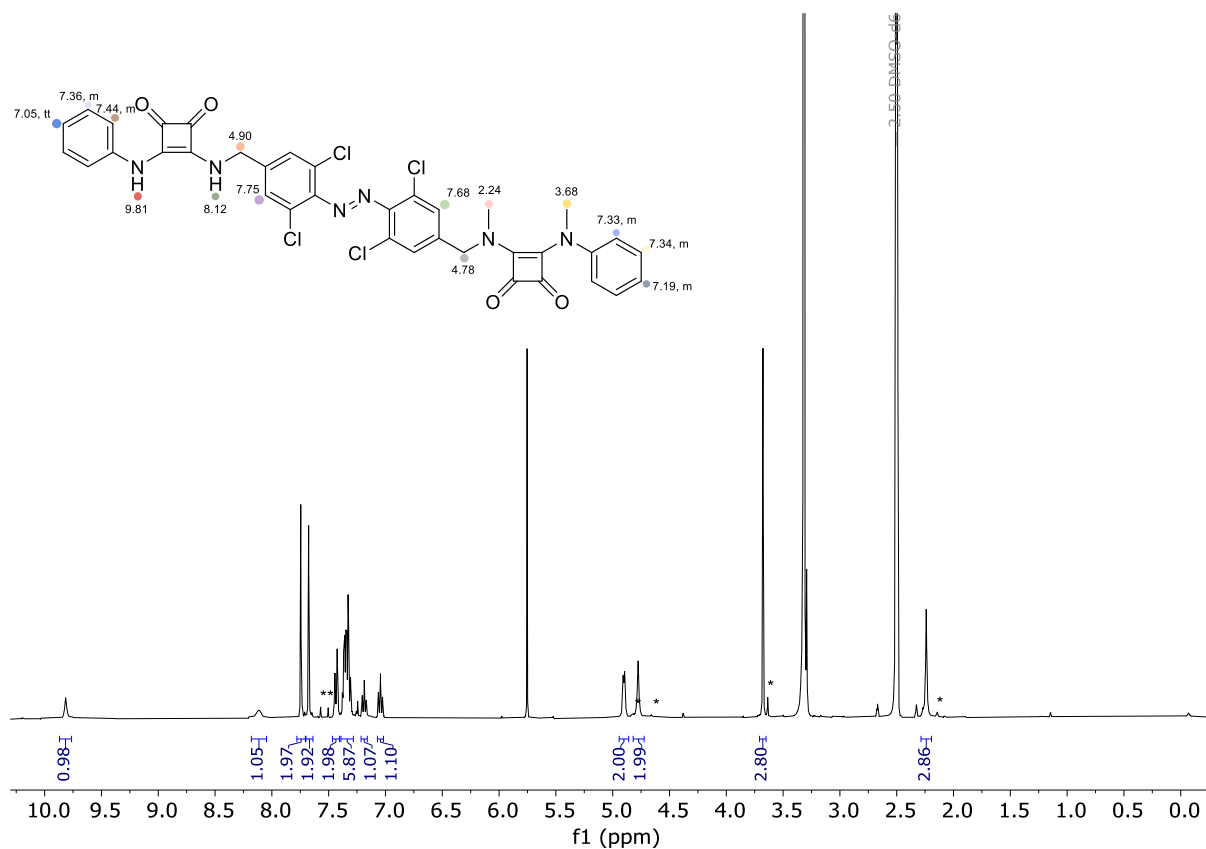


Figure S68. ¹H NMR spectrum of **4** (DMSO-d₆, 298 K). **Z-4** signals labelled as *.

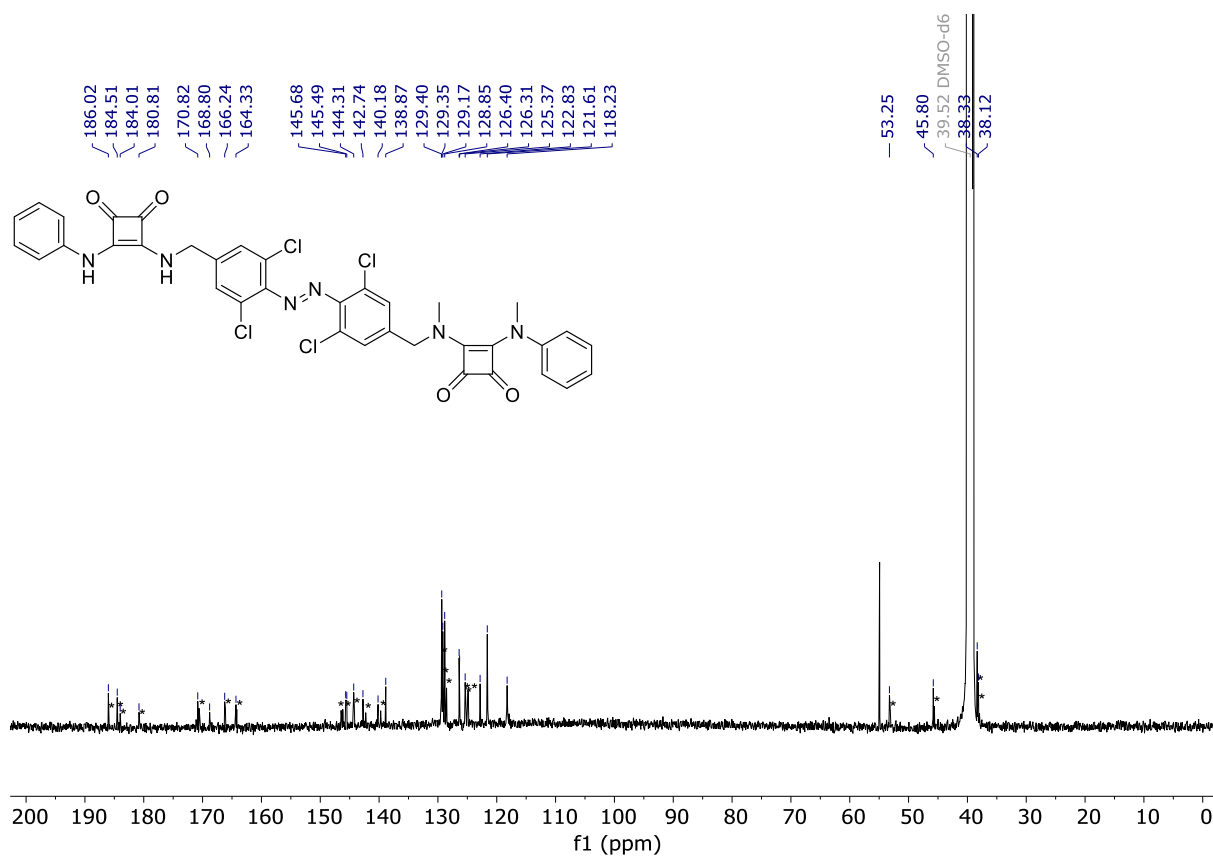


Figure S69. ¹³C NMR Spectrum of **E-1i**. (DMSO-d₆, 298 K). **Z-4** signals labelled as *.

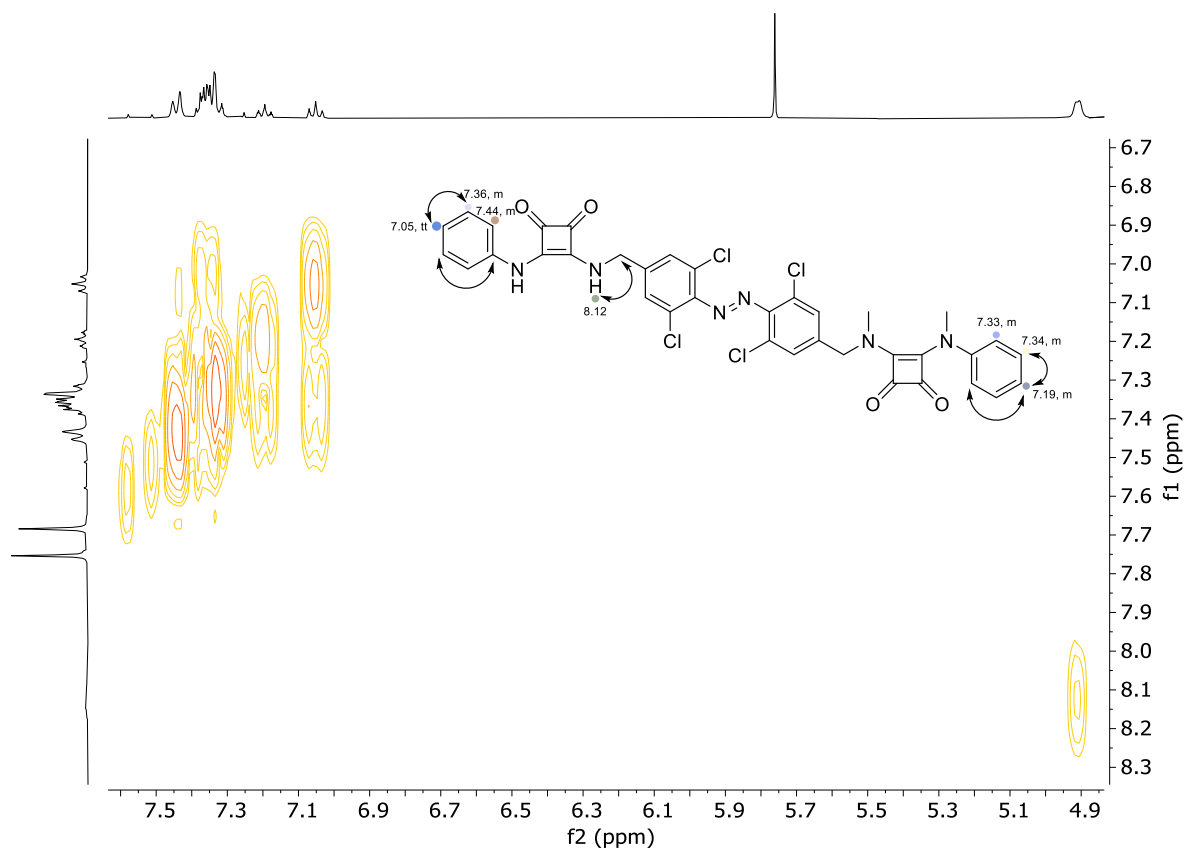


Figure S70. COSY of 4. Key ^1H – ^1H correlations highlighted. (DMSO- d_6 , 298 K).

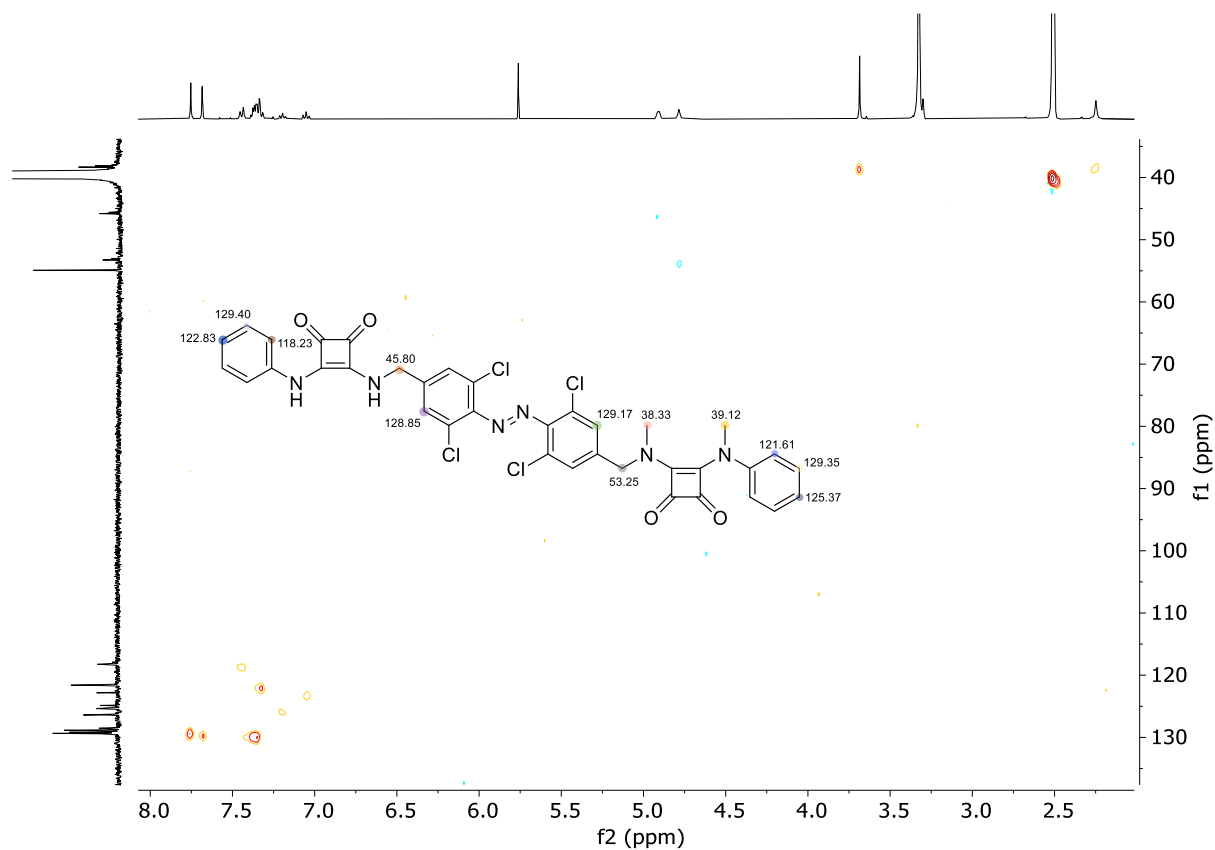


Figure S71. HSQC of 4. Key ^1H – ^{13}C correlations highlighted. (DMSO- d_6 , 298 K).

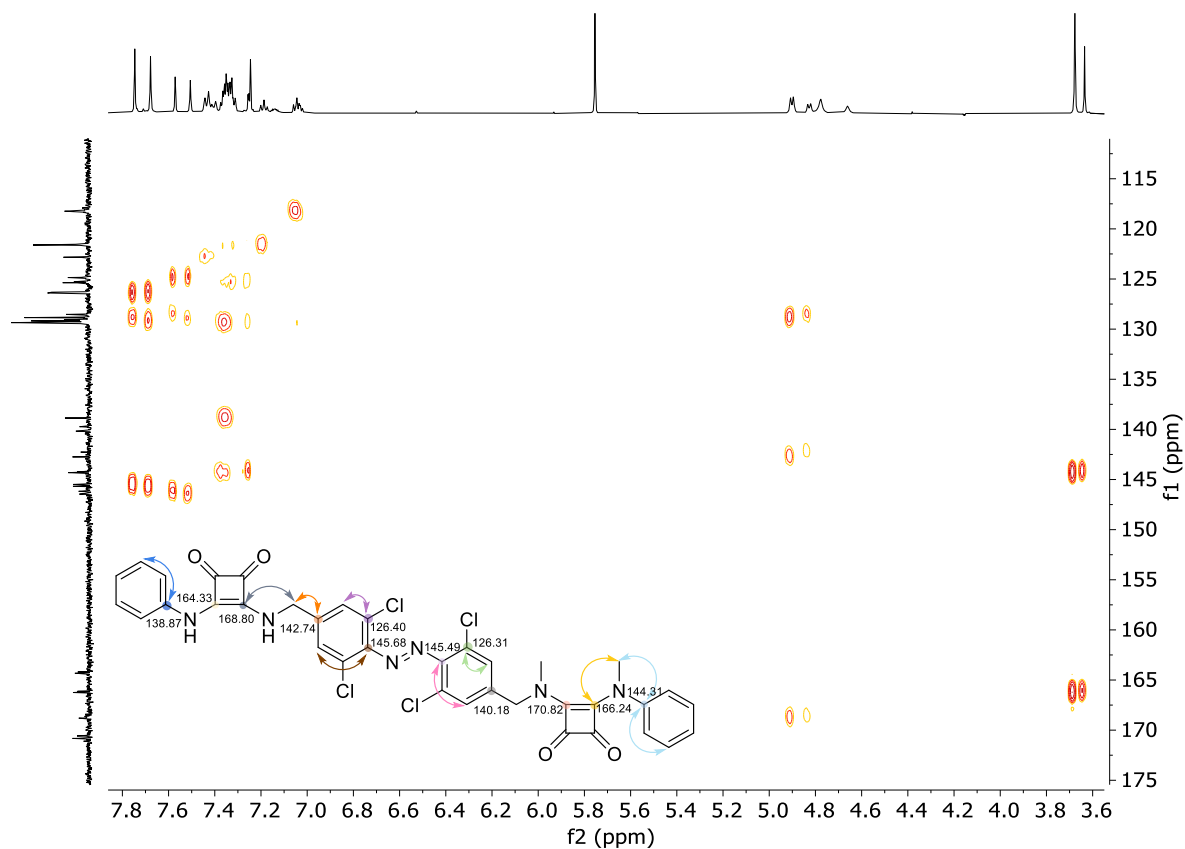


Figure S72. HMBC of **4**. Key ^1H - ^{13}C correlations highlighted. (DMSO- d_6 , 298 K).

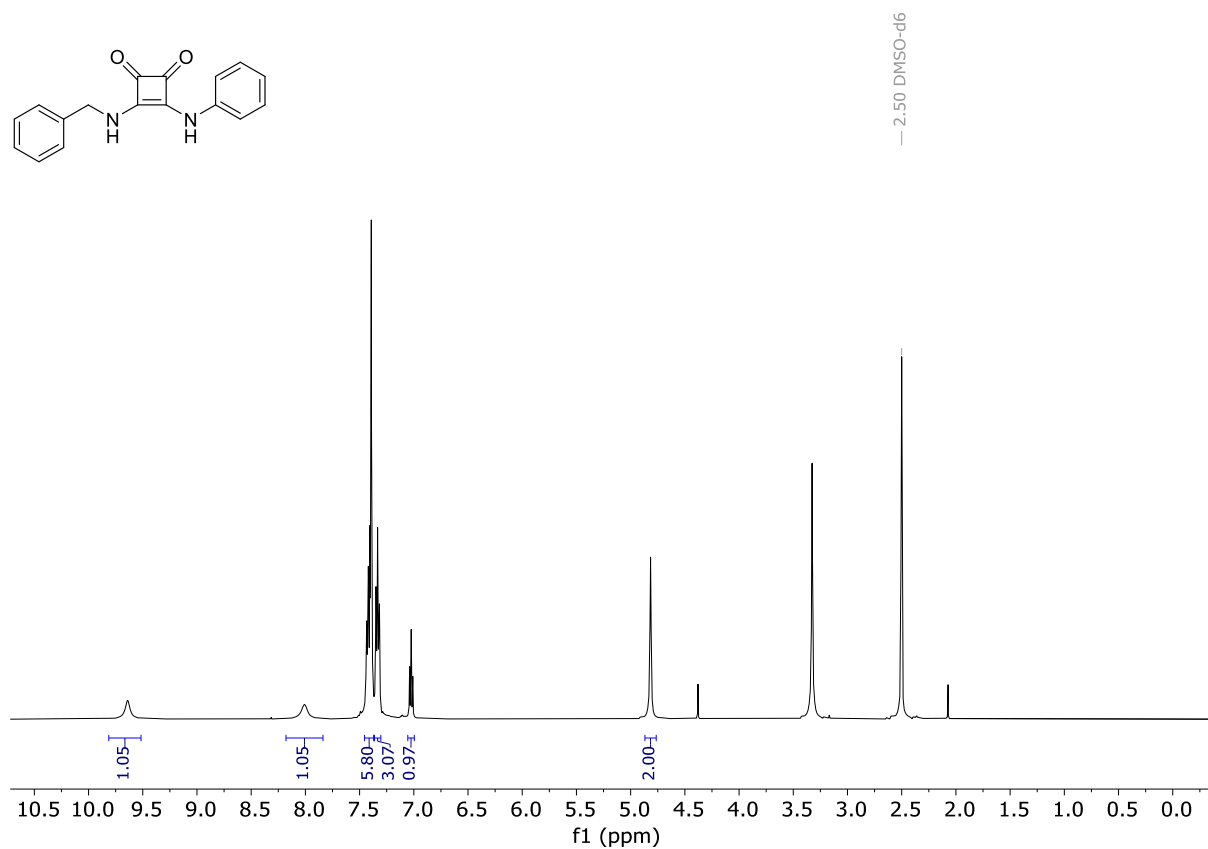


Figure S73. ^1H NMR spectrum of **37** (DMSO- d_6 , 298 K).

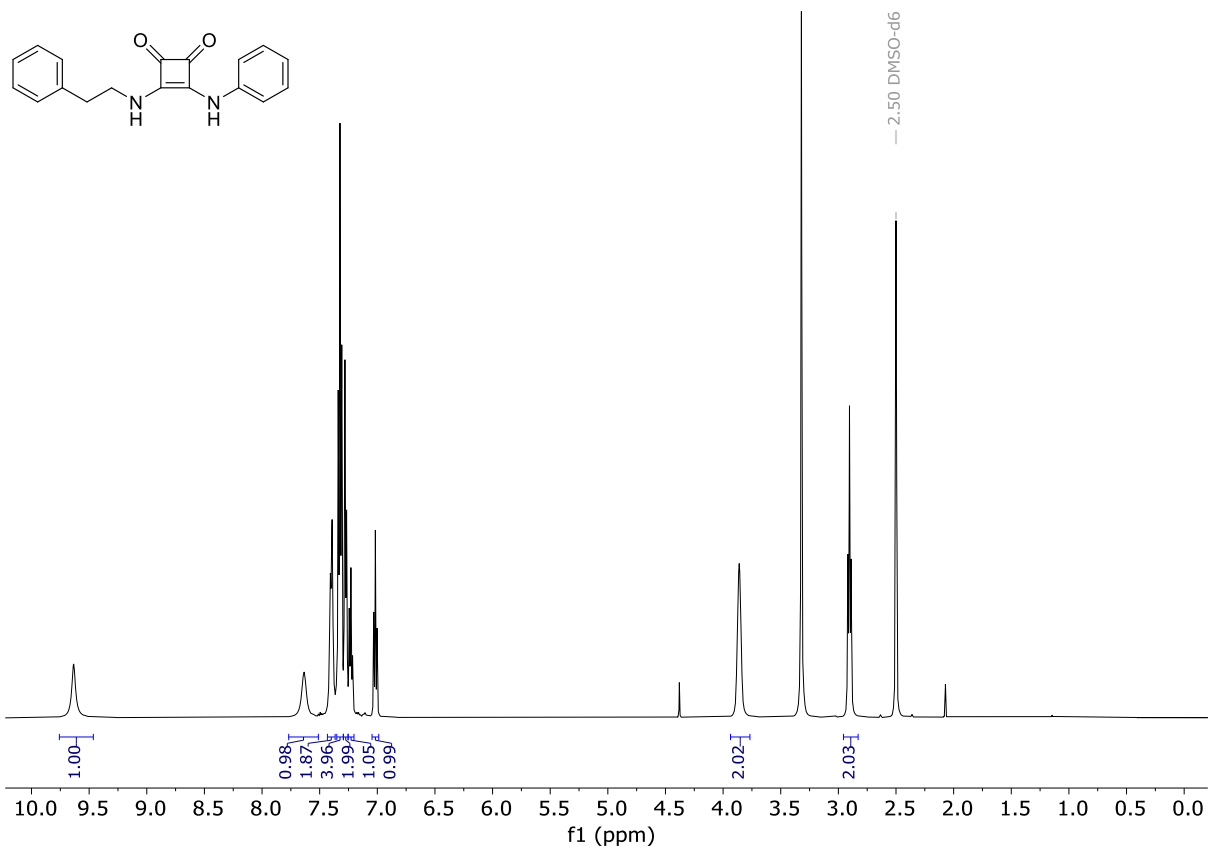


Figure S74. ¹H NMR spectrum of **38** (DMSO-d₆, 298 K).

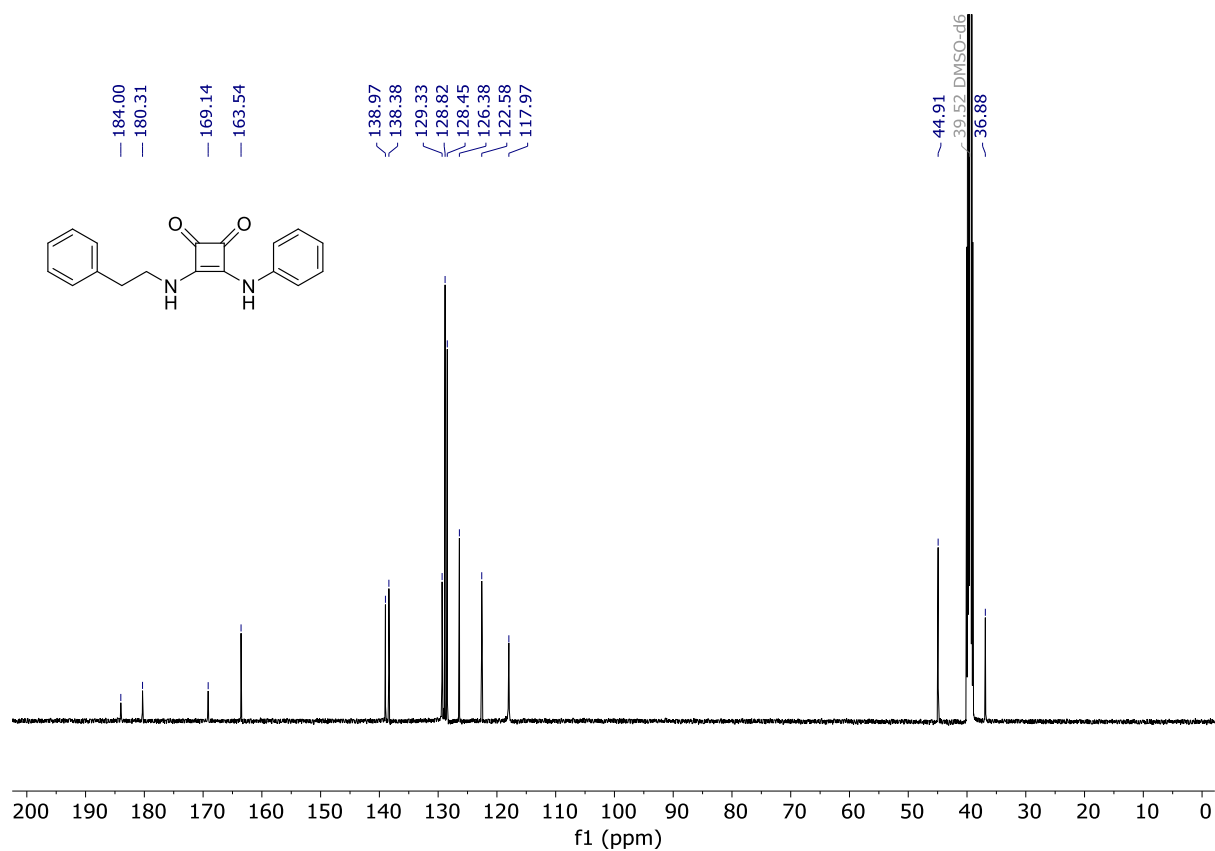


Figure S75. ¹³C NMR spectrum of **38** (DMSO-d₆, 298 K).

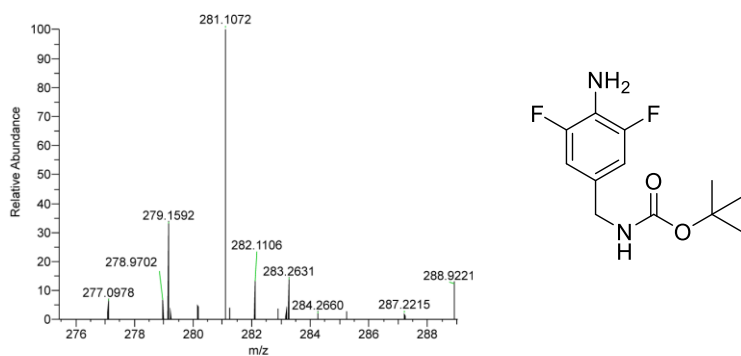


Figure S76. HRMS spectrum of **8**. HRMS-ESI (m/z) Calculated for $C_{12}H_{16}O_2N_2F_2$ $[M+Na]^+$, 281.1072; found 281.1072.

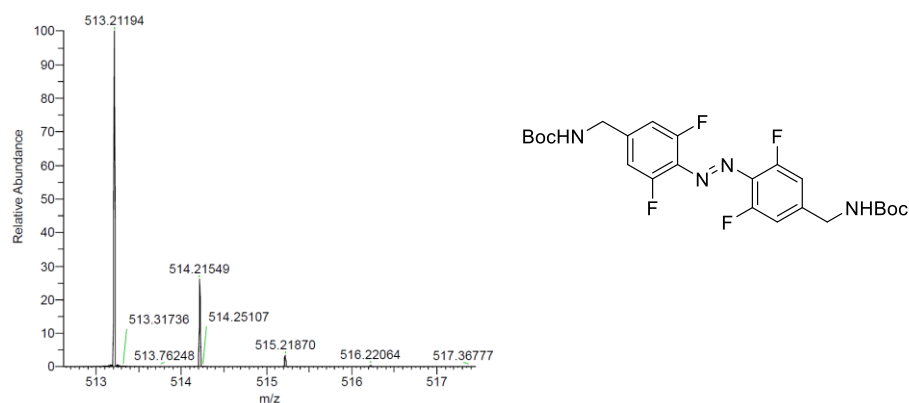


Figure S77. HRMS spectrum of **9**. HRMS-ESI (m/z) Calculated for $C_{24}H_{28}F_4N_4O_4$ $[M+H]^+$, 513.2119; found 513.2119.

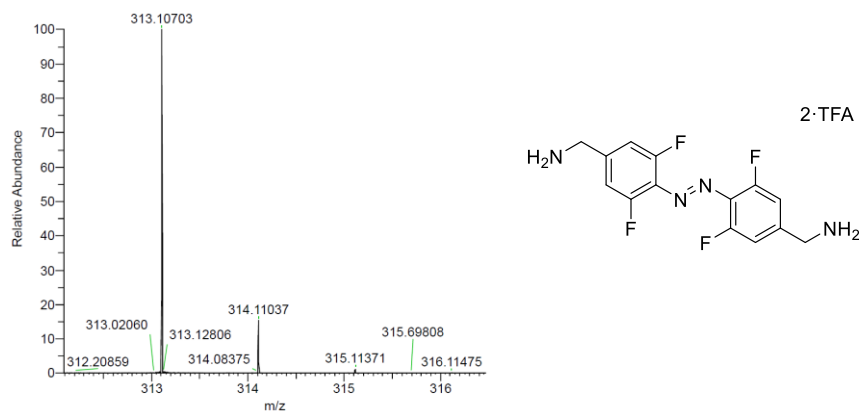


Figure S78. HRMS spectrum of **10**. HRMS-ESI (m/z) Calculated for $C_{14}H_{12}F_4N_4$ $[M+H]^+$, 313.1071; found 313.1070.

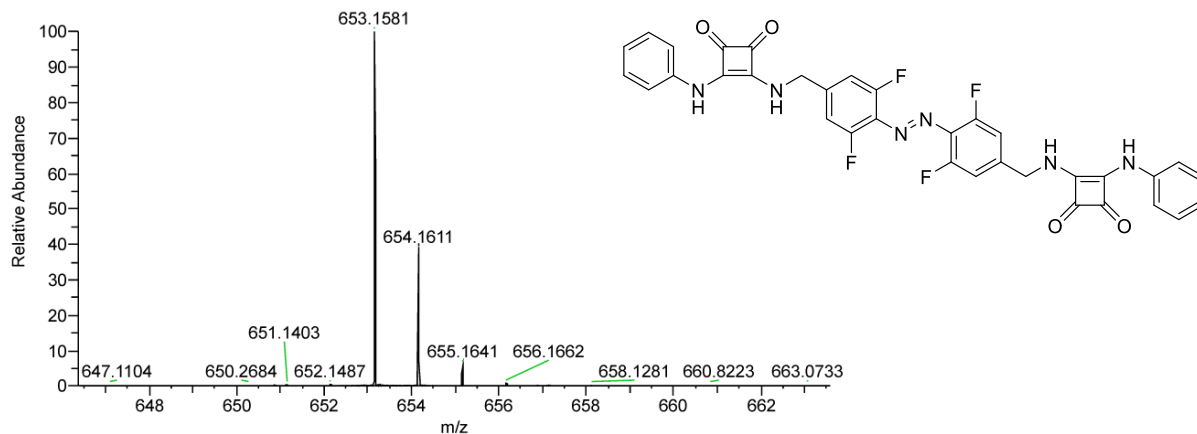


Figure S79. HRMS spectrum of **1b**. HRMS-ESI (m/z) calculated for $C_{34}H_{21}F_4N_6O_4^-$ [M-H]⁻, 653.1566, found 653.1581.

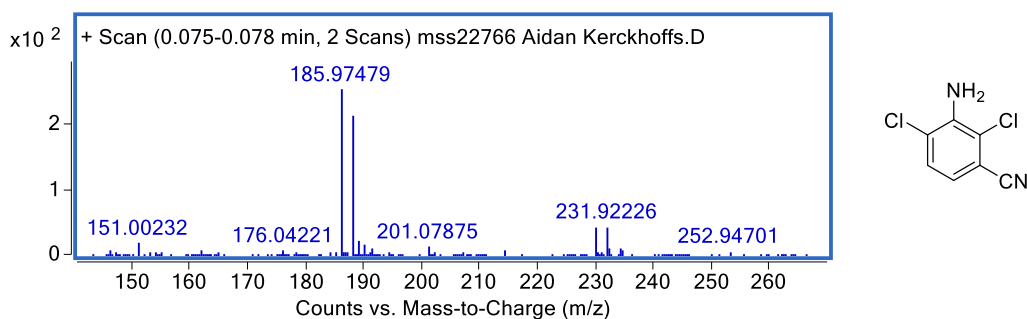


Figure S80. HRMS spectrum of **S4**. HRMS-EI (m/z) Calculated for $C_7H_4Cl_2N_2$ 185.9752; found 185.9748

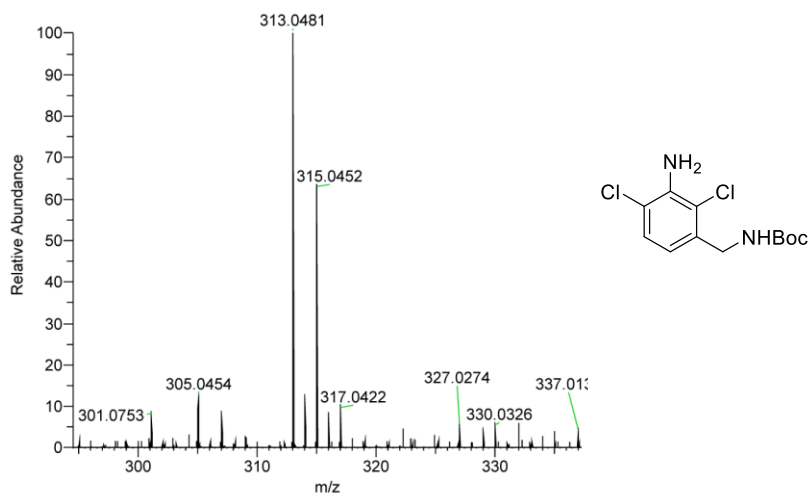


Figure S81. HRMS spectrum of **12**. HRMS-ESI (m/z) Calculated for $C_{12}H_{16}Cl_2N_2O_2$ [M+Na]⁺, 313.0481; found 313.0481.

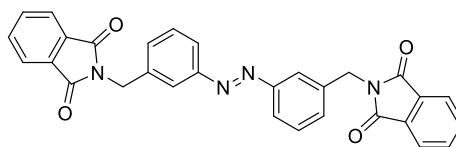
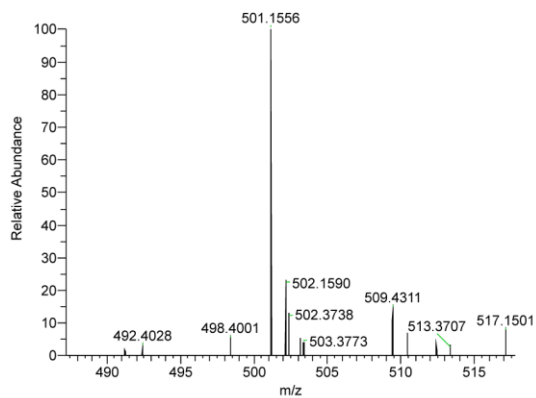


Figure S82. HRMS spectrum of **16**. HRMS-ESI (m/z) Calculated for $C_{30}H_{20}N_4O_4$ $[M+H]^+$, 501.1557; found 501.1556

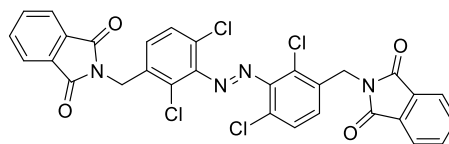
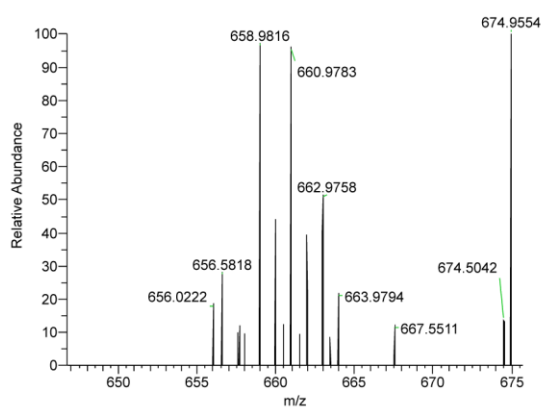


Figure S83. HRMS spectrum of **17**. HRMS-ESI (m/z) Calculated for $C_{30}H_{16}Cl_4N_4O_4$ $[M+Na]^+$, 658.9823; found 658.9816

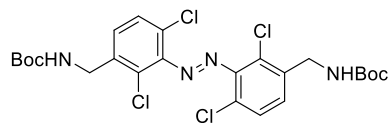
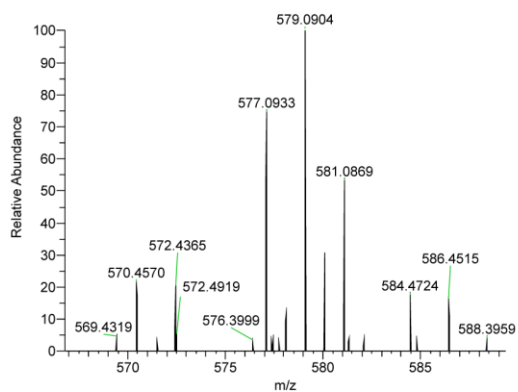


Figure S84. HRMS spectrum of **13**. HRMS-ESI (m/z) Calculated for $C_{24}H_{28}Cl_4N_4O_4$ $[M+H]^+$, 577.0937; found 577.0933.

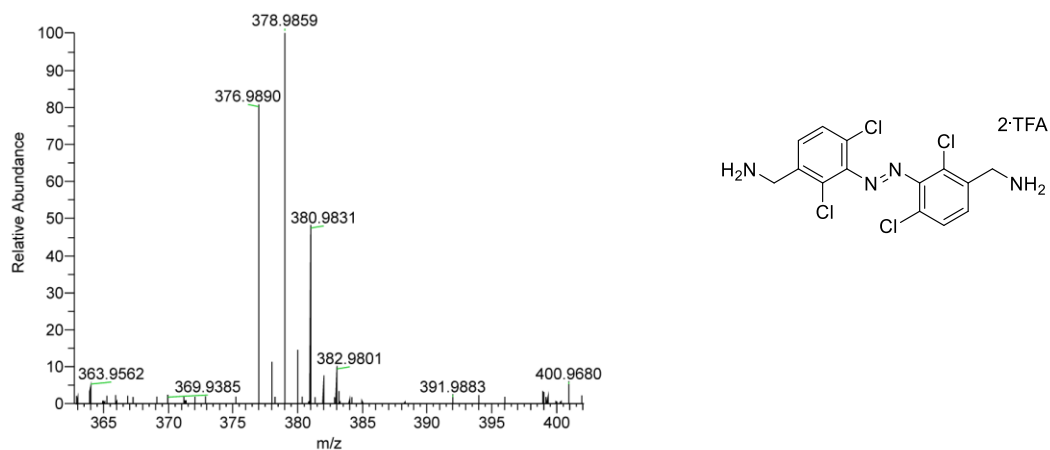


Figure S85. HRMS spectrum of **18**. HRMS-ESI (m/z) Calculated for $C_{14}H_{12}Cl_4N_4$ $[M+H]^+$, 376.9889; found 376.9890.

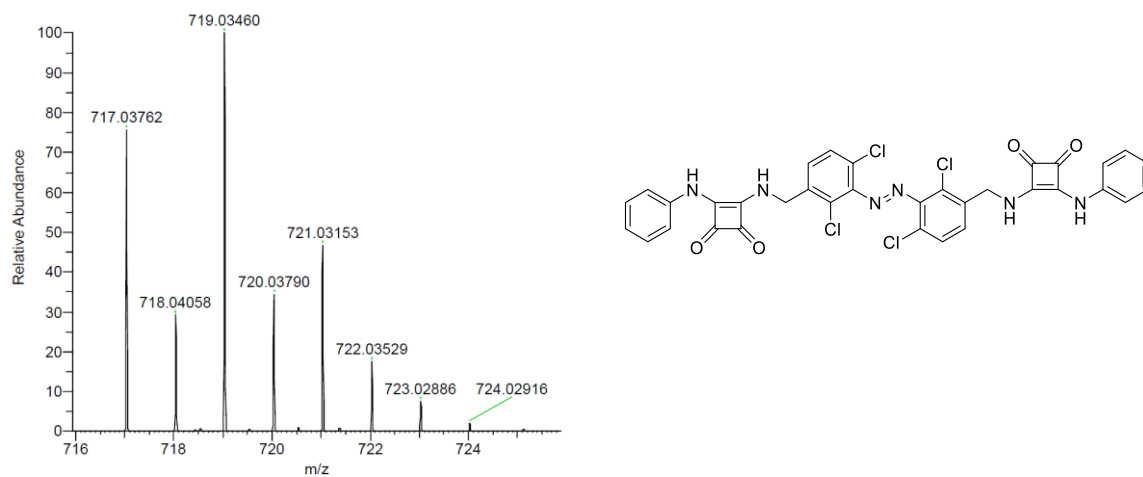


Figure S86. HRMS spectrum of **2**. HRMS-ESI (m/z) Calculated for $C_{34}H_{22}Cl_4N_6O_4$ $[M-H]^-$, 717.0373; found 717.0376.

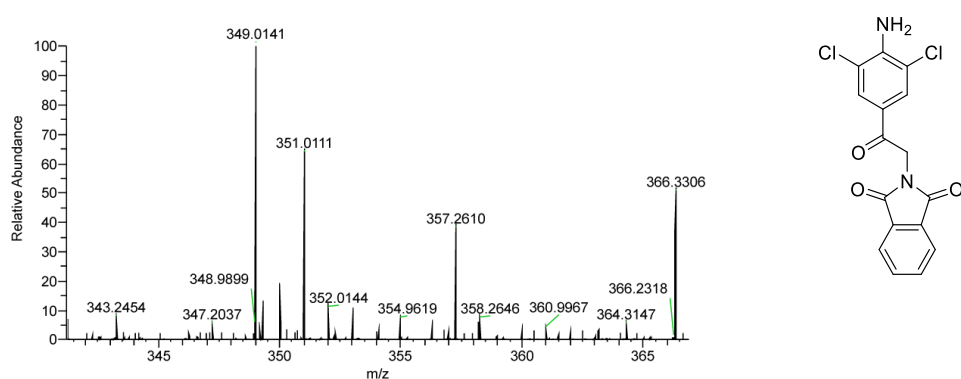


Figure S87. HRMS spectrum of **22**. HRMS-ESI (m/z) calculated for $C_{16}H_{10}Cl_2N_2O_3^+$ $[M+H]^+$, 349.0141; found 349.0141.

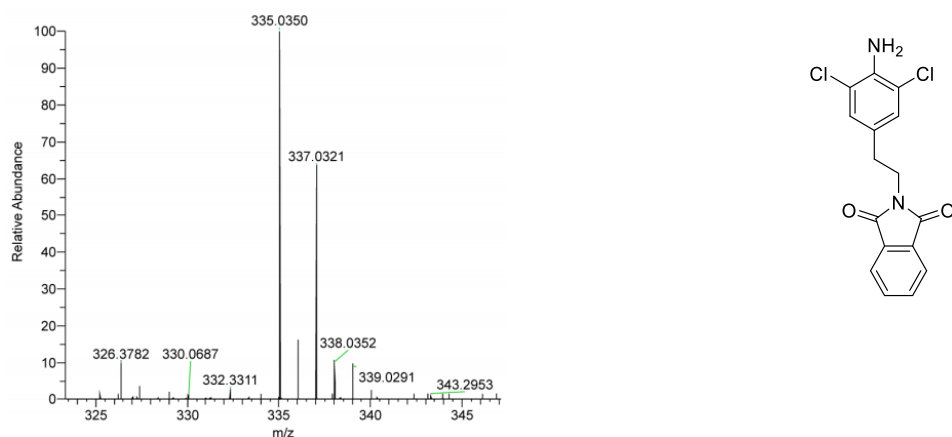


Figure S88. HRMS spectrum of **23**. HRMS-ESI (m/z) calculated for $C_{16}H_{13}Cl_2N_2O_2^+$ $[M+H]^+$, 335.0349, found 335.0350.

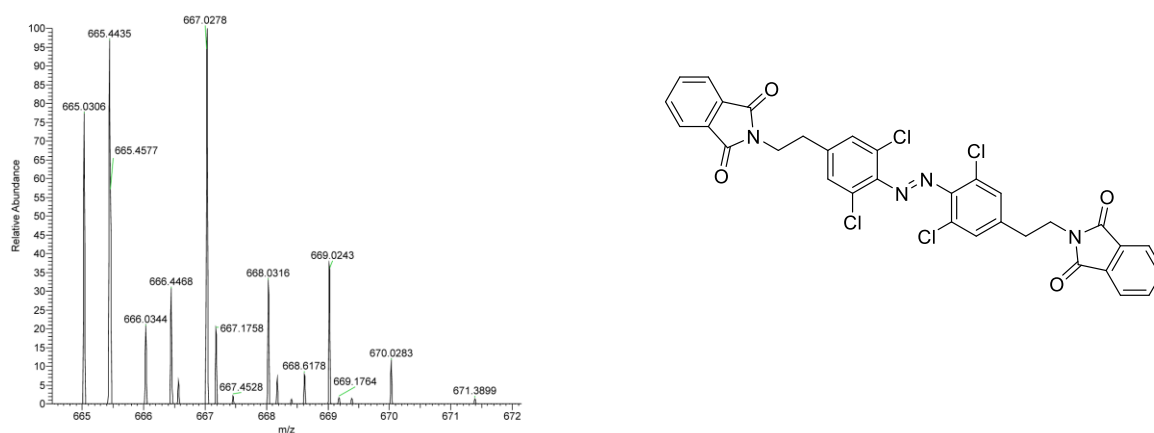


Figure S89. HRMS spectrum of **24**. HRMS-ESI (m/z) calculated for $C_{32}H_{21}Cl_4N_4O_4^+$ $[M+H]^+$, 665.0317; found 665.0306.

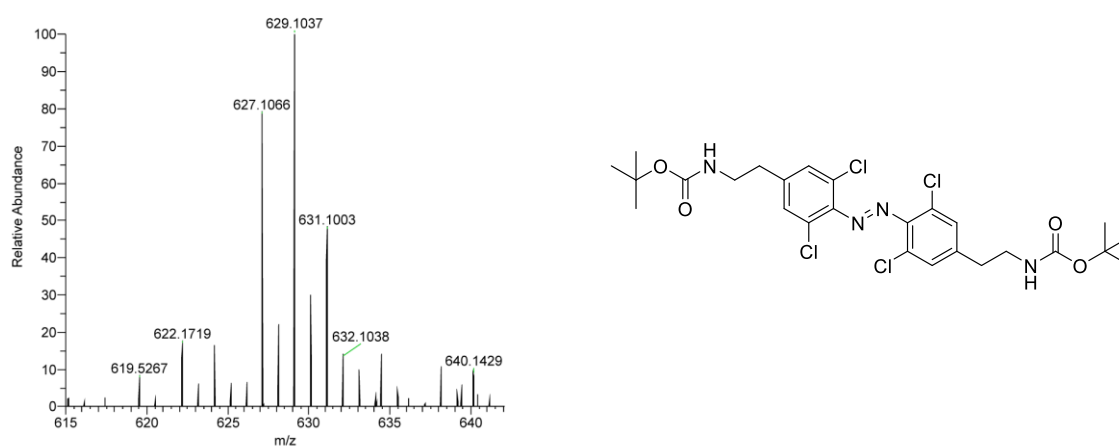


Figure S90. HRMS spectrum of **25**. HRMS-ESI (m/z) calculated for $C_{26}H_{32}Cl_4N_4O_4Na^+$ $[M+Na]^+$, 629.1042; found 629.1037.

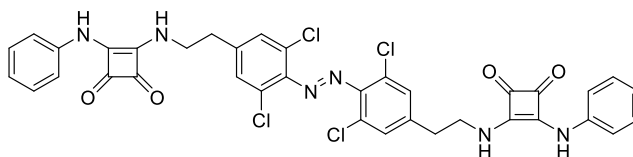
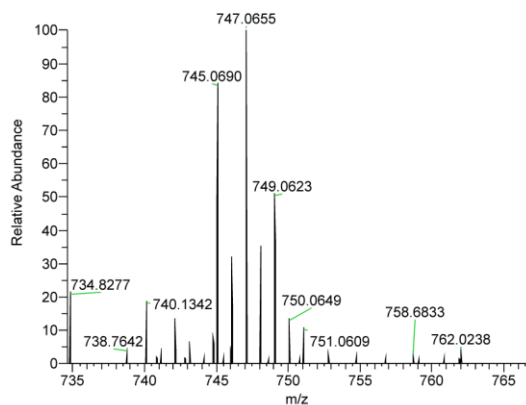


Figure S91. HRMS spectrum of **3**. HRMS-ESI (m/z) Calculated for $C_{36}H_{26}Cl_4N_6O_4$ [M-H]⁻, 745.0697; found 745.0690

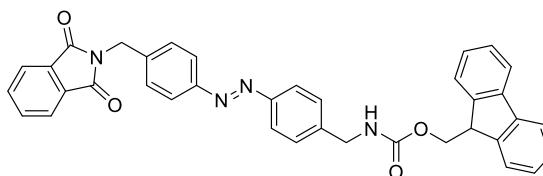
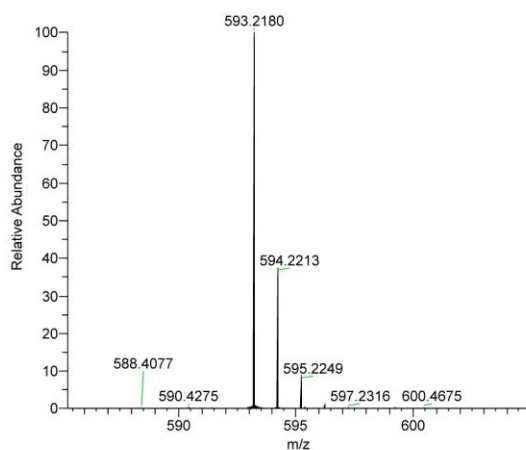


Figure S92. HRMS spectrum of **30**. HRMS-ESI (m/z) Calculated for $C_{37}H_{28}N_4O_4$ [M+H]⁺, 593.2183; found 593.2180

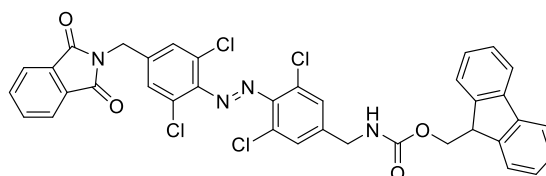
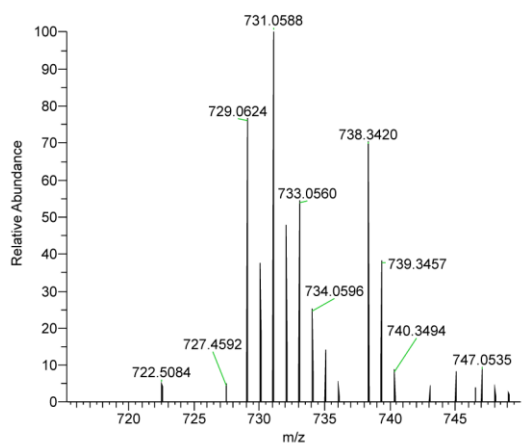


Figure S93. HRMS spectrum of **31**. HRMS-ESI (m/z) Calculated for $C_{37}H_{24}Cl_4N_4O_4$ [M-H]⁻, 729.0624; found 729.024

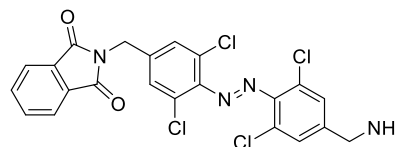
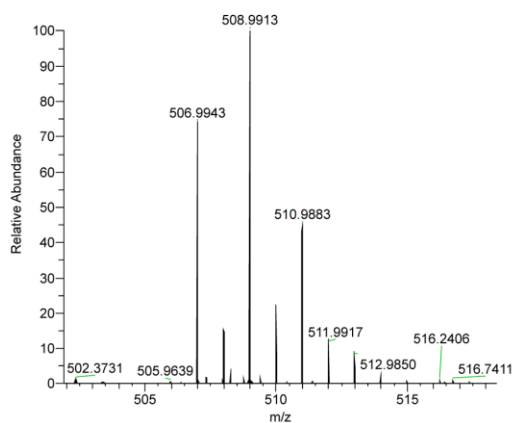


Figure S94. HRMS spectrum of **32**. HRMS-ESI (m/z) Calculated for $C_{22}H_{14}Cl_4N_4O_2$ $[M+H]^+$, 506.9944; found 506.9943

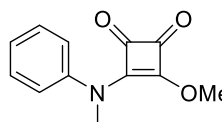
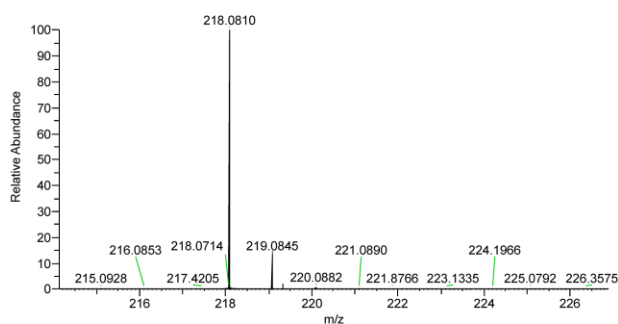


Figure S95. HRMS spectrum of **33**. HRMS-ESI (m/z) Calculated for $C_{12}H_{11}NO_3$ $[M+H]^+$, 218.0812; found 218.0810

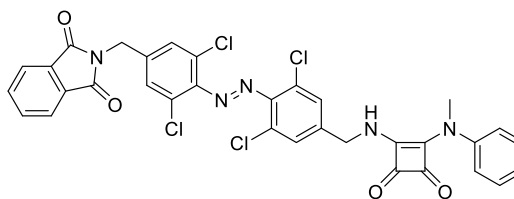
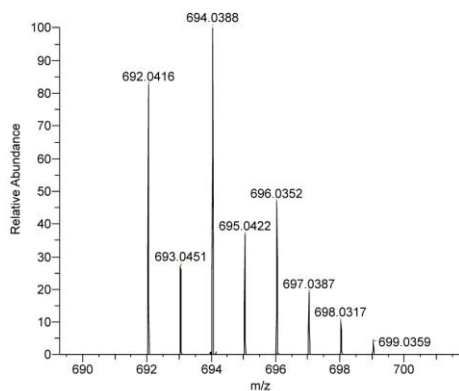


Figure S96. HRMS spectrum of **34**. HRMS-ESI (m/z) Calculated for $C_{33}H_{21}Cl_4N_5O_4$ $[M+H]^+$, 692.0420; found 692.0416

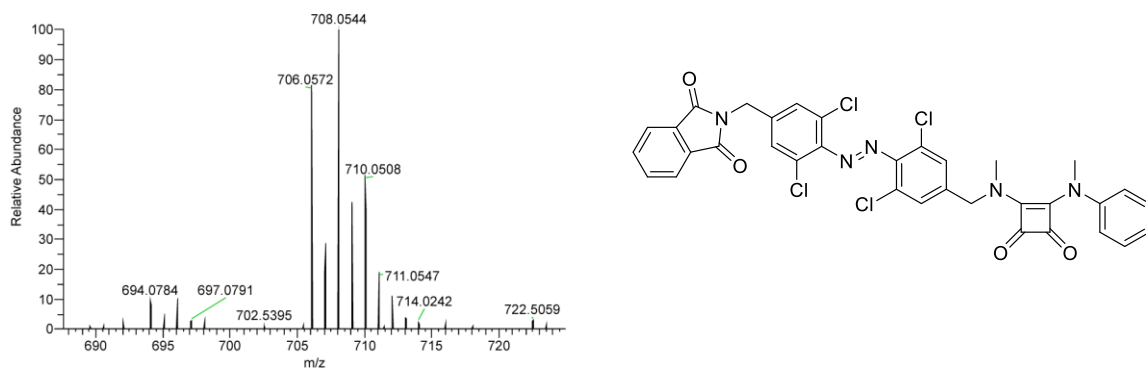


Figure S97. HRMS spectrum of **35**

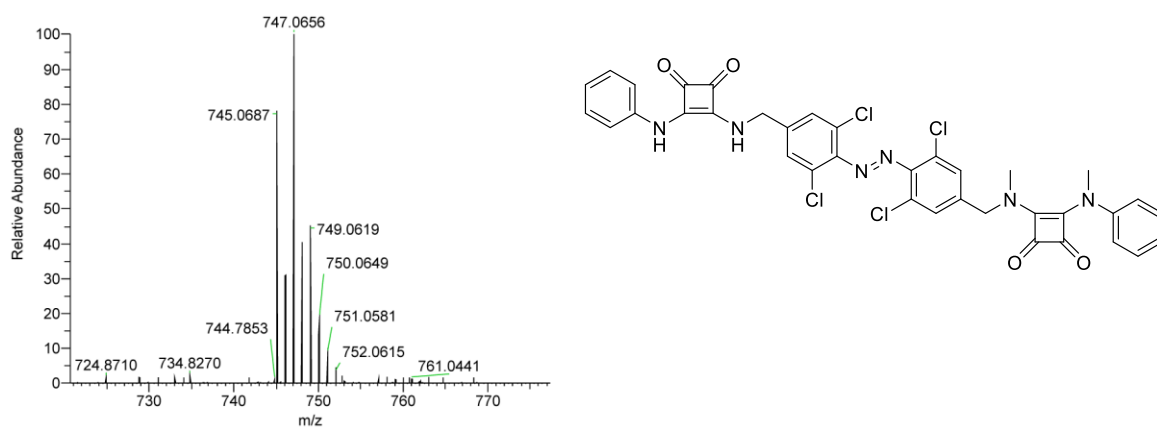


Figure S98. HRMS spectrum of **4**. HRMS-ESI (m/z) Calculated for $C_{36}H_{26}Cl_4N_6O_4$ [M-H]⁻, 745.0697; found 745.0687.

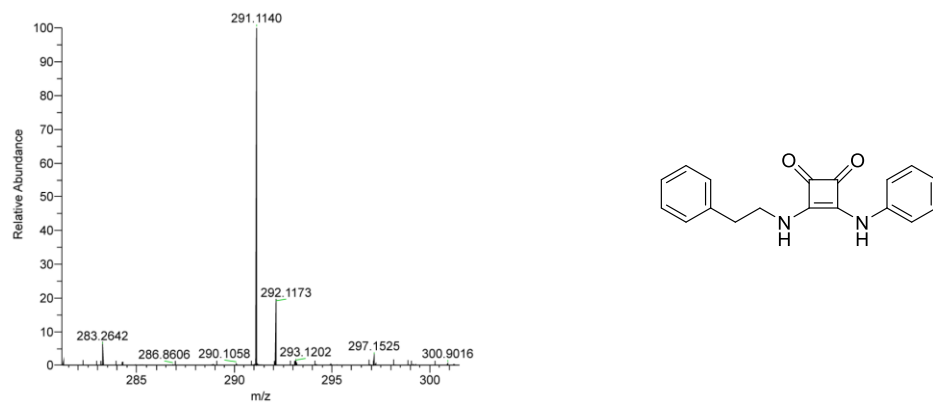


Figure S99. HRMS spectrum of **S38**

3. Photo-switching experiments

Photo-irradiation of liquid samples was carried out using Thorlabs high-power mounted LEDs (models M625L4 (red, 625 nm); M530L4 (green, 530 nm), M455L4 (blue, 455 nm) and M405L4 (purple, 405 nm) in-house custom built set-ups using optical components supplied by Thorlabs, as described in reference ¹

All UV-vis spectra were determined in DMSO solution. Extinction coefficients were determined by recording a UV-vis spectra for the *E* isomer at 10, 20, 30, 40 μM in DMSO respectively. The absorbance at the maximum of the $\pi - \pi^*$ transition of the *E*-isomers was plotted against concentration (Beer-Lambert plot) to determine the molar extinction coefficient ϵ . For each compound, the *E* isomer sample at 40 μM was irradiated with the appropriate wavelength of light to generate the photo-stationary state, and another spectrum was run. This spectrum was normalised to units of ϵ and overlaid with the dark (100% *E* isomer) spectrum

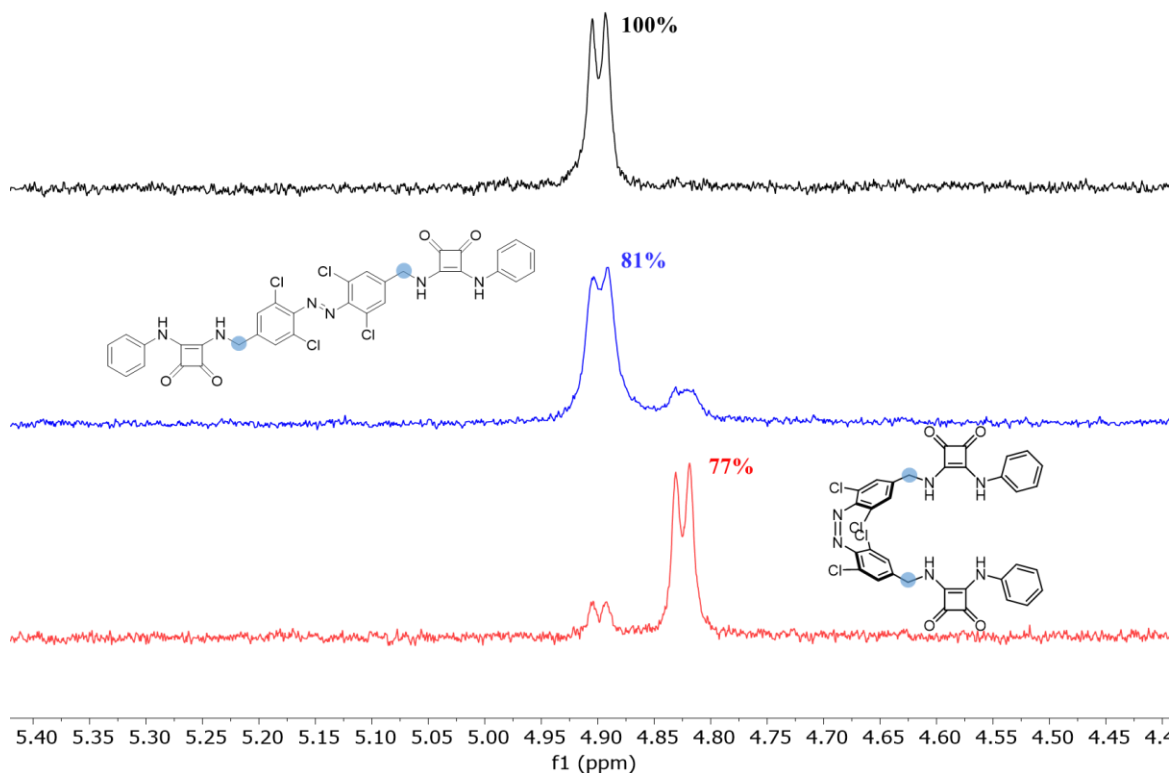


Figure S100. Partial ^1H NMR spectrum of **1a** in the dark (100% *E*), and PSS achieve by irradiation with blue 455 nm (81% *E*) and red 625 nm (77% *Z*) light.

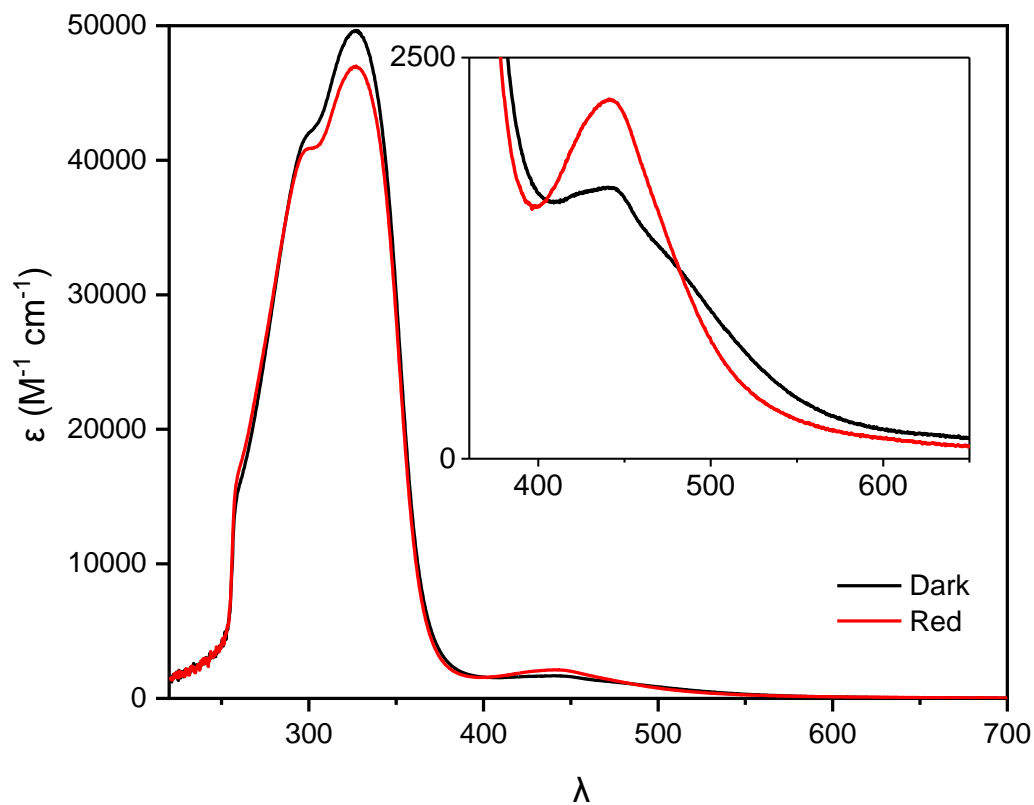


Figure S101. UV-vis Spectrum of **1a** in the dark (100% *E*) and red (77% *Z*) state.

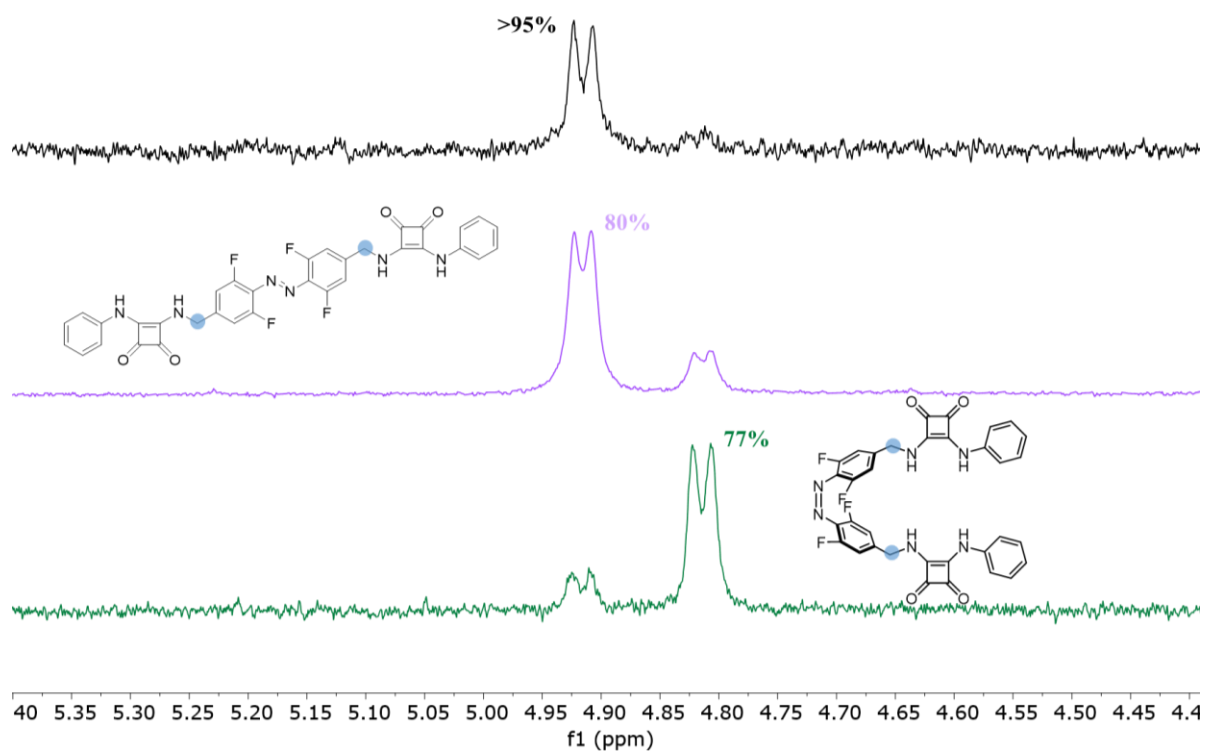


Figure S102. Partial ^1H NMR spectrum of **1b** in the dark (100% *E*), and PSS achieve by irradiation with purple 405 nm (80% *E*) and green 530 nm (77% *Z*) light.

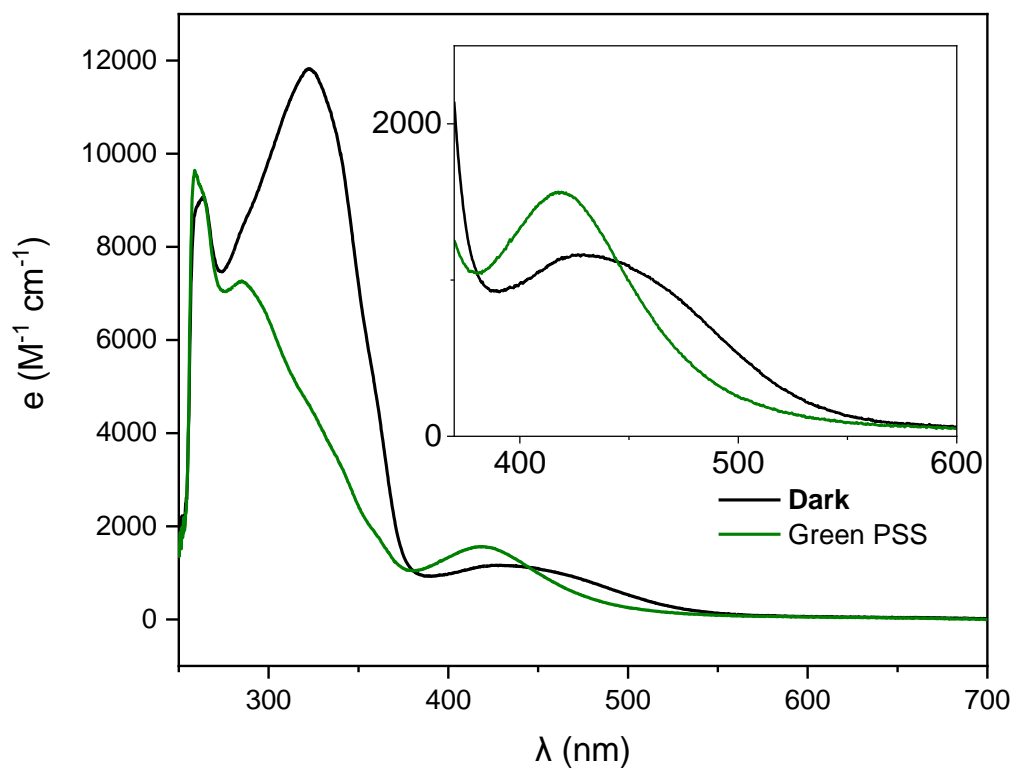


Figure S103. UV-vis spectrum of **1b** in the dark (100% *E*) and green (77% *Z*) state.

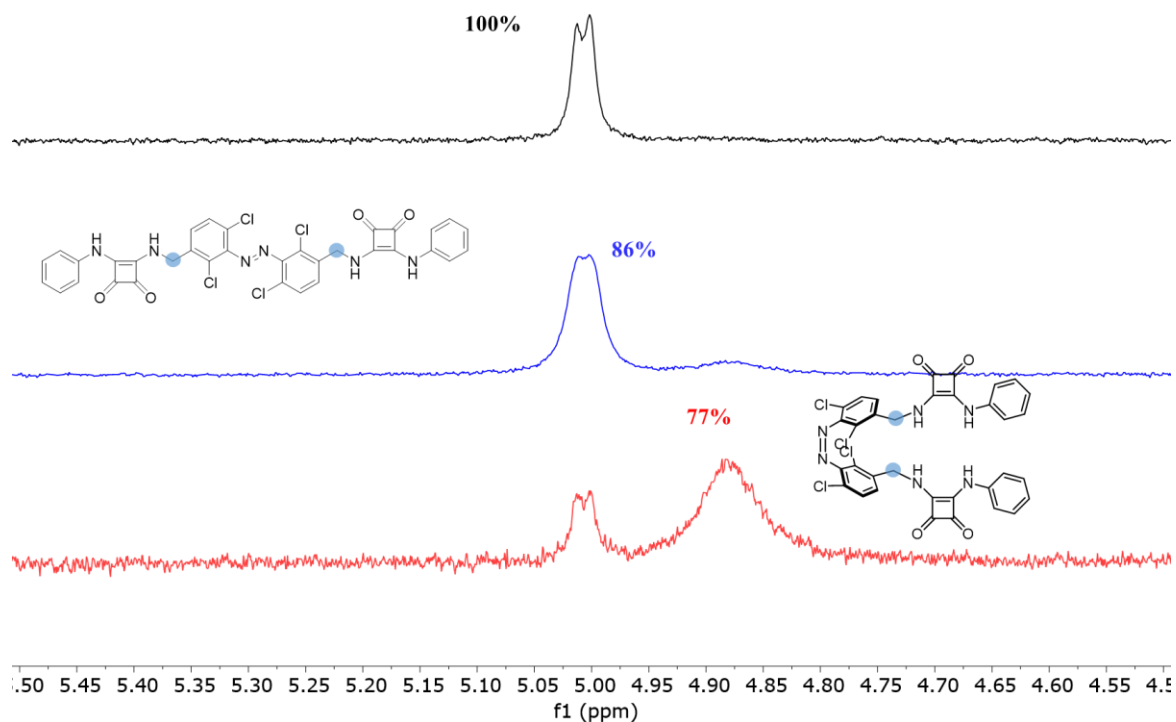


Figure S104. Partial ^1H NMR spectrum of **2** in the dark (100% *E*), and PSS achieved by irradiation with blue 455 nm (86% *E*) and red 625 nm (77% *Z*) light.

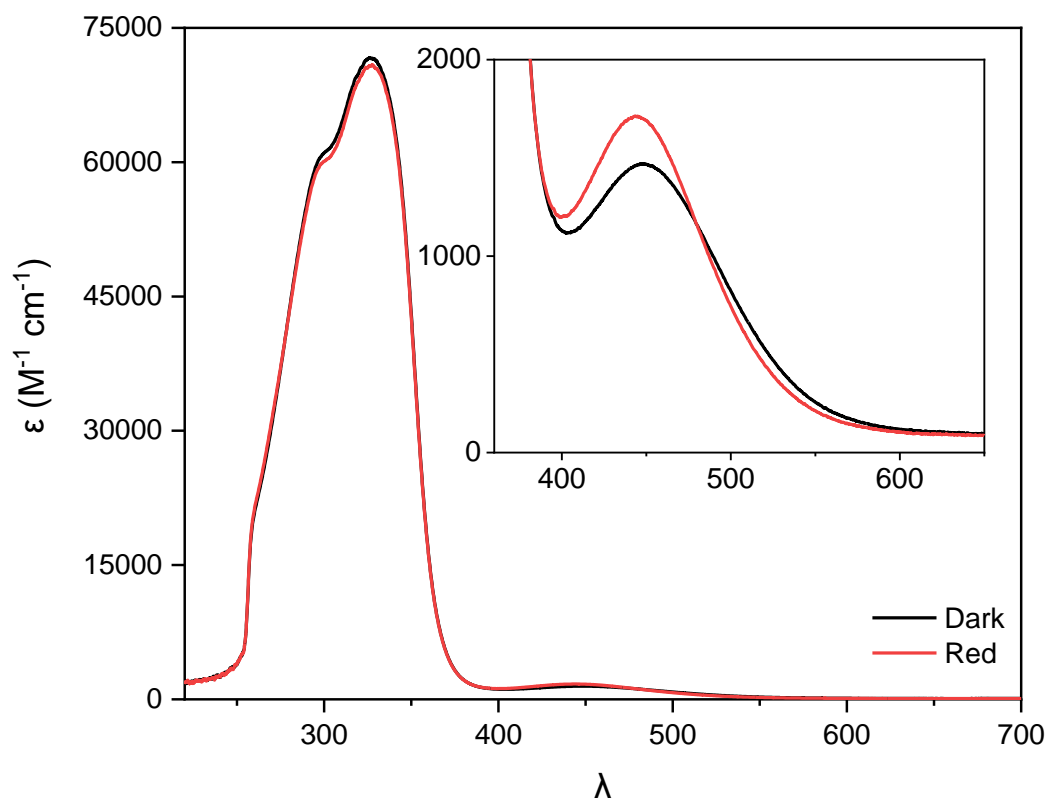


Figure S105. UV-vis spectrum of **2** in the dark (100% *E*) and red (77% *Z*) state.

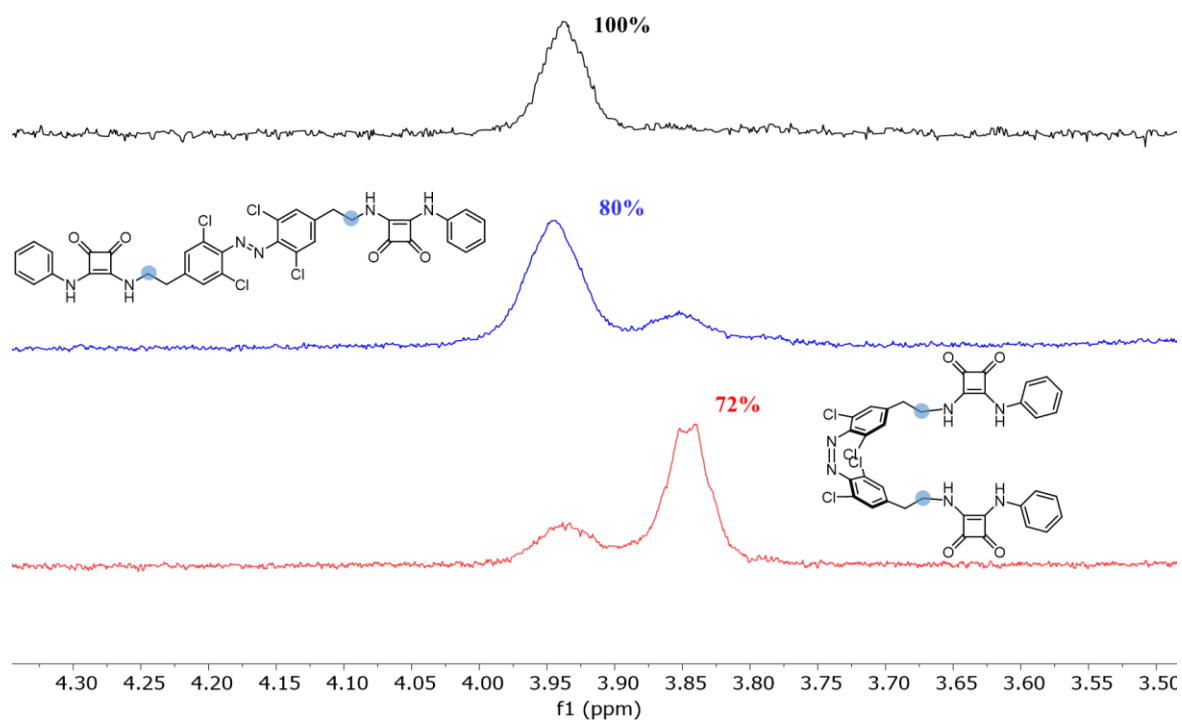


Figure S106. Partial ^1H NMR spectrum of **3** in the dark (100% *E*), and PSS achieved by irradiation with blue 455 nm (80% *E*) and red 625 nm (72% *Z*) light.

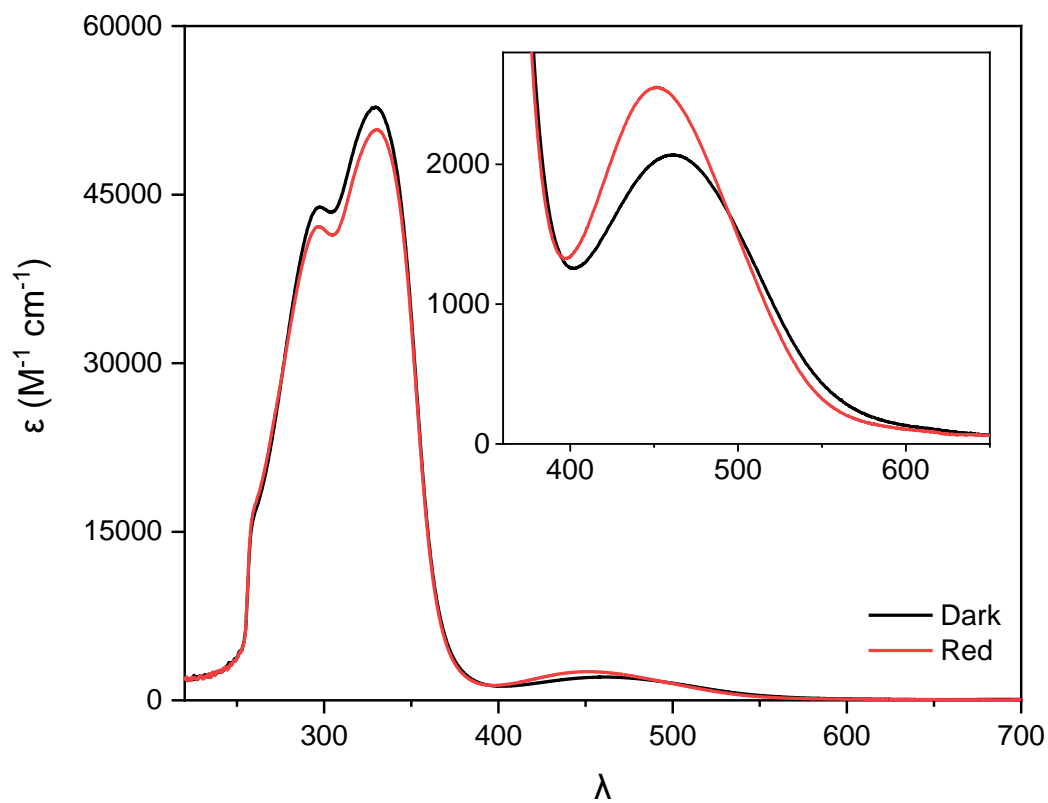


Figure S107. UV-vis Spectrum of **3** in the dark (100% *E*) and red (72% *Z*) state.

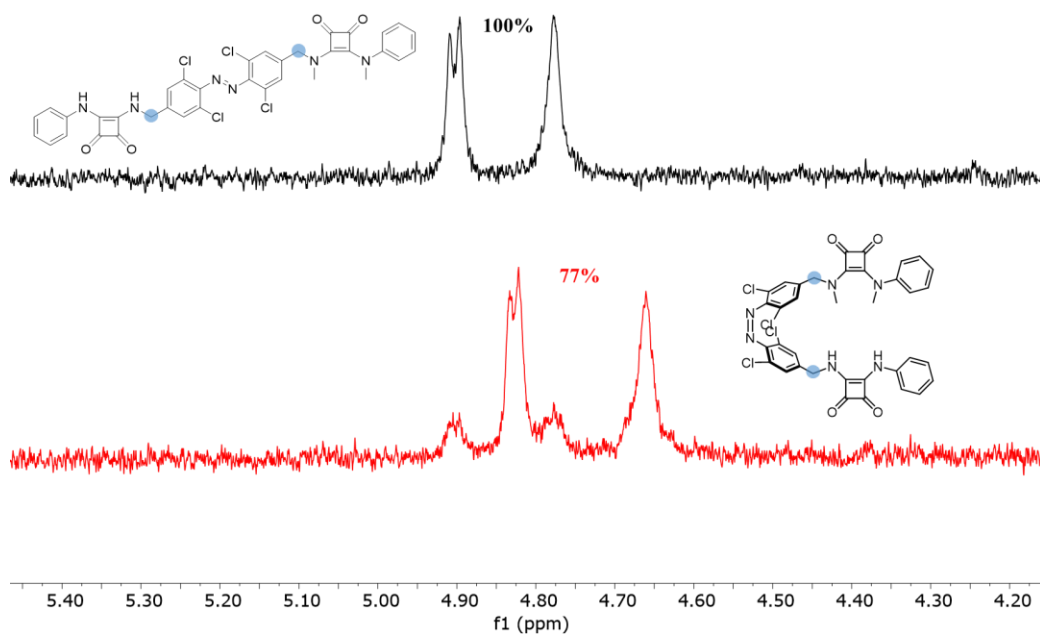


Figure S108. Partial ^1H NMR spectrum of **4** in the dark (100% *E*) and PSS achieve by irradiation with red 625 nm (77% *Z*) light.

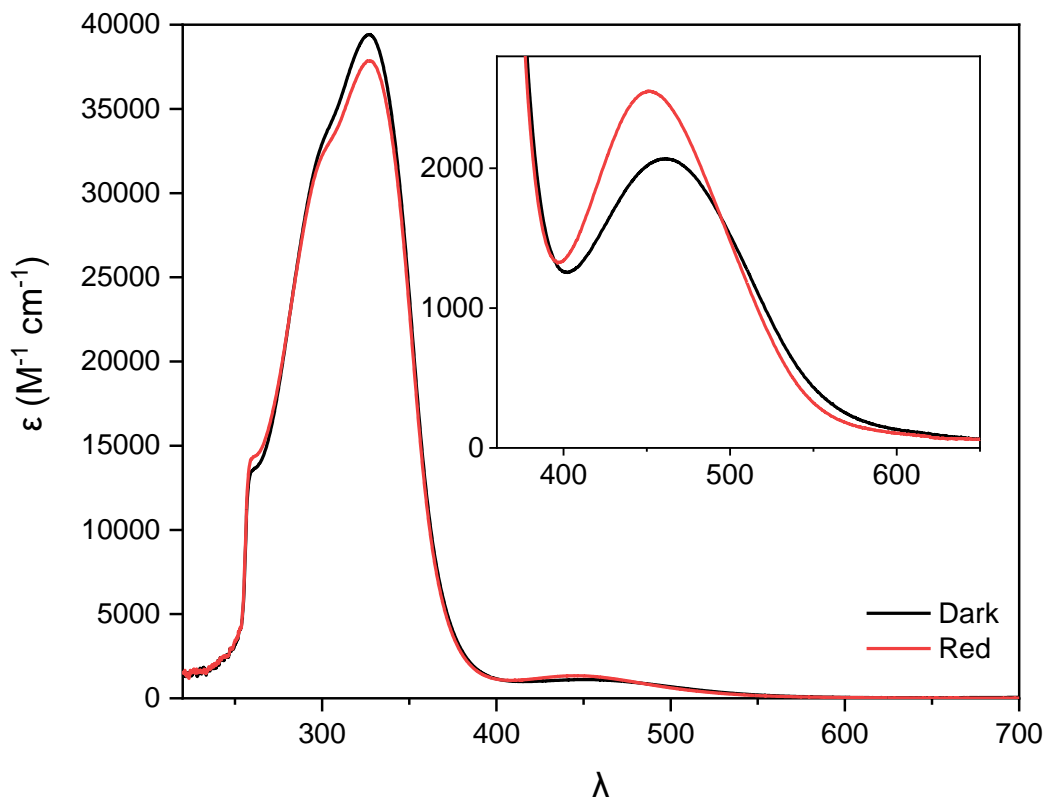
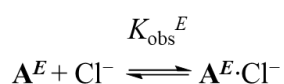


Figure S109. UV-vis Spectrum of **4** in the dark (100% *E*) and red (77% *Z*) state.

4. NMR titration experiments

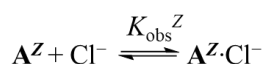
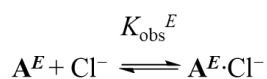
All binding constants were measured by ^1H NMR titrations in a Bruker AVIII 500 spectrometer at 500 MHz and 298 K. The host (squaramide azobenzene derivative) was dissolved in d_6 -DMSO and added at 1 mM concentration and a known volume (0.5 mL) added to the NMR tube. Known volumes of guest (chloride, added as the TBA salt) in d_6 -DMSO were added, and the spectra were recorded after each addition. The chemical shifts of the host spectra, where resolved, were monitored as a function of guest concentration. The data was analysed using a global fit procedure for all three data sets simultaneously in the Dynafit software program,^[10] using non-linear least squares analysis to obtain the best fit between observed and calculated chemical shifts, as described in further detail below. Errors were calculated as two times the standard deviation from the average value of two repeats. In all experiments the association of guest and host was fast on the NMR timescale.

***E* isomer:** Chloride binding to a dark adapted sample of the transporter (compound **1b**, **2**, **3** and **4**, denoted here by the symbol **A**) as the *E* isomer (>99% *E*) was determined by NMR titration analysis in d_6 -DMSO as described above, fitting to a 1:1 binding model:



Binding of a second equivalent of chloride, to form a 1:2 host:guest complex, was not observed in DMSO, as inferred from the failure to fit the data to 1:2 binding models. This is presumably due to inter-anion repulsion in the 1:2 complex, leading to negligible association of the second anion in this competitive polar solvent. In contrast 1:1 binding models in our analysis gave excellent fits to the experimental data for all compounds studied.

***Z* isomer:** A 1 mM sample of **1-4** in d_6 -DMSO was irradiated with red or green light until the PSS was reached, before the titration experiment was conducted as described above. The PSS ratio was maintained throughout the titration for all derivatives. The binding constant for 1^Z – 4^Z derivatives to chloride were obtained by fitting the data, using a global fit procedure, to the following equilibria where K_1^E is fixed, and obtained from the previous titration with the *E* isomer.



$[\text{A}^E] + [\text{A}^Z] = 1 \text{ mM}$; $[\text{A}^Z] = 1 - x^E \text{ mM}$; $[\text{A}^E] = 1 - x^Z \text{ mM}$ where x^E and x^Z are the mole-fractions of the *E* and *Z* isomer in the photo-stationary state, respectively.

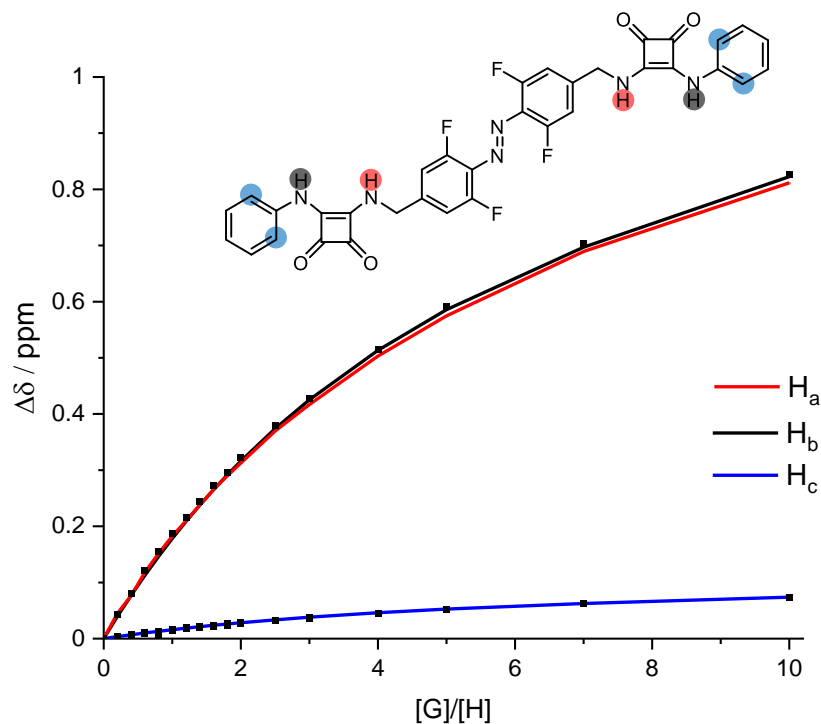


Figure S110. Plots of chemical shift changes of *E-1a* upon addition of TBACl. Shifts are normalised by subtraction to give an initial value of 0.

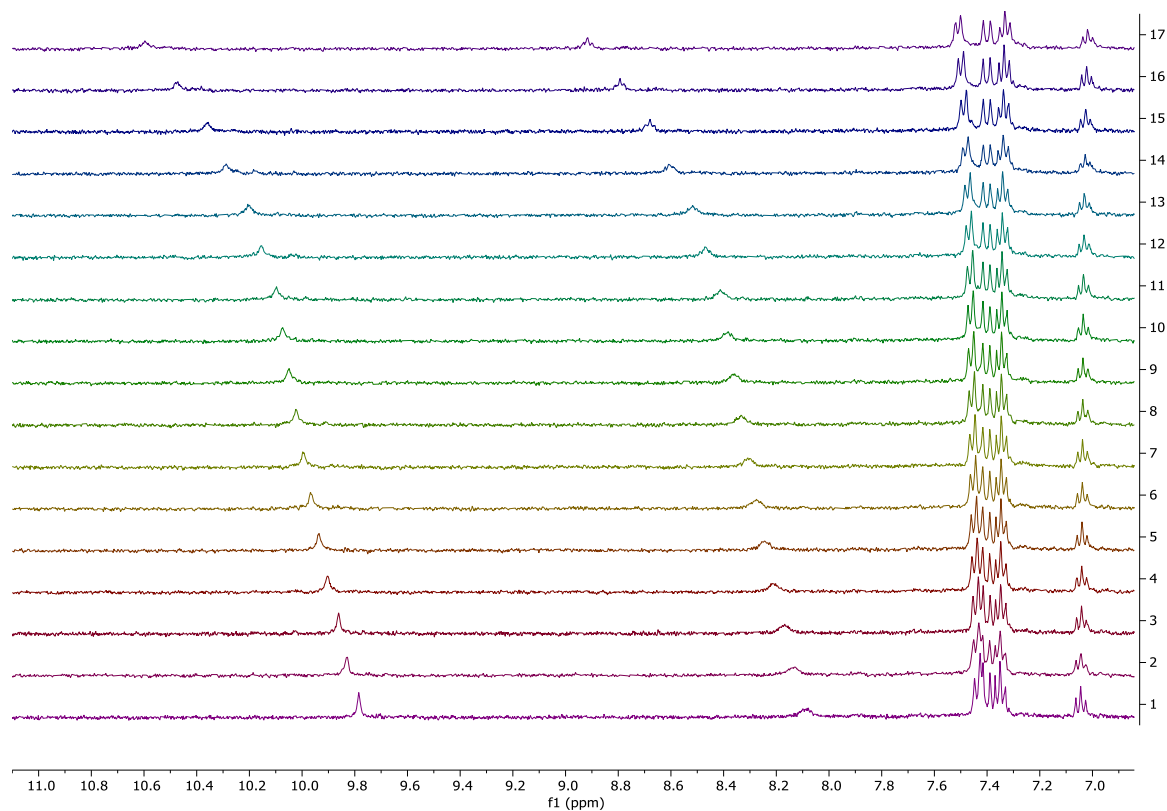


Figure S111. Stacked partial ^1H NMR spectra of *E-1a* with increasing equivalents of TBACl

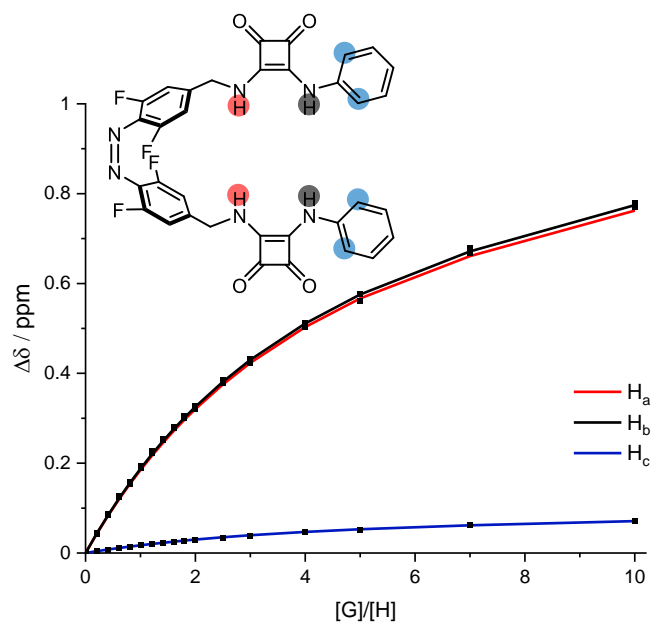


Figure S112. Plots of chemical shift changes of **Z-1a** upon addition of TBACl

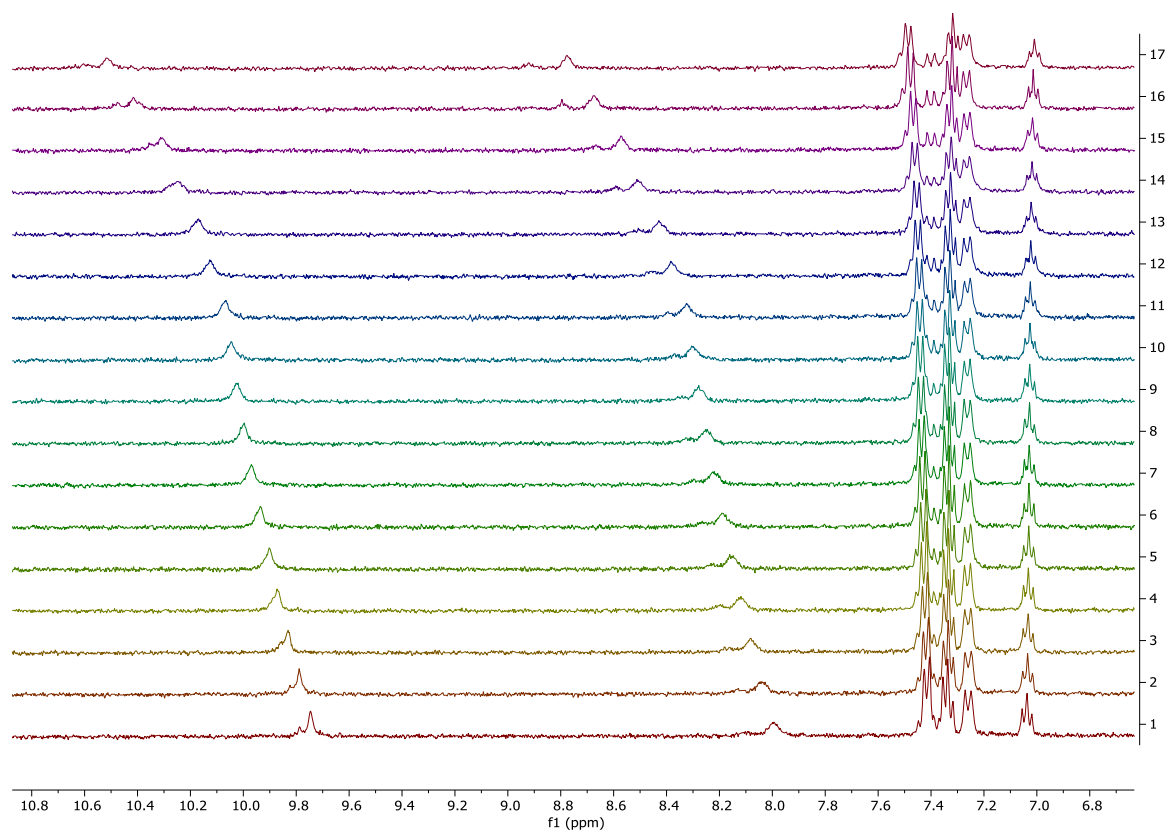


Figure S113. Stacked partial ^1H NMR spectra of **Z-1a** with increasing equivalents of TBACl

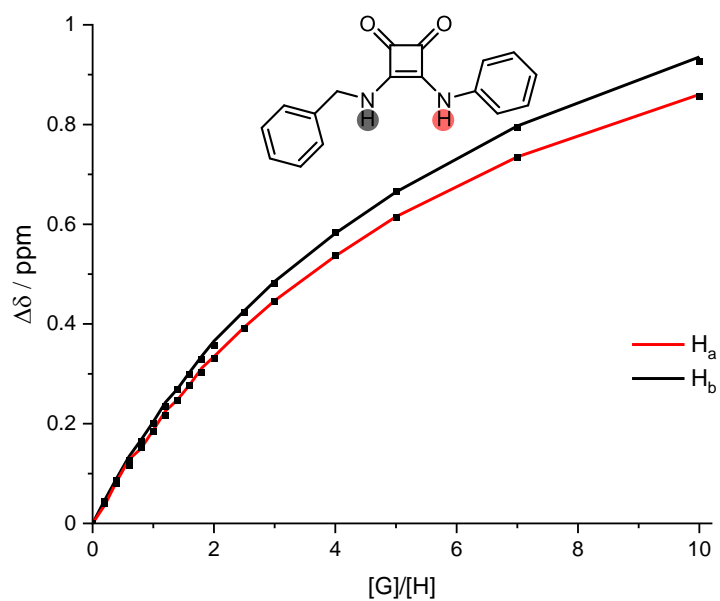


Figure S114. Plots of chemical shift changes of **37** upon addition of TBACl

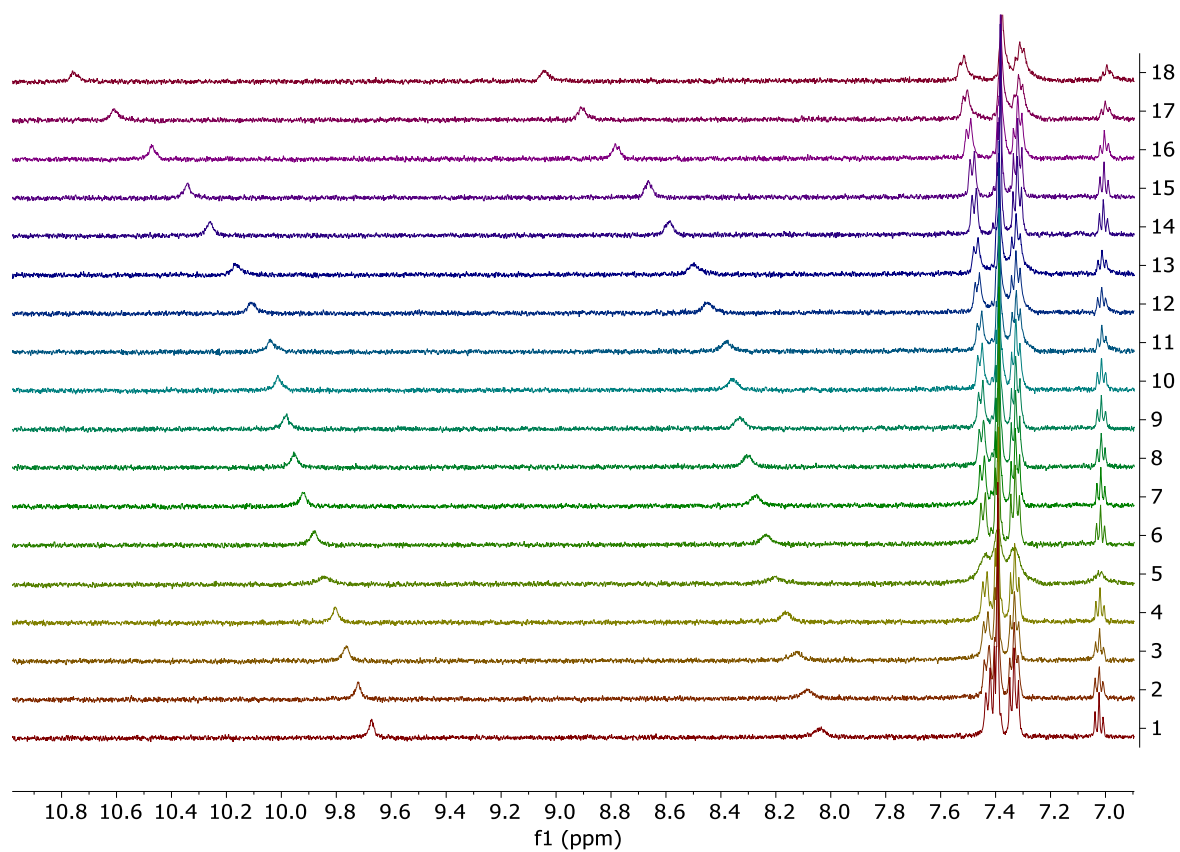


Figure S115. Stacked partial ^1H NMR spectra of **37** with increasing equivalents of TBACl

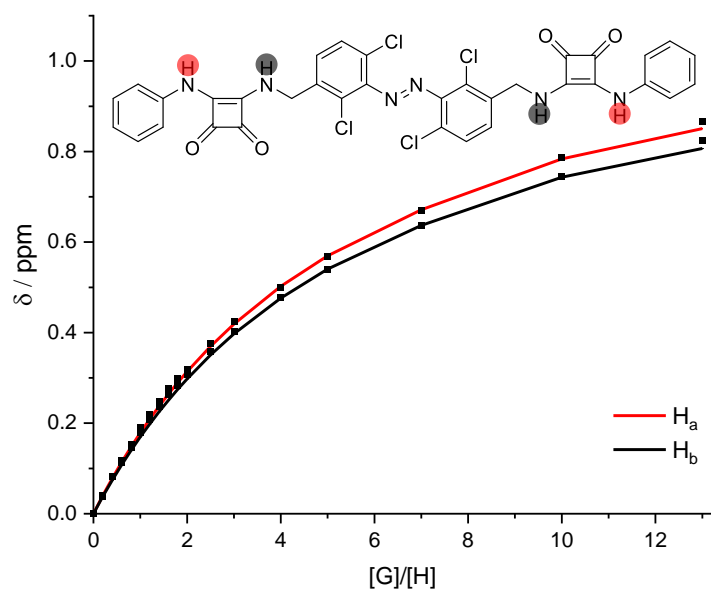


Figure S116. Plots of chemical shift changes of *E-2* upon addition of TBACl

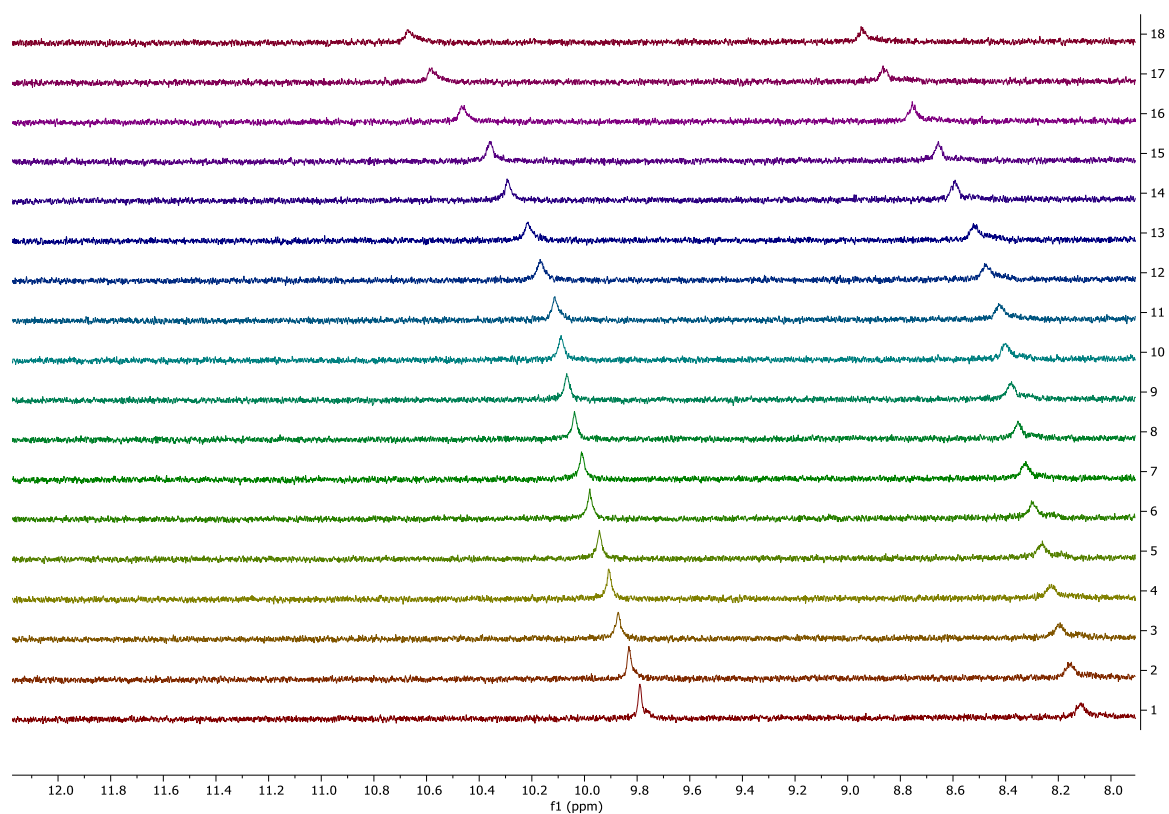


Figure S117. Stacked partial ^1H NMR spectra of *E-2* with increasing equivalents of TBACl

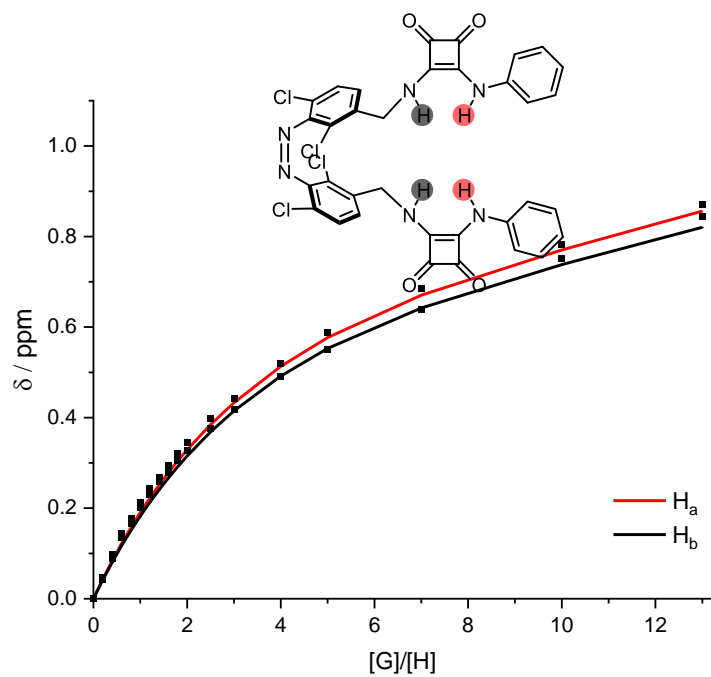


Figure S118. Plots of chemical shift changes of **Z-2** upon addition of TBACl

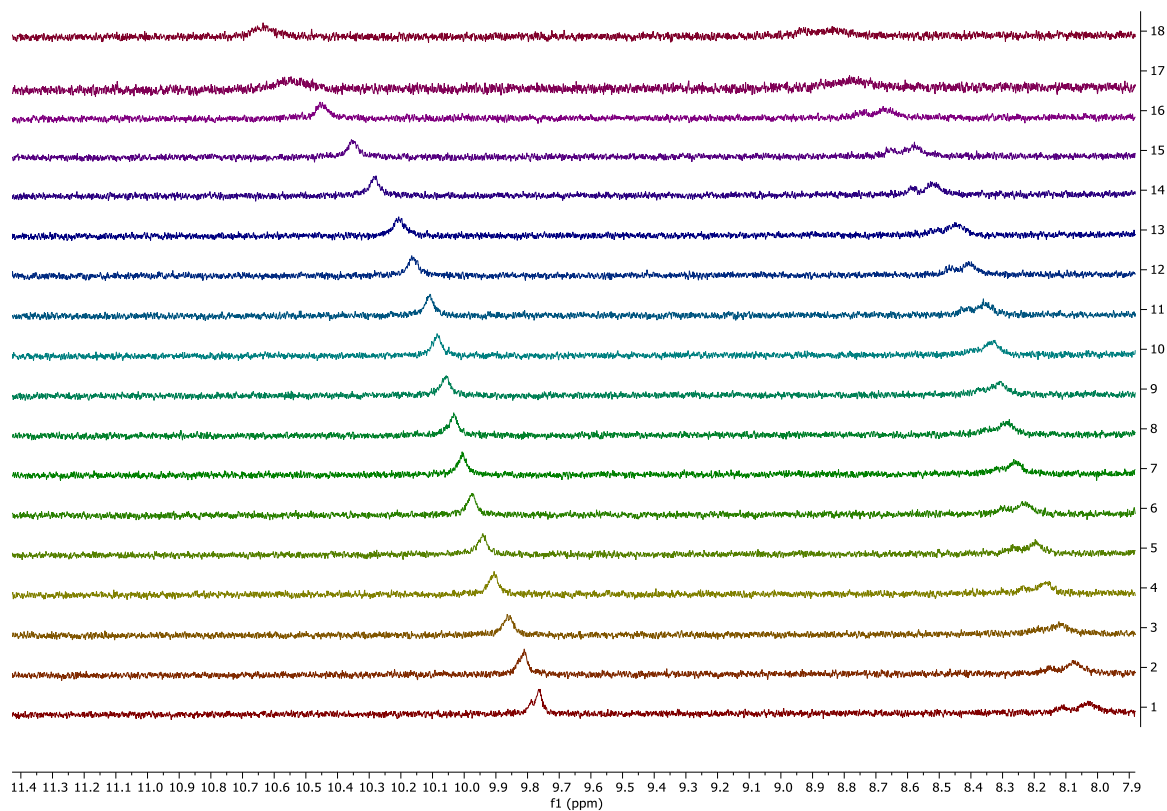


Figure S119. Stacked partial ^1H NMR spectra of **Z-2** with increasing equivalents of TBACl

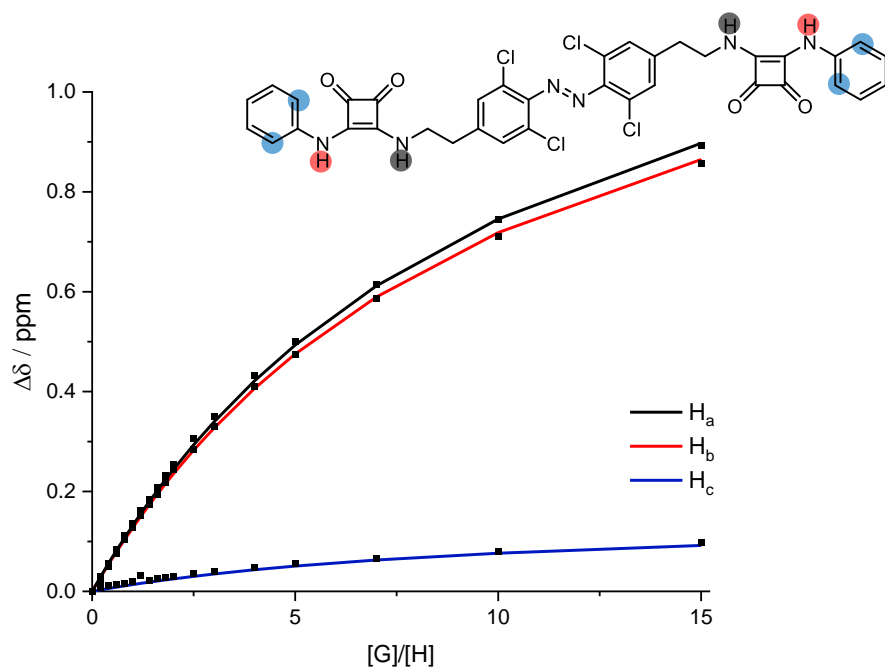


Figure S120. Plots of chemical shift changes of *E-3* upon addition of TBACl

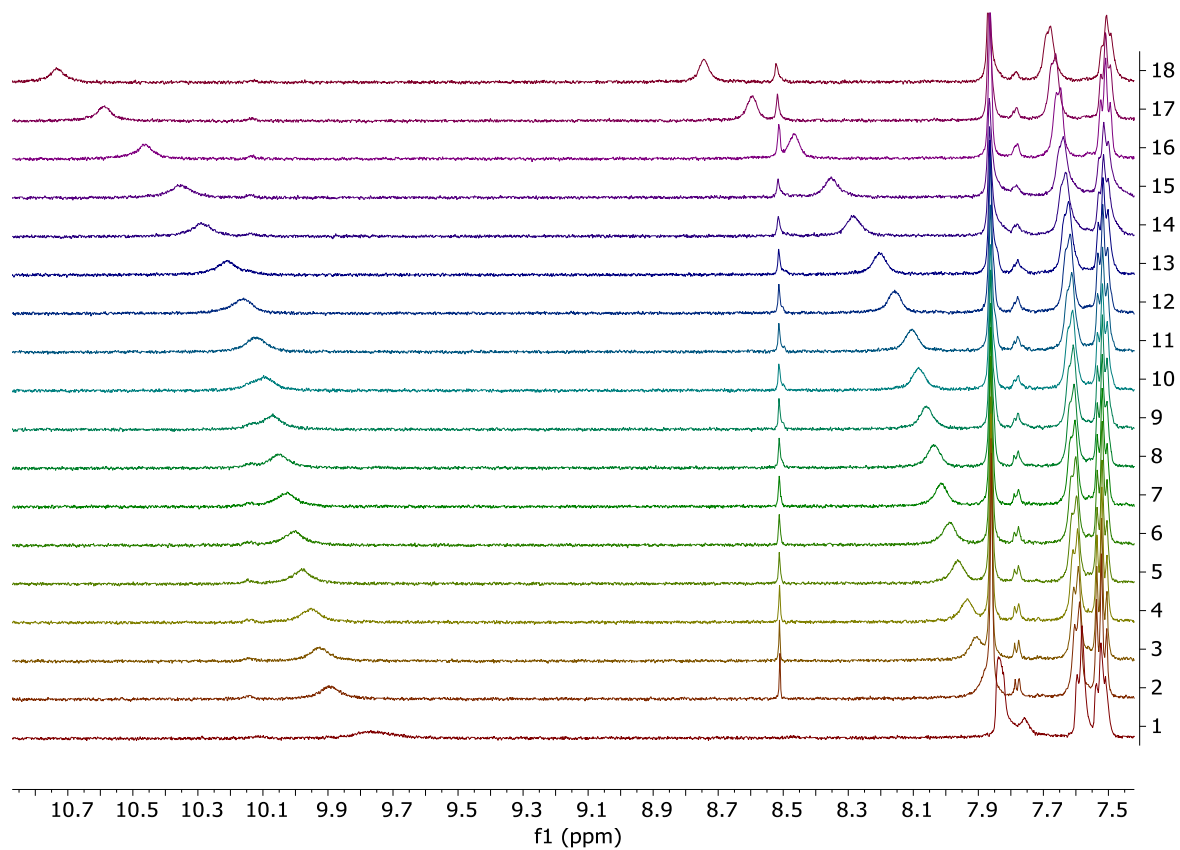


Figure S121. Stacked partial ^1H NMR spectra of *E-3* with increasing equivalents of TBACl

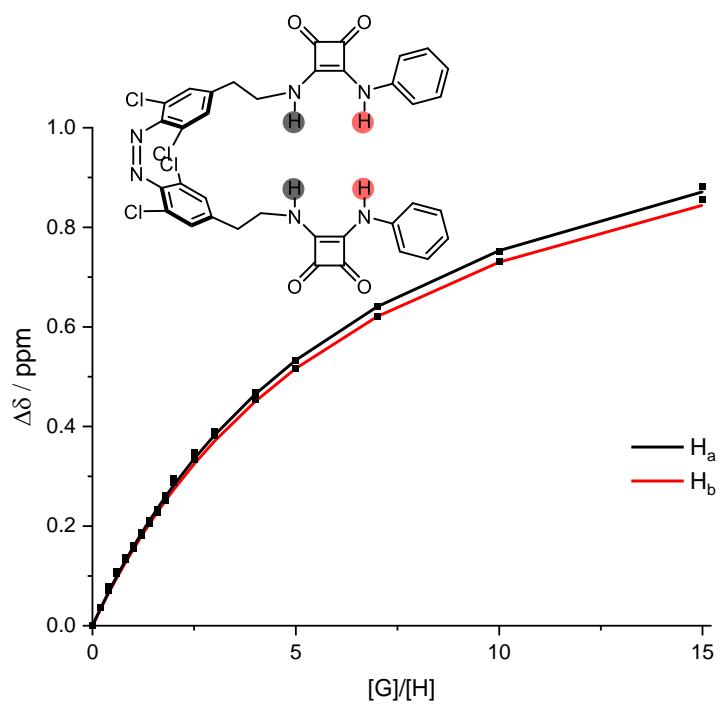


Figure S122. Plots of chemical shift changes of Z-3 upon addition of TBACl

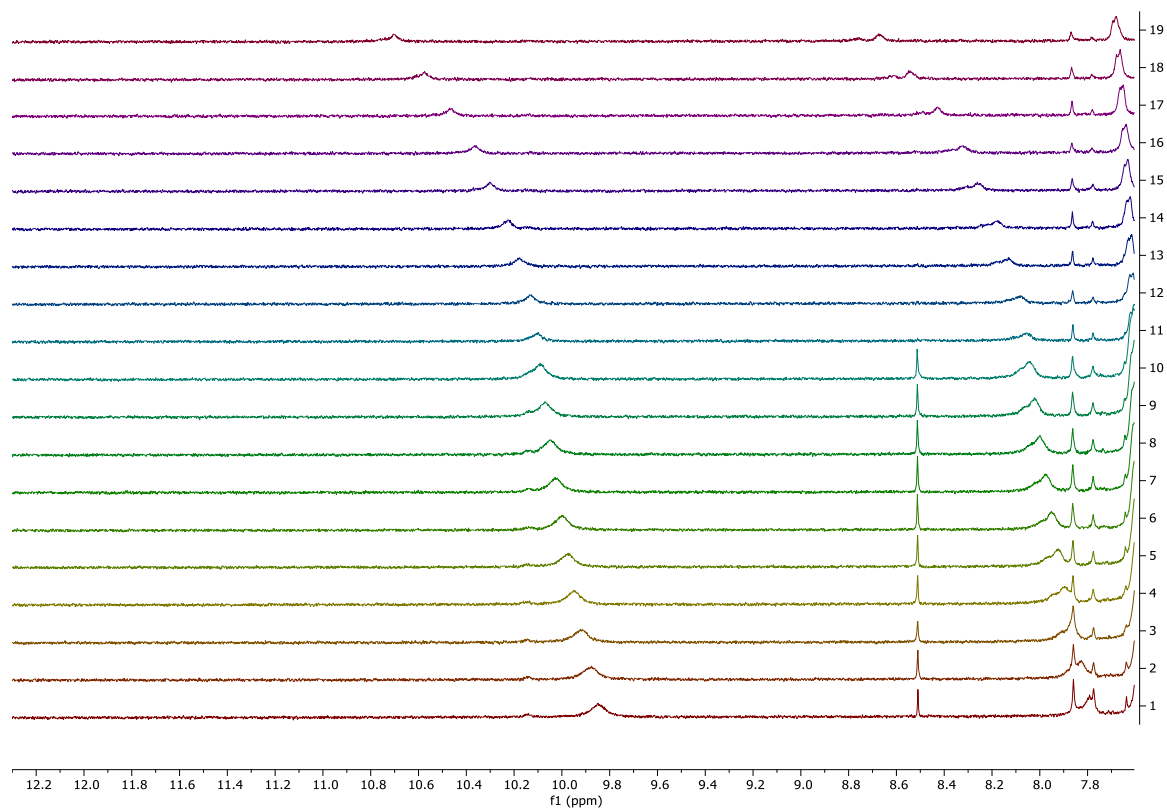


Figure S123. Stacked partial ^1H NMR spectra of Z-3 with increasing equivalents of TBACl

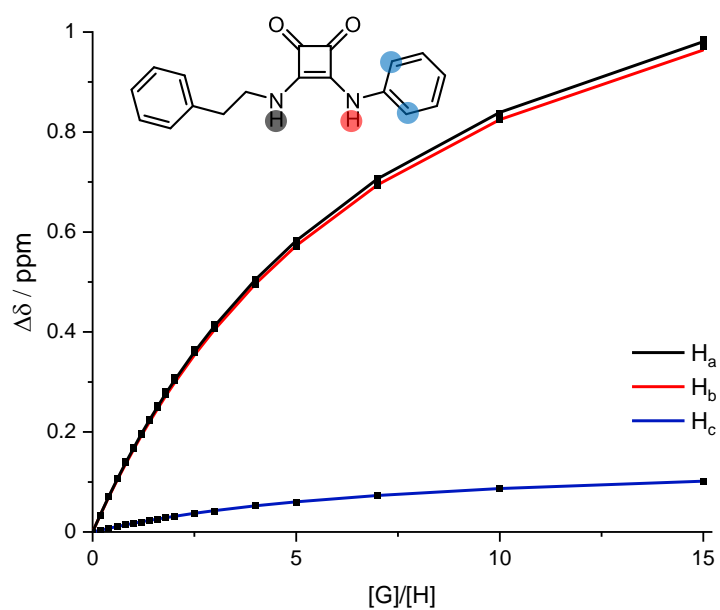


Figure S124. Plots of chemical shift changes of **38** upon addition of TBACl

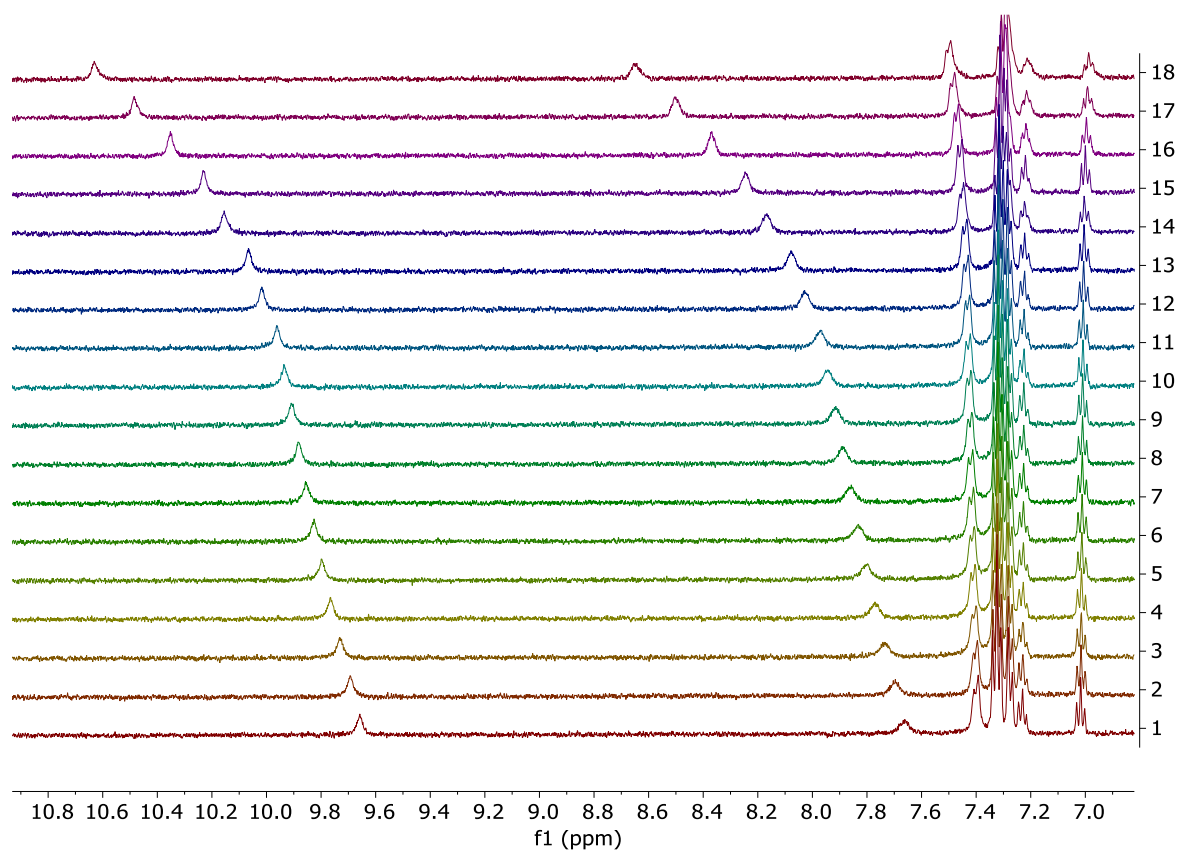


Figure S125. Stacked partial ^1H NMR spectra of **S38** with increasing equivalents of TBACl

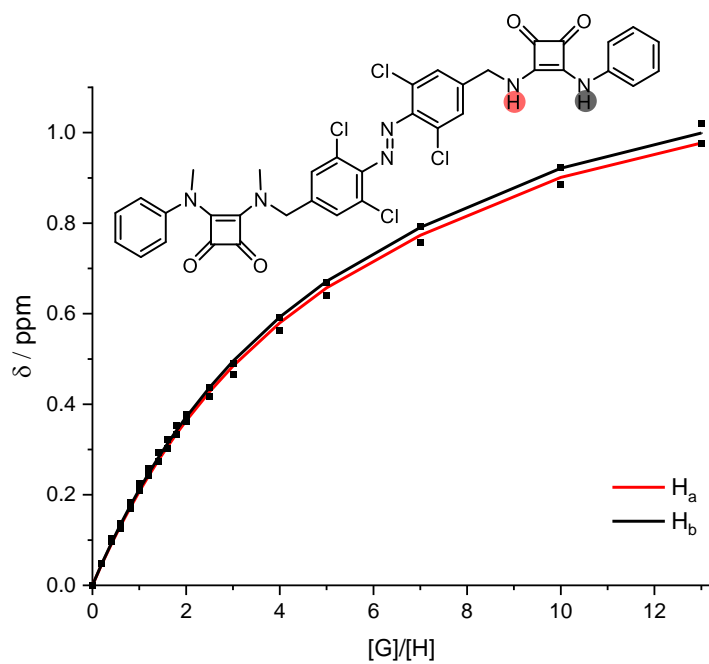


Figure S126. Plots of chemical shift changes of *E-3* upon addition of TBACl

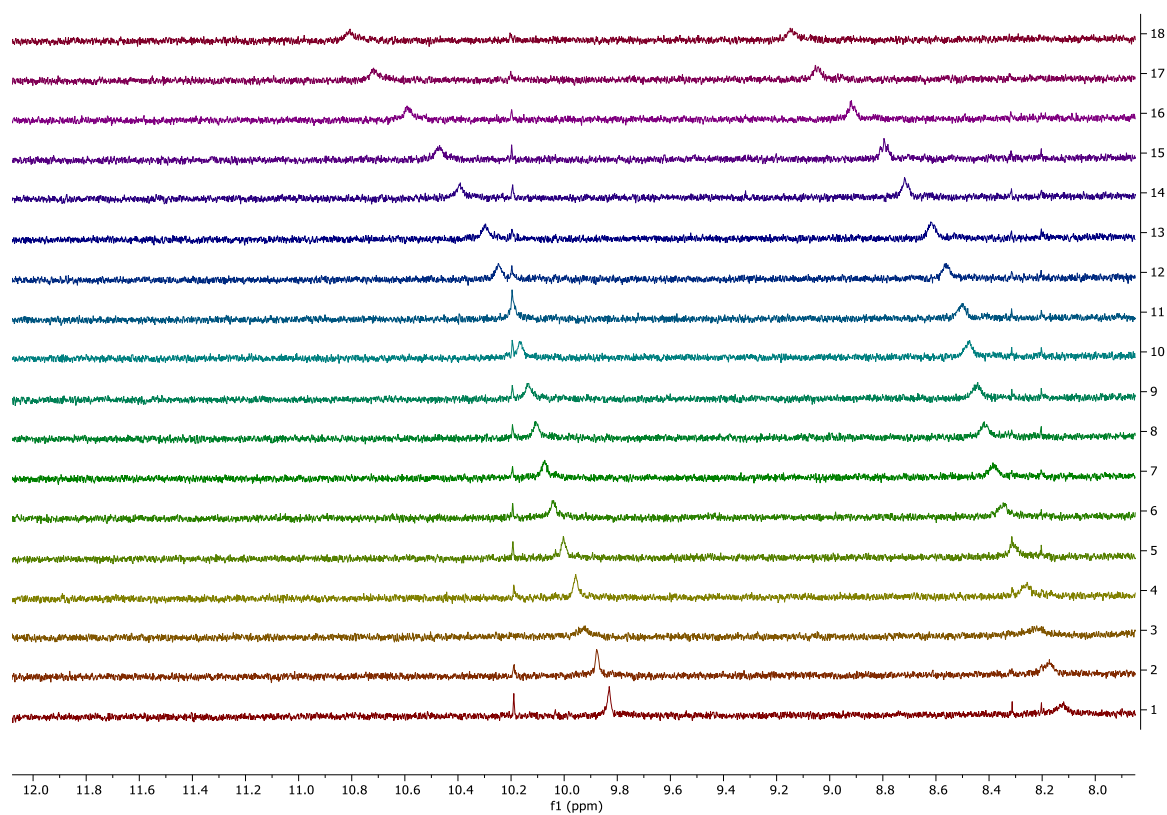


Figure S127. Stacked partial ^1H NMR spectra of *E-3* with increasing equivalents of TBACl

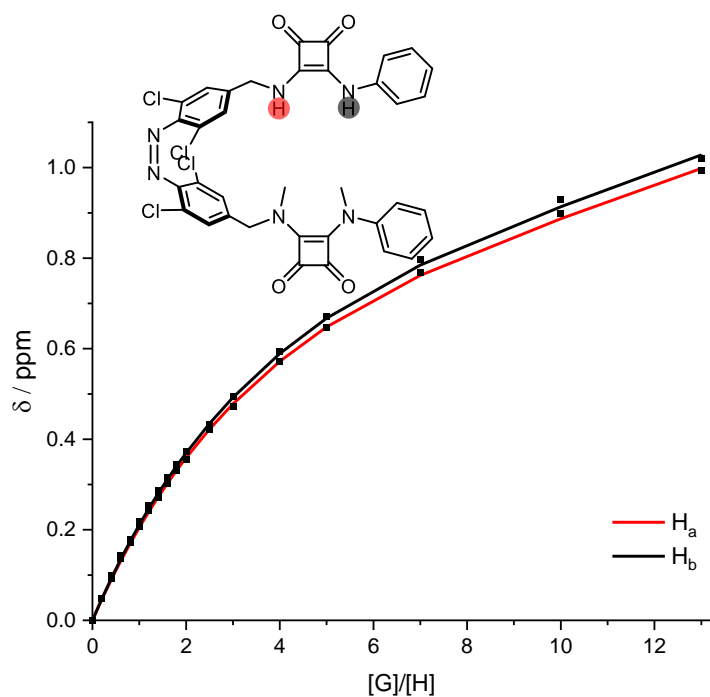


Figure S128. Plots of chemical shift changes of Z-4 upon addition of TBACl

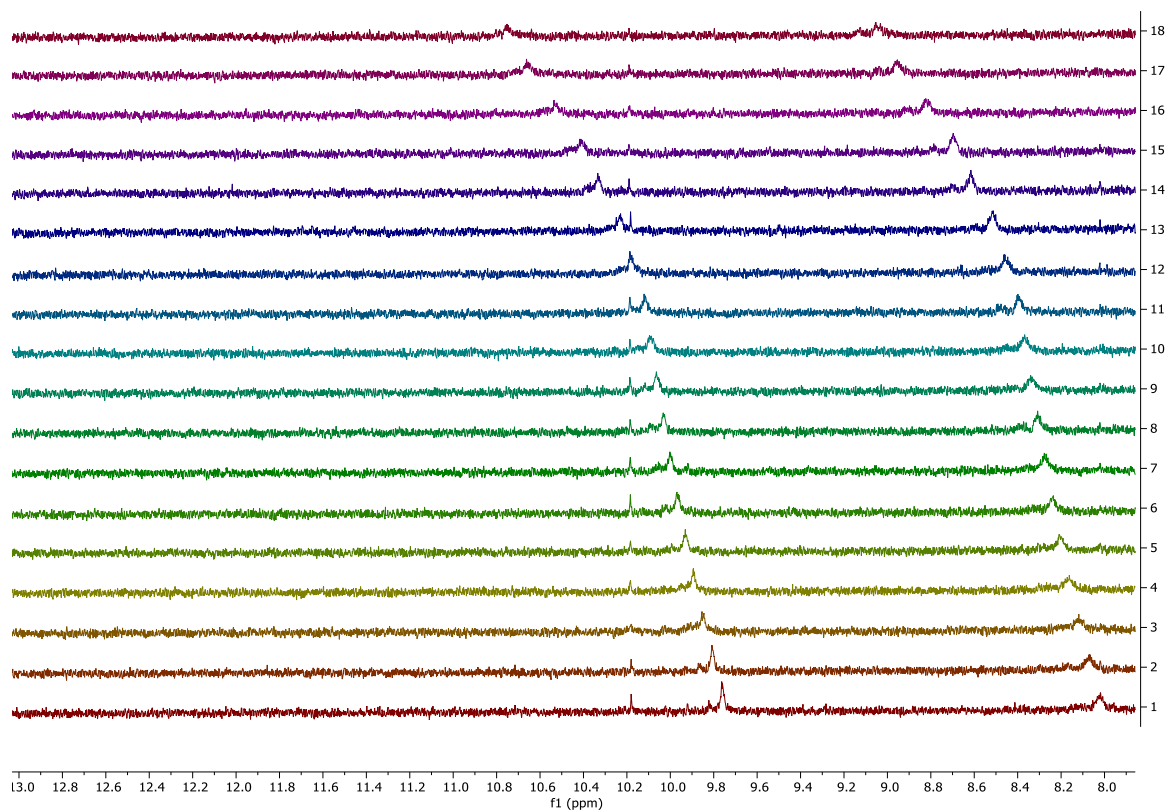


Figure S129. Stacked partial ^1H NMR spectra of Z-4 with increasing equivalents of TBACl

5. Anion transport studies

Vesicle preparation. A thin film of lipid (1-palmitoyl-2-oleoyl-*sn*-3-phosphatidylcholine POPC, egg-yolk phosphatidylglycerol EYPG or dipalmitoyl phosphatidylcholine DPPC) was formed by evaporating a chloroform solution under a stream of nitrogen gas, and then under high vacuum for 6 hours. The lipid film was hydrated by vortexing with the prepared buffer (100 mM NaCl, 10 mM HEPES, 1 mM 8-Hydroxypyrene-1,3,6-trisulfonic acid trisodium salt (HPTS), pH 7.0). The lipid suspension was then subjected to 5 freeze-thaw cycles using liquid nitrogen and a water bath (40°C), followed by extrusion 19 times through a polycarbonate membrane (pore size 200 nm) at rt. Extrusion was performed at 50°C in the case of DPPC lipids. Extra-vesicular components were removed by size exclusion chromatography on a Sephadex G-25 column with 100 mM NaCl, 10 mM HEPES, pH 7.0. Final conditions: LUVs (2.5 mM lipid); inside 100 mM NaCl, 10 mM HEPES, 1 mM HPTS, pH 7.0; outside: 100 mM NaCl, 10 mM HEPES, pH 7.0. Vesicles for the sodium gluconate assay were prepared by the same procedure, substituting NaCl for NaGluconate in the buffer solution.

Transport assays with HPTS. In a typical experiment, the LUVs containing HPTS (25 μ L, final lipid concentration 31 μ M) were added to buffer (1950 μ L of 100 mM NaCl, 10 mM HEPES, pH 7.0) at 25°C under gentle stirring. A pulse of NaOH (20 μ L, 0.5 M) was added at 20 secs to initiate the experiment. At 80 s the test transporter (various concentrations, in 5 μ L DMSO) was added, followed by detergent (25 μ L of Triton X-100 in 7:1 (v/v) H₂O-DMSO) at 300 secs to calibrate the assay. The fluorescence emission was monitored at $\lambda_{em} = 510$ nm ($\lambda_{ex} = 460/405$ nm). The fractional fluorescence intensity (I_{rel}) was calculated from Equation S4, where R_t is the fluorescence ratio at time t , (ratio of intensities 460 nm / 405 nm excitation) R_0 is the fluorescence ratio at time 77 s, and R_d is the fluorescence ratio after the addition of detergent.

$$I_{rel} = \frac{R_t - R_0}{R_d - R_0} \quad (\text{S4})$$

The fractional fluorescence intensity (I_{rel}) at 290 s just prior to lysis, defined as the fractional activity y , was plotted as a function of the ionophore concentration (x / μ M). Hill coefficients (n) and EC₅₀ values were calculated by fitting to the Hill equation (Equation S5),

$$y = y_0 + (y_{max} - y_0) \cdot \frac{x^n}{EC_{50}^n + x^n} \quad (\text{S5})$$

where y_0 is the fractional activity in the absence of transporter, y_{max} is the fractional activity in with excess transporter, x is the transporter concentration in the cuvette.

Exposure of the sample to the excitation beam was minimised by closing the shutter immediately after each measurement, and using a short integration time (0.05 s) / narrow excitation band pass (5 nm). The extent of *Z* to *E* isomerisation under these conditions during the anion transport assays was previously estimated for tetra-*ortho*-chloro azobenzene transporters to be <5% by analysis of the UV-vis spectra of sample subjected to the assay measurement conditions.¹

For each compound as the *E* and *Z* isomer, Hill plots were fitted to at-least 8, and up to 12 data points spanning the required concentration range, and each individual concentration was repeated at-least twice and averaged (>16 independent measurements per isomer). Experiments with DPPC lipids were conducted in the same way. For elevated temperature studies, the sample was equilibrated at 45°C (using the Peltier temperature controller) for 5 minutes prior to initiating the experiment.

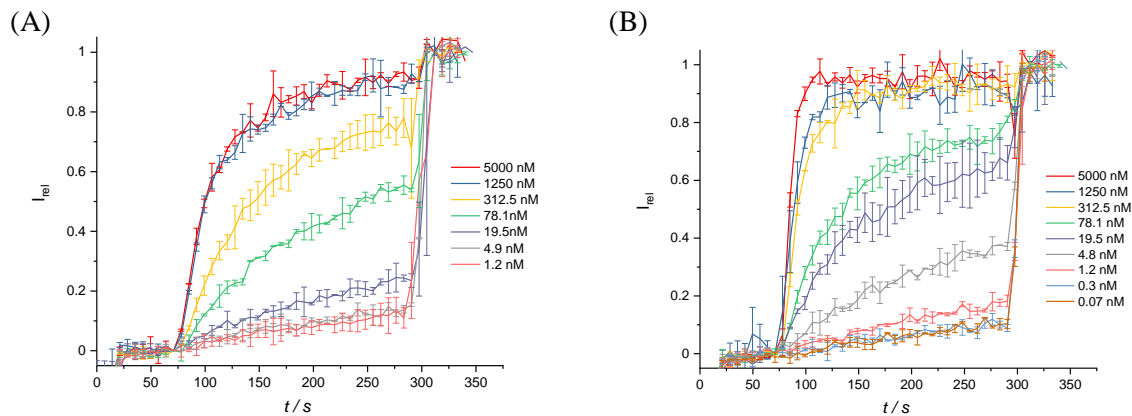


Figure S130. Original data for HPTS assay for (A) *E-1b* (B) PSS *Z-1b* (77%)

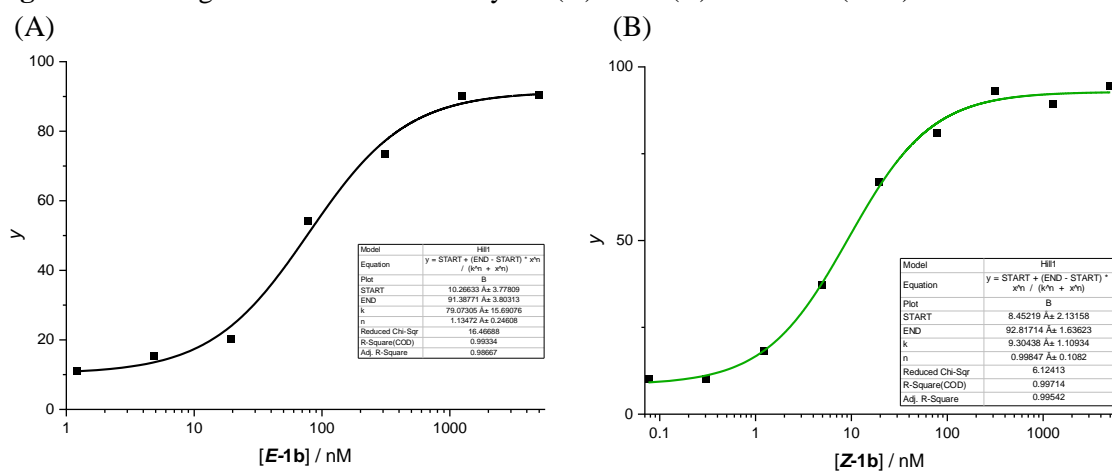


Figure S131. Hill plot for (A) *E-1b* (B) PSS *Z-1b* (77%).

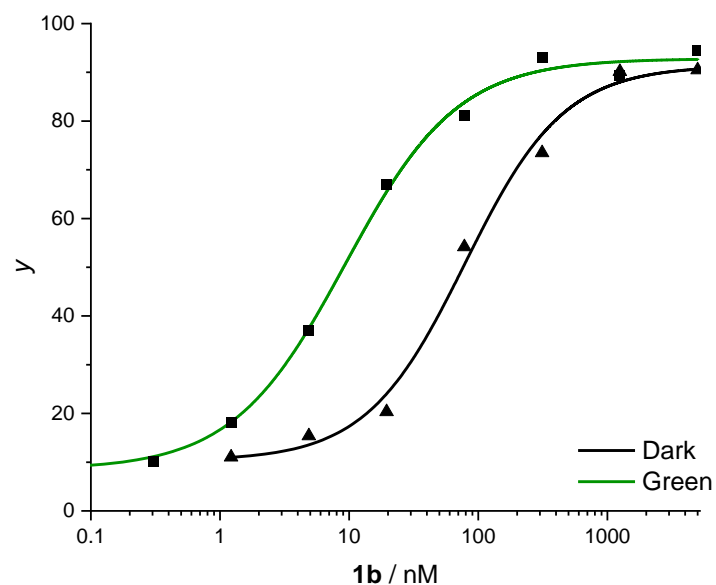


Figure S132. Stacked Hill plot for *E-1b* and PSS *Z-1b* (77%).

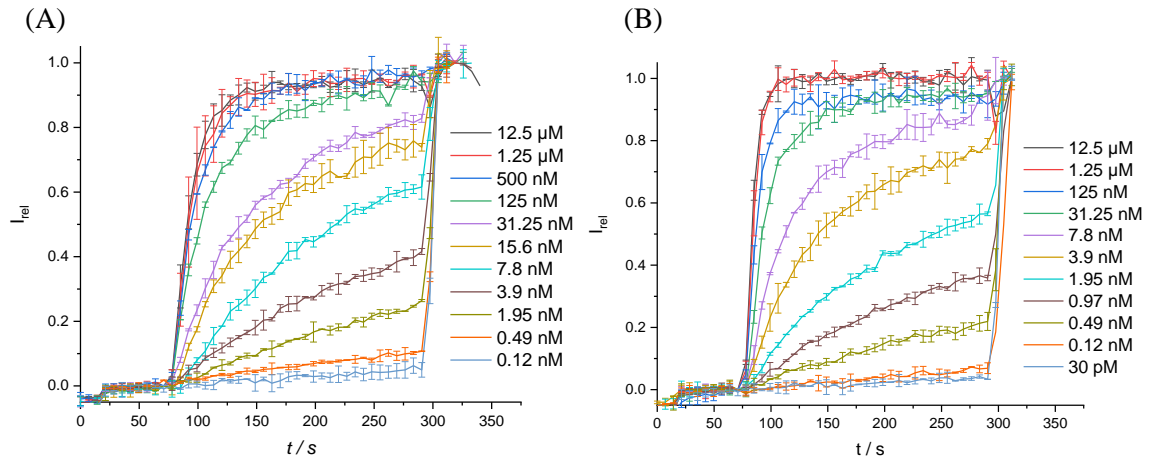


Figure S133. Original data for HPTS assay for (A) *E-2* (B) PSS *Z-2* (77%)

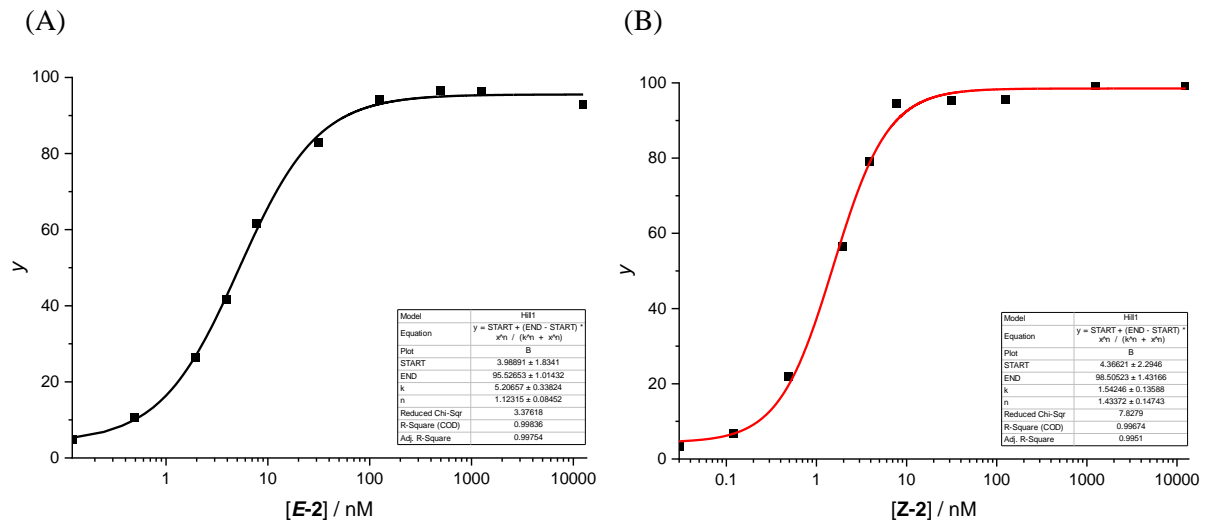


Figure S134. Hill plot for (A) *E-2* (B) PSS *Z-2* (77%).

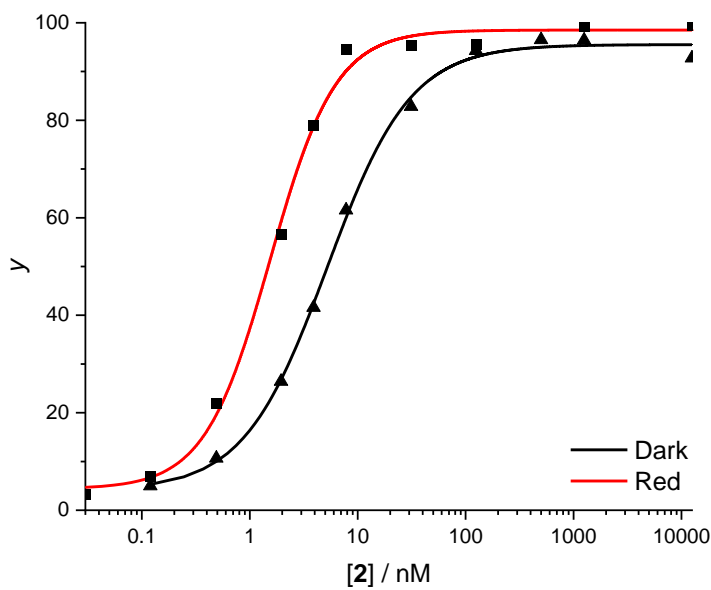


Figure S135. Stacked Hill plot for *E-2* and PSS *Z-2* (77%).

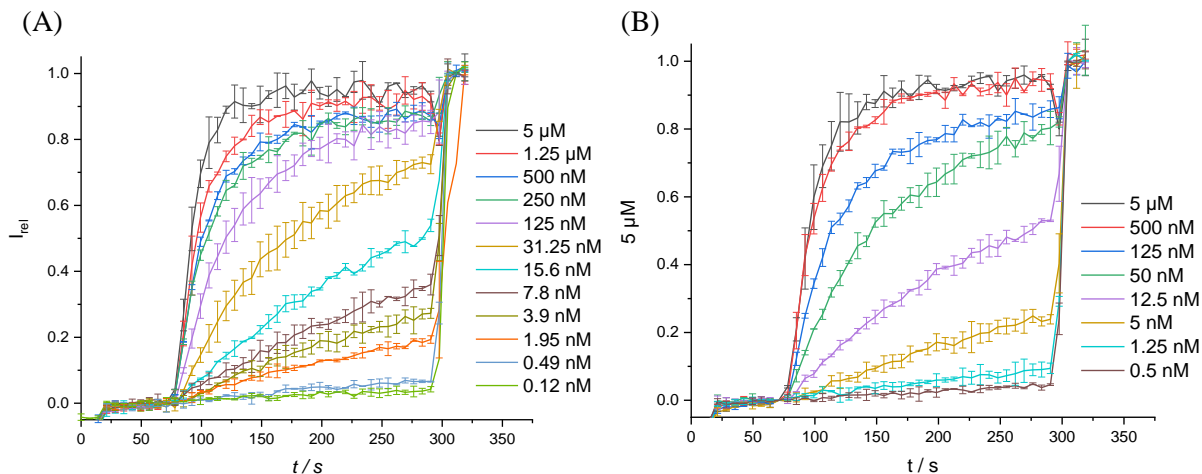


Figure S136. Original data for HPTS assay for (A) *E-3* (B) PSS *Z-3* (77%)

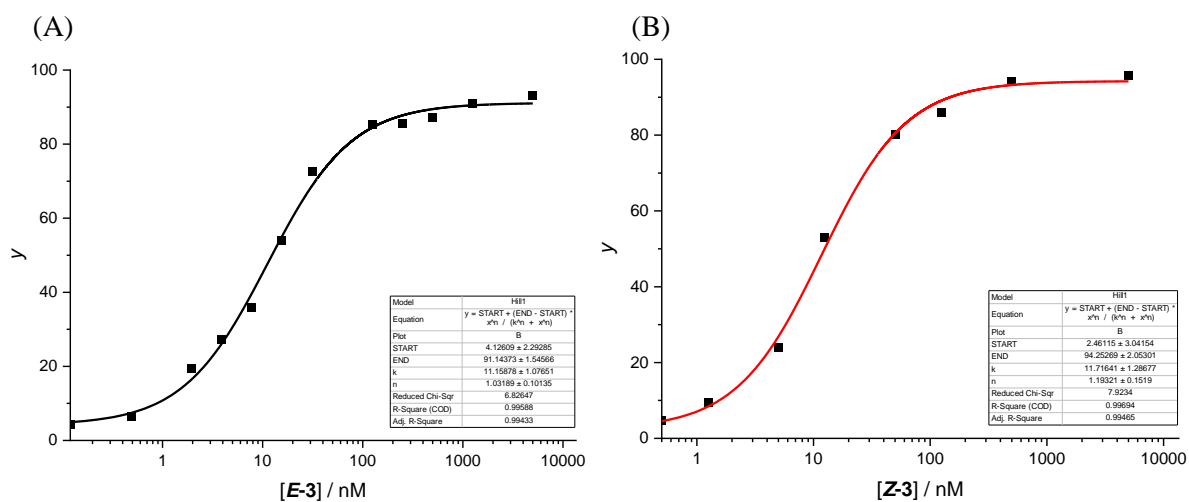


Figure S137. Hill plot for (A) *E-3* (B) PSS *Z-3* (77%).

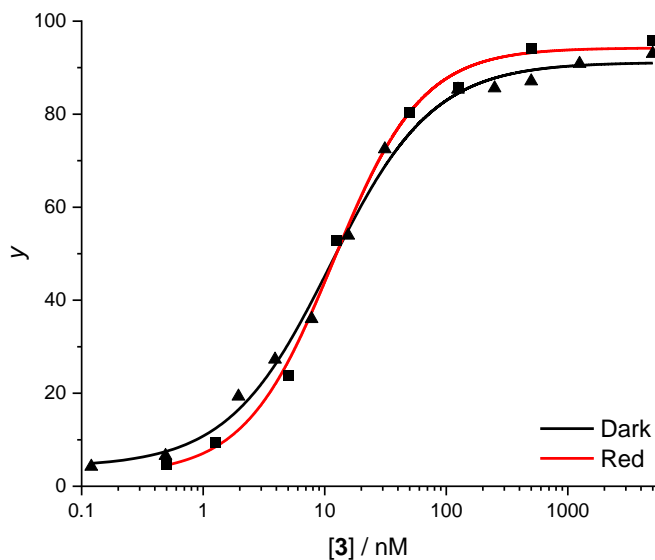


Figure S138. Stacked Hill plot for *E-3* and PSS *Z-3* (77%).

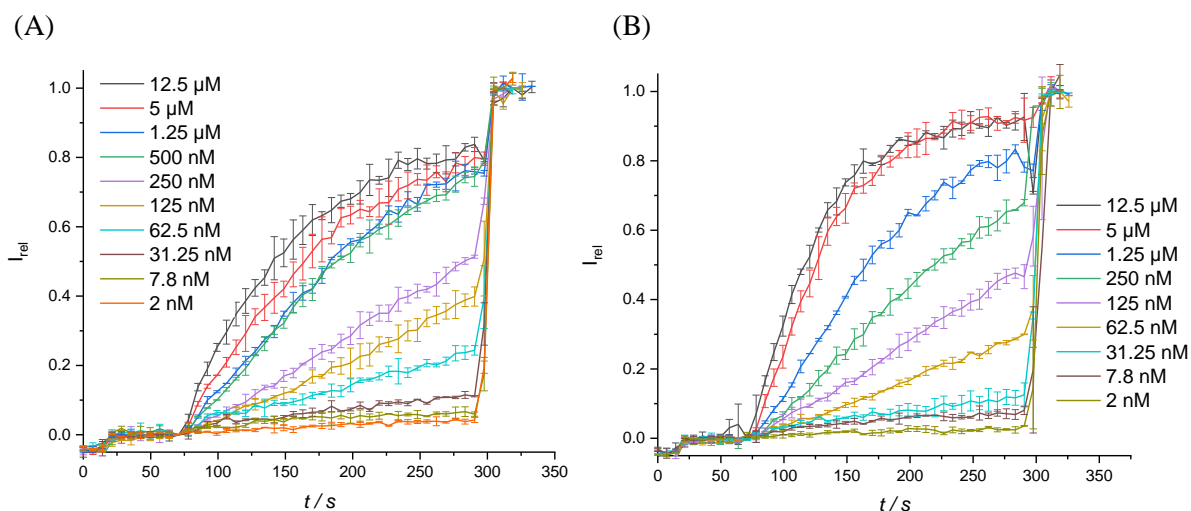


Figure S139. Original data for HPTS assay for (A) *E-4* (B) PSS *Z-4* (77%)

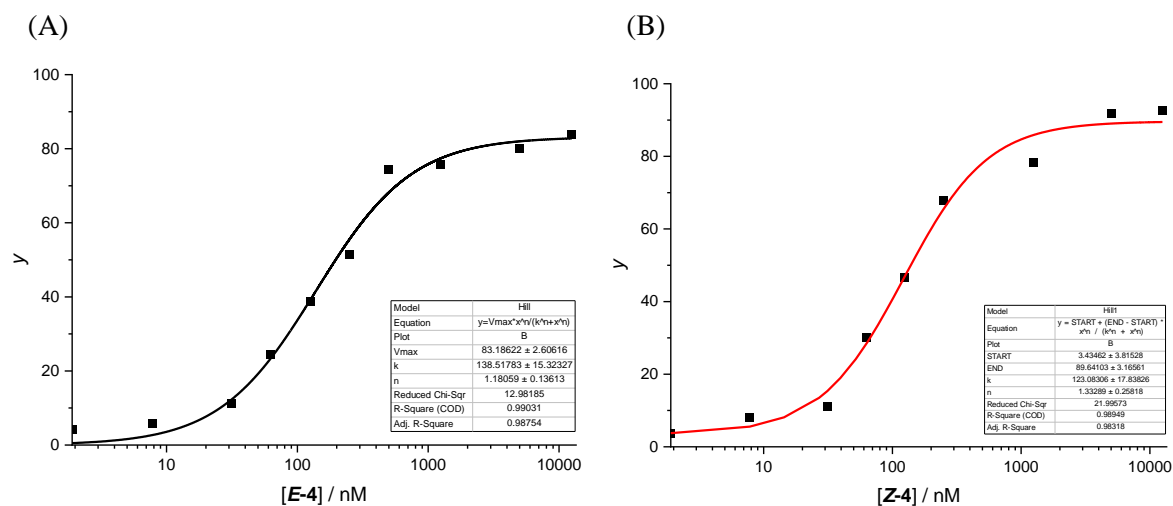


Figure S140. Hill plot for (A) *E-4* (B) PSS *Z-4* (77%).

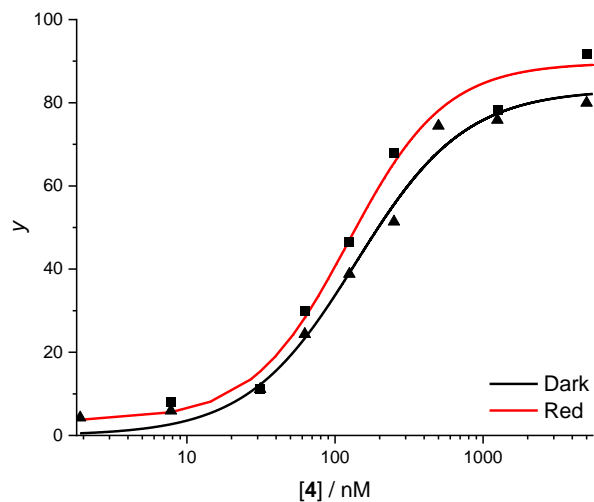


Figure S141. Stacked Hill plot for *E-4* and PSS *Z-4* (77%).

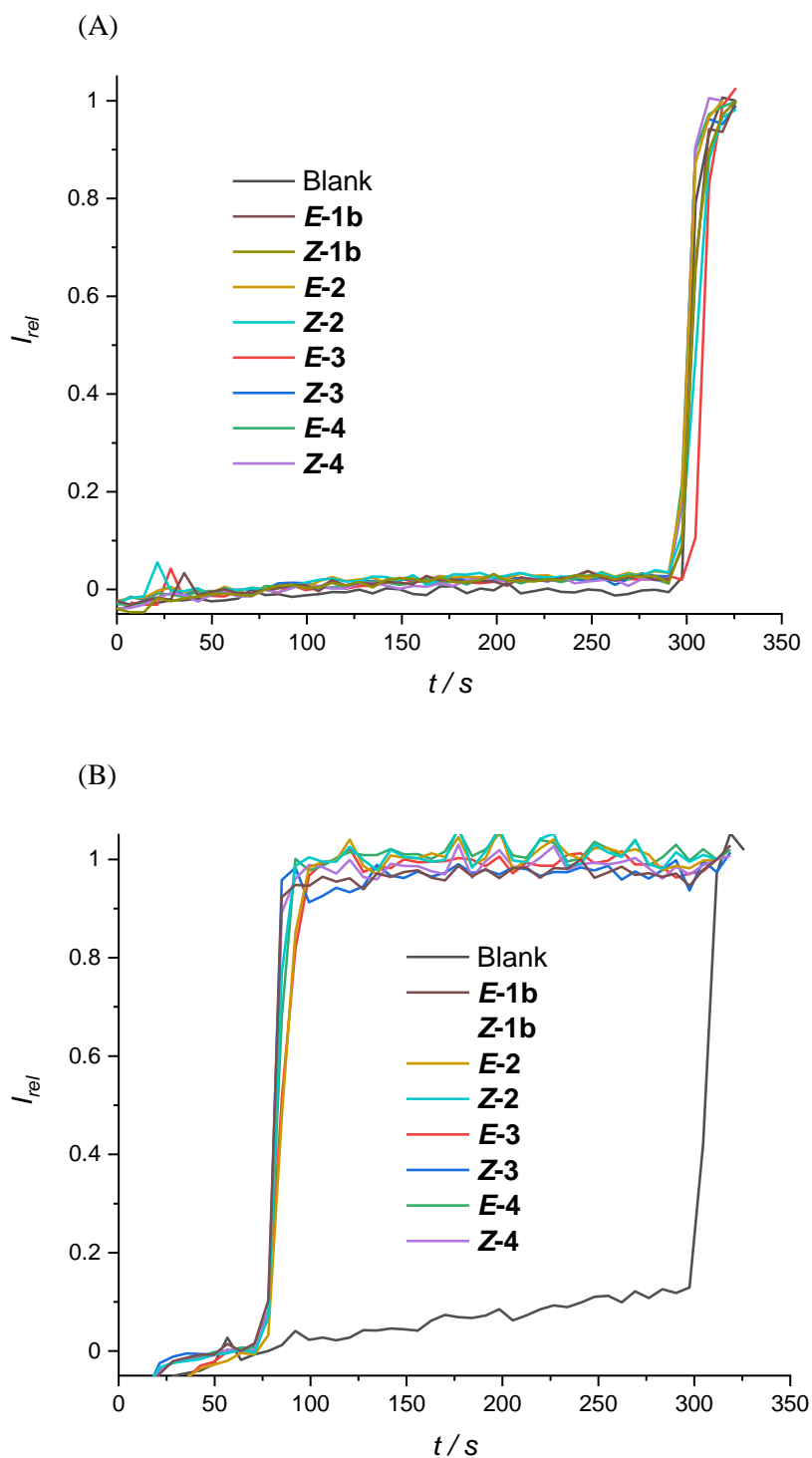


Figure S142. HPTS assay using DPPC LUVs at (A) 25 °C (B) 45 °C at 1 μ M carrier concentration. Blank runs are shown for comparison. Data normalised using Triton X-100

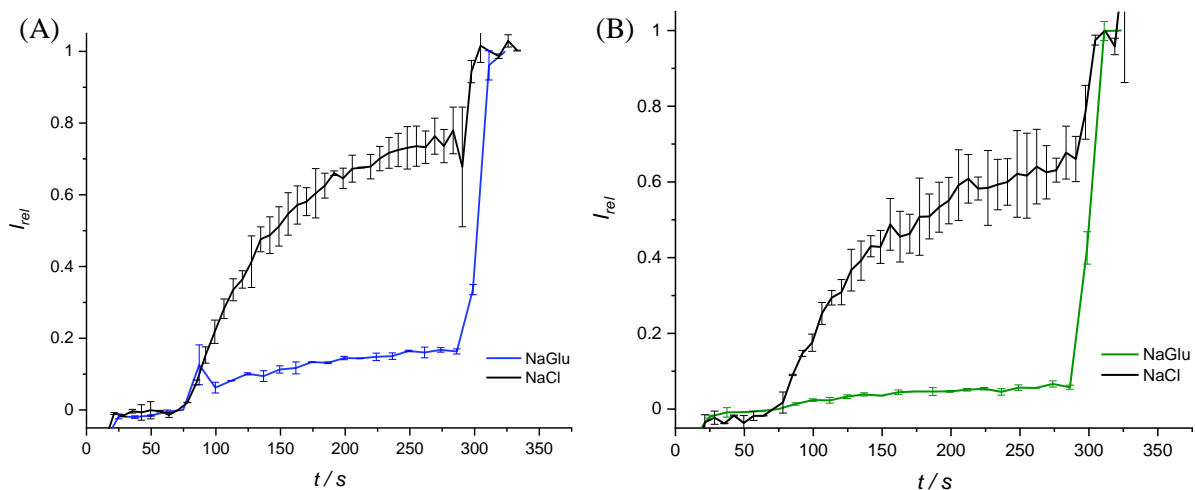


Figure S143. HPTS assay using 100mM sodium gluconate vs 100mM NaCl for (A) *E-1b* at 250 nM carrier concentration and (B) *Z-1b* at 250 nM carrier concentration.

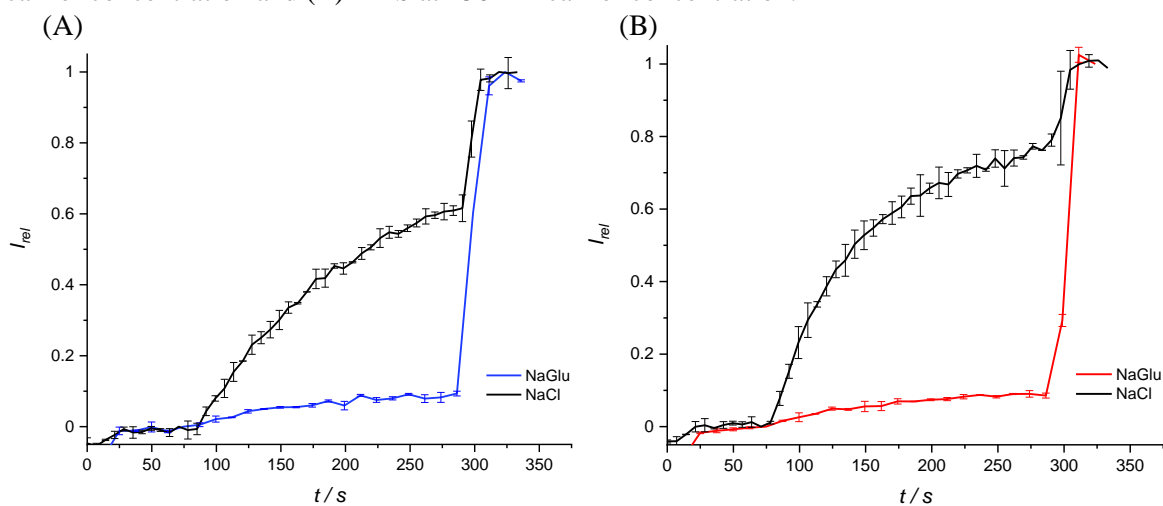


Figure S144. HPTS assay using 100mM sodium gluconate vs 100mM NaCl for (A) *E-2* at 8 nM carrier concentration and (B) *Z-2* at 4 nM carrier concentration.

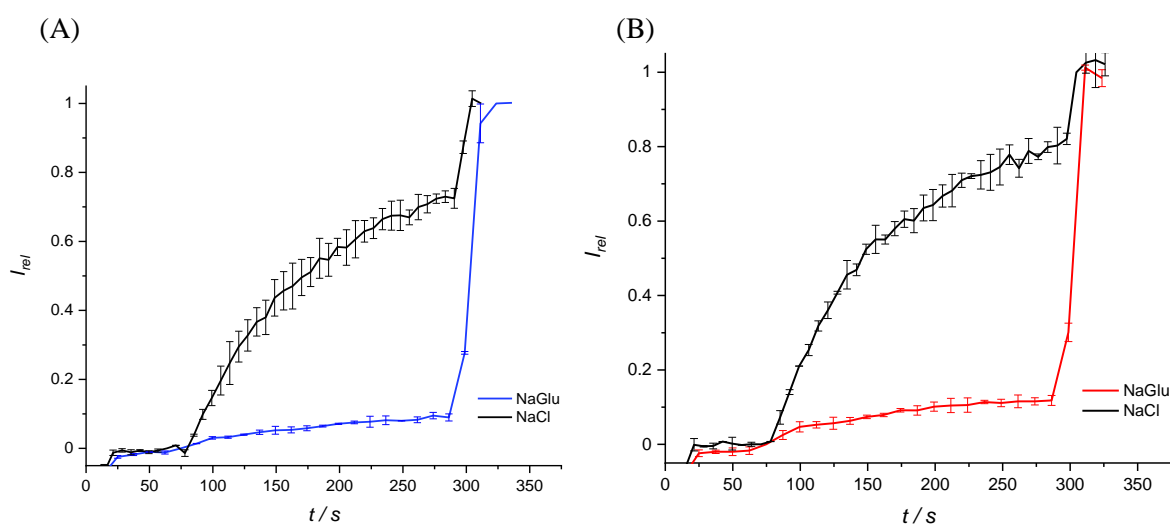


Figure S145. HPTS assay using 100mM sodium gluconate vs 100mM NaCl for (A) *E-3* at 31.25 nM carrier concentration and (B) *Z-3* at 50 nM carrier concentration.

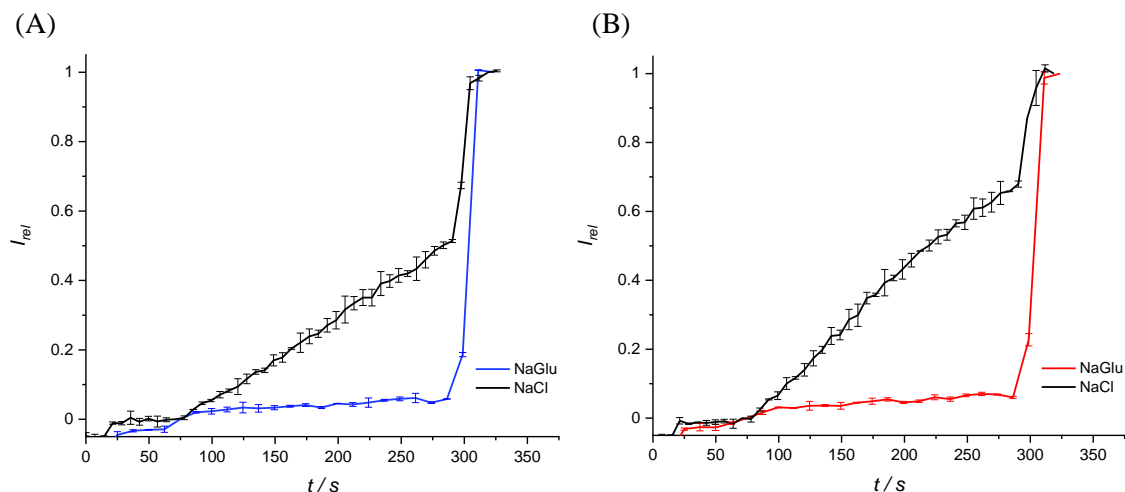


Figure S146. HPTS assay using 100mM sodium gluconate vs 100mM NaCl for (A) **E-4** at 250 nM carrier concentration and (B) **Z-4** at 250 nM carrier concentration.

Calcein leakage assay

POPC vesicles were prepared containing calcein (Internal buffer: 100 mM NaCl, 10 mM HEPES, 100 mM calcein, pH 7.0. External buffer: 100 mM NaCl, 10 mM HEPES, pH 7.0). Each transport experiment was carried out as follows; the calcein-containing POPC vesicles (25 μ L, 2.5 mM) were suspended in the external buffer (1925 μ L, 100 mM NaCl, 10 mM HEPES, pH 7.0) at 25°C and gently stirred. At 60 s, the carriers were administered in 5 μ L DMSO. The assay was calibrated at 250 s with detergent (25 μ L of Triton X-100 in 7:1 (v/v) H₂O-DMSO). The time-dependent change in fluorescence intensity ($\lambda_{\text{ex}} = 490$ nm, $\lambda_{\text{em}} = 520$ nm) was monitored, and normalised according to Equation S6:

$$I_{\text{rel}} = \frac{I_t - I_0}{I_{\text{max}} - I_0} \quad (\text{S6})$$

where $I_0 = I_t$ before transporter addition, $I_{\text{max}} = I_t$ after lysis.

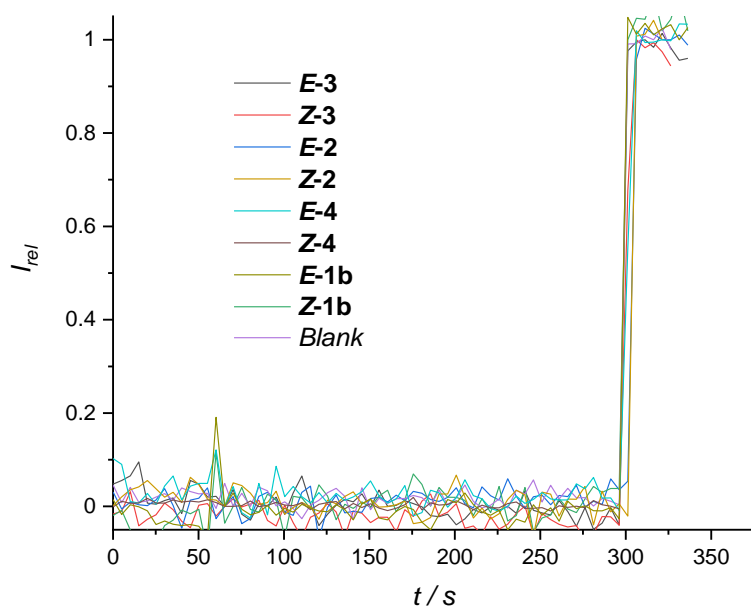


Figure S147. Calcein leakage assay: change in relative fluorescence intensity over time of **1-4**

Estimating the effective concentration of transporters in the membrane

The effective concentration of a receptor or transporter in a vesicle membrane is higher than that in bulk solution, because it is confined only to the small volume occupied by the membrane itself.

We can approximate this effective concentration using Equation S7:

$$[\mathbf{T}]_{\text{memb}} = [\mathbf{T}]_{\text{solution}} / V_{\text{m}}[\text{lipid}] \quad (\text{S7})$$

where $[\mathbf{T}]_{\text{memb}}$ is the concentration of the transporter in the membrane, $[\mathbf{T}]_{\text{solution}}$ is the overall concentration of transporter in the assay, V_{m} is the molar volume of phospholipid ($0.84 \text{ dm}^3 \text{ mol}^{-1}$ for POPC).

Under the HPTS assay conditions, working at the EC_{50} value of **1a**: $[\mathbf{1a}]_{\text{solution}} = 22 \text{ nM}$, $[\text{lipid}] = 31,000 \text{ nM}$ and $[\mathbf{1a}]_{\text{memb}} = 0.84 \text{ mM}$, this equates to a ~40,000-fold enhancement in concentration assuming all transporters are confined within the membrane.

6. Computational

Parametrization of anion transporter $1a^Z$

The anion transporter $1a^Z$ complex was optimised in ORCA (version 4.2.1)^[11] at the SMD(DMSO)- ω B97X-D3/def2-SVP level of theory (ma-def2-SVP on the Cl^- anion),^[12-15] which includes Grimme's D3 dispersion correction.^[16] To speed up the calculations, the resolution-of-identity chain-of-spheres exchange (RIJCOSX) approximation was employed.^[17]

The optimised structure was then used for charges calculations following the RESP protocol. To do so, the electrostatic potential (EFP) was generated in Gaussian 16 software^[18] at the HF/6-31G* level of theory using the Merz-Singh-Kollman scheme^[19] with 6 density points in each layer (IOp(6/33=2, 6/42=6, 6/50=1)) with a tight convergence criterion and a UltraFine grid (99,590 grid). The initial atomic charges of each molecule were then calculated by RESP fitting, along with the assignment of GAFF atom types,^[20-21] using the antechamber module, as implemented in the AMBER software suite.^[22]

Molecular dynamics simulations

For $1a^Z$, two systems were simulated in explicit DMSO, $1a^Z$ as a free ligand and in complex with chloride. For $1a^E$ dimer, the system was simulated in explicit DMSO, water and POPC.

MD simulations were performed in the GROMACS (v.2019.2),^[23] employing the AMBER99SB-IDLN force field.^[24] GAFF parameters for DMSO were taken as described by Coleman *et al.*^[25-26] Water molecules were described by TIP3P water model.^[27] POPC parameters were described by Slipid parameters.^[28] Chloride anion parameters were taken from Li *et al.*,^[29] these parameters have been found to reproduce the QM hydrogen bond lengths between the chloride anion and squaramide NH protons ($d_{NH-Cl} = 2.4 \text{ \AA}$, Fig. S148).

In each case, the system was inserted in a cubic box and solvated with either water or DMSO molecules. 0.15 M NaCl was added also included in the $1a^Z$ complex system. The system was further neutralised and minimised using the steepest descent algorithm until the maximum force was below $1000 \text{ kJ mol}^{-1} \text{ nm}^{-1}$. Five independent runs were performed with random initial velocities generated according to the Maxwell–Boltzmann distribution at 298 K (100 ps, 2 fs timestep), followed by equilibration under an NPT ensemble (100 ps, 2 fs timestep). Production simulations were performed in the NPT ensemble during 200 ns (2 fs timestep, 298 K and 1 bar). All simulations were performed with three-dimensional periodic boundary conditions. Long-range electrostatics was described with the Particle Mesh Ewald (PME) algorithm.^[30,31] Temperature of the system was maintained at 298 K using the V-rescale thermostat.^[32] Pressure was controlled by the Parrinello-Rahman barostat at 1.0 bar, with an isothermal compressibility of $4.5 \times 10^{-5} \text{ bar}^{-1}$.^[33] All bond lengths involving hydrogen atoms were constrained using the LINCS algorithm.^[34]

To study the behaviour of the $1a^E$ dimer in POPC, the dimer was placed in the centre of a pre-equilibrated POPC membrane. The system was first minimised and equilibrated as described above. In each case, the system was equilibrated under an NPT (500 ps, 1 fs timestep) ensemble and production MD simulations were run for 50 ns (2 fs timestep at 298 K and 1.0 bar).

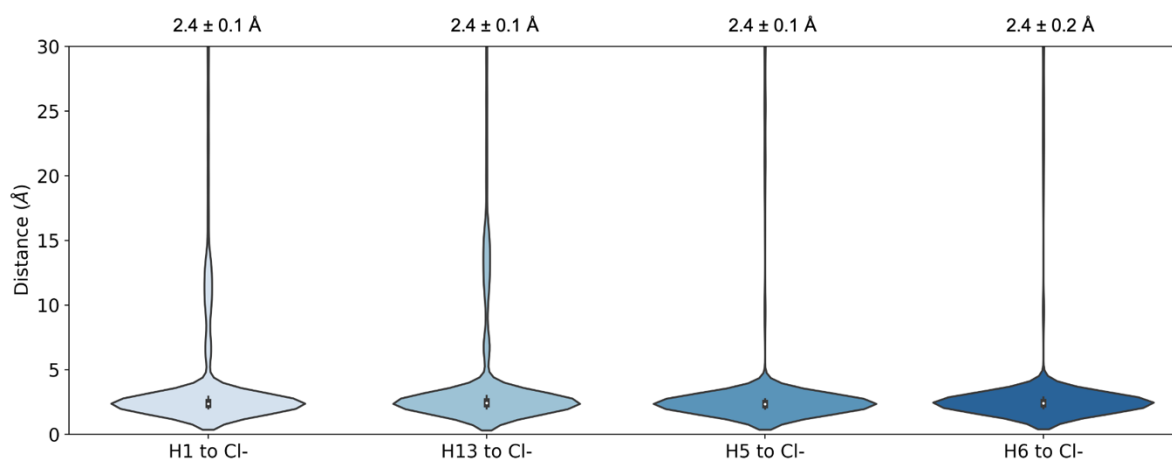


Figure S148. Distance of hydrogen bond between the squaramide NH protons to the Cl^- anion ($d_{\text{NH-Cl}}$) in a $1\mathbf{a}^Z$ complex in DMSO over 5×200 ns explicitly solvated MD simulations, resulting in $1 \mu\text{s}$ of total sampling time.

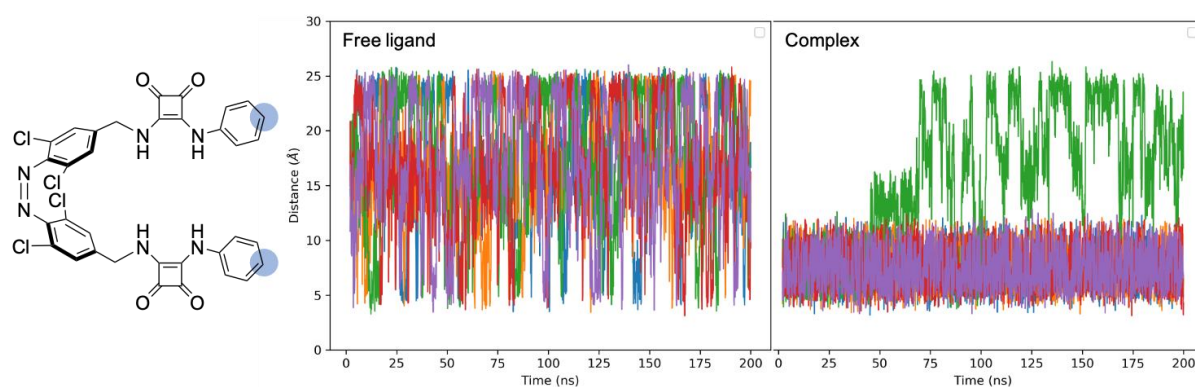


Figure S149. Time evolution of the end-to-end distance of $1\mathbf{a}^Z$ as a free ligand and as a 1:1 complex with chloride over 5×200 ns explicitly solvated MD simulations, resulting in $1 \mu\text{s}$ of total sampling time per system.

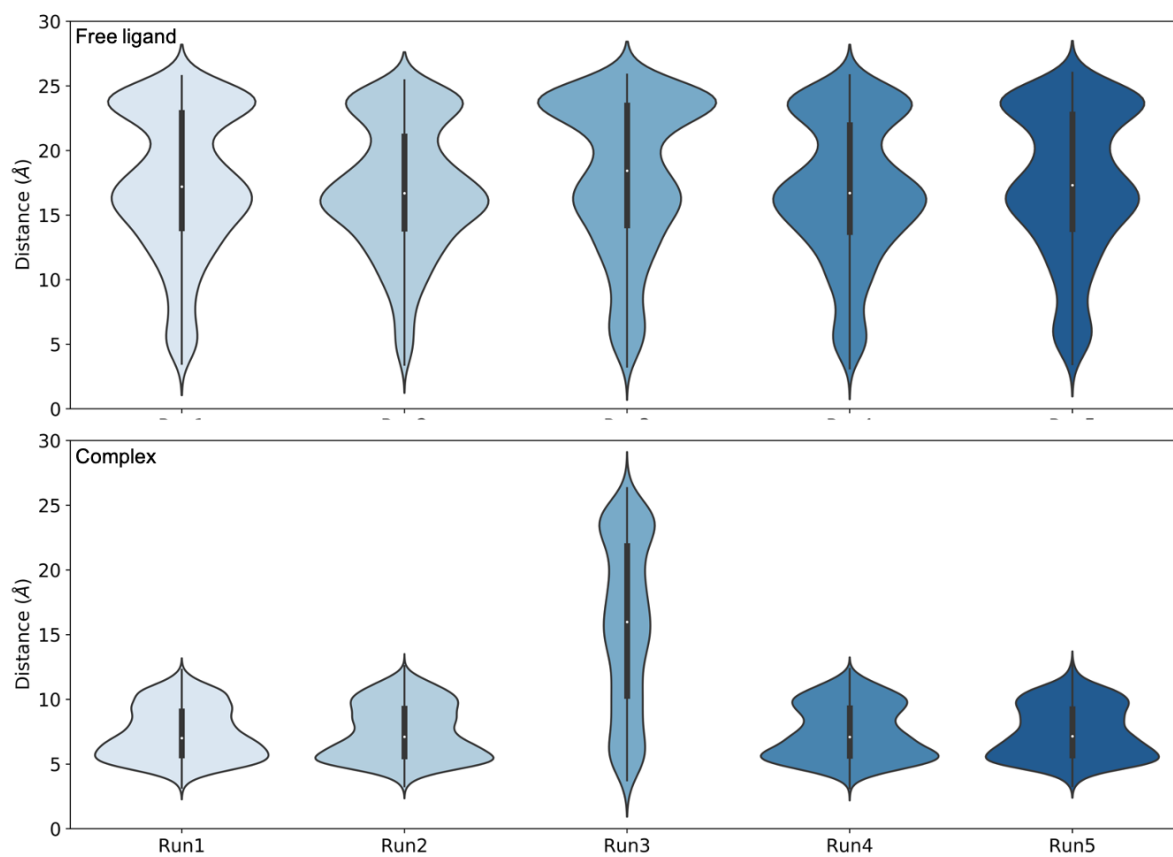


Figure S150. Comparison of the distributions of the end-to-end distance of $1a^Z$ as a free ligand (top) and in complex with chloride (bottom) across of 5 replicates of 200 ns explicitly solvated MD simulations, resulting in 1 μ s of total sampling time per system.

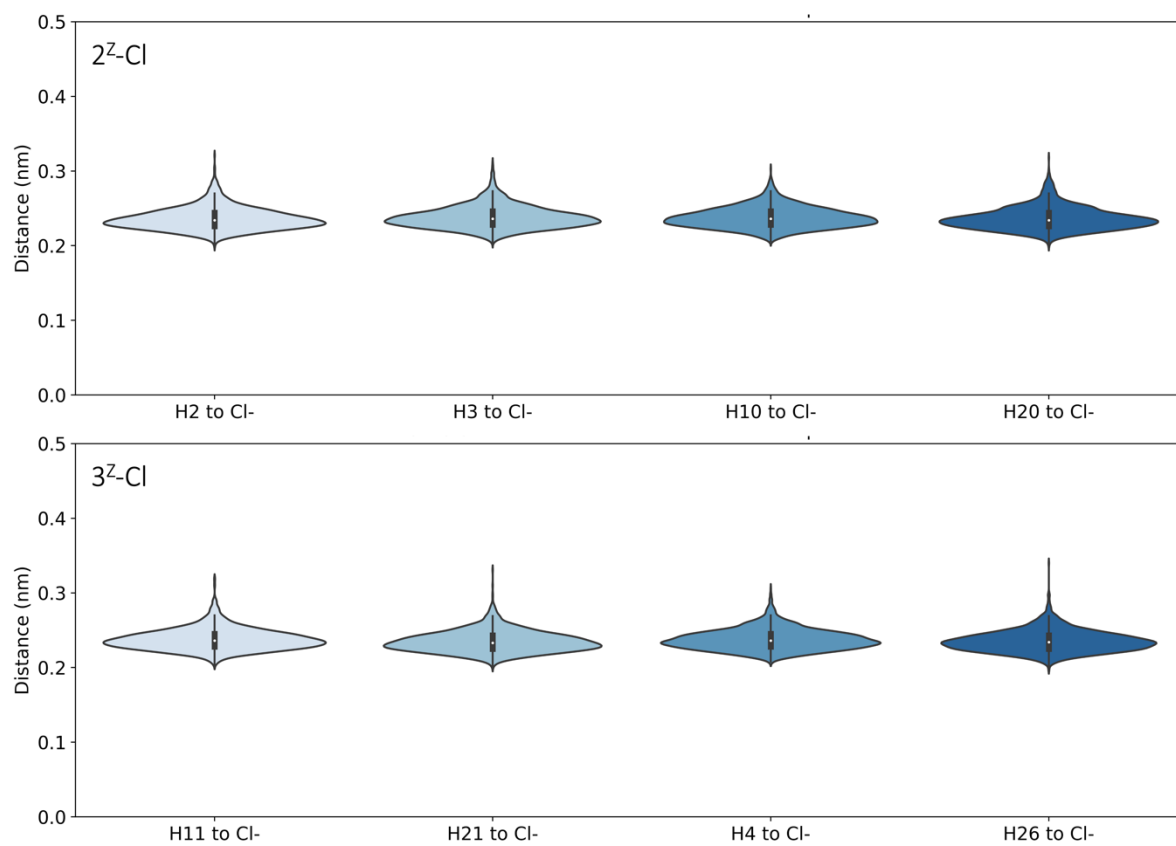


Figure S151. Distance of hydrogen bond between the squaramide NH protons to the Cl⁻ anion ($d_{\text{NH-Cl}}$) in a 2^Z and 3^Z complex in DMSO over a 200 ns explicitly solvated MD simulation.

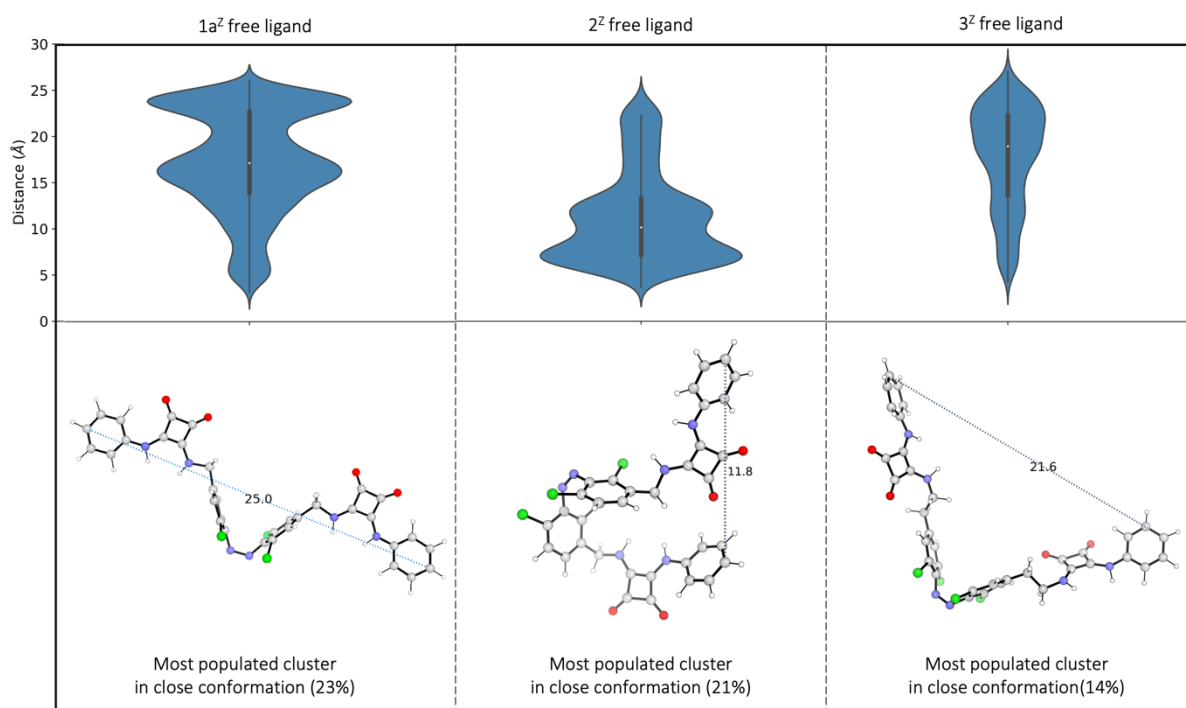


Figure S152. Top: Distance histograms of the end-to-end distance of $1a^Z$, 2^Z and 3^Z as a free ligand in DMSO. Bottom: The structure and percentage population of the most populated clusters, with their corresponding d_{RR} shown as blue dash lines.

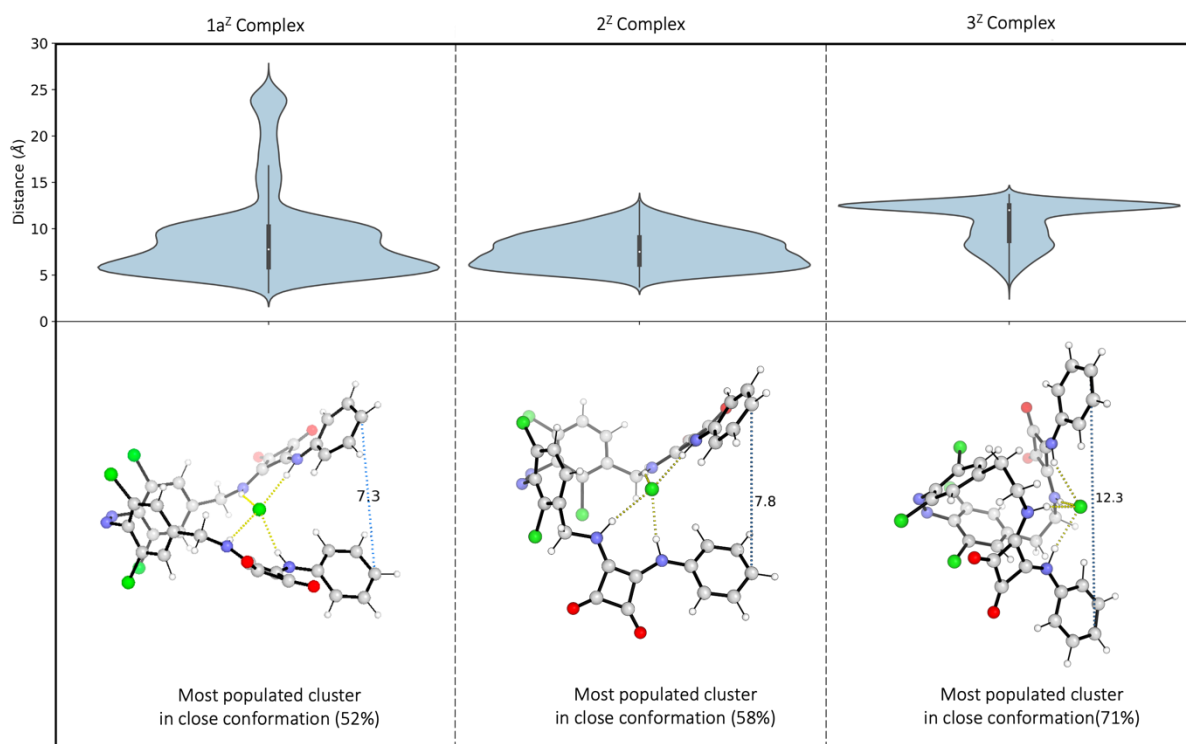


Figure S153. Top: Distance histograms of the end-to-end distance of $1a^Z$, 2^Z and 3^Z as a 1:1 complex with a chloride anion in DMSO. Bottom: The structure and percentage population of the most populated clusters, with their corresponding d_{RR} shown as blue dash lines.

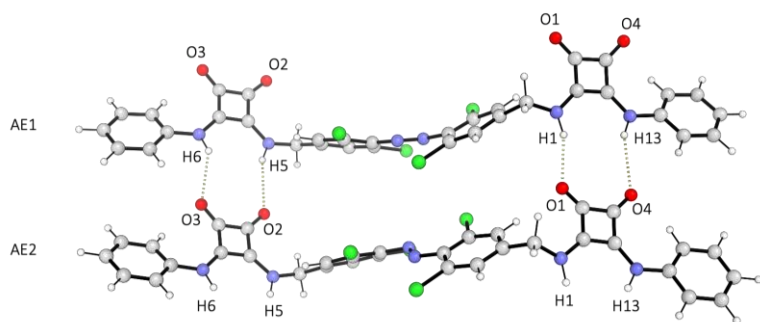


Figure S154. Ball-and-stick representation of the starting structure of the $1a^E$ dimer.

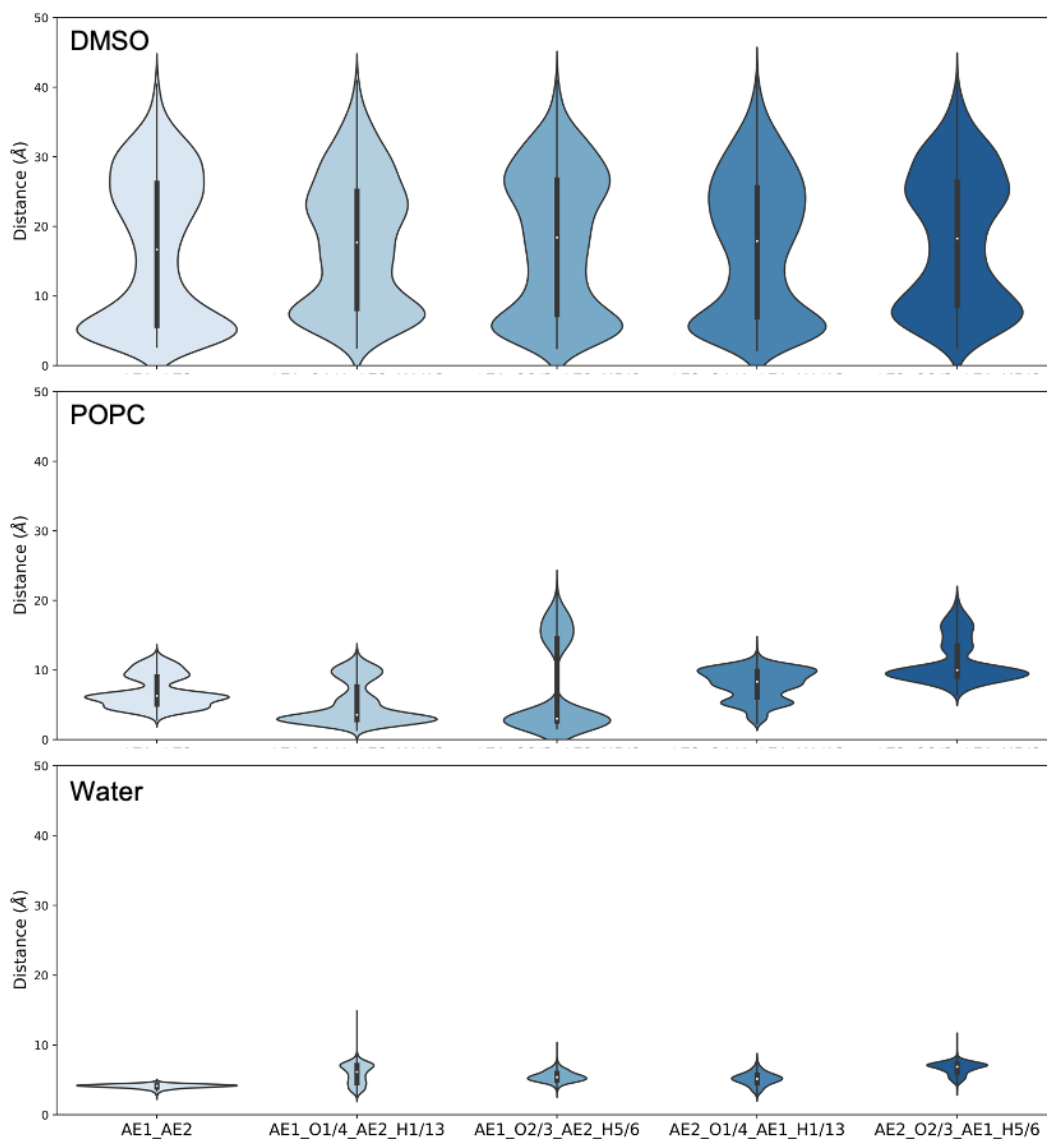


Figure S155. Distance histograms between the two $1a^E$ monomers over 5 x 50 ns simulations in DMSO, POPC membrane and water, resulting in 250 ns of total sampling time per system.

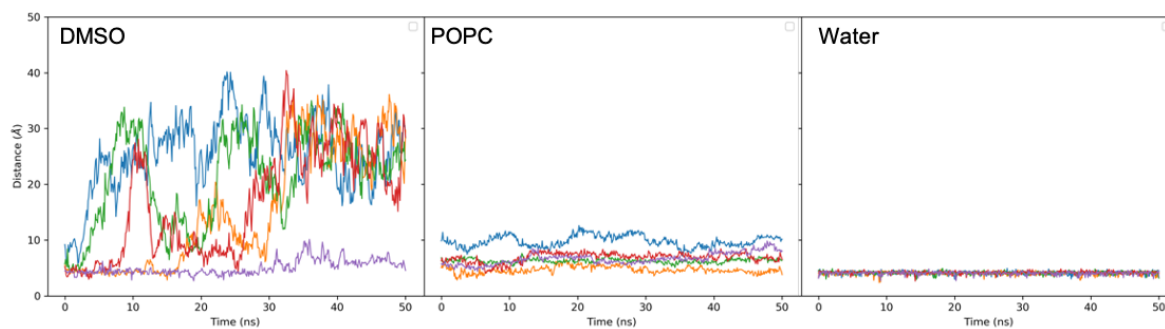


Figure S156. Time evolution of distance (\AA) between the two $1a^E$ monomers over 5 x 50 ns simulations in DMSO, a POPC membrane and water.

7. References

1. A. Kerckhoffs and M. J. Langton, *Chem. Sci.*, 2020, **11**, 6325–6331.
2. B. Heinrich, K. Bouazoune, M. Wojcik, U. Bakowsky, O. Vázquez, *Org. Biomol. Chem.*, 2020, **17**, 1827-1833.
3. ASSEMBLY BIOSCIENCES, INC.; L. Li, L. D. Arnold, D. Lee, S. Reddy WO2018/169907, 2018, A1
4. VICHEM CHEMIE KUTATÓ KFT.; GREFF, Zoltán; VARGA, Zoltán; KÉRI, György; NÉMETH, Gábor; ÖRFI, László; SZÁNTAI KIS, Csaba WO2011/77171, 2011, A1
5. G. Yan, L. Hao, Y. Niu, W. Huang, W. Wang, F. Xu, L. Liang, C. Wang, H. Jin and P. Xu, *Eur. J. Med. Chem.*, 2017, **137**, 462-475.
6. A. González-Antuña, I. Lavandera, P. Rodríguez-González, J. Rodríguez, J. I. García Alonso and V. Gotor, *Tetrahedron*, 2011, **67**, 5577-5581.
7. M. A. Lucherelli, J. Raya, K. F. Edelthammer, F. Hauke, A. Hirsch, G. Abellán, A. Bianco, *Chem. Eur. J.*, 2019, **25**, 13218-13223
8. Mahlooji, I.; Shokri, M.; Manoochehri, R.; Mahboubi-Rabbani, M.; Rezaee, E.; Tabatabai, S. A., **353** (8), 2000052.
9. Tran-Hoang, N.; Kodadek, T., *ACS Combinatorial Science*, 2018, **20** (2), 55-60.
10. P. Kuzmič, *Analytical Biochemistry*, 1996, **237**, 260–273.
11. F. Neese, F. Wennmohs, U. Becker, C. Riplinger, *J. Chem. Phys.*, 2020, **152**, 224108.
12. A. V. Marenich, C. J. Cramer, D. G. Truhlar, *J. Phys. Chem. B.*, 2009, **113**, 6378–6396
13. F. Weigend, R. Ahlrichs, *Phys. Chem. Chem. Phys.*, 2005, **7**, 3297-305.
14. F. Weigend, *Phys. Chem. Chem. Phys.*, 2006, **8**, 1057-65.
15. J. Zheng, X. Xu, D.G. Truhlar, *Theor Chem Acc*, 2011, **128**, 295–305
16. J.-D. Chai, M. Head-Gordon, *Phys. Chem. Chem. Phys.*, 2008, **10**, 6615 —6620
17. R. Izsak and F. Neese, *J. Chem. Phys.*, 2011, **135**, 144105
18. Gaussian 16, Revision C.01, M. J. Frisch, G. W. Trucks, H. B. Schlegel, G. E. Scuseria, M. A. Robb, J. R. Cheeseman, G. Scalmani, V. Barone, G. A. Petersson, H. Nakatsuji, X. Li, M. Caricato, A. V. Marenich, J. Bloino, B. G. Janesko, R. Gomperts, B. Mennucci, H. P. Hratchian, J. V. Ortiz, A. F. Izmaylov, J. L. Sonnenberg, D. Williams-Young, F. Ding, F. Lipparini, F. Egidi, J. Goings, B. Peng, A. Petrone, T. Henderson, D. Ranasinghe, V. G. Zakrzewski, J. Gao, N. Rega, G. Zheng, W. Liang, M. Hada, M. Ehara, K. Toyota, R. Fukuda, J. Hasegawa, M. Ishida, T. Nakajima, Y. Honda, O. Kitao, H. Nakai, T. Vreven, K. Throssell, J. A. Montgomery, Jr., J. E. Peralta, F. Ogliaro, M. J. Bearpark, J. J. Heyd, E. N. Brothers, K. N. Kudin, V. N. Staroverov, T. A. Keith, R. Kobayashi, J. Normand, K. Raghavachari, A. P. Rendell, J. C. Burant, S. S. Iyengar, J. Tomasi, M. Cossi, J. M. Millam, M. Klene, C. Adamo, R. Cammi, J. W. Ochterski, R. L. Martin, K. Morokuma, O. Farkas, J. B. Foresman, and D. J. Fox, Gaussian, Inc., Wallingford CT, 2016.
19. U. C. Singh and P. A. Kollman. *J. Comp. Chem.* **1984**, *5*, 129 – 145
20. J. Wang, W. Wang, P.A. Kollman, D.A. Case, *J. Mol. Graph. Mod.* **2006**, 247260.
21. J. Wang, R.M. Wolf, J.W. Caldwell, P.A. Kollman, D.A. Case, *J. Comp. Chem.*, 2004, **25**, 1157-1174.
22. D.A. Case, H.M. Aktulga, K. Belfon, I.Y. Ben-Shalom, S.R. Brozell, D.S. Cerutti, T.E. Cheatham, III, V.W.D. Cruzeiro, T.A. Darden, R.E. Duke, G. Giambasu, M.K. Gilson, H. Gohlke, A.W. Goetz, R. Harris, S. Izadi, S.A. Izmailov, C. Jin, K. Kasavajhala, M.C. Kaymak, E. King, A. Kovalenko, T. Kurtzman, T.S. Lee, S. LeGrand, P. Li, C. Lin, J. Liu, T. Luchko, R. Luo, M. Machado, V. Man, M. Manathunga, K.M. Merz, Y. Miao, O. Mikhailovskii, G. Monard, H. Nguyen, K.A. O’Hearn, A. Onufriev, F. Pan, S. Pantano, R. Qi, A. Rahnamoun, D.R. Roe, A. Roitberg, C. Sagui, S. Schott-Verdugo, J. Shen, C.L. Simmerling, N.R. Skrynnikov, J. Smith, J. Swails, R.C. Walker, J. Wang, H. Wei, R.M. Wolf,

- X. Wu, Y. Xue, D.M. York, S. Zhao, and P.A. Kollman (2021), Amber 2021, University of California, San Francisco.
23. M.J. Abraham, D. van der Spoel, E. Lindahl, B. Hess, and the GROMACS development team, GROMACS User Manual version 2019, <http://www.gromacs.org>
 24. K. Lindorff-Larsen, S. Piana, K. Palmo, P. Maragakis, J.L. Klepeis, R.O. Dror, D.E. Shaw *Proteins*, 2010, **78**, 1950
 25. C. Caleman, P. J. van Maaren, M. Hong, J. S. Hub, L. T. Costa and D. van der Spoel *J. Chem. Theory Comput.*, 2012, **8**, 61-74
 26. D. van der Spoel, P. J. van Maaren and C. Caleman *GROMACS Molecule & Liquid Database, Bioinformatics* 2012, **28**, 752-753
 27. D. J. Price and C. L. Brooks, *J Chem Phys.* 2004 121,10096-103
 28. J. P. M. Jämbeck, A. P. Lyubartsev, *J. Chem. Theory Comput.*, 2012, **8**, 2938–2948
 29. P. Li, L. F. Song, and K. M. Merz, *J. Chem. Theory Comput.* 2015, 11, 4, 1645–1657
 30. T. Darden, D. York, and L. Pedersen, *J. Chem. Phys.*, 1993, **98** 10089–10092
 31. U. Essmann, L. Perera, M.L. Berkowitz, T. Darden, H. Lee, and L.G. Pedersen, *J. Chem. Phys.*, 1995, **103** 8577–8592
 32. G. Bussi, D. Donadio, M. Parrinello, *J. Chem. Phys.* 2007, **126**, 014101
 33. M. Parrinello, A. Rahman *J. Appl. Phys.* 1981, **52**, 7182
 34. B. Hess, H. Bekker, H. J. C. Berendsen, J. G. E. M. Fraaije, *J. Comp. Chem.*, 1997, **18**, 1463–1472